University of Trento
Center for Mind/Brain Sciences (CIMeC)

Doctoral Programme in Cognitive and Brain Sciences
(XXXVII Cycle)

Beyond visual processing: A multi-method investigation into the role of early visual areas during reaching, grasping, and haptic exploration without vision

PhD Candidate:
Samantha Sartin

PhD Supervisor:
Prof. Simona Monaco

A thesis submitted in fulfillment of the requirements for the degree of Doctor of Philosophy in Cognitive and Brain Sciences

Academic Year 2024-2025

To everyone who held a piece of the puzzle.

Abstract

The human hand enables goal-directed actions, like reaching and grasping, and haptic object exploration, allowing us to interact with but also to perceive and contextualize our surroundings. Most of the time, we use vision to guide these processes as it is the dominant sense for extracting information about object properties that are relevant for appropriate hand-object interactions. Yet there are many situations in which visual information is not available, for example when we search for our keys in a pocket, or we reach for a door handle in complete darkness. In such circumstances we need to rely on memory and previous experience, as well as on somatosensory feedback to guide our actions and execute appropriate movements to achieve our goals.

The present work is about the neural mechanisms behind grasping, reaching, and haptic exploration, particularly focusing on the role of the ventral visual stream and Early Visual Cortex (EVC), when visual input is unavailable. In fact, while the existing literature overall agrees on the neural underpinnings of visually guided, skilled hand actions, which consistently recruit dorsal stream areas in parietal cortex as well as somatomotor-related areas, no consensus has been reached on the brain areas subtending the execution of the same actions in the absence of visual information. Specifically, it remains a matter of debate whether early visual and ventral stream areas are consistently involved in the execution of reaching and grasping actions without visual input. In addition, the EVC, including the primary visual cortex (V1), also seems to be involved in haptic object exploration even in the absence of visual information, further pointing to a role of early visual areas that goes beyond unisensory processing of visual information. Yet it is unclear whether attributes of objects explored only through active touch might be represented in early visual areas, and whether this could be a mere epiphenomenon of top-down visual imagery. Finally, it has not yet been thoroughly investigated whether haptic processing in early visual areas might also be functionally relevant for behaviour.

Therefore, the contribution of this work is three-fold. First, I show that across published neuroimaging studies there is consistent univariate activation of dorsal stream areas during the execution of skilled hand actions irrespective of the availability of visual information, and of ventral visual stream areas, along with the EVC, only when online visual input is available. Second, I provide evidence for the role of V1 in haptic processing of object size by showing that activity patterns in V1 can be used to decode the size of unseen, haptically explored stimuli, but not visually imagined ones, even if participants never had visual experience of the stimuli, thereby suggesting that haptic processing in V1 is not merely due to visual imagery. Finally, I present behavioural data on manual size estimation of unseen haptically explored stimuli. The behavioural results show that the location of the hand exploring the unseen target, relative to gaze direction and body midline, does not significantly modulate haptic size estimation, and suggest that haptic size processing likely occurring in V1 might be functionally relevant for behavior. However, future research is needed to replicate our findings and further elucidate whether and how V1 contributes to haptic size processing.

Overall, this work contributes to our understanding of the neural mechanisms underlying the execution of skilled hand actions and haptic processing of object features in the absence of visual information, particularly addressing the controversial role of early visual areas. The findings of this thesis suggest that the visual system, particularly V1, acts in concert with well-established action-related and somatosensory brain networks. In particular, early visual areas show cross-modal modulations that can be explained within the predictive coding framework, wherein they might process haptic and action-related information to guide behaviour even when visual input is absent.

Acknowledgments

"*All we have to decide is what to do with the time that is given us*" (Tolkien, 1954, Chapter 2).

Looking back, the decision to pursue a PhD was unexpectedly one of the easiest I have ever made. It was a choice that matured early on, during the first years of my Bachelor's studies, as a result of a growing fascination with Cognitive Neuroscience. While the road of both personal and academic life since then has been long and winding at times, that initial spark of curiosity never faded. Nevertheless, while the decision was mine, the journey was made possible only through the collective time, expertise, and personal support of many others.

To my supervisor, Simona Monaco: thank you for believing in me, sometimes even more than I believed in myself. Thank you for giving me the chance to bring this project to life and for helping me achieve this beautiful milestone. Your expert guidance kept me on the right path whenever doubts arose. Beyond your academic mentorship, I am forever grateful for your empathy during the challenging personal circumstances I unexpectedly had to navigate.

I would also like to express my gratitude to Prof. Luigi Cattaneo and Luca Turella for their insightful feedback provided during the oversight committee's meetings that helped refine some aspects of this research. A special thank you goes to Prof. Irene Sperandio, as well as to all the co-authors of the papers included in this thesis; your collaboration and expertise were fundamental to the scientific quality of this work.

To the technicians of the University's laboratories, especially Massimo Vescovi and Andrea Vitale: thank you for helping me define the strategies for data acquisition and analysis. Beyond your technical mastery, your kindness was a constant and invaluable support. I would also like to extend my thanks to the administrative staff and the department secretaries who contribute in the background to the fulfillment of research and doctoral duties.

To the "Monks' lab"—Margherita, Fabio, Eleonora, and Isotta: thank you for sharing the everyday adventures of this academic journey. Thank you for the "shared traumas", the important "scientific" debates between Marghe and Fabio, and the unique, funny ways of saying things "invented" by Ele that never failed to lighten the mood. You were the *Fellowship* I needed to navigate the highs and lows of the last year. Between our rigorous scientific meetings and

our legendary culinary discussions and classes, you provided the laughter and the friendship that turned the lab into a second home, and you made this final year a chapter I will always cherish.

To all my office neighbors, including (but not limited to) Chiara, Matteo, Alex, Valentina, Marco, and Elena: thank you for the shared lunches, the coffee breaks, and for being such wonderful companions during our daily downtime. Even if only for a brief period, your presence made the long hours in the office much more enjoyable.

To the many former interns who assisted across various stages of this research—Federica D., Fabio, Federica A., Domenico, Laura, Federica C., Elena, Greta, Arefeh, Thomas, and Francesca: thank you for your invaluable time. This work would not have been possible without your hands and your hearts. I am also grateful to all the participants who volunteered their time for this research.

Importantly, this research was made possible by the financial support provided by the European Commission and the Italian Ministry of University and Research within the Next generation EU programme Young Researchers [Grant 40104258].

Finally, to my family, the foundation upon which all my accomplishments rest. To my mum Gabriella and grandmother Bruna: you have both faced such difficult times in these last years with a strength that I can only hope to emulate. I have worked for this milestone also for you, and knowing that you feel proud of me is my greatest reward. To my sister Sara, my brothers Matteo and Mirco, and the entire family: thank you for your constant love and for being proud of this journey. In particular to my brother, Matteo: you may not realize it, but you were the very first person to motivate me toward my goals, giving everything you could to support my growth as a person and my academic path. A profound thank you goes to the other half of my heart, Nicholas: you have literally walked this path beside me, supporting me from the very first day of my academic studies in ways I could never have imagined. Without you both, I am certain I would not be here today, writing the final lines of this thesis.

Lastly, to my beloved nieces Giorgia, Gaia, Gioia, and my nephew Brandon: I hope that this work somehow serves as an inspiration for you. I hope I can be a guide as you begin to dream

of your own futures and careers; remember that no quest is too long if you have the heart to pursue it.

Ultimately, this thesis is dedicated to all of you. Every one of you held a vital piece of the puzzle, and it is only because of your support, expertise, time, and *love*, that the picture is finally complete.

Thank you.

Abbreviations

AIP: anterior intraparietal area
aIPS: anterior intraparietal sulcus
ALE: activation likelihood estimation
BA: Brodmann area
BOLD: blood oxygen level dependent
CBMA: coordinate-based meta-analysis
CIP: caudal intraparietal area
CoS: collateral sulcus
dPM: dorsal premotor area
EP: exploratory procedure
EVC: early visual cortex
FFA: fusiform face area
fMRI: functional magnetic resonance imaging
GLM: general linear model
HE: haptic exploration
hMT+/V5: human middle temporal area/area V5
IFG: inferior frontal gyrus
ILOTC: inferolateral occipitotemporal cortex
IPL: inferior parietal lobule
IPS: intraparietal sulcus
ITC: inferotemporal cortex
ITG: inferior temporal gyrus
ITI: inter-trial interval
LO: lateral occipital cortex
LOC: lateral occipital complex
LOtv: lateral occipital tactile-visual area
M1: primary motor cortex
MA: modelled activation
MFG: middle frontal gyrus
MNI: Montreal neurologic institute
MOC: medial occipital cortex
MRI: magnetic resonance imaging
MTG: middle temporal gyrus
MVPA: multivoxel pattern analysis
NIBS: non-invasive brain stimulation
OP: occipital pole
OP1, 3, 4: operculum parietalis 1,3,4
PCS: postcentral sulcus
PET: positron emission tomography
pIPS: posterior intraparietal sulcus
PO: parietal operculum

PoCG: postcentral gyrus
PPA: parahippocampal place area
PPC: posterior parietal cortex
PPI: psychophysiological interaction analysis
PreCG: precentral gyrus
preSMA: presupplementary motor area
RFX: random effects
ROI: region of interest
S1/SI: primary somatosensory cortex
S2/SII: secondary somatosensory cortex
SFG: superior frontal gyrus
SMA: supplementary motor area
SPL: superior parietal lobule
SPOC: superior parieto-occipital cortex
TAL: Talairach
TMS: transcranial magnetic stimulation
V1: primary visual cortex
VI: visual imagery
vIPS: ventral intraparietal sulcus
vPM: ventral premotor area
VTC: ventral temporal cortex
VWFA: visual word form area

List of Publications

Sartin, S., Danaj, F., Del Giudice, F., Chen, J., Schwarzkopf, D. S., Sperandio, I., & Monaco, S. (2026). Decoding haptic and imagined stimulus size in the human cortex. *NeuroImage*, 121774. https://doi.org/10.1016/j.neuroimage.2026.121774

Sartin, S., Dal Monte, D., Del Giudice, F., Caleca, L., Prosperi, E., Carini, F., Danaj, F., Sperandio, I., & Monaco, S. (2025). Behavioural significance of foveal cortical processing for haptic size estimation. *Journal of Vision, 25*(9), 2601. https://doi.org/10.1167/jov.25.9.2601 [Abstract from the 25th Annual Meeting of the Vision Sciences Society (VSS), St. Pete Beach, Florida, USA]

Sartin, S., Dal Monte, D., Del Giudice, F., Caleca, L., Mattioli, G., Prosperi, E., Carini, F., Danaj, F., Sperandio, I., & Monaco, S. (2024). Behavioural relevance of foveal cortex processing for haptic size estimation. *Perception, 53*, 113. [Abstract from the 46th European Conference on Visual Perception (ECVP), Aberdeen, Scotland]

Sartin, S., Danaj, F., Del Giudice, F., Sperandio, I., & Monaco, S. (2023). Cortical areas involved in imagery and haptic exploration of object size. *Journal of Vision, 23*(9), 4991. https://doi.org/10.1167/jov.23.9.4991 [Abstract from the 23rd Annual Meeting of the Vision Sciences Society (VSS), St. Pete Beach, Florida, USA]

Sartin, S., Ranzini, M., Scarpazza, C., & Monaco, S. (2023). Cortical areas involved in grasping and reaching actions with and without visual information: An ALE meta-analysis of neuroimaging studies. *Current Research in Neurobiology, 4*, 100070. https://doi.org/10.1016/j.crneur.2022.100070

Monaco, S., Dal Monte, D., Del Giudice, F., Caleca, L., Danaj, F., **Sartin, S.**, & Sperandio, I. (2022). Behavioural relevance of haptic processing of object size in the primary visual cortex. *Perception, 51*, 54. https://doi.org/10.1177/03010066221141167 [Abstract from the 44th European Conference on Visual Perception (ECVP), Nijmegen, The Netherlands]

Table of contents

Chapter 1

General Introduction

In our daily interactions with the environment, our hands constantly enable us to translate our motor intentions into real goal-directed actions. On top of that, what makes the human hand a particularly powerful biological tool is the fact that it can simultaneously act as an effector of action and a receptor for perception. Whether we are reaching to grasp a cup of tea in a dimly lit room or assessing the ripeness of fruit through active touch (i.e., haptics), the brain must continuously translate multisensory inputs into precise motor commands. This process involves intricate sensorimotor transformations and real-time perceptual updates; yet, despite this underlying computational complexity, the resulting movements appear effortless.

While typically guided by vision, the motor system allows us to perform actions with remarkable precision even without online visual feedback by relying on somatosensory feedback. In addition to support non-visually guided actions, the haptic system allows us to perceive our surroundings by extracting information about object's attributes like size, shape, and texture, that enable us to recognize objects through touch.

The neural underpinnings of visually guided action and perception are classically and consistently mapped to the dorsal and ventral visual stream with the dual-visual stream theory. However, the neural mechanisms supporting the execution of actions and haptic object exploration when vision is not available are less understood and more inconsistent. Specifically, the recruitment of early visual areas in action and haptic exploration in absence of visual information is a matter of debate. Therefore, the main objective of this thesis is to elucidate the neural bases of these processes, with a particular focus on the debated role of the ventral visual stream and the Early Visual Cortex (EVC). Specifically, we will examine whether and how early visual areas contribute to action execution and haptic processing when visual input is unavailable.

1.1 The dual-visual stream theory

Ungerleider and Mishkin were among the first to suggest that the visual system of the macaque monkey consists of two anatomically and functionally specialized visual subsystems (Ungerleider & Mishkin, 1982). The authors postulated that a ventral and a dorsal visual stream originate from the primary visual cortex (V1), and project to the infero-temporal cortex and posterior parietal cortex, respectively. In addition to this anatomical distinction between the two streams, the authors proposed that the two visual streams receive and process two different types of visual information: objects features, like colour, texture, and shape in the ventral visual stream, vs. the spatial relations between objects, motion, orientation, and depth in the dorsal visual stream. As such, while the ventral visual stream supports the identification of objects ('what'), the dorsal visual stream supports the localization of objects in space ('where').

A decade later, Milner and Goodale put forward a new interpretation of this hypothesis based on neuropsychological observations, as well as electrophysiological and behavioural findings, thus giving rise to the "perception-action model" (Goodale & Milner, 1992) which has since then been further expanded (Milner & Goodale, 2006, 2008). According to this re-interpretation, both the ventral and dorsal visual streams receive and process the same type of visual information (i.e., about objects' features and spatial position), and they transform this information differently to support different functions. As proposed by the model, the ventral visual stream transforms the visual input into a perceptual representation of the object, thus playing a role in visual perception (e.g., object identification and recognition; 'what'), whereas the dorsal visual stream supports the visual control and guidance of actions performed toward an object (e.g., reaching and grasping; 'how'). Furthermore, the authors proposed that the two visual systems store visual inputs for different periods of time. The ventral stream maintains the perceptual representation of objects over a sustained period of time in order to enable the recognition of objects regardless of changes in viewing conditions and perspective, whereas the

dorsal stream registers and continuously updates the visual information about the goal object in order to determine the appropriate coordinates for the effector being used (Milner & Goodale, 2008). In other words, on one side, the dorsal visual stream supports the immediate control of actions toward target objects, and, on the other side, the ventral visual stream supports the control of actions when a delay is interposed between the visual presentation of the target object and the response.

Despite the consistent body of evidence supporting the division of labour between the two visual pathways, the extent of the dichotomy between them is still a matter of debate. For instance, a review conducted by Schenk and McIntosh (2010) challenged the idea that the two visual systems are functionally independent, and rather suggested that their functional specialization might be relative. Furthermore, the dual-visual stream theory has been revised to address evidence indicating that the two visual streams do indeed interact with each other (Milner, 2017). Hence, in the next sections, we will discuss the evidence supporting the involvement of the dorsal and ventral visual streams in the visual guidance of actions and in object recognition, respectively, but we will also discuss an emerging body of evidence that extend previous findings about the role of the two streams. Importantly, since the two-stream hypothesis is based on behavioural findings in neurologically intact and brain damaged individuals, here we examine the extent to which neuroimaging results published so far align with the behavioural findings that motivated and explained the dual visual-stream theory.

1.1.1 The role of the dorsal visual stream in action execution

A consistent portion of the existing literature points to the involvement of dorsal stream areas in the visual guidance of skilled actions, such as reaching, pointing and grasping, and in the control of eye movements. For the purpose of this thesis, in the next sections we are going to focus on the evidence investigating the neural underpinnings of the visual guidance of hand reaching and grasping actions.

One of the first pieces of evidence in support of the role of the dorsal visual pathway in the visual guidance of actions like reaching and grasping comes from neuropsychological observations of patients with damage to dorsal stream areas who suffer from a neurological deficit named 'optic ataxia'. For example, patient A.T. exhibited the symptoms associated with this disorder as a consequence of a bilateral lesion in the posterior parietal cortex (Jeannerod et al., 1994). Patients like A.T. show the inability to correctly reach to a visual target located in their peripheral visual field; the misreach becomes even more pronounced when patients are not allowed to look at the object while performing the reaching action (Borchers et al., 2013; Jeannerod, 1986; Perenin & Vighetto, 1988). Despite their reaching impairments, optic ataxia patients can accurately recognize target objects and perceive their spatial location even when these objects are presented in their peripheral visual field (Pisella et al., 2009). The lesion site common to patients suffering from optic ataxia is located in the parietal cortex and spans the superior parietal lobule (SPL) along with areas around the intraparietal sulcus (IPS) (Andersen et al., 2014).

Lesion studies and electrophysiological recordings in macaques supported the role of the dorsal visual stream in visually guided actions (e.g., Gallese et al., 1994; Hyvärinen & Poranen, 1974; Sakata et al., 1995; Taira et al., 1990; for reviews, see Jeannerod et al., 1995; Sakata & Taira, 1994; Sakata et al., 1997). For instance, Taira et al. (1990) identified 55 macaque's neurons in area 7 of the posterior parietal cortex that responded to the active movement of the hand (i.e., manipulation of objects). The majority of these hand-movement-related neurons showed higher activation during hand manipulation in the light than in the dark; moreover, they showed selectivity for the type of object being manipulated and for its orientation in space, thus suggesting that these neurons are involved in the guidance of hand actions, specifically by matching them with object features (Taira et al., 1990). Murata et al. (2000) further investigated the response properties of hand-manipulation-related neurons of the

macaque anterior intraparietal area (AIP) while the animals grasped and manipulated 3D objects. They confirmed that among the visually responsive neurons that were active during both object fixation and hand-manipulation tasks, many showed shape selectivity, size and orientation selectivity (Murata et al., 2000). Taken together, these findings suggest that the dorsal visual stream underpins the processing of objects' features such as size, shape, and orientation which are relevant for the visual control of actions toward objects.

The investigation of the neural bases of goal-directed actions like grasping and reaching through functional imaging experiments in humans further corroborated the involvement of parietal areas in the visual guidance of such actions (e.g., Cavina-Pratesi et al., 2010b; Culham, Danckert, et al., 2003; Di Bono et al., 2015; Monaco et al., 2014; for reviews, see Culham, Cavina-Pratesi, & Singhal, 2006; Gallivan & Culham, 2015). In particular, parietal areas involved in grasping and reaching are the anterior intraparietal sulcus (aIPS), superior parietal lobe (SPL), superior parieto-occipital cortex (SPOC), and, as expected, the primary somatosensory area (S1). Additional areas of the frontal lobe are also involved in grasping actions, such as the ventral premotor region (vPM), dorsal premotor region (dPM), supplementary motor area (SMA), and as expected the primary motor cortex (M1).

Overall, these findings show that there is plenty of evidence that dorsal stream areas are recruited during visually guided reaching and grasping actions.

1.1.2 The role of the dorsal visual stream in perception

Despite the evidence reviewed above indicating the involvement of the dorsal stream in action control, some studies found evidence that the dorsal visual stream is also involved in object perception. Therefore, over the years some aspects of the model proposed by Goodale and Milner (1992) or, more broadly, the functional specialization between the two streams, has been revised.

While some authors adapted and extended the Milner and Goodale-model by suggesting the existence of additional anatomically and functionally distinct subsystems within the dorsal visual pathway (e.g., Binkofski & Buxbaum, 2013; Kravitz et al., 2011; Pisella et al., 2006; Rizzolatti & Matelli, 2003), others raised concerns about the linear hierarchical organization of the two pathways (de Haan & Cowey, 2011) or directly challenged the clear cut functional distinction between the visual ventral and dorsal streams. For example, Pisella et al. (2009) conducted a review of some divergent results in the dorsal and ventral visual streams literature, based on which the authors hypothesized that the dorsal stream is also involved in the perception of objects together with the ventral stream. The evidence that supports their proposal comes from neuropsychological observations of patients with damage to the posterior parietal cortex, but intact ventral stream, and with no primary visual field defect: in particular, these patients show an impaired performance in perceptual tasks. For instance, as reported by the authors, patients with hemineglect are unable to consciously perceive visual stimuli presented on the left visual hemifield, patients with simultagnosia are unable to consciously perceive parts of the visual field, and patients suffering from pure optic ataxia also show perceptual impairments in the periphery of the visual field despite having an intact ventral visual stream (Pisella et al., 2009).

In line with the proposal of Pisella et al. (2009), a growing body of evidence suggests that posterior regions of the dorsal visual stream may be involved in object perception along with the ventral visual stream (for reviews, see Erlikhman et al., 2018; Freud et al., 2016; Freud et al., 2020). Indeed, several studies show the existence of object representations in dorsal regions (Bettencourt & Xu, 2013; Freud et al., 2015; Konen & Kastner, 2008; Xu, 2009) which are independent of action execution and might cooperate with the ventral stream to enable normal object recognition (e.g., Sim et al., 2015). As Freud et al. (2016) claim in their review, the posterior and medial regions of the dorsal stream might hold perceptual representations of

objects, whereas the more anterior and lateral regions might support representations related to the actions to be performed. However, one might hypothesize that the representations of objects in the dorsal stream could be the result of input signals from the representations stored in the ventral stream (Freud et al., 2017, 2016). To test this hypothesis, a recent study conducted by Freud et al. (2017) further investigated the nature of the dorsal stream object representations using neuroimaging and behavioural measures. The authors found that not only dorsal stream areas are involved in the representation of the global structure of 3D objects, but also that there are different object representations in the dorsal and ventral visual streams. Therefore, this dissociation is not the result of inputs coming from ventral stream representations of objects. Concerning the functional role that the dorsal visual stream representations might play, they seem not to be sufficient for the perception of objects as indicated by the poor performance of patients with a ventral stream lesion in the perceptual tasks employed. Instead, the authors suggest that they could support the processing of the structural information of objects, which is fundamental for planning and guiding actions.

Further evidence in non-human primates supports the hypothesis that dorsal visual stream representations may play a functional role in object perception (e.g., Jeong & Xu, 2016; Van Dromme et al., 2016; Zachariou et al., 2015). For instance, Van Dromme et al. (2016) investigated the functional interaction between the macaque dorsal visual stream (caudal intraparietal area, CIP) and ventral visual stream (inferotemporal cortex, ITC) during the processing of 3D object information. They used reversible inactivation and microstimulation of these areas during fMRI to visualize changes in brain activity. The results of this study showed that inactivation of CIP, but not ITC, led to a reduced fMRI activation in both ventral and dorsal stream areas, in addition to a perceptual deficit in a depth-structure categorization task. Therefore, these findings suggest that visual information of 3D objects flows from the posterior

parietal cortex to the inferotemporal cortex, and that the former seems to be involved in the processing of objects' perceptual information.

Taken together, these studies indicate that the dorsal stream is involved not only in the visual guidance of skilled actions, such as reaching and grasping, but also in the perception of objects' features potentially supplementing the ventral visual stream with additional information about the target object to enable accurate object recognition with the ultimate goal of acting upon objects.

1.1.3 The role of the ventral visual stream in perception

We have so far provided a broad overview of the consistent body of evidence suggesting the involvement of the dorsal stream in the visual guidance of skilled actions on one side, and in the perception of objects' global 3D structure on the other side. As for the role of the ventral visual stream, many studies have provided evidence supporting the involvement of the ventral visual stream in object perception and recognition.

The main source of evidence in support of this hypothesis comes from neuropsychological observations of patients suffering from visual form agnosia as a result of damage to the ventral visual pathway. In comparison to the behaviour shown by patients suffering from optic ataxia, a reverse pattern of deficits was observed in patients with visual form agnosia (Goodale et al., 1991; Karnath et al., 2009). One of the most famous patients with this deficit is patient D.F. who, consequently to a bilateral damage to the occipito-temporal cortex, developed visual agnosia of shapes (Milner et al., 1991) that is, she failed at recognizing objects and their features (e.g., shape, size or orientation) through vision (Goodale et al., 1991). Despite her perceptual impairment, her ability to reach for an object and grasp it was spared and quite similar to that of healthy subjects. Patient D.F. has been the subject of further research using fMRI (e.g., James et al., 2003) which confirmed that, on one side, her inability to recognize objects is attributable to ventral stream damage, including the lateral occipital cortex

(LO), and, on the other side, her visuomotor skills are preserved thanks to the intact dorsal stream processing. In addition, it has been demonstrated that damage to distinct regions of the occipito-temporal cortex can be at the basis of different agnosia categories (e.g. Konen et al., 2011; Schiltz et al., 2006; for a review, see Martinaud, 2017) thus confirming the importance of the visual ventral stream in visual recognition and categorization.

Further evidence demonstrating the pivotal role of ventral stream areas in visual object perception and categorization comes from many neuroimaging studies (for reviews see Grill-Spector, 2003; Grill-Spector & Weiner, 2014; Grill-Spector et al., 2001). While neurons in early visual areas, including the primary visual cortex (V1) and secondary visual areas (V2-V3), respond to simple objects' features like local contours (i.e., edges), neurons in higher-level visual areas in the occipito-temporal cortex (OTC) integrate the information received by early visual areas to encode more complex representations, such as objects' shapes or even specific objects' categories. Indeed, it is these high-level visual areas that play a crucial role in visual perception and recognition (Grill-Spector et al., 2000; Moutoussis & Zeki, 2002). Several studies investigated the types of visual information that the OTC processes and, among them, we find information about visual object category and identity (Haxby et al., 2001; Kriegeskorte et al., 2008). It has been suggested the existence of category-selective regions with a preference for exemplars of one category of objects, that is, groups of regions that show a stronger response for exemplars belonging to the same object category than for exemplars of different categories. To name the most studied ones, the extrastriate body area (i.e., EBA in the fusiform gyrus) shows selectivity for human body parts (e.g., Peelen & Downing, 2005), the visual word form area (a region in the left inferior temporal lobe) for letter strings (Cohen et al., 2000), the fusiform face area (FFA) for face perception (Kanwisher et al., 1997), and the parahippocampal place area (PPA) for places (Epstein & Kanwisher, 1998). Furthermore, distributed object representations also lay in the VTC, as highlighted by Edelman et al. (1998) and Ishai et al.

(1999). More recently, Margalit et al. (2020) conducted an ultra-high-resolution fMRI study to investigate the nature of object representations in the human OTC. Their results suggest that the representations in the lateral OTC are organized at the level of domains (e.g., objects) while those in the medial OTC are organized at the category-specific level (e.g., cars, instruments).

A complete review of the literature on visual perception and categorization, however, goes beyond our scope. For our purpose, it is important to be aware of the enormous body of evidence indicating that the main functional role of the ventral visual stream is object perception and recognition.

1.1.4 The role of the ventral visual stream in action execution

As we already mentioned above, the clear-cut functional distinction between the two visual streams has raised some doubts as compelling evidence in favour of a complementary role of the two systems in both cognitive functions continues to emerge. We have already examined the pieces of evidence suggesting that the dorsal pathway plays a role in object recognition, and now we are going to introduce literature which points to the involvement of the ventral visual stream in functions other than object recognition that is, the control of delayed (or memory-based) hand grasping actions, when online visual information is not available.

The literature reviewed above indicates that the dorsal stream supports the guidance of reaching and grasping actions when online visual feedback is available during action execution. However, when such online visual feedback is not available (e.g., when a time delay separates the visual presentation of the target object and the onset of the action), the properties of the target object must be recruited from memory. More than a decade ago, Milner and Goodale (2008) demonstrated that the ventral visual stream is involved in the short-term maintenance of the object representation in memory, and consequently, it is thought to support the guidance of delayed grasping. This evidence is supported by neuropsychological observations of patients suffering from optic ataxia, on one side, and patients with visual agnosia, on the other side. On

the one hand, patients with optic ataxia show a better performance while executing pointing actions toward a target object when a delay is interposed between object presentation and reaching to grasp it (Milner et al., 2001; Milner et al., 1999). On the other hand, patients with visual agnosia show a poor performance when the same delay is introduced (Goodale et al., 1994). Therefore, these observations suggested that during the delay period, when visual information of the object is not available, the ventral stream might store a perceptual representation of the target object which would be subsequently recruited and used by the dorsal stream to guide movements. Further evidence supporting a role of the ventral visual stream in delayed actions comes from a transcranial magnetic stimulation study (TMS) on neurologically intact subjects indicating that TMS to the ventral visual stream caused impairments in delayed grasping (Cohen et al., 2009). In line with these results, an fMRI study conducted by Singhal et al. (2013) showed that the V1 and the lateral occipital complex were reactivated during delayed grasping actions performed in the dark. Moreover, their results also showed sustained activation in dorsal stream areas (i.e., aIPS, SMA, and dPM) throughout the delay period. Hence, based on these findings it seems that both the dorsal and ventral streams are involved in controlling delayed grasping, and that ventral stream areas supplement the dorsal stream with a stored perceptual object representation that is needed to execute an efficient grasping action even in the absence of direct visual information. Further, the ventral visual stream is reactivated during an action towards an object even if the object has been previously haptically explored in absence of any visual information (Monaco et al., 2017). Overall, these results suggest that the perceptual information stored in the ventral visual stream is independent of the modality initially used to explore the object (vision or touch).

Other studies, however, found sustained activation in the dorsal, but not the ventral, stream during the delay period. For instance, a study conducted by Fiehler et al. (2011) suggests that the control of both immediate and memory-based grasping movements is supported by a

similar cortical network located in the dorsal visual stream and in motor areas. Similar results were found for immediate and delayed reaching actions in both healthy subjects and an optic ataxia patient by Himmelbach et al. (2009). Similarly, a single neuron recording study with macaques indicated that the anterior intraparietal area remained activated throughout the duration of the delay periods (Murata et al., 1996). In addition, some findings also suggest that the ventral visual stream might not be crucial during the execution of delayed action. For instance, a TMS study conducted by Smyrnis et al. (2003) found that the stimulation of the posterior parietal cortex in healthy participants impairs the ability to perform delayed pointing movements.

Overall, the studies investigating the involvement of ventral stream areas in the guidance of grasping actions do not reach a consensus: some indicate that the ventral stream plays a crucial role in the guidance of delayed actions by storing a perceptual representation of the object that is accessed by the dorsal stream, others suggest that both streams are involved in controlling memory-guided grasping, while a few other studies provide evidence for the involvement of the dorsal, but not the ventral, stream in this process. Therefore, the debate is still open. This lack of consensus may be a byproduct of methodological constraints. It is possible that standard univariate analysis used by most studies over the past 20 year lacks the sensitivity to consistently detect action-related processes within early visual and ventral visual stream areas. In contrast, emerging work using MVPA has demonstrated different representations for grasping and reaching action planning with and without visual input in visual areas (Monaco et al., 2019, 2020; Velji-Ibrahim et al., 2022; Gallivan et al., 2013, 2019). Therefore, while the visual system might not be consistently engaged in motor and haptic tasks in terms of peak activation levels, it may still contain action-related information reflected by distributed activity patterns that can be detected and classified with MVPA but not univariate

approaches. As such, MVPA appears to be a promising tool for uncovering whether ventral stream and early visual areas have a representation of action planning and execution.

Up to this point we have focused on vision as the dominant sense that guides perception and action. However, haptic information is crucial when vision is not available. Despite its importance, the haptic system remains under-explored in cognitive neuroscience compared to the visual domain. The next session of the introduction will focus on research in the haptic domain, its neural underpinnings and its role in processing object properties in absence of visual information.

1.2 Haptic object processing in visual cortex

The term "haptics" refers to the cutaneous and kinesthetic inputs acquired through active movements of our hands to retrieve the properties of an object (James et al., 2007). Hence, haptic object recognition defines the ability to recognize object properties through tactile exploration. This aspect is crucial not only for blind people but also for sighted individuals performing daily tasks in low or no light conditions, or in situations in which one cannot gaze towards the object that is being haptically explored.

An object can be defined by several somatosensory attributes that can be haptically processed, including shape, size, surface texture, weight, temperature, and hardness (Lederman & Klatzky, 1993). For instance, to recognize an object, such as a key, solely through touch we may use our fingers to explore the edges of the entire object to gain information about its overall shape, including the curvature of the blade, the angle of the teeth, and any other unique features of a key's shape. To sense information about the material it is made of, typically metal, we would move our fingers on the surface of the object. Therefore, we perform specific types of hand movements to haptically explore an object and extract relevant information on its material

(e.g., weight, texture, hardness, thermal) and geometric or spatial (e.g., size, shape) attributes. More specifically, depending on the object dimension that we aim to explore, we typically perform a precise pattern of stereotypical hand movements that Lederman & Klatzky (1987) termed as "exploratory procedure" (EP) which is indeed property specific. For instance, the EP "contour following" represents an exploration technique in which the hand follows the contour of an object to extract information about its volume and precise shape while "lateral motion" is used to assess its texture (Lederman & Klatzky, 1987).

So far, we provided a broad overview of the perceptual abilities of the human haptic system (for reviews, see Kappers & Bergmann Tiest, 2013; Lederman & Klatzky, 1993). In the next sections, we will focus on the neural mechanisms that support these processes which are at the basis of our ability to interact with the external world.

1.2.1 Overview of the peripheral and neural mechanisms of haptic object exploration

How does the haptic system convey sensory information to the brain to enable the perception of object attributes? Here we provide a general overview of the peripheral and neural mechanisms involved in haptic object recognition.

When we haptically explore an object, our skin is the first major source of input. In fact, it contains receptors that constitute the peripheral sensory system which detects inputs from the external world. Thanks to specialized mechanisms, the incoming input is then translated into electrical signals to transmit sensory information to dedicated subcortical and cortical structures. Receptors in the skin are divided into groups based on the type of input they sense, and these include mechanoreceptors, which detect physical change (e.g., vibration, pressure, touch, stretch), thermoreceptors that sense changes in temperature, and nociceptors for pain detection. An additional group of receptors is that of proprioceptors; these are located in muscles, tendons, and joints, and are responsible, among others, for detecting sensations of

body parts position and movement (Tsay et al., 2016). Both cutaneous and kinesthetic inputs are processed by the haptic system and thus contribute to haptic object exploration (Lederman & Klatzky, 2009).

Inputs from the periphery are then transmitted through afferent nerve fibers (i.e., ascending pathways which pass through the brainstem and thalamus) to the neocortex where they are subject to further processing. Here, sensory inputs are combined to build a representation that can be compared with existing object representations stored in memory (Lederman & Klatzky, 1993). Several neocortical areas in the human brain process haptic stimuli. The primary sensory area for haptic processing is the primary somatosensory cortex (S1). It is located in the postcentral gyrus and is composed of four distinct cytoarchitectonic regions each containing a map of the human body surface (i.e., sensory homunculus, initially described by Penfield & Boldrey, 1937): Brodmann's areas (BAs) 3a, 3b, 2, and 1 (Kaas et al., 1979). Each one of these subregions receives specific inputs from different regions of the thalamus and displays a complex pattern of reciprocal connections both among them and with higher order brain regions (Delhaye et al., 2018). For instance, BA 3b responds to cutaneous stimuli, BA 3a receives mainly proprioceptive inputs, BA 1 exhibits primarily cutaneous responses, while BA 2 responds to both types of inputs (for a review, see Delhaye et al., 2018). While these regions are considered an early stage for cutaneous and proprioceptive information processing, the secondary somatosensory cortex (S2) is classically treated as a higher order processing stage in the somatosensory system. S2, which lies in the parietal operculum (PO), is a portion of cortex that also contains a somatotopic map and comprises multiple opercular subfields known as OP1, OP3, and OP4 (Eickhoff et al., 2007). This higher-order region, along with additional brain areas, receives projections from S1 and plays a crucial role in haptic object recognition (James et al., 2007). Apart from somatosensory cortical areas that are classically associated with touch, haptic object processing recruits also brain areas located in the posterior

parietal (Rolls et al., 2023) and visual cortices (Sathian, 2016). We will return to the involvement of visual cortical areas in a later section.

Interestingly, it has been proposed that haptic object processing is organized along two pathways, namely the ventral and dorsal routes (Dijkerman & de Haan, 2007; James et al., 2007; Reed et al., 2005), similar to those described in the visual system (Goodale & Milner, 1992; Ungerleider & Mishkin, 1982). Recently, de Haan and Dijkerman (2020) put forward a model to describe the functional organization of the somatosensory system. The authors suggest that it includes a unit for basic somatosensory processing which sends input to multiple networks, each subserving a distinct subfunction including haptic object recognition. According to this model, the network for haptic object recognition comprises brain regions supporting the encoding and maintenance of tactile information (S1), as well as the short and long-term storage of haptic information in memory. While short-term haptic memory is thought to be stored in S2, inferior parietal cortex, ventral and dorsal premotor cortices, and anterior cingulate cortex, the long-term haptic memory is stored in superior parietal cortex, intraparietal sulcus, medial and lateral prefrontal cortices. Tactile imagery is also considered in the model, and it is suggested to recruit sensory areas (e.g., S1) for modality-specific tactile imagery processes, and a more extended network (e.g., S1, retrosplenial cortices, prefrontal cortex, precuneus) for amodal mental imagery.

1.2.2 Cortical areas involved in haptic processing of object attributes

In the last few decades, several neuroimaging studies have investigated the neural basis of haptic processing of the various somatosensory attributes (for reviews, see J.-H. Kim & S.-P. Kim, 2023; Sathian, 2016). Overall, activation elicited by haptic object attributes has been detected in cortical regions inside but also outside the classical somatosensory areas previously mentioned. This stands true, for example, for object shape, texture, and motion. Figure 1 provides an overview of the major human brain areas involved in haptic processing. Since we

are mainly interested in the potential role of visual cortical areas in haptic object processing, here we summarize the main findings that shed light onto the cortical areas involved in haptic processing of the attributes previously anticipated.

A substantial body of literature investigated the neural basis of haptic shape processing (for reviews, see Sathian, 2016; Yau et al., 2016). At the cortical level, the brain areas which appear to mainly support haptic perception of shape are the postcentral sulcus (PCS) which corresponds to BA 2 (e.g., Lee Masson et al., 2016; Stilla & Sathian, 2008), the postcentral gyrus (PoCG) corresponding to BA 1 (e.g., Stilla & Sathian, 2008), the ventral premotor cortex (vPM) (Snow et al., 2015; Stilla & Sathian, 2008), the anterior intraparietal sulcus (aIPS) (e.g., Roland et al., 1998; Stilla & Sathian, 2008), the posterior IPS (pIPS) (e.g., Stilla & Sathian, 2008; Van De Winckel et al., 2005), and the ventral IPS (vIPS) (e.g., Stilla & Sathian, 2008). Interestingly, these portions of the IPS were reported to be involved in haptic but also visual shape processing (Stilla & Sathian, 2008).

In addition to parietal areas, shape-related activity has also been observed in brain regions commonly associated with visual information processing, like lateral occipital complex (LOC) (e.g., Amedi et al., 2001, 2002; for a review, see Lacey et al., 2009; Lee Masson et al., 2016; Stilla & Sathian, 2008). In fact, LOC was originally associated with visual object processing (e.g., Kourtzi & Kanwisher, 2001; Malach et al., 1995) and more specifically with shape perception (e.g., Drucker & Aguirre, 2009; Op de Beeck et al., 2008). In a seminal study conducted by Amedi et al. (2001), the authors showed that tactile 3D objects compared to shapeless tactile textures elicited activation in the occipitotemporal cortex. Specifically, the somatosensory activation overlapped with a subregion of LOC which has been named lateral occipital tactile-visual area (LOtv) based on its visuo-haptic response property (Amedi et al., 2002). From then on, LOtv has been proposed to store a supramodal visuo-haptic representation of object shape (Ricciardi et al., 2014). More recently, an fMRI study employing multivariate

cross-decoding analyses (Tian et al., 2023) confirmed that the occipital cortex stores a modality-independent representation (i.e., shared by haptic and visual modalities) of basic shape features like curvature and rectilinear. Snow et al. (2014) further extended this line of research by showing that shape perception of familiar objects recruited not just a single subregion but the entire LO, in addition to low- and intermediate-level visual areas like the primary visual cortex (V1) and V4. Further evidence for the recruitment of early visual areas in haptic shape processing comes from the study by Monaco et al. (2017) who found haptic shape-related activation in the occipital pole (OP) and similar activations in LOtv for haptic and visual exploration of unfamiliar shapes. This line of research suggests that haptic object perception recruits the entire visual ventral stream, that is the visual pathway including the temporal-occipital cortex which is relevant for visual perception and recognition (Goodale & Milner, 1992). The functional magnetic resonance imaging (fMRI) study conducted by Lee Masson et al. (2016) also revealed the existence of haptic shape representations in the early visual cortex (EVC) in addition to bilateral LOC although visual inputs were unavailable. However, the EVC and the right LOC, but not left LOC, were recruited to represent haptic shape information only when participants visually explored object shape prior to haptic exploration. Based on these results, the authors proposed that the EVC and right LOC may be recruited by top-down pathways to support visual imagery processes during haptic shape processing. Overall, the literature reviewed so far points to (or provides correlational evidence for) the involvement of the occipitotemporal cortex, and partly also the EVC, in haptic shape processing. Yet, the notion that especially the LOC is crucial for representing object shape not only in vision but also in touch has been challenged by evidence from a patient with lesions in bilateral LOC (Snow et al., 2015). In fact, patient M.C. showed impaired object recognition in the visual but not in the tactile modality. Moreover, fMRI results showed that neither haptic nor visual object exploration elicited activation in LOC, while the overall brain activation elicited by haptic

exploration was similar to that of healthy participants. Therefore, this result suggests that LOC is not crucial for haptic shape perception. In sum, these findings raised important questions about the role of primary and higher-order visual areas in haptic object processing. Relative to this, we will discuss the main hypotheses that have been proposed in the next section.

Tactile texture perception recruits various brain regions including the PoCG, likely corresponding to S1 (e.g., Deshpande et al., 2008; Sathian et al., 2011; Stilla & Sathian, 2008), and the PO (S2) including OP1, OP3 and OP4 (e.g., Sathian et al., 2011; Stilla & Sathian, 2008).

Similar to haptic shape perception, also tactile texture processing was found to elicit activation in the occipital cortex. In fact, early visual areas in the medial occipital cortex (MOC) showed activation in response to visual but also haptic textures (Eck et al., 2013; Sathian et al., 2011; Stilla & Sathian, 2008). Quite similar results were found by Podrebarac et al. (2014), who observed visual and haptic texture-selective activation in the medial occipitotemporal cortex in the collateral sulcus (CoS) although the visual and haptic activations did not overlap.

Another haptic object property that received attention, though to a smaller extent compared to shape and texture, is object motion. The investigation of the neural basis of haptic motion perception, compared to static motion, revealed inconsistent results relative to the involvement of S1. While some studies did find activation of S1 in response to tactile motion (Planetta & Servos, 2012; Summers et al., 2009; Wacker et al., 2011), others did not (e.g., Matteau et al., 2010). Similarly, it is not clear yet whether the posterior parietal cortex (PPC), including the IPS and the inferior parietal lobule (IPL), plays a role in tactile motion perception as suggested by several findings (e.g., Kitada et al., 2003; Nakashita et al., 2008; Summers et al., 2009; Van Kemenade et al., 2014) considering also the limitations related to experimental stimuli (Summers et al., 2009; Van Kemenade et al., 2014) and/or paradigm (Kitada et al., 2003; Nakashita et al., 2008). Interestingly, as we previously anticipated, there is evidence which shows that also haptic tactile motion elicits activation in the visual cortex. Specifically, tactile

motion recruits a visual motion-selective area named V5/human middle temporal (V5/hMT+) complex as demonstrated in sighted participants (Blake et al., 2004; Hagen et al., 2002; Summers et al., 2009; Van Kemenade et al., 2014; Wacker et al., 2011) and in congenitally blind people (e.g., Matteau et al., 2010; Ricciardi et al., 2007), although contradictory findings have also been reported (Jiang et al., 2015).

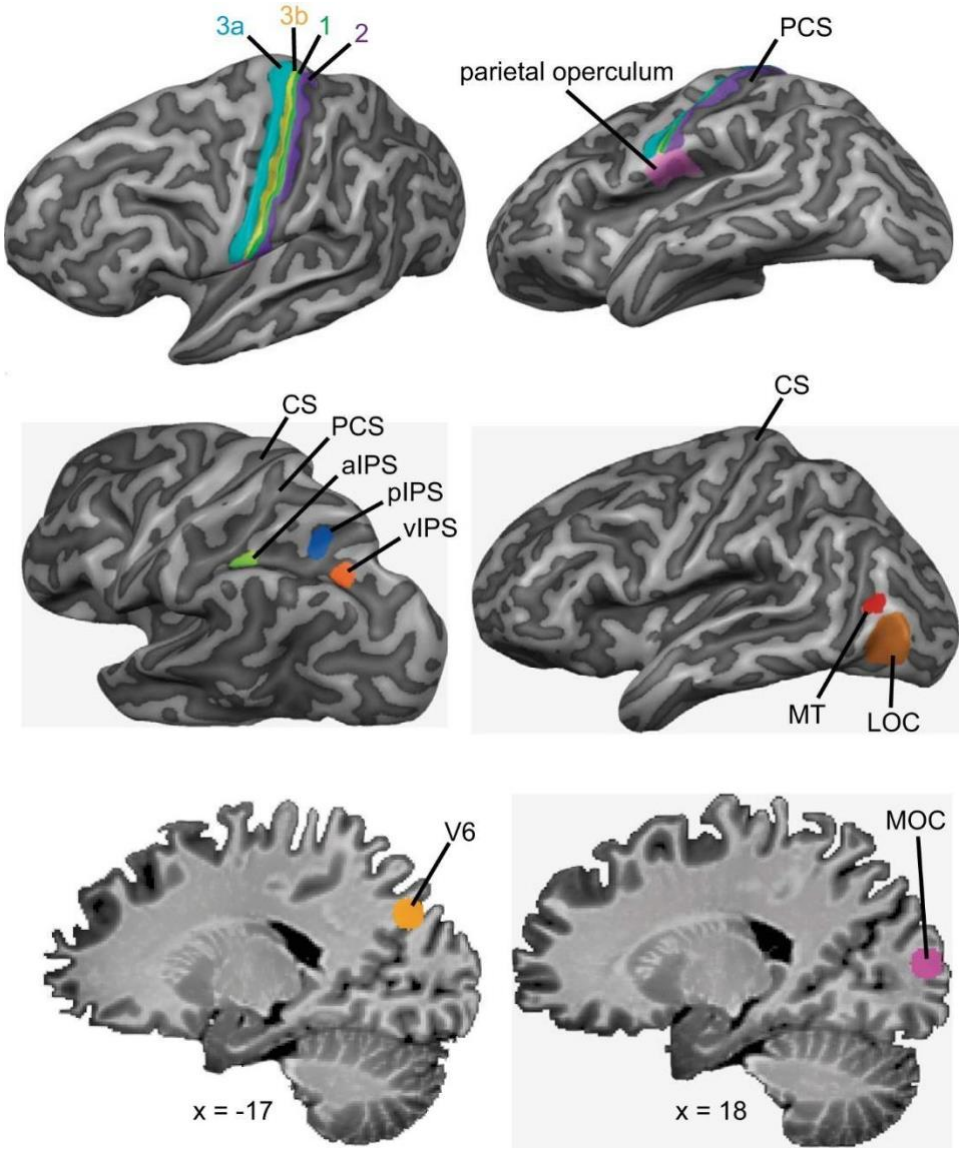

Figure 1. Overview of the major human brain areas processing somatosensory information. Neocortical areas are depicted on partially inflated views of the left cerebral hemisphere or on sagittal slices (Talairach x coordinate indicates slice position). 3a, 3b, 1, and 2: Brodmann's areas that form the primary somatosensory cortex (S1). PCS, postcentral sulcus; CS, central sulcus; aIPS, pIPS, vIPS: anterior, posterior, and ventral intraparietal sulcus; MT, human MT complex; LOC, lateral occipital complex; MOC, medial occipital cortex; V6, 6th visual area. Reproduced from Sathian (2016). Copyright © 2016, The American Physiological Society.

1.3 Role of the early visual cortex in haptic tasks

The evidence reviewed in the previous paragraph supports the recruitment of visual cortical areas during haptic perception of object attributes (for a review, see Lacey & Sathian, 2014). In blind individuals, the evidence for the engagement of the early visual cortex in tactile tasks (e.g., Braille reading and tactile discrimination; Sadato et al., 1998) reflect neuroplastic changes and cortical reorganization consequent to the absence of visual input (Silva et al., 2018; for reviews, see Mašić et al., 2020; Merabet & Pascual-Leone, 2010). However, the fact that both the blind and the sighted recruit visual cortical areas during haptic and tactile tasks also indicates a possible shared functional organization of visual areas across blind and sighted individuals. Yet, the mechanisms underlying the recruitment of visual areas for haptic processing, especially in the sighted, are still a matter of debate. What role could visual areas play in haptic object perception? To date, the literature proposes two possible top-down mechanisms that might explain the recruitment of early visual areas during haptic tasks. One hypothesis is that the recruitment of visual areas is mediated by visual imagery processes and is, therefore, epiphenomenal rather than functionally relevant for haptic processing per se. The alternative view posits that visual areas store abstract and multisensory representations of object attributes that are accessible both through vision and touch. Based on the latter, the occipital and occipitotemporal cortices might play a fundamental role in haptic tasks. In the next sections, we briefly review the literature investigating both hypotheses.

1.3.1 Mental visual imagery

According to the visual imagery hypothesis, the activation observed in occipital areas is related to the creation of a mental visual image of the object and its attributes, hence to visual imagery. In line with this hypothesis, the EVC including the primary and secondary visual cortices (V1 and V2, respectively), along with other brain regions are recruited for visual

imagery (e.g., Dijkstra et al., 2017; for a review, see Pearson, 2019). Recent meta-analytical evidence shows that the generation of visual mental images heavily relies on a network of brain areas encompassing frontoparietal, anterior temporal and hippocampal regions, along with a crucial node in the left ventrotemporal cortex, while the EVC does not seem to be crucially recruited (Spagna et al., 2021, 2024).

Despite the controversial role of the EVC in visual mental imagery, its involvement in haptic perception has been investigated especially in the context of object shape. Notably, Zhang et al. (2004) found that ratings of visual imagery vividness strongly correlated with activation levels in the right LOC during haptic shape perception. To note, while the left LOC also showed haptic shape-selective responses while stimuli were explored (or perceived) with the right hand, this haptic-related activation did not correlate with visual imagery vividness, suggesting a functional dissociation between left and right LOC. Similar results were reported by Lee Masson et al. (2016) who found that the recruitment of EVC and right, but not left, LOC during haptic shape perception with the right hand is mediated by top-down visual imagery signals. Altogether, these findings suggest that visual imagery may account for some, but not all cross-modal activations observed in visual areas. To specifically tackle the question relative to the role of visual imagery in recruiting visual areas for non-visual shape-related tasks, researchers investigated haptic shape processing in early/congenitally blind individuals. In fact, it was traditionally assumed that congenitally blind individuals cannot mentally generate a visual representation due to the lack of visual experience. With this assumption in mind, the fact that also the blind recruit visual cortical areas for haptic object processing suggested that visual object imagery cannot explain the observed results. This has been argued for haptic shape, texture, and motion processing in visual areas (see *Section 1.2.2*). For instance, LOC showed haptic shape-selective responses also in early/congenitally blind individuals (e.g., Amedi et al., 2010; Xu et al., 2023) although they cannot rely on any visual but only tactile

experience of the object. It is important to note, however, that there is compelling evidence suggesting that the congenitally blind engage in mental imagery by relying on verbal, semantic, haptic, or purely spatial (i.e., without visual content) representations, rather than visual ones, in the absence of vision (for a review, see Cattaneo et al., 2008). In addition, it was suggested that occipital areas mediate tactile imagery processes in blind individuals (Uhl et al., 1994). Therefore, we should be cautious when excluding a priori the role of any imagery processes in driving the blind's occipital cortex activation during haptic tasks.

Altogether, the pieces of evidence reported here do not provide clear answers to the question of whether imagery processes mediate the recruitment of visual areas during haptic object processing. In fact, based on the reviewed literature, it is difficult to completely rule out the role of visual and non-visual imagery in the sighted and the blind, respectively, during haptic processing without vision.

1.3.2 Multisensory object representations

In contrast to the visual imagery hypothesis, it has been proposed that the visual cortex plays a fundamental role in haptic object perception as it stores multisensory representations of object attributes like shape. In support of the existence of multisensory processing mechanisms in the occipital/occipitotemporal cortex is the evidence for perceptual interactions between touch and vision for orientation, shape, texture, and motion perception (for a review, see Sathian & Lacey, 2022).

The hypothesis of a multimodal representation of object properties is especially supported by studies employing multivariate approaches which precisely assess whether overlapping or distinct neural populations within a given area are recruited to access the same object representation through different sensory modalities, i.e., touch and vision. In fact, multi-voxel pattern analysis (MVPA), as opposed to more traditional univariate analysis, accounts for the representational content stored in brain regions rather than just activation levels elicited by

a given sensory stimulus. For instance, relative to shape, a recent study used fMRI and MVPA to characterize the brain regions implementing shape and conceptual representations of objects in blind and blindfolded sighted participants (Xu et al., 2023). Subjects heard words referring to manmade objects and were asked to focus on either their shape or function and to judge with a yes/no response a set of shape characteristics or object's functions, respectively. The authors found evidence for a supramodal shape representation in both blind and sighted participants' inferolateral occipitotemporal cortex (ILOTC), and argue against the visual imagery hypothesis. Concerning object motion, MVPA results revealed that the motion-selective visual area hMT+/V5 stores information about the direction of moving stimuli that is accessible through both touch and vision (Van Kemenade et al., 2014). This result can be taken as evidence for multimodal, visuo-tactile processing mechanisms in the visual cortex, precisely hMT+/V5. Hence, this visual area seems to play a supportive role in tactile motion perception. The authors also argue that their findings cannot be explained by visual imagery although they cannot completely rule out this possibility.

In sum, there is evidence for the existence of multisensory representations of object attributes like shape and motion in visual cortical areas. However, the evidence is not yet conclusive and more extensive research is warranted to corroborate the role of visual areas in storing shared representation of haptic object properties, especially in sighted individuals.

1.3.3 Complementary or mutually exclusive mechanisms?

More than a decade ago, a few neuroimaging findings advanced the idea that the role of visual cortical areas in haptic object processing might be explained by both visual imagery and multisensory object representations, and that these two hypotheses are not mutually exclusive (e.g., Deshpande et al., 2008; Lacey et al., 2014).

A study on effective connectivity during haptic object perception assessed whether the two hypotheses were complementary or mutually exclusive, and if so, which one was true

(Deshpande et al., 2008). The results showed that the two hypotheses were not necessarily mutually exclusive, that is they were both true though in different experimental contexts. These results were corroborated by later findings investigating the neural underpinnings of haptic shape perception of familiar and unfamiliar objects, and visual object imagery (Deshpande et al., 2010; Lacey et al., 2010). For instance, using effective and functional connectivity analyses of fMRI data, Deshpande et al. (2010) found that haptic perception of familiar shapes and visual imagery tasks recruited similar networks including connections from prefrontal cortex into LOC, while haptic perception of unfamiliar objects activated a different network consisting of inputs from the somatosensory cortex into LOC. Later, a another study further suggested that the network involved in haptic processing of unfamiliar shapes also includes spatial imagery processes supported by parietal regions including the IPS and its surrounding (Lacey et al., 2014).

Overall, these findings may support the notion of multisensory, flexible representations stored in the EVC and LOC. This is in line with the conceptual framework proposed for visual and haptic object representation which integrates both the visual (spatial and object) imagery and multisensory components of object processing (Lacey et al., 2009, 2014; Lacey & Sathian, 2014) (Fig. 2).

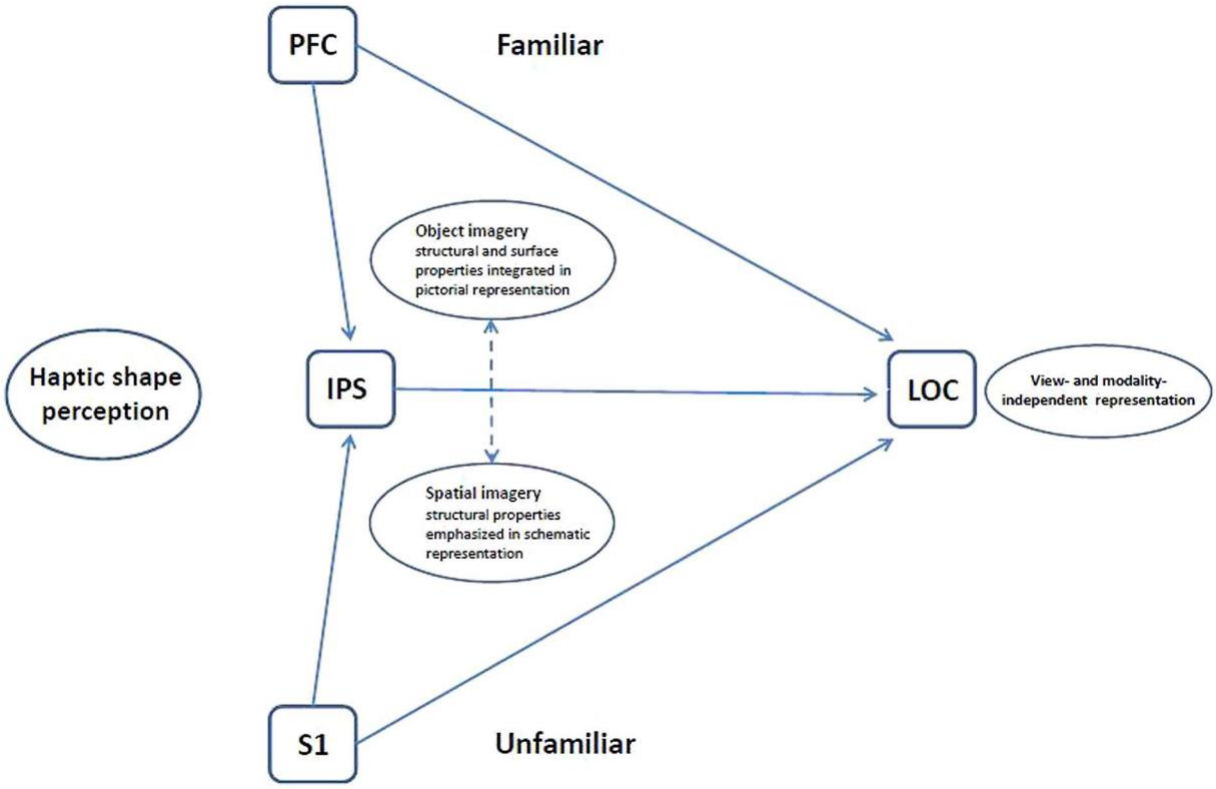

Figure 2. Model of haptic object representation in LOC with modulation of LOC activity by object familiarity and imagery type. Reproduced from Lacey & Sathian (2014). Copyright © 2014 Lacey and Sathian.

1.3.4 Functional relevance for haptic processing

The hypothesis of multisensory visuo-tactile representations of object attributes in the occipital and temporal cortices raises a critical question: does the recruitment of the visual cortex have functional behavioural relevance or is it epiphenomenal? In other words, does our behavioural performance in haptic tasks necessarily depend on haptic information processing in the visual cortex?

Lesion approaches, including irreversible (i.e., lesion studies) and reversible (i.e., non-invasive brain stimulation, NIBS) methods, are generally used to investigate the functional relevance of brain areas for specific behaviours. The case report of a congenitally blind patient revealed that, despite intact somatosensory cortex, the patient became unable to read Braille following bilateral occipital stroke and showed deficits in fine tactile spatial discrimination

while the ability to discriminate everyday objects remained intact (Hamilton et al., 2000; Merabet et al., 2004), thereby supporting the functional relevance of occipital cortex recruitment in high-level cognitive and tactile processing, at least for the visually impaired. Patient M.C. revealed preserved haptic shape recognition despite extensive bilateral occipitotemporal infarctions, suggesting that lesioned cortical visual areas are not necessary for object recognition through touch (Snow et al., 2015). Nevertheless, this finding may also indicate potential cortical reorganization, with intact areas compensating for haptic shape processing. Taken together, the two case reports apparently show divergent results relative to the functional relevance of the visual cortex for haptic processing: while the congenitally blind patient failed at fine tactile spatial discrimination, patient M.C. succeeded at haptic shape recognition. However, the observed discrepancy might reflect a task-specific role of the visual cortex for haptic processing, in as much as it may be crucial for fine, high-resolution spatial tactile tasks, but not for gross shape recognition.

To further elucidate the functional relevance of visual areas for haptic information processing, NIBS studies investigated the effects of their transient disruption on behaviour. Notably, transcranial magnetic stimulation (TMS) studies found that transient disruption of the occipital cortex impairs Braille reading and tactile discrimination in early onset blind but not sighted individuals (Cohen et al., 1997). Likewise, the study by Ptito et al. (2008) also showed that TMS applied to the occipital cortex induced tactile sensations in the early blind, but not in blindfolded sighted subjects suggesting the existence of a polysynaptic cortical pathway between the somatosensory and visual cortex through the parietal lobe which drives visual cortex responses to tactile input specifically in the blind. In addition, the reorganization of the visual cortex in the blind seems functionally relevant also for higher-level cognitive processing of tactile input (Kupers et al., 2007). Importantly, the functional relevance of the visual cortex for somatosensory processing may depend on critical developmental periods. In fact, Cohen et

al. (1999) found that while congenitally and early blind individuals showed altered behavioural performance following transient disruption of visual cortices, late-onset blind people did not, suggesting that there may be a critical period during development for repurposing of the visual cortex consequent to sensory loss.

Nevertheless, functionally relevant cross-modal recruitment of the visual cortex is not unique to blind individuals. In the sighted, TMS studies found that extrastriate visual areas are functionally relevant for the processing of specific tactile features, like orientation (Zangaladze et al., 1999) and motion (Amemiya et al., 2017). Additional evidence in the sighted shows that the visual cortex become functionally relevant for tactile processing after five days of blindfolding (Merabet et al., 2008) and following intensive training on Braille reading (Bola et al., 2017, 2019; Siuda-Krzywicka et al., 2016), suggesting the rapid unmasking of latent connections and large-scale reorganization as possible mechanisms at the basis of these cross-modal responses, respectively. In fact, nine months of Braille training in sighted adults led to anatomical and functional changes in the visual cortex, including increased connectivity to somatosensory and motor cortices (Bola et al., 2017). In addition, fMRI data showed that Braille reading activated the visual cortex and the visual word form area (VWFA), with increased resting-state functional connectivity between VWFA and somatosensory cortex. Complementarily, temporary disruption of VWFA induced by TMS impaired Braille reading accuracy. These changes suggested large-scale cortical reorganization and cross-modal plasticity resulting from long-term training can occur also in the normal, adult brain (Bola et al., 2017; Siuda-Krzywicka et al., 2016). Importantly, they also reveal that functionally specialized visual areas like the VWFA can be recruited by the somatosensory modality and be functionally relevant for the tactile task though it is not clear whether visual or tactile representations of letters mediate these results.

Overall, while findings demonstrating the functional relevance of the visual cortex for haptic processing in the blind are consistent (e.g., Cohen et al., 1997; Kupers et al., 2007), the same is not true for the sighted. In fact, while Cohen et al. (1997) found no effect of TMS disruption of the visual cortex on performance of sighted subjects in tactile tasks, other studies found functional relevance for tactile orientation and motion perception (Amemiya et al., 2017; Zangaladze et al., 1999). However, the conditions under which the cross-modal recruitment of the occipital cortex in the sighted was found to be functionally relevant vary across the literature. An increasing number of studies showing cross-modal tactile responses in visual areas of sighted subjects adopt protocols which involve temporary visual deprivation via blindfolding (e.g., Merabet et al., 2008) or intensive training on Braille reading (e.g. Siuda-Krzywicka et al., 2016) which likely induce the recruitment of latent connections or rapid cortical reorganization as previously mentioned. Conversely, Amemiya et al. (2017) and Zangaladze et al. (1999) found TMS to have an effect on tactile perception without using a sensory deprivation protocol, even though the effects were observed in specific extrastriate areas like V5/hMT+ for tactile motion perception. Therefore, it remains unclear whether the visual cortex is functionally relevant for haptic perception in sighted individuals under normal, non-deprived conditions. Exploring this is crucial to understanding whether the visual cortex functions as a metamodal processing system for spatial tasks (Pascual-Leone & Hamilton, 2001) especially in the sighted or if its engagement during haptic tasks required some type of cortical reorganization triggered by training or sensory loss.

1.4 Thesis Aim and Organization

Thus far, I have outlined two major lines of research examining the potential role of ventral stream areas and the EVC in reaching, grasping, and haptic exploration of objects, each presenting critical open questions. The first one is related to the brain areas involved in the execution of hand actions like reaching and grasping. While the scientific community agrees on the role of the dorsal visual stream in the control and guidance of immediate and delayed actions with and without visual feedback, the role of ventral visual stream areas in delayed actions without online visual feedback remains controversial due to inconsistent results across the literature. Are both streams involved in the control of reaching and grasping actions with and without visual information? Is the recruitment of the ventral pathway mediated by the availability of visual information during action execution? The second line of research is represented by studies investigating the involvement of visual cortical areas in haptic tasks in sighted individuals despite the absence of visual information. The open question is whether the underlying neural mechanisms are due to visual mental imagery processes or not. Further, is the involvement of visual areas during haptic tasks relevant for behaviour? These are some crucial aspects that still need to be clarified.

This thesis addresses these unresolved questions with three specific contributions. (i) The first contribution capitalized on coordinate-based Activation Likelihood Estimation (ALE) meta-analysis of neuroimaging studies to assess the consistency of results across the literature on the role of the ventral visual stream and the EVC, along with the dorsal stream, in the execution of reaching and grasping actions, when visual information about the target object and/or the hand is available and when it is not (Sartin et al., 2023). Lastly, based on the evidence showing higher activation for grasping than reaching in the ventral stream (Singhal et al., 2013; Monaco et al., 2017), this meta-analysis also investigated whether and where the two visual streams are differentially recruited during reaching and grasping actions. To the best of our

knowledge, this work represented the first attempt to clarify the debate on the potential involvement of occipital and temporal areas in the guidance and execution of skilled hand actions, by assessing the spatial convergence across the literature of brain areas involved in grasping and reaching with and without visual feedback. Importantly, we showed that the dorsal stream was consistently involved in both actions regardless of the availability of visual information, thereby confirming its role in the guidance and execution of skilled hand actions. As for the ventral stream, our findings revealed that it was consistently involved in the execution of these actions only with online visual input, with similar activations for grasping and reaching. Overall, this work contributes to the improvement of our knowledge on the neural basis of skilled hand actions by shedding light onto the consistent role of the ventral and dorsal stream areas in the guidance and execution of reaching and grasping actions, with and without visual input. This work has been published in Current Research in Neurobiology in 2023: Sartin, S., Ranzini, M., Scarpazza, C., & Monaco, S. (2023). Cortical areas involved in grasping and reaching actions with and without visual information: An ALE meta-analysis of neuroimaging studies. *Current Research in Neurobiology, 4*, 100070. https://doi.org/10.1016/j.crneur.2022.100070.

While the meta-analysis focused on studies that employed standard univariate analysis, more recent multivoxel pattern analyses have started to unveil representations of action-related information in the EVC despite the lack of visual information (e.g., Gallivan et al., 2019; Monaco et al., 2020). What aspects are processed in the EVC? To investigate whether patterns of activation in the visual cortex represent object properties, like size, that might be used for planning appropriate hand-object interactions, we conducted a second project.

(ii) The second contribution addresses the critical question about the potential role of the EVC in haptic object processing in sighted individuals despite the absence of online visual input by focusing on object size, an easily isolatable and manipulable object property.

Specifically, we used fMRI and MVPA to explore the neural mechanisms at the basis of haptic size processing of unseen stimuli and the role of visual imagery. To this aim, we investigated whether size information from haptic exploration and visual imagery can be decoded in early visual areas. Accurate decoding of haptic but not imagined size in EVC would suggest processing of size information acquired through motor and haptic systems via hypothetical feedback signals, thereby challenging the visual imagery hypothesis. In addition, Psychophysiological interaction analysis (PPI) allowed us to examine the task-related functional connections between the EVC and the rest of the brain. Notably, size representations were examined not only in early visual areas but also in regions of the frontal and parietal cortices, as well as in lateral occipital and temporal cortical areas. In fact, these areas may encode object properties like size that are relevant for action and/or object recognition and may therefore be involved in the processing of size information through haptic exploration and visual imagery. Overall, this work allowed us to shed light on the controversial involvement of the EVC in haptic processing and the potential role of visual imagery vs feedback mechanisms, by showing that early visual areas represent haptic, but not visually imagined size, thus indicating that haptic processing in the EVC is not the mere reflection of mental visualization during the haptic task. In addition, our results revealed overlapping but distinct haptic and imagined size representations in higher-order regions like LOtv, aIPS, pIPS, dPM, and SMA. Further, IPS and dPM also showed decoding of size across haptic and visual imagery tasks, revealing a task-independent representation of stimulus size. Interestingly, we found that V1 and OP had a stronger functional connection with aIPS and LOtv during the haptic compared to the imagery task, possibly indicating the involvement of feedback mechanisms from multisensory and associative regions. This study was presented at several National and International conferences, including the Minerva-Gentner Symposium 2022 (Perception, Recognition and Control of Goal-Directed Actions: From Cognitive to Neural Representations)

in Regensburg (Germany), the CAOs 2023 Workshop (Concepts, Actions, and Objects: Functional and Neural Perspectives) in Rovereto (Italy), the 23rd Annual Meeting of the Vision Sciences Society (VSS) 2023 in Florida (USA), and it earned the Best Abstract/Poster Award which resulted in a monetary prize and an invited oral presentation at CAOs Workshop 2025 in Rovereto (Italy). This work has been published in NeuroImage in 2026: Sartin, S., Danaj, F., Del Giudice, F., Chen, J., Schwarzkopf, D. S., Sperandio, I., & Monaco, S. (2026). Decoding haptic and imagined stimulus size in the human cortex. *NeuroImage, 121774*. https://doi.org/10.1016/j.neuroimage.2026.121774.

While haptic size information is represented in the EVC, this representation does not necessarily prove that the visual cortex is behaviourally relevant. To investigate this, we conducted the third study.

(iii) The third contribution tackles the question of the functional relevance of V1 for haptic size processing. To do so, we designed three distinct behavioural experiments requiring participants to haptically explore the size of occluded cylinders while fixating a cross on the screen, and to later report perceptual size estimates of the explored stimuli. Specifically, the first experiment investigated if and how the location of the target and the exploring hand relative to gaze direction and body midline during haptic exploration of unseen objects modulates manual size estimation. Thus, this study aimed to explore how haptic size information is processed and stored in terms of frames of reference. Furthermore, it served the purpose of defining the optimal experimental setup for two subsequent behavioural studies where we needed to isolate the potential effects of these variables from additional effects of interest. In the second experiment, we adapted a behavioural paradigm used in studies on visual perception (e.g., Fan et al., 2016) to physiologically disrupt the foveal cortex via a dynamic patch of visual noise presented in fovea, while participants encoded haptic size information of unseen stimuli. We then analysed size estimations of previously haptically explored stimuli when visual noise

was present and when it was not. This approach enabled us to test the hypothesis that if haptic information processing recruits V1 in a functionally relevant way such as to support perceptual size estimation, then the presentation of competing visual noise information should conflict with the simultaneously acquired haptic size information, thereby hampering the processing of size-related information necessary to perform the size estimation task. Finally, the third behavioural experiment aimed at assessing whether the potential effects of foveal visual noise on haptically-guided size estimation might be modulated by task difficulty which was increased by using a larger set of more closely spaced stimuli. Altogether, this contribution suggests a functional role of the EVC in haptic size processing by showing that foveal visual noise presented during haptic size exploration may influence the precision or accuracy of the subsequent perceptual size estimation, based on task demands. While these behavioural findings need to be replicated in future studies, they point toward a potentially context-dependent role for the EVC that requires further investigation. This work was presented at several National and International conferences, including the European Conference on Visual Perception (ECVP) 2022 in Nijmegen (The Netherlands), the CAOs 2024 Workshop (Concepts, Actions, and Objects: Functional and Neural Perspectives) in Rovereto (Italy), the ECVP 2024 in Aberdeen (Scotland), the 43° European Workshop on Cognitive Neuropsychology (EWCN) 2025 in Bressanone (Italy), the 25th Annual Meeting of the Vision Sciences Society (VSS) 2025 in Florida (USA).

Chapter 2

Cortical areas involved in grasping and reaching actions with and without visual information: An ALE meta-analysis of neuroimaging studies

The content of this chapter has been published as: Sartin, S., Ranzini, M., Scarpazza, C., & Monaco, S. (2023). Cortical areas involved in grasping and reaching actions with and without visual information: An ALE meta-analysis of neuroimaging studies. *Current Research in Neurobiology, 4*, 100070. https://doi.org/10.1016/j.crneur.2022.100070

Abstract

The functional specialization of the ventral stream in Perception and the dorsal stream in Action is the cornerstone of the leading model proposed by Goodale and Milner in 1992. This model is based on neuropsychological evidence and has been a matter of debate for almost three decades, during which the dual-visual stream hypothesis has received much attention, including support and criticism. The advent of functional magnetic resonance imaging (fMRI) has allowed investigating the brain areas involved in Perception and Action, and provided useful data on the functional specialization of the two streams. Research on this topic has been quite prolific, yet no meta-analysis so far has explored the spatial convergence in the involvement of the two streams in Action. The present meta-analysis (N = 53 fMRI and PET studies) was designed to reveal the specific neural activations associated with Action (i.e., grasping and reaching movements), and the extent to which visual information affects the involvement of the two streams during motor control. Our results provide a comprehensive view of the consistent and spatially convergent neural correlates of Action based on neuroimaging studies conducted over the past two decades. In particular, occipital-temporal areas showed higher activation likelihood in the Vision compared to the No vision condition, but no difference between reach and grasp actions. Frontal-parietal areas were consistently involved in both reach and grasp actions regardless of visual availability. We discuss our results in light of the well-established dual-visual stream model and frame these findings in the context of recent discoveries obtained with advanced fMRI methods, such as multivoxel pattern analysis.

keywords: meta-analysis, ventral stream, dorsal stream, grasping, reaching

2.1 Introduction

Over the last three decades, the investigation of the neuroanatomical substrates of goal-directed hand action has received increasing attention. Indeed, hand movements not only allow us to interact with our surroundings, but also enable us to satisfy our basic needs. A deep and comprehensive understanding of the neural mechanisms underlying goal-directed hand action is crucial for advancements in many research areas, such as the ever-growing field of brain-computer interfaces for individuals who have limited or no ability to perform volitional movements.

One of the most prominent theories about action and perception was put forward by Goodale and Milner in 1992 and is based on behavioural and neuropsychological findings that show a specialization of the dorsal stream in action and the ventral stream in perception (Goodale and Milner, 1992). Specifically, the original model describes the functional specialization of the parietal cortex in processing spatial information that is relevant for planning and executing action, and the temporal-occipital cortex in recognition of contents. The proposed two-visual streams model has received much interest, including support and criticism, and it has been a matter of debate for almost three decades (see Freud et al., 2016; Whitwell et al., 2014).

The advent of functional magnetic resonance imaging (fMRI) has allowed investigating the brain areas involved in action and perception and provided useful data on this topic. Despite the challenges related to studying the execution of motor actions with neuroimaging techniques, among which the confined environment of the MR and the risk of inducing motion artifacts, research on the functional specialization of the two streams has been quite prolific (e.g., Cavina-Pratesi et al., 2007; Culham et al., 2003; Króliczak et al., 2007, 2008; Singhal et al., 2013; Fiehler et al., 2011; Prado et al., 2005; Begliomini et al., 2007; Desmurget et al., 2001). Yet very little attempt has been made so far to determine the consistency in neuroimaging results

across the published studies, with only one recent study which summarizes the existing data with systematic research and a meta-analytical approach (Ranzini et al., 2022).

In addition to the specialization of the dorsal and ventral stream in action and perception, respectively, according to the dual-stream theory both streams are involved in processing vision for action, but with different purposes (Goodale and Milner, 1992; Milner and Goodale, 2008). Specifically, while the dorsal visual stream is specialized in the online control of visually-guided actions, the ventral visual stream processes short-term maintenance of the object representation in memory, and, as a consequence, it is thought to support the guidance of delayed actions in absence of online visual information (i.e. when the brief visual presentation of a stimulus and the action towards it are separated by a delay). Seminal evidence comes from neuropsychological observations of patients suffering from optic ataxia (Perenin and Vighetto, 1988), on the one side, and patients suffering from visual agnosia, on the other side (Riddoch and Humphreys, 1987). Optic ataxia is due to dorsal stream lesions and consists of a deficit in reaching towards objects in the visual periphery. Visual agnosia is caused by ventral stream lesions which impair the visual recognition of objects and shapes. Importantly, while optic ataxia patients perform more accurate actions with than without a delay (Milner et al., 1999, 2001), visual agnosia patients show the opposite pattern (Goodale et al., 1994), in line with the idea that while the dorsal stream is crucial for online control of immediate actions, the ventral stream permits maintenance of object representation in memory for delayed actions. The importance of such findings about delayed actions resides in the fact that in principle they comprise a big portion of the actions that we perform in our everyday life. For example, when we grab our car keys from a pocket or change the shift while keeping our eyes on the street, we need to retrieve information from memory about our keys and car shift as we cannot directly look at them while we plan and perform the action.

Ventral and dorsal visual streams are also differently recruited for immediate and delayed actions. Specifically, while the dorsal stream (i.e., intraparietal sulcus) plays a role in immediate and delayed actions, the ventral stream (i.e., lateral temporal-occipital cortex) might have a more prominent role in delayed actions only. In particular, neuroimaging studies showed that during delayed actions areas in the dorsal and ventral stream are re-activated when a movement is performed in absence of visual information (Himmelbach et al., 2009; Monaco et al., 2017; Singhal et al., 2013). In addition to these findings, some fMRI studies showed that the early visual cortex (EVC), on or slightly above the Calcarine sulcus, is reactivated during delayed actions in the dark (Chen et al., 2014; Monaco et al., 2017; Singhal et al., 2013). Further, transcranial magnetic stimulation (TMS) studies determined that while the dorsal stream has a causal role in performing immediate and delayed actions (Cohen et al., 2009; Smyrnis et al., 2003), the ventral stream is crucial for delayed but not immediate actions (Cohen et al., 2009).

One of the controversies about previous findings on the involvement of dorsal and ventral stream areas in goal-directed hand actions arises from the fact that not all results point to the involvement of the ventral stream and the EVC in delayed actions without online visual feedback. Indeed, some fMRI studies found reactivation in dorsal but not ventral stream areas during the execution of an action after a delay (Fiehler et al., 2011), while other studies found reactivation in the ventral stream and EVC during action execution in the dark after a delay (Chen et al., 2014; Monaco et al., 2017; Singhal et al., 2013). Further, the reactivation in visual areas for delayed actions in the dark was higher for grasping than reaching actions, perhaps because grasping requires the retrieval of more detailed information, such as size and shape, than reaching. Yet, no attempt has been made to assess the consistency of results across the literature in a systematic manner.

In this study we exploited the potential of coordinate-based Activation Likelihood Estimation (ALE) meta-analysis of neuroimaging studies (Laird et al., 2005; Turkeltaub et al., 2002), to explore the neural bases of hand reaching and grasping, performed with and without online visual feedback (i.e., after a delay following the presentation of the target object or in total darkness). We focused on studies investigating hand reaching and grasping because reach-to-grasp is probably the most representative human skilled-action, and it has been extensively investigated to test and confirm the dual-visual stream theory (Goodale and Milner, 1992). We based our literature search and article selection on a recent study by Ranzini et al. (2022), where a systematic review and meta-analysis of neuroimaging studies on the execution of reach and grasp actions has been provided for a comparison between brain areas involved in number processing and grasping and reaching actions. Meta-analytical studies have proven to be important for the assessment of consistency across neuroimaging studies (Wager et al., 2009). Indeed, they enable us to get a summary of the brain areas (i.e., activation clusters) that are active during a particular task, or involved in a cognitive domain, across all the studies published so far.

The main objective of the current study was to elucidate the brain areas consistently recruited during the execution and guidance of skilled actions, specifically hand reaching and grasping actions, when visual information of the target object and/or the hand is available, and when it is not. More specifically, the present work aimed at addressing two main aims. First, we investigated whether activation in the ventral stream and EVC is found only during the execution of actions with vision or also in complete darkness (aim 1). The former hypothesis would be expected based on the wide body of evidence showing the involvement of temporal-occipital areas in the processing of visual information ranging from simple to complex visual features. The latter hypothesis is suggested by findings that show reactivation of ventral stream areas and EVC during delayed actions performed in complete darkness after a brief presentation

of a stimulus (Singhal et al., 2013). This reactivation is likely related to memory components. To address this aim, we performed two meta-analyses, one including all the studies investigating the execution of reaching and grasping with online visual feedback, and the other one including the experiments exploring the execution of the same actions without visual feedback, and therefore relying on memory. We then directly compared (through a contrast analysis) the two sets of studies (i.e., reaching and grasping with vision vs. without vision) to identify the visual areas that show consistently higher activation for actions executed with as compared to without visual input. Given the well-known role of the ventral stream and EVC in visual perception, we expected to find it consistently activated during actions executed with online visual feedback, as the visual input of the target or the hand approaching the target are being processed (Bracci et al., 2010; Malach et al., 1995). The critical question was whether the ventral stream and early visual areas also show consistent activation during actions performed without visual feedback, given the divergent results on the involvement of ventral stream areas in delayed actions (i.e., Fiehler et al., 2011; Singhal et al., 2013). Second, we assessed whether reaching and grasping differentially recruit ventral and dorsal stream areas (aim 2). Some studies have shown that grasping elicits higher activation than reaching actions in the ventral stream and EVC (Monaco et al., 2017; Singhal et al., 2013). This might be related to the fact that grasping, but not reaching, requires detailed information about the object properties, such as size and shape, to perform an accurate movement. Although in these studies the visual component of the object is ruled out by the contrast of Grasp vs. Reach, the way in which the object is processed differs between the two actions. Indeed, grasping requires processing the object by taking into account also cognitive aspects, for instance: 1) where to place the digits on the object for accurate, stable, and comfortable grasp; 2) the size of the object; 3) the texture of the object to determine whether it is slippery. Some of these properties are known to be processed in ventral stream areas (Cant et al., 2009; Cavina-Pratesi et al., 2010a; Chouinard et

al., 2009). As such, we hypothesized consistently higher activation in ventral stream and early visual areas for grasp than reach tasks. To address this aim, we performed two meta-analyses including the experiments investigating: grasping, on one side, and reaching, on the other side. Lastly, we ran a contrast analysis between grasping and reaching (i.e., grasping vs. reaching).

2.2 Materials and methods

2.2.1 Studies selection

The procedure used for the selection of the studies is described in detail in Ranzini et al. (2022). The data associated with this study is publicly available and can be found at: https://osf.io/48w69/?view_only=633d3ad74a1346ab86b65d6766f79753.

To summarize, the literature search was conducted until December 30, 2020 (for a detailed description of the literature searching process, see PRISMA flow diagram, Annex A). To the best of our knowledge, there was no study published after this date that could be included in this meta-analysis. We identified 565 studies through a database search with Pubmed and bioRxiv on hand reaching and grasping. Further, 454 studies were identified with the use of the "related articles" function, available in the Pubmed database, and the backward and forward snowballing search strategy, i.e., reference list and citations of primary articles, reviews, and meta-analyses. This selection process led to a total of 1020 studies. After removing duplicates, a total of 954 studies were originally identified to undergo further scrutiny at a later stage.

Studies had to respect the following inclusion criteria to be included in the current meta-analysis:

- to have written the paper in the English language.
- to use a hand reaching and/or grasping task.

- to investigate brain activity during the action execution phase (i.e., studies that focused on brain activity during the planning phase were excluded). This ensured consistency across the selected studies, where the elicited activation reflected somatosensory feedback and motor outputs, which are absent during the planning phase preceding action execution. This criterion was added to the ones used in the study by Ranzini et al. (2022), where the execution as well as the planning phase preceding the movement were considered. As such, five studies were excluded from our meta-analysis (Beurze et al., 2007, 2009; Chapman et al., 2007; Chen et al., 2014; Majdandžić et al., 2007).
- to use fMRI or positron emission tomography (PET) to collect data about neural activity.
- to have conducted whole-brain analyses (e.g., studies that use a region of interest (ROI) approach were excluded, as it focuses on predefined areas of the image rather than reporting all activated clusters and could thus bias the result of the meta-analysis; Müller et al., 2018).
- to have performed univariate analyses (i.e., papers that conducted multivoxel pattern analysis (MVPA) or functional connectivity analyses were not included). It is important to note that MVPA and univariate analysis produce different types of data (i.e., percentage of classification accuracy vs. extent of activation). Therefore, the meta-analysis of multivariate data is based on values of decoding accuracies (e.g., Bhandari et al., 2018), which cannot be collapsed with univariate results. To date, the number of MVPA studies on this topic is not large enough to conduct a meta-analytic procedure (Gallivan et al., 2013, 2019; Gallivan, McLean, Valyear, et al., 2011; Gutteling et al., 2015; Monaco et al., 2019, 2020; Velji-Ibrahim et al., 2022).
- to report a contrast that shows larger activation level for reaching or grasping than the control condition, i.e., when the contrast shows activation rather than deactivation. The control condition differs from the experimental condition only in the dimension of

interest. As such, it depends on the task used in each original study. Examples of control conditions are passive viewing (look), reach, colour detection, simple fingers movement, etc.

- to report findings in either Talairach (Talairach and Tournoux, 1988) or Montreal Neurologic Institute (MNI) coordinate space (i.e., studies not reporting results in a standardized coordinate space were excluded).
- to have included only healthy adults in the experiment.
- to test a sample size of at least 5 participants.

2.2.2 Systematic review

The literature was screened in detail and the articles that met the inclusion criteria were selected in accordance with PRISMA guidelines (Moher et al., 2009) by Ranzini et al. (2022). We checked that the screening procedure was in line with the updated PRISMA guidelines that have been recently published (Page et al., 2021). In addition, we followed recent recommendations on how to conduct a proper neuroimaging meta-analysis (Müller et al., 2018). The screening procedure is described in more detail in the PRISMA flow diagram available in Annex A. For the current meta-analysis, 53 studies met the inclusion criteria reported in the previous section. The complete list of included studies is presented in Annex B.

Data were extracted from the studies and then checked. We then created a database containing the following information of the selected articles on hand reaching and grasping actions: the sample size, the percentage of females, the mean age of participants, the technique (either fMRI or PET), the experimental task (only grasp, only reach, or reach and grasp), the control task, additional information about the task and stimuli, the relevant contrast selected, the coordinate system, the coordinates of foci and their anatomical labels, the p-value criteria (corrected, uncorrected), and the related statistic (z score, t value).

In the case of multiple contrasts performed in a single study and on the same group of participants, only the most relevant one was considered (i.e., the contrast that best represents the process under investigation in the present meta-analysis). This approach ensures that there is no dependence across the activation maps of the included experiments which would instead negatively impact the validity of meta-analytic results (Müller et al., 2018). As a result of the application of this approach, we eventually selected only one contrast from each of the eligible studies, thus yielding a final list of 53 experiments (i.e., contrasts), consisting of 528 foci, included in the current meta-analysis. We then divided the studies into four categories consisting of two movements (Grasp and Reach) and two levels of visual information (Vision and No vision), as described here below.

2.2.3 Data categorization

For the purpose of the current meta-analysis, we further analysed each of the 53 studies in order to extract additional information about the experimental task and the contrast used. In fact, while Ranzini et al. (2022) performed a meta-analysis of the areas involved in grasping and reaching actions by collapsing the availability of visual information, we further categorized the 53 studies depending on the level of visual information isolated by the contrast. Further, we performed a direct comparison between grasping and reaching studies that was not performed by Ranzini et al. (2022).

Reaching tasks consisted of moving the hand towards the object with the pointing finger or the knuckles. Grasping tasks consisted of moving the hand towards the object and grasping it with a precision or a whole hand grasp. While some of the studies in this meta-analysis employed either reach or grasp tasks, others included both movement types. Some studies also included ad-hoc control conditions (i.e., passive viewing of the target object). Tasks consisting in moving the arm and hand to the target, without a grip component, were categorized as Reach. Tasks that included the grip component, with or without the movement of the arm towards the

target, were categorized as Grasp. For example, the contrasts of: (Grasp vs. Reach), and (Grasp vs. Passive viewing) were both labelled as Grasp, as they both included the grip component (note that this procedure partially differs from the one of Ranzini et al. (2022), where a distinction between reach-only, grasp-only, and reach-to-grasp studies was made).

We then assessed whether the experimental paradigm required participants to perform goal-directed hand actions in total darkness (i.e., participants could not see their moving hand or the target object; No vision condition) or in a dimly light room (i.e., participants could see their own hand moving and the target object or a visual stimulus projected onto a screen; Vision condition). For experiments performed under dim light illumination sufficient to process visual stimuli during action execution, we determined whether the contrast used in the study allowed subtracting neural activity elicited by the visual stimuli and/or the hand performing the movement. If so, we included these contrasts in the No vision condition along with the studies in which participants performed goal-directed movements in complete darkness.

As a result, we classified the selected studies into the following categories: 1) reaching experiments that isolated neural activity elicited by the somato-motor component of the reaching movement without vision (Reach No vision; number of studies (N) = 13); 2) reaching experiments in which visual information about the hand or the target was present in addition to the somato-motor component of the reaching movement (Reach Vision; N = 3); 3) grasping experiments that isolated neural activity elicited by the somato-motor component of the grasping movement without vision (Grasp No vision; N = 20); 4) grasping experiments in which vision was present in addition to the somato-motor component of the grasping movement (Grasp Vision; N = 17). The No vision category includes studies in which vision was not available during the task, as well as studies in which vision of the object was available before movement execution but was removed by the contrast used. The Vision category includes visual processing of the object, hand, or both. Specifically, there are studies where vision was

available: 1) before action execution, allowing only vision of the target (i.e., Verhagen et al., 2008); 2) during the execution of the movement, allowing vision of the target and the moving hand (i.e., Begliomini et al., 2015); and 3) throughout the movement, and the contrast used (Grasp > Reach) removed information about the object but not visual processing of the grasping hand (i.e., Cavina-Pratesi et al., 2010b). The Grasp category includes studies in which the grip component is isolated with or without the transport component. The Reach category includes studies where a grip component is not present.

Table 1 reports a summary of the studies, contrasts, and isolated components included in each category.

Table 1. Components isolated by the contrasts used in the studies included for each category in the meta-analysis.

Category in the meta-analysis	Contrasts used in the original studies	Isolated components	Studies
Grasp with Vision	(Grasp > reach) with vision or (Grasp > other grasps) with vision or Grasp with vision > look at object or Grasp with vision > fixation	Somato-motor component of the grasp (grip only, grip and transport components) And Vision of the target object and/or Vision of the moving hand	8, 11, 14, 15, 16, 19, 22, 25, 26, 27, 28, 35, 36, 38, 44, 46, 49
Grasp No vision	(Grasp > reach) with no vision or (Grasp > other grasps) with no vision or Delayed grasp > look at object	Somato-motor component of grasp	1, 5, 6, 10, 18, 20, 23, 31, 37, 39, 40, 41, 42, 43, 45, 47, 50, 51, 52, 53
Reach with Vision	Reach with vision > fixation or Reach with vision > reach with no vision	Somato-motor component of reach and Vision of the target object and/or Vision of the moving hand	3, 13, 34
Reach No vision	(Reach > other reaches) with no vision Reach with no vision > fixation (Reach > other tasks) with no vision	Somato-motor component of reach	2, 4, 7, 9, 12, 17, 21, 24, 29, 30, 32, 33, 48

Note: Numbers refer to studies reported in Annex B.

2.2.4 Activation likelihood estimation meta-analysis

We conducted a coordinate-based meta-analysis (CBMA) which uses the coordinates of activation peaks (i.e., activation foci) reported in a standardized coordinate space. We employed the ALE method (Laird et al., 2005; Turkeltaub et al., 2002) to conduct the coordinate-based meta-analysis of selected fMRI and PET experiments. In particular, the revised version of the ALE algorithm (Eickhoff et al., 2009, 2017) was run with BrainMap GingerALE software version 3.0.2 (Research Imaging Institute; http://brainmap.org/ale/). The MNI coordinates of activation peaks were converted into Talairach space before performing the meta-analysis. We transformed the coordinate space for as few studies as possible. Since more than half of the studies included in this meta-analysis (30 out of 53) reported coordinates in TAL space, we converted the MNI coordinates to TAL space.

The ALE algorithm aims at evaluating the brain areas of spatial convergence of activated foci across neuroimaging experiments using the coordinates of the peak activations extracted from individual studies. In particular, the algorithm models the reported activated foci of each experiment as three-dimensional Gaussian probability distributions. The number of participants in each experiment is considered to compute the size of the probability distributions. The uncertainty associated with the spatial location of activated foci due to between-study variances (e.g., between-subject and between-template variances; Eickhoff et al., 2009) is considered, quantified and used by the ALE algorithm to compute the width of each Gaussian distribution. The probability distributions of all activation foci extracted from an experiment are then combined voxelwise to obtain a Modelled Activation (MA) map, that is a map (i.e., 3D volume) of activation likelihood that is generated for each included experiment. For each meta-analysis, all the MA maps are combined voxelwise to create an ALE map. Each voxel of this image contains an ALE score which represents the spatial convergence of activated foci at exactly that position (Eickhoff et al., 2009). The ALE scores are then tested against a null hypothesis

according to which the concordance in spatial activation between experiments can occur by chance and is therefore random (noise; Eickhoff et al., 2016), by applying a random-effects spatial inference (i.e., random effects model) instead of a fixed-effects inference to evaluate the agreement on activation peaks across studies. The ALE algorithm uses a permutation procedure to assign each voxel a P value which stems from the probabilities of obtaining an ALE value not equal to the ALE value of the very same voxel based on the null-distribution. We employed Mango software (http://ric.uthscsa.edu/mango/), a multi-image analysis program, to visualize the results of the meta-analysis by overlaying ALE maps onto an anatomical image in Talairach space.

2.2.4.1 Single dataset and contrast analyses

We ran four single dataset and two contrast analyses to examine the areas involved in the execution of reaching and grasping movements with and without the availability of visual information. While single dataset analysis indicates the main results of the studies included in each category, the contrast analysis allows comparing results between two different categories (i.e., datasets). In order to examine which areas are consistently involved in visual and non-visual reaching and grasping actions, we performed two meta-analyses separately for each of the two visual conditions across action types: 1) Reach and Grasp Vision, and 2) Reach and Grasp No vision. Further, to investigate which areas are selectively involved in online visual processing during action execution, we performed a contrast analysis of: 3) Reach and Grasp Vision > Reach and Grasp No vision. To investigate the cortical areas specifically involved in grasping and reaching tasks, regardless of the availability of visual information, we ran two single dataset analyses for each action type (Grasp, Reach) across the two visual conditions: 4) Grasp Vision and No vision, 5) Reach Vision and No vision. Lastly, to determine which areas consistently show higher activation for grasping than reaching movements, we ran the contrast analysis of: 6) Grasp > Reach.

For the single dataset meta-analyses, all the resulting statistical ALE maps were thresholded by means of a cluster-level family-wise error (cFWE) correction at $p < 0.05$ (5,000 permutations) with a cluster-forming threshold of $p < 0.001$ (uncorrected), in line with the latest recommendations for neuroimaging meta-analyses (Müller et al., 2018).

To perform the contrast analyses, we followed the recommendation of Eickhoff et al. (2016) according to which two datasets are comparable when one is at most four times bigger than the other one (and vice versa), in terms of number of studies. Therefore, the sample size of studies included in the contrast analyses was: Reach and Grasp Vision (N = 20) vs. Reach and Grasp No vision (N = 33), and Grasp (N = 37) vs. Reach (N = 16). During the analysis, the ALE algorithm repeatedly and randomly splits the pooled list of foci into two separate sets of data while keeping their original sizes. Afterwards, an ALE map is generated for each new dataset, and one is subtracted from the other one (and vice versa); eventually, for each voxel the difference is computed between this new experimental ALE map and the original ALE map. For the current meta-analysis, the ALE algorithm used 10,000 permutations to perform the contrast analyses. The uncorrected threshold and the minimum cluster volume were set at $p < 0.05$ and to 100 mm^3, respectively.

2.3 Results

An overview of all areas involved in the execution of reaching and grasping actions, regardless of whether or not vision is available, can be found in Ranzini et al. (2022) (see in the article by Ranzini et al., 2022: Figure 2, Panel b; Figure 4, Panels a and b).

2.3.1 Meta-analytical map of Reach and Grasp Vision

The Reach and Grasp Vision ALE meta-analysis included a total of 298 subjects, and 168 foci extracted from 20 eligible experiments. Results showed five significant clusters (Fig. 1, Panel a; Table 2).

The most significant peaks of activity were located in the left precentral gyrus (cluster 1; TAL coordinates: −32, −30, 56, BA4), the right medial frontal gyrus (cluster 2; TAL coordinates: 2, −12, 50, BA6), the right cerebellar dentate (cluster 3; TAL coordinates: 16, −50, −20), the left inferior temporal gyrus (cluster 4; TAL coordinates: −44, −68, 2, BA37), and the right inferior frontal gyrus (cluster 5; TAL coordinates: 50, 6, 14, BA44). Cluster 1 (5776 mm^3) showed two activation peaks in the left hemisphere, and it extended from the postcentral gyrus (42.3% of experiments) to the precentral gyrus (38.4%), and the inferior parietal lobule (19.4%). Cluster 2 (1280 mm^3) consisted of two activation peaks, and it spanned both the left and right hemispheres (52% and 48% of experiments, respectively); more precisely, it was located in the medial frontal gyrus (BA6; 97.3%), and it spread slightly to the paracentral lobule (BA31; 2.7%). Cluster 3 (1264 mm^3) was found with one activation peak in the right cerebellar hemisphere; the cluster spanned the anterior lobe (98.7%), and slightly spread to the posterior lobe of the cerebellum (1.3%). Cluster 4 (1064 mm^3) consisted of one activation peak in the left hemisphere; it was primarily located in the inferior temporal gyrus (40.4%), the middle temporal gyrus (29.8%), and the middle occipital gyrus (29.8%). Cluster 5 (720 mm^3) was found with one activation peak in the right hemisphere; it was located mainly in the precentral gyrus (BA44; 66.7%), and the inferior frontal gyrus (BA6; 33.3%).

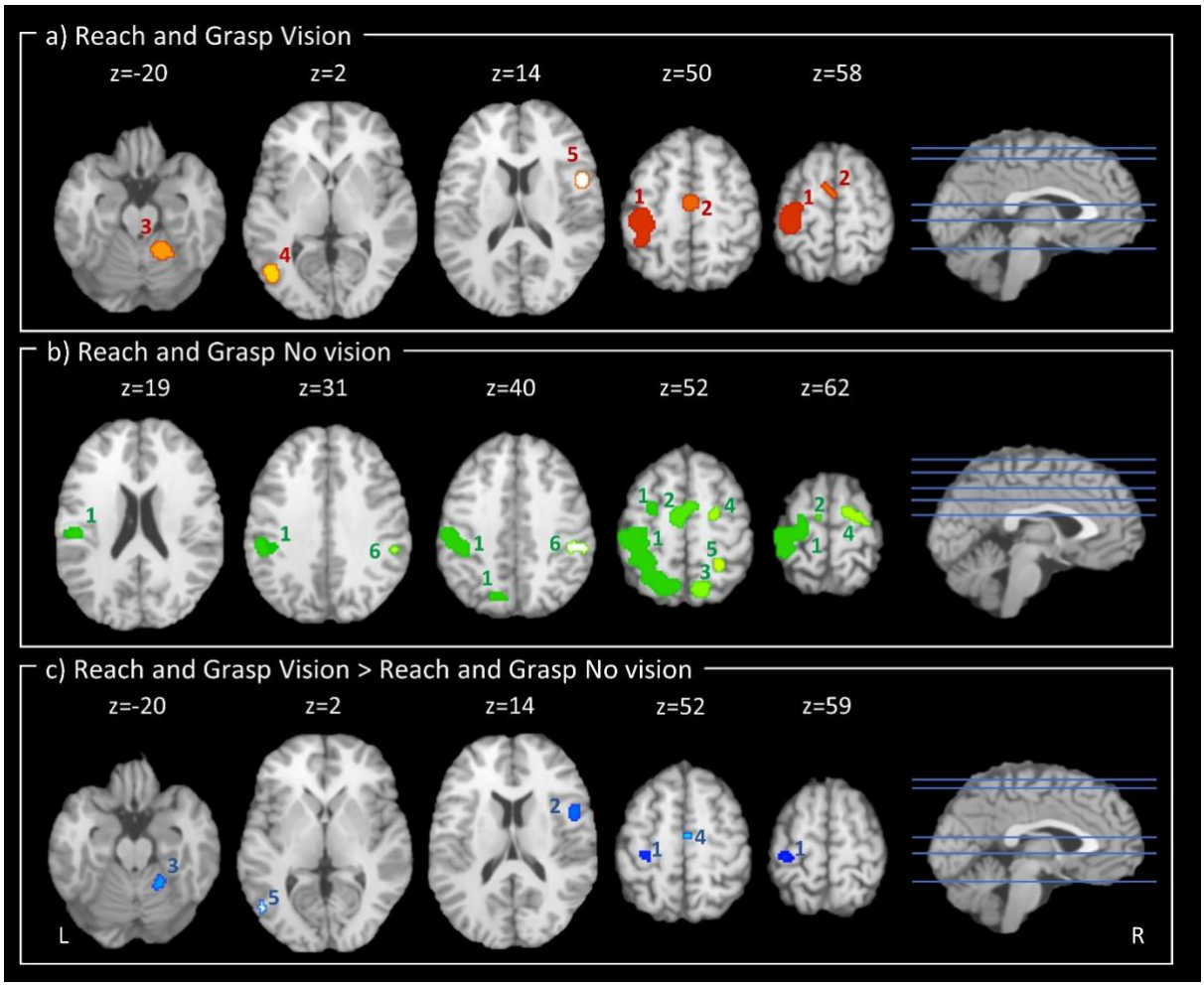

Fig 1. Schematic representation of the results for the Reach and Grasp Vision meta-analysis (Panel **a**), Reach and Grasp No vision meta-analysis (Panel **b**), and the Reach and Grasp Vision and Reach and Grasp No vision contrast analysis (i.e., Reach and Grasp Vision > Reach and Grasp No vision; Panel **c**). Results are shown in the axial view. TAL z coordinates are shown above the slices. Numbers within the slices (1–6) refer to clusters (Panel **a**: 1 = left precentral gyrus, left postcentral gyrus, left inferior parietal lobule, 2 = left and right medial frontal gyrus, 3 = right cerebellum, 4 = left middle temporal gyrus, left inferior temporal gyrus, left middle occipital gyrus, 5 = right precentral gyrus, right inferior frontal gyrus; Panel **b**: 1 = left insula, left postcentral gyrus, left inferior parietal lobule, left supramarginal gyrus, left precuneus, left precentral gyrus, left superior parietal lobule, left sub-gyral, left middle frontal gyrus, left superior frontal gyrus, 2 = left and right medial frontal gyrus, 3 = right precuneus, right superior parietal lobule, 4 = right sub-gyral, right middle frontal gyrus, right superior frontal gyrus, right precentral gyrus, 5 = right precuneus, right sub-gyral, 6 = right inferior parietal lobule, right supramarginal gyrus; Panel **c**: 1 = left precentral gyrus, left postcentral gyrus, 2 = right precentral gyrus, right inferior frontal gyrus, right insula, 3 = right cerebellum, 4 = right medial frontal gyrus, 5 = left inferior temporal gyrus, left middle occipital gyrus).

Table 2. Results of the single dataset meta-analysis on Reach and Grasp Vision. TAL: Talairach; Hemi: hemisphere; BA: Brodmann Area; Cluster size: size of clusters in mm^3.

Cluster	Cluster size	ALE value	p value	z-score	Hemi	Anatomical Labelling	BA	TAL coordinates		
								x	y	z
1	5776	0.048	<0.001	8.81	L	Precentral gyrus	4	-32	-30	56
		0.017	<0.001	4.36	L	Inferior parietal lobule	40	-38	-42	52
2	1280	0.023	<0.001	5.35	R	Medial frontal gyrus	6	2	-12	50
		0.012	<0.001	3.48	L	Medial frontal gyrus	6	-6	0	58
3	1264	0.023	<0.001	5.37	R	Cerebellum (anterior lobe, dentate)	-	16	-50	-20
4	1064	0.022	<0.001	5.32	L	Inferior temporal gyrus	37	-44	-68	2
5	720	0.019	<0.001	4.78	R	Inferior frontal gyrus	44	50	6	14

2.3.2 Meta-analytical map of Reach and Grasp No vision

The Reach and Grasp No vision ALE meta-analysis included a total of 476 subjects, and 360 foci extracted from 33 eligible experiments. Results showed six significant clusters (Fig. 1, Panel b; Table 3).

The most significant peaks of activity were located in the left postcentral gyrus (cluster 1; TAL coordinates: −34, −30, 50, BA3), the left medial frontal gyrus (cluster 2; TAL coordinates: −6, −12, 54, BA6), the right precuneus (cluster 3; TAL coordinates: 12, −68, 48, BA7), the right middle frontal gyrus (cluster 4; TAL coordinates: 22, −8, 56, BA6), the right precuneus (cluster 5; TAL coordinates: 28, −46, 46, BA7), and the right supramarginal gyrus (cluster 6; TAL coordinates: 54, −36, 36, BA40). Cluster 1 (21,288 mm^3) showed twelve activation peaks in the left hemisphere; it extended across the postcentral gyrus (32.5% of experiments), the inferior parietal lobule (18.6%), the precuneus (15.2%), the precentral gyrus

(14.6%), the superior parietal lobule (12.3%), and it slightly spread to the middle frontal gyrus (3.5%), the sub-gyral (1.7%) and the insula (1%). Cluster 2 (3536 mm^3) consisted of three activation peaks, and it spanned both the left and right hemispheres (73.5% and 26.5% of experiments, respectively); more precisely, it was located in the medial frontal gyrus (73.5%), the cingulate gyrus (25.2%), and the paracentral lobule (1.3%). Cluster 3 (2056 mm^3) had two activation peaks in the right hemisphere; the cluster was located primarily in BA7, and particularly, it spanned the precuneus (69.3%), and the superior parietal lobule (30.7%). Cluster 4 (1744 mm^3) consisted of three activation peaks in the right hemisphere; it was located in the middle frontal gyrus (54.6%), the precentral gyrus (16.7%), the superior frontal gyrus (14.8%), the sub-gyral (12%), and the medial frontal gyrus (1.9%). Cluster 5 (1664 mm^3) had one activation peak in the right BA7; in particular, it spanned the precuneus (65.3%) and the superior parietal lobule (34.7%). Cluster 6 (896 mm^3) consisted of two activation peaks in the right hemisphere; it was primarily located in the inferior parietal lobule (84.8%), and it spread slightly to the supramarginal gyrus (8.7%), and the postcentral gyrus (6.5%).

Table 3. Results of the single dataset meta-analysis on Reach and Grasp No vision. TAL: Talairach; Hemi: hemisphere; BA: Brodmann Area; Cluster size: size of clusters in mm^3.

Cluster	Cluster size	ALE value	p value	z-score	Hemi	Anatomical Labelling	BA	TAL coordinates		
								x	y	z
1	21,288	0.034	<0.001	6.25	L	Postcentral gyrus	3	-34	-30	50
		0.033	<0.001	6.08	L	Postcentral gyrus	3	-38	-26	54
		0.030	<0.001	5.75	L	Precuneus	7	-20	-62	52
		0.029	<0.001	5.59	L	Postcentral gyrus	2	-46	-26	48
		0.029	<0.001	5.55	L	Postcentral gyrus	40	-34	-34	58
		0.027	<0.001	5.34	L	Inferior parietal lobule	40	-36	-40	56
		0.024	<0.001	4.91	L	Superior parietal lobule	7	-28	-58	54

		0.023	<0.001	4.81	L	Precentral gyrus	4	-22	-24	62
		0.023	<0.001	4.70	L	Superior parietal lobule	7	-10	-64	54
		0.021	<0.001	4.39	L	Sub-gyral	6	-24	-6	56
		0.020	<0.001	4.31	L	Inferior parietal lobule	40	-42	-34	36
		0.019	<0.001	4.21	L	Postcentral gyrus	40	-52	-24	22
2	3536	0.029	<0.001	5.65	L	Medial frontal gyrus	6	-6	-12	54
		0.020	<0.001	4.33	R	Medial frontal gyrus	6	6	-2	48
		0.020	<0.001	4.24	R	Medial frontal gyrus	6	2	-4	48
3	2056	0.030	<0.001	5.80	R	Precuneus	7	12	-68	48
		0.015	<0.001	3.47	R	Superior parietal lobule	7	22	-60	56
4	1744	0.019	<0.001	4.14	R	Middle frontal gyrus	6	22	-8	56
		0.018	<0.001	4.00	R	Superior frontal gyrus	6	16	-8	62
		0.016	<0.001	3.56	R	Precentral gyrus	6	30	-16	60
5	1664	0.025	<0.001	5.07	R	Precuneus	7	28	-46	46
6	896	0.020	<0.001	4.24	R	Supramarginal gyrus	40	54	-36	36
		0.017	<0.001	3.78	R	Inferior parietal lobule	40	44	-34	40

2.3.3 Contrast: Reach and Grasp Vision > No vision

The contrast meta-analysis (Reach and Grasp Vision > Reach and Grasp No vision) pooled data from a total of 528 foci, extracted from an overall group of 53 experiments and 774 participants (Reach and Grasp Vision: 168 foci, 20 experiments, 298 subjects; Reaching and Grasp No vision: 360 foci, 33 experiments, 476 subjects). The analysis revealed five significant ALE clusters. The results are represented in Fig. 1 (Panel c); for more details, see Table 4.

The most significant peaks of activation were found in the left precentral gyrus (cluster 1; TAL coordinates: −31, −28, 55, BA4), the right precentral gyrus (cluster 2; TAL coordinates:

49, 2, 12, BA44), the culmen of the right cerebellum (cluster 3; TAL coordinates: 22, −48, −22), the right medial frontal gyrus (cluster 4; TAL coordinates: 4, −14, 54, BA6), and the left inferior temporal gyrus (cluster 5; TAL coordinates: −48, −70, 2). Cluster 1 (648 mm^3) was found with one peak in the left hemisphere, and it was located in the precentral gyrus (BA4; 58%), and the postcentral gyrus (BA3; 42%). Cluster 2 (576 mm^3) consisted of three peaks of activation in the right hemisphere, and it was mainly located in the precentral gyrus (BA44), and the inferior frontal gyrus (BA44). Cluster 3 (344 mm^3) showed one activation peak in the right cerebellar hemisphere; it was located in the cerebellar culmen (88.4%), and slightly extended into the cerebellar dentate nucleus (11.6%). Cluster 4 (128 mm^3) revealed one activation peak in the right hemisphere, and it was located in the medial frontal gyrus (BA6; 100%). Cluster 5 (112 mm^3) showed one activation peak in the left hemisphere; it was located in the inferior temporal gyrus (61.5%), the middle occipital gyrus (30.8%), and the middle temporal gyrus (7.7%).

Table 4. Results of the contrast analysis (Reach and Grasp Vision > No vision). TAL: Talairach; Hemi: hemisphere; BA: Brodmann Area; Cluster size: size of clusters in mm^3.

Cluster	**Cluster size**	**p value**	**z-score**	**Hemi**	**Anatomical Labelling**	**BA**	**TAL coordinates**		
							x	y	z
1	648	0.002	2.83	L	Precentral gyrus	4	-31	-28	55
2	576	0.014	2.19	R	Precentral gyrus	44	49	2	12
		0.016	2.16	R	Precentral gyrus	44	47.8	6.5	11.8
		0.016	2.13	R	Inferior frontal gyrus	44	48	6	18
3	344	0.010	2.31	R	Cerebellum (anterior lobe; culmen)	-	22	-48	-22
4	128	0.033	1.85	R	Medial frontal gyrus	6	4	-14	54
5	112	0.030	1.88	L	Inferior temporal gyrus	-	-48	-70	2

2.3.4 Meta-analytical map of Grasp

The Grasp ALE meta-analysis included a total of 563 subjects, and 294 foci extracted from 37 eligible experiments. Results showed five significant clusters (Fig. 2, Panel a; Table 5).

The most significant peaks of activity were located in the left postcentral gyrus (cluster 1; TAL coordinates: −34, −30, 56, BA3), the right cerebellar dentate (cluster 2; TAL coordinates: 16, −50, −20), the left medial frontal gyrus (cluster 3; TAL coordinates: 0, −10, 52, BA6), the right precentral gyrus (cluster 4; TAL coordinates: 36, −26, 48, BA3), and the left inferior temporal gyrus (cluster 5; TAL coordinates: −44, −66, 2, BA37). Cluster 1 (12,528 mm^3) showed six significant activation peaks in the left hemisphere; it was located in the postcentral gyrus (46.7% of experiments), the inferior parietal lobule (27.5%), the precentral gyrus (22.7%), and the superior parietal lobule (1.9%). Cluster 2 (2200 mm^3) consisted of one peak of significant activation in the right cerebellar hemisphere; the cluster was mainly located in the anterior lobe of the cerebellum (96.7%) and only slightly spread to the posterior lobe (3.3%). Cluster 3 (2024 mm^3) was found with one peak of activation in both the left and right hemispheres (76.9% and 23.1%, respectively); the cluster was located primarily in the medial frontal gyrus (BA6; 98.5%) and activation also spread slightly to the paracentral lobule (BA31; 1.5%). Cluster 4 (1352 mm^3) consisted of two activation peaks in the right hemisphere; it was located in the postcentral gyrus (73.3%), the precentral gyrus (25.6%), and activation also spread slightly to the inferior parietal lobule (1.2%) Cluster 5 (1104 mm^3) was found with two peaks in the left hemisphere; it was located in the inferior temporal gyrus (45%), the middle temporal gyrus (27.5%), the middle occipital gyrus (20%), the fusiform gyrus (5%), and the inferior occipital gyrus (2.5%).

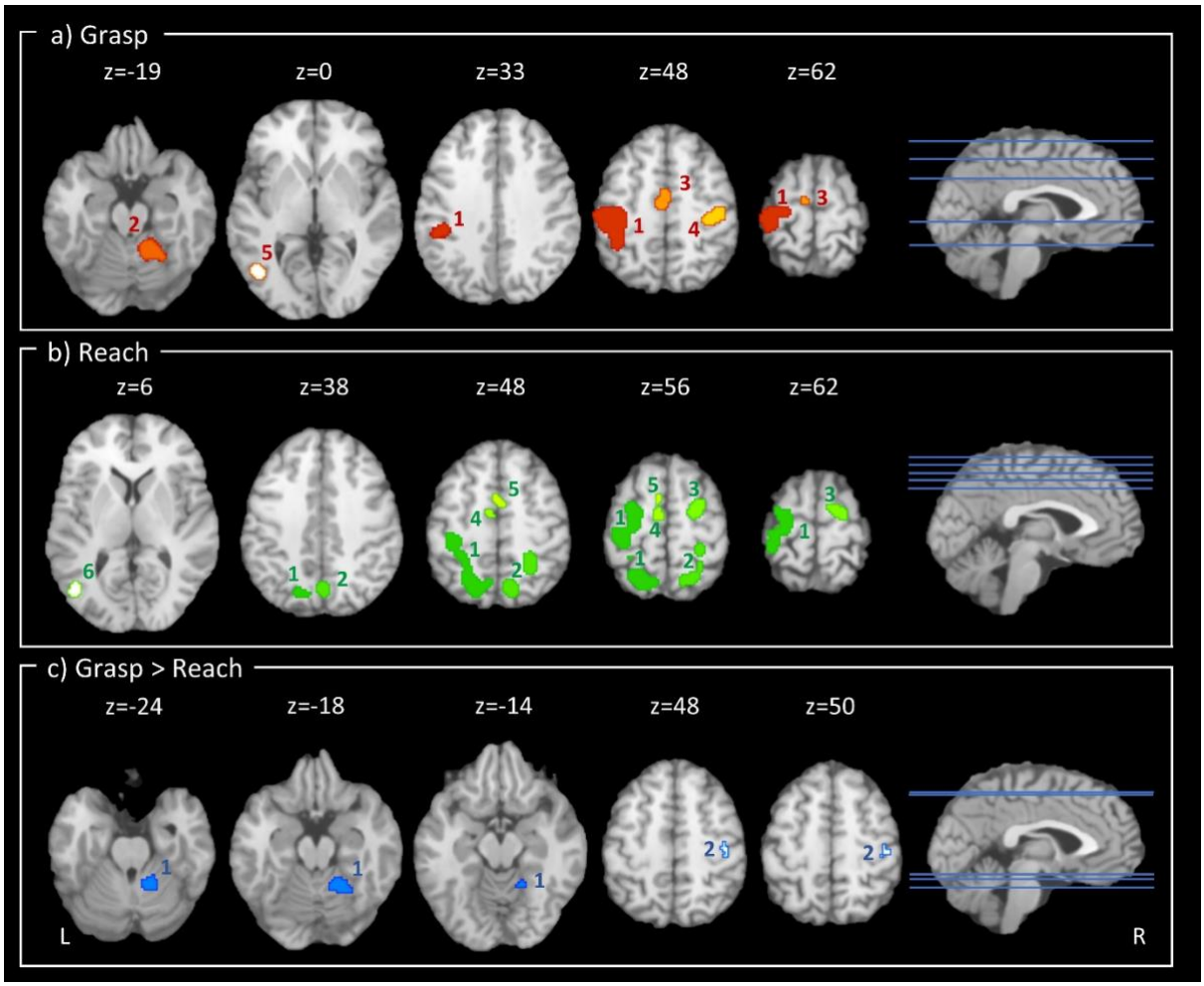

Fig. 2. Schematic representation of the results for the Grasp meta-analysis (Panel **a**), the Reach meta-analysis (Panel **b**), and the Grasp and Reach contrast analysis (i.e., Grasp > Reach; Panel **c**). Results are shown in the axial view. TAL z coordinates are shown above the slices. Numbers within the slices (1–6) refer to clusters (Panel **a**: 1 = left precentral gyrus, left postcentral gyrus, left inferior parietal lobule, left supramarginal gyrus, 2 = right cerebellum, 3 = left and right medial frontal gyrus, left and right paracentral lobule, 4 = right precentral gyrus, right postcentral gyrus, 5 = left Inferior temporal gyrus, left inferior occipital gyrus, left middle occipital gyrus, left middle temporal gyrus, 6 = right precentral gyrus, right inferior frontal gyrus; Panel **b**: 1 = left precuneus, left inferior and superior parietal lobule, left precentral and postcentral gyrus, left sub-gyral, left paracentral lobule, left middle frontal gyrus, left superior frontal gyrus, 2 = left and right precuneus, right superior and inferior parietal lobule, right sub-gyral, right paracentral lobule, right postcentral gyrus, 3 = right middle frontal gyrus, right sub-gyral, right superior frontal gyrus, right middle frontal gyrus, right precentral gyrus, 4 = left medial frontal gyrus, 5 = left and right cingulate gyrus, left and right medial frontal gyrus, 6 = left middle occipital gyrus, left middle temporal gyrus; Panel **c**: 1 = right cerebellum, 2 = right postcentral gyrus).

Table 5. Results of the single dataset meta-analysis on Grasp. TAL: Talairach; Hemi: hemisphere; BA: Brodmann Area; Cluster size: size of clusters in mm^3.

Cluster	Cluster size	ALE value	p value	z-score	Hemi	Anatomical Labeling	BA	TAL coordinates		
								x	y	z
1	12,528	0.051	<0.001	8.35	L	Postcentral gyrus	3	-34	-30	56
		0.038	<0.001	6.89	L	Postcentral gyrus	2	-42	-28	50
		0.038	<0.001	6.78	L	Inferior parietal lobule	40	-36	-40	54
		0.023	<0.001	4.79	L	Inferior parietal lobule	40	-40	-36	36
		0.017	<0.001	3.87	L	Precentral gyrus	6	-18	-18	66
		0.015	<0.001	3.65	L	Superior parietal lobule	7	-30	-56	54
2	2200	0.034	<0.001	6.37	R	Cerebellum (anterior lobe; dentate)	-	16	-50	-20
3	2024	0.025	<0.001	5.14	L	Medial frontal gyrus	6	0	-10	52
4	1352	0.021	<0.001	4.53	R	Precentral gyrus	3	36	-26	48
		0.021	<0.001	4.50	R	Postcentral gyrus	3	42	-22	48
5	1104	0.024	<0.001	4.96	L	Inferior temporal gyrus	37	-44	-66	2
		0.015	<0.001	3.65	L	Fusiform gyrus	19	-42	-70	-10

2.3.5 Meta-analytical map of Reach

The Reach ALE meta-analysis included a total of 211 subjects, and 234 foci extracted from 16 eligible experiments. Results showed six significant clusters (Fig. 2, Panel b; Table 6).

The most significant peaks of activity were located in the left precuneus (cluster 1; TAL coordinates: −20, −62, 52, BA7), the right precuneus (cluster 2; TAL coordinates: 26, −46, 46,

BA7), the right sub-gyral (cluster 3; TAL coordinates: 26, −4, 54, BA6), the left medial frontal gyrus (cluster 4; TAL coordinates: −4, −12, 52, BA6; cluster 5; TAL coordinates: −4, 4, 52, BA6), and the middle temporal gyrus (cluster 6; TAL coordinates: −44, −70, 6, BA37). Cluster 1 (12,320 mm^3) showed eight peaks of activity in the left hemisphere; it was located in the precuneus (29.1% of experiments), the precentral gyrus (19%), the postcentral gyrus (18.4%), the superior parietal lobule (18.2%), the middle frontal gyrus (10.8%), the sub-gyral (2.7%), and the inferior parietal lobule (1.7%). Cluster 2 (5088 mm^3) consisted of six activation peaks, and it spanned primarily the right hemisphere (96.6%) and, to a lesser extent, the left hemisphere (3.4%); more precisely, it was located in the precuneus (59.9%), the superior parietal lobule (24.1%), the sub-gyral (7.6%), the postcentral gyrus (6.3%), and the cuneus (1.3%). Cluster 3 (2144 mm^3) was found with two activation peaks in the right hemisphere, particularly in BA6; the cluster spanned the middle frontal gyrus (55.3%), the superior frontal gyrus (22%), the sub-gyral (14.6%), the precentral gyrus (5.7%), and the medial frontal gyrus (2.4%). Cluster 4 (928 mm^3) consisted of two activation peaks in the left hemisphere; it was primarily located in the medial frontal gyrus (BA6; 82.9%), and the cingulate gyrus (BA24, BA31; 17.1%). Cluster 5 (864 mm^3) was found with three activation peaks in both the right and left hemispheres (50.9% and 49.1%, respectively). The latter cluster was located mainly in the medial frontal gyrus (79.2%), and activity also spread slightly to the superior frontal gyrus (13.2%), and the cingulate gyrus (7.5%). Cluster 6 (624 mm^3) showed one activation peak in the left hemisphere; it was located in the middle occipital gyrus (58.8%), the middle temporal gyrus (32.4%), and the inferior temporal gyrus (8.8%).

Table 6. Results of the single dataset meta-analysis on Reach. TAL: Talairach; Hemi: hemisphere; BA: Brodmann Area; Cluster size: size of clusters in mm^3.

Cluster	Cluster size	ALE value	p value	z-score	Hemi	Anatomical Labeling	BA	TAL coordinates		
								x	y	z
1	12,320	0.031	<0.001	6.53	L	Precuneus	7	-20	-62	52
		0.024	<0.001	5.42	L	Postcentral gyrus	3	-34	-30	54
		0.021	<0.001	5.01	L	Middle frontal gyrus	6	-22	-10	58
		0.018	<0.001	4.49	L	Sub-gyral	40	-26	-44	52
		0.018	<0.001	4.38	L	Precuneus	7	-8	-64	52
		0.016	<0.001	4.08	L	Precentral gyrus	6	-24	-18	58
		0.013	<0.001	3.45	L	Inferior parietal lobule	40	-34	-46	40
		0.012	<0.001	3.33	L	Superior parietal lobule	7	-26	-56	42
2	5088	0.022	<0.001	5.09	R	Precuneus	7	26	-46	46
		0.020	<0.001	4.75	R	Precuneus	7	12	-70	48
		0.017	<0.001	4.26	R	Superior parietal lobule	7	20	-60	56
		0.017	<0.001	4.25	R	Precuneus	7	2	-68	38
		0.014	<0.001	3.71	R	Postcentral gyrus	40	28	-36	56
		0.011	<0.001	3.18	R	Cuneus	19	4	-78	36
3	2144	0.022	<0.001	5.08	R	Sub-gyral	6	26	-4	54
		0.017	<0.001	4.29	R	Superior frontal gyrus	6	16	-8	64
4	928	0.019	<0.001	4.72	L	Medial frontal gyrus	6	-4	-12	52
		0.012	<0.001	3.44	L	Cingulate gyrus	24	-10	-6	44
5	864	0.013	<0.001	3.53	L	Medial frontal gyrus	6	-4	4	52
		0.013	<0.001	3.50	R	Medial frontal gyrus	6	6	-4	52
		0.012	<0.001	3.36	L	Medial frontal gyrus	6	-6	0	58
6	624	0.019	<0.001	4.65	L	Middle temporal gyrus	37	-44	-70	6

2.3.6 Contrast: Grasp > Reach

The contrast ALE meta-analysis (Grasp > Reach) included a total of 774 participants and 528 foci, extracted from an overall group of 53 experiments (Grasp: 294 foci, 37 experiments, 563 subjects; Reach: 234 foci, 16 experiments, 211 subjects). The analysis revealed two significant ALE clusters for activation. The results are represented in Fig. 2, Panel c; for more details, see Table 7.

The most significant peaks of activation were found in the right cerebellar dentate nucleus (cluster 1; TAL coordinates: 16.8, −51.2, −24.8), and in the right postcentral gyrus (cluster 2; TAL coordinates: 44, −24, 52, BA3). Cluster 1 (1488 mm^3) was found with five peaks in the right cerebellum; this cluster was located in the anterior lobe (97.8%) and activation spread slightly into the posterior lobe (2.2%) of the cerebellum. Cluster 2 (184 mm^3) consisted of two peaks of activation in the right hemisphere, and it was primarily located in the parietal lobe, more specifically in the postcentral gyrus (BA3; 100%).

Table 7. Results of the contrast analysis (Grasp > Reach). TAL: Talairach; Hemi: hemisphere; BA: Brodmann Area; Cluster size: size of clusters in mm^3.

Cluster	Cluster size	p value	z-score	Hemi	Anatomical Labeling	BA	TAL coordinates		
							x	y	z
1	1488	0.010	2.34	R	Cerebellum (anterior lobe; dentate)	-	16.8	-51.2	-24.8
		0.015	2.16	R	Cerebellum (anterior lobe)	-	20	-48	-24
		0.017	2.13	R	Cerebellum (anterior lobe; culmen)	-	24	-53	-22
		0.017	2.13	R	Cerebellum (anterior lobe; culmen)	-	28	-54	-18
		0.017	2.12	R	Cerebellum (anterior lobe; culmen)	-	22.2	-50.9	-16.7

2	184	0.033	1.85	R	Postcentral gyrus	3	44	-24	52
		0.037	1.78	R	Postcentral gyrus	3	40	-20	48

2.4 General discussion

In the present study we conducted a coordinate-based meta-analysis to investigate the brain areas consistently recruited during hand reaching and grasping with and without online visual feedback, with a focus on ventral stream and early visual areas. As for the dorsal stream, we found that it was consistently involved in grasping as well as reaching actions, regardless of the availability of visual information. This is in line with the dual-stream theory, postulating that the dorsal stream is involved in the execution of reach and grasp actions. As for the ventral stream, we found that it was involved in actions executed with but not without online visual feedback. Specifically, the temporal-occipital cortex showed higher activation likelihood for the Vision than No vision condition. In addition, the ventral stream showed comparable activation likelihood for grasping and reaching actions. Below, we discuss the main findings of the present meta-analysis and the potential functional role of ventral stream areas in action guidance and execution.

2.4.1 Processing of visual information during goal-directed hand actions

The two single-dataset meta-analyses on actions with and without vision, and the contrast analysis between Vision and No vision enabled us to examine the role of vision in temporal-occipital areas during action execution (aim 1).

The meta-analytical map on hand reaching and grasping with vision (Fig. 1, Panel a) revealed consistent activation across the studies in frontal, parietal, and right cerebellar regions, as well as in the occipito-temporal cortex. These findings are expected given the known role of

the dorsal stream in action and the ventral stream in perception. Indeed, the inferior temporal gyrus (ITG) and the lateral occipital cortices are known to be involved in visual perception and recognition of object categories and body parts, including the hand (Bracci et al., 2010; Herath et al., 2001; Ishai et al., 1999; Malach et al., 1995; for reviews see Grill-Spector, 2003; Grill-Spector and Weiner, 2014). Similarly, the posterior areas of the middle temporal gyrus (MTG) process category and motion-related information (Chao et al., 1999). These results are consistent with the fact that in the selected Vision conditions participants viewed the target and their moving hand while approaching the target.

As for actions performed without online visual feedback, the meta-analytical map showed significant activation in six cortical clusters covering both the left and right hemispheres; specifically, they included parietal areas, such as bilateral inferior parietal lobule (IPL), precuneus, superior parietal lobule (SPL), and left postcentral gyrus (PoCG), and frontal areas like bilateral precentral gyrus (PreCG), middle frontal gyrus (MFG), superior frontal gyrus (SFG), and left insula. The clusters in the posterior parietal cortex for the No vision category are likely related to motor planning and reliance on somatosensory feedback. Another possible and non-exclusive interpretation is related to the recruitment of working memory mechanisms in the parietal cortex that support the guidance of actions in absence of visual information (Bettencourt and Xu, 2016; Fiehler et al., 2011). Importantly, no cluster was found in the ventral visual stream (Fig. 1, Panel b). Therefore, despite some evidence supporting the involvement of the ventral stream in goal-directed actions performed in the dark after a delay (Monaco et al., 2017; Singhal et al., 2013), there is no consistency in support of the recruitment of ventral visual stream areas during the control and execution of skilled actions in the absence of visual input. In line with this result, the contrast analysis did not reveal any cluster in the temporal-occipital cortex (Fig. 1, Panel c). Interestingly, the contrast did reveal clusters of activation spanning the left PreCG and PoCG, two clusters in the right hemisphere located

mainly in frontal areas, such as PreCG, inferior and middle frontal gyrus (IFG and MFG, respectively), and an additional cluster in the anterior lobe of the right cerebellar hemisphere. Therefore, these areas are more engaged when visual information is available as opposed to when it is not. The higher consistency in brain activation for Vision than No vision in motor-related areas is in line with a seminal neurophysiology study in primates by Graziano et al. (1997), which demonstrated the presence of bimodal visual and tactile neurons in macaques' ventral premotor cortex, typically known to be involved in motor control. Our results suggest that bimodal neurons might also be present in humans' premotor cortex, which is recruited by vision of a target to be acted upon that requires the processing of affordances and spatial information for accurate action performance.

We found no activation cluster in the EVC for Vision and No vision conditions. The lack of activation clusters in the EVC in the Vision condition can be explained by the fact that some of the studies included in the Vision condition used a contrast of Grasp > Look. Therefore, the visual processing of the object was removed by the contrast. Since in such tasks vision of the hand was available throughout the movement, we included these studies in the Vision condition. However, the inclusion of contrasts subtracting some activity related to visual processing might have reduced the sensitivity to detect activation in early visual areas. Also, while univariate analysis might lack the sensitivity to reveal activation in ventral stream areas and EVC under lack of vision, recent MVPA studies have shown different representations for grasping and reaching action planning with and without visual information in ventral stream and early visual areas (Monaco et al., 2019, 2020; Velji-Ibrahim et al., 2022; Gallivan et al., 2013, 2019). This difference in results indicates that univariate and multivariate analysis provide complementary and not necessarily equivalent information, with MVPA being more sensitive to distributed representation of information of content, and univariate analysis that shows more sensitivity to

the overall engagement in a task (Coutanche, 2013; Davis et al., 2014; Jimura and Poldrack, 2012).

Overall, these results indicate the consistent involvement of the parietal and frontal cortex in the execution of grasping and reaching actions regardless of the availability of visual information, while the temporal-occipital cortex is recruited only when vision is available. Notably, the same frontal and parietal areas have been recently shown to process magnitude representations (Cona et al., 2021). Consistently, grasping and reaching actions require the processing of space-related magnitude information, such as the location of the target in space for reaching, as well as its size for grasping.

2.4.2 Processing of grasping and reaching

The second aim of the current study was to assess whether ventral and dorsal stream areas are differentially recruited during the execution of reaching and grasping (aim 2).

The meta-analytical map of hand grasping revealed consistent activation clusters in the frontal and parietal cortex, as well as in the anterior lobe of the right cerebellar hemisphere (Fig. 2, Panel a). Moreover, a significant cluster of activation was located in the left inferior temporal cortex, more precisely in the ITG, and the fusiform gyrus. The inferior temporal cortex, including the ITG, plays a well-known role in the visual perception and recognition of objects, scenes, and hands (Bracci et al., 2010; Grill-Spector and Weiner, 2014; Kanwisher, 2010; Malach et al., 1995) and it has been shown that the fusiform gyrus might store semantic information about the object shape (Chao et al., 1999; see also Sakreida et al., 2016). Therefore, neural activation in these areas might underpin the visual processing of object properties and semantic representation during grasping actions.

Similarly, the meta-analytical map of hand reaching revealed five cortical clusters covering both hemispheres (Fig. 2, Panel b). Specifically, a network of frontal, parietal, and temporal-occipital regions was consistently activated across the literature. Moreover, the

network for reaching appeared more bilateral than the one for grasping, in line with previous findings that show a lateralization of the activation for grasping movements (Blangero et al., 2009; Ranzini et al., 2022).

Although we initially hypothesized that the ventral stream may show more clusters of activation for grasping than reaching, the results of our contrast do not support our hypothesis. Indeed, no temporal-occipital area was found in the meta-analytical contrast of Grasp vs. Reach (Fig. 2, Panel c). A possible explanation is related to the fact that the single dataset analyses for grasping and reaching showed similar results. This could be due to the inclusion of tasks that isolated the grip as well as the transport component (12 out of 37 studies) in our Grasp category. Further, the anterior intraparietal sulcus (aIPS), typically known to be involved in grasping actions, does not show any activation cluster with the contrast of Grasp vs. Reach. This (lack of) finding can be explained by the fact that the aIPS is sensitive to the precision required by a grasping movement, rather than the number of digits or lift component (Cavina-Pratesi et al., 2018). Part of the studies included in our Grasp category have contrasted between types of grasps that required different hand configurations but the same precision (e.g., gentle precision grip vs. firm precision grip, Kuhtz-Buschbeck et al., 2001). Overall, these meta-analyses revealed that reaching and grasping under the two visual conditions recruited similar networks that span the temporal-occipital and frontal-parietal cortex. Indeed, the contrast analysis showed only a few clusters in the right cerebellum and precentral gyrus, likely related to the finer motor control of the fingers during a grasping as compared to a reaching movement. The right lateralization of the post-central gyrus for the contrast of Grasp vs. Reach is unexpected and could be due to the use of grasp tasks that required moving the left hand (Begliomini et al., 2015; Gallivan, McLean, and Culham, 2011; Ward and Frackowiak, 2003).

2.4.3 Strengths and limitations of the study

The present meta-analysis has important strengths, as it is the first work to define the consistency across neuroimaging studies on goal-directed hand actions with and without online visual information over the last two decades. In addition, this study provides a further confirmation of the brain areas involved in the control of skilled actions (Culham et al., 2006; Gallivan and Culham, 2015; for additional meta-analytical results, see also Ranzini et al., 2022). Furthermore, we provide an overview of the areas recruited while reaching out and grasping objects, with and without online visual feedback. This aspect is of particular importance. Indeed, despite the consensus in the literature on the involvement of the frontal and parietal cortex in the guidance of reaching and grasping, there is compelling evidence suggesting that also the temporal-occipital cortex might play a role (e.g., Cohen et al., 2009; Milner and Goodale, 2008; Monaco et al., 2017; Singhal et al., 2013), especially in recent neuroimaging studies that have employed multivariate analysis which allows identifying representations rather than extent of activation (Gallivan et al., 2013, 2019; Gutteling et al., 2015; Monaco et al., 2019, 2020; Velji-Ibrahim et al., 2022). Therefore, our meta-analysis attempted to clarify the debate on the potential involvement of the temporal-occipital cortex in the guidance of skilled actions as investigated with univariate analysis.

There are also some limitations to our work. One of them consists in the fact that half of the experiments categorized as Grasp Vision used a contrast that included visual processing elicited by the view of the reaching limb and grasping hand (i.e., Grasp > Look) or view of the grasping hand only (i.e., Grasp > Reach, Grasp > Point, Grasp > Touch, Grasp > Different grasp). However, this fine-grained categorization might have hampered the possibility to find consistent activation in brain areas associated with visual processing during action execution in presence of vision. As a consequence, it might have likely hindered the contrast analysis

between the two vision conditions (i.e., Reach and Grasp Vision > No vision) which did not show any significant cluster of activation associated with visual processing in the EVC.

2.5 Conclusion

To the best of our knowledge, this coordinate-based meta-analysis is the first attempt to investigate spatial convergence across the available literature in relation to the involvement of temporal-occipital and frontal-parietal cortex in reaching and grasping actions performed with and without online visual feedback. Our findings reconcile the existing neuroimaging literature on actions that employed standard univariate analysis, by emphasizing the complementary role of more recent techniques, such as multivoxel pattern analysis, to the current knowledge on cortical areas involved in hand movements.

Chapter 3

Decoding haptic and imagined stimulus size in the human cortex

The content of this chapter has been published as: Sartin, S., Danaj, F., Del Giudice, F., Chen, J., Schwarzkopf, D. S., Sperandio, I., & Monaco, S. (2026). Decoding haptic and imagined stimulus size in the human cortex. *NeuroImage*, 121774. https://doi.org/10.1016/j.neuroimage.2026.121774

Abstract

Human neuroimaging studies indicate that the early visual cortex (EVC), including the primary visual cortex (V1), is involved in haptic exploration of objects, even when visual information is not available. However, it remains unknown whether the features of haptically explored objects, like size, are represented in the EVC. Here, we investigated whether we can use the activity patterns in the EVC and other task-relevant brain regions to decode stimulus size during haptic exploration, and whether this effect is due to visual imagery. Twenty-five right-handed participants haptically explored or imagined the size of three rings (small, medium, large) in a slow-event-related fMRI study. Participants were blindfolded during the training and fMRI sessions. Using multivariate pattern analysis, we found that V1 and the occipital pole (OP) showed accurate decoding of stimulus size during haptic exploration, but not imagery trials. This suggests that the activity patterns observed in the haptic condition cannot be explained by visual imagery. Frontal and parietal regions, as well as the multisensory lateral occipital tactile-visual area (LOtv), showed accurate size decoding during both haptic and imagery conditions, suggesting a flexible representation of stimulus size that adapts to task demands. In addition, stimulus size could be decoded across tasks in the anterior and posterior intraparietal sulcus (aIPS, pIPS), and dorsal premotor cortex (dPM). Psychophysiological interaction analysis indicated that V1 and OP showed stronger functional connectivity with ventral and dorsal visual stream areas during the haptic as compared to the imagery task. Overall, stimulus size information is similarly represented in frontal and parietal cortices across haptic exploration and imagery, but not in early visual areas, demonstrating that only regions specialized for haptic exploration and imagery support generalized size representations.

keywords: size, haptic exploration, visual imagery, early visual cortex, functional magnetic resonance imaging (fMRI), multivoxel pattern analysis (MVPA), psychophysiological interactions

3.1 Introduction

To make sense of the outside world, our brain constantly processes and filters incoming sensory information. Although our understanding of how this occurs in the visual domain has advanced considerably, much remains to be learned about the neural mechanisms that enable object recognition when sensory information is gained solely through haptics (i.e., active touch).

Existing studies suggest that brain areas commonly associated with visual processing are also recruited for processing tactile information (for reviews, see Lacey & Sathian, 2014; Sathian, 2016). However, it is still unclear the extent to which early visual areas respond to haptic object signals in the absence of visual information. For instance, the specific role they play and whether this role might be related to visual imagery, still need to be thoroughly investigated. A major source of evidence for the involvement of the visual cortex in tactile processing comes from research on blind individuals, which has shown that the early visual cortex (EVC) is engaged in tactile tasks such as Braille reading and tactile discrimination (Sadato et al., 1998). These findings can be explained by neuroplastic changes induced by the absence of visual input (Silva et al., 2018). Yet, they might also reflect a broader functional organization of visual areas that is shared by both blind and sighted individuals.

Studies of haptic object exploration in sighted participants have provided evidence for EVC activation during haptic exploration of objects in the absence of online visual input (Merabet et al., 2007; Monaco et al., 2017; Singhal et al., 2013; Snow et al., 2014). These findings suggest that, even with an intact visual system, haptic exploration of unseen stimuli recruits the EVC. However, the specific aspects of haptic exploration that elicit this activity remain unclear. The cross-modal influence of visual areas could be driven by at least two non-mutually exclusive neural mechanisms. First, somatosensory and motor signals elicited during haptic exploration might convey information about object properties, like size and shape, to the

EVC via feedback connections. Second, activation in the EVC could result from visual imagery elicited during haptic exploration, which might facilitate the mental reconstruction of the explored object. Exploring the relative contributions of these mechanisms is crucial in order to understand whether and how the EVC supports the representation of object-related properties across sensory modalities and task demands.

In the present study, we focused on a specific object feature, namely size, because it can be rigorously controlled within the experimental setting. Specifically, we systematically varied object size while keeping other features (e.g., shape) constant. By using circular stimuli of different sizes, we ensured that the explored dimension remained consistent regardless of how the stimulus was explored.

In doing so, we aimed to determine the neural mechanisms underlying haptic stimulus size processing, and whether the haptic and visual imagery systems share the same size representation. Specifically, we pursued two main goals using functional magnetic resonance imaging (fMRI). First, we investigated whether the size of visually imagined and haptically explored, unseen stimuli can be decoded from activity patterns in early visual areas, including the primary visual cortex (V1) and the occipital pole (OP), which corresponds to central vision. Accurate decoding of haptic size in EVC would indicate that EVC processes size information acquired through the motor and haptic system, either via feed-back mechanisms, or indirectly via visual imagery. Further, if size can be accurately decoded during haptic exploration, but not visual imagery, this would argue against the visual imagery hypothesis. Second, we tested whether an abstract representation of size is shared across haptic exploration and visual imagery. If V1 and OP have such a task-independent representation of size, this would support the hypothesis of a more abstract coding mechanism that is not strictly tied to task demands. Importantly, we examined these size representations not only in early visual areas but also in regions of the frontal and parietal cortices known for their roles in action planning, execution,

and imagery, as well as in lateral occipital and temporal areas involved in visual object recognition. Indeed, these areas may encode object properties, like size, that are relevant for action and/or object recognition, and thus, influence the activity of early visual areas through feedback connections. For example, it is well established that frontal and parietal regions are involved in hand movements and action plans (Filimon, 2010; Gallivan & Culham, 2015). Specifically, parietal regions, like the anterior intraparietal area (aIPS), play a role in computing object properties such as size for the selection of appropriate hand configurations to enable accurate hand-object interactions (Cavina-Pratesi et al., 2007; Monaco et al., 2014). Meanwhile, occipito-temporal regions contain high-dimensional object representations, and as such, they contribute to the recognition of object identity and category, as well as to semantic processing (for a review, see Bracci & Op de Beeck, 2023).

To achieve our aims, we blindfolded our participants and asked them to either haptically explore or visually imagine the size of three, concentric rings engraved on a plastic surface. During both the Haptic exploration and Visual imagery tasks, we acquired participants' fMRI data and applied multivoxel pattern analysis (MVPA) to examine the representational content associated with each ring size. Specifically, we tested whether a classifier could accurately discriminate between the three stimulus sizes based on voxel activity patterns in EVC and higher-level cortical areas during Haptic exploration, Visual imagery, and across the two tasks. By analyzing decoding accuracies for Haptic exploration and Visual imagery separately, we could test whether early visual areas and other brain regions encode size consistently within each task. In addition, the performance of the classifier trained on Haptic exploration and tested on Visual imagery, and vice versa, informed us about the existence of abstract representations of size shared across conditions, regardless of whether size was haptically explored or visually imagined. Significant cross-decoding accuracy would suggest that similar neural mechanisms underlie the processing of stimulus size in both the Haptic and Visual imagery tasks. In contrast,

distinct activation patterns would indicate specialized neural representations specific to each task.

3.2 Materials and methods

3.2.1 Participants

Twenty-five participants were recruited for this study (13 females; age: M = 25.11, SD = 3.98). Participants were all right-handed, had normal or corrected-to-normal vision, and no history of neurological or psychiatric disorders. This research adhered to the guidelines outlined in the Declaration of Helsinki. The Human Research Ethics Committee of the University of Trento approved the experimental protocol of this study (protocol 2021-040). All participants provided written informed consent to participate in the experiment and received a monetary reimbursement for their participation.

3.2.2 Experimental design and paradigm

We used a slow event-related fMRI design to measure the blood-oxygenation-level dependent (BOLD) signal (Ogawa et al., 1992) while participants performed Haptic exploration and Visual imagery tasks. The two tasks consisted of haptically exploring one of three differently sized rings with the right (dominant) hand or visually imagining them. Therefore, we had a 2 x 3 repeated measures design (Fig. 1A) with factors: “task” (Haptic exploration vs. Visual imagery) and “size” (Small, Medium, and Large). This design resulted in six conditions: Touch Small, Touch Medium, Touch Large, Imagine Small, Imagine Medium, and Imagine Large. Importantly, participants were blindfolded throughout the entire experiment and had not seen the stimuli prior to the experimental session, which included a training phase followed by fMRI data acquisition.

At the beginning of the experiment, participants rested their right hand with the index finger and thumb placed together at the centre of a tablet, in correspondence of a small groove that served as a reference point for the resting position. Each trial started with an auditory instruction indicating the task to be performed (Touch or Imagine) and the size of the target circle (Small, Medium, or Large) (Fig. 1B). After 6 s, a “Stop” sound instructed participants to either stop exploring the circle and return their fingers to the resting position (Haptic trials), or to stop imagining the circle (Visual imagery trials). The "Stop" instruction served two main purposes: (1) to ensure that Haptic and Visual imagery trials had similar durations, and (2) to maintain a consistent return-phase duration across different movement types, thereby preventing potential differences in brain activation from being attributed to variations in Haptic task duration. The next trial started after 12 s of inter-trial interval (ITI). This ITI duration enabled the fMRI response to return to baseline before the onset of the next trial, thus avoiding contamination of the BOLD signal in the subsequent trial (e.g., Gallivan, McLean, Valyear, et al., 2011; Monaco et al., 2019; Singhal et al., 2013). During the ITI and imagery trials, participants kept their hand in the resting position.

To instruct participants about the size of the target circle to be explored, we used three letters (J, P, and Q) to be associated with the three stimulus sizes (e.g., Small = P, Medium = J, Large = Q). Therefore, the auditory cues consisted of: “Touch J”, “Touch P”, “Touch Q”, “Imagine J”, “Imagine P”, and “Imagine Q”. This weakened the possible influence of quantitative information about spatial magnitude that the words “small”, “medium”, and “large” clearly convey (e.g., Moretto & di Pellegrino, 2008). We identified all the nine possible associations between the three letters and the three object sizes and we randomly assigned them to our participants. Prior to the scanning session, each participant underwent a short training session (10-15 min) to learn the predefined letter-size associations and become familiar with

the two tasks. All auditory cues were created using a freely available voice synthesizer (https://voicemaker.in/).

Participants were asked to keep their eyes closed and wore an eye-mask throughout the training and scanning sessions to prevent visual processing of the stimulus and the workspace. Therefore, they never saw the stimulus, neither before, nor during the experiment. Since participants had no prior visual experience of the stimuli, the initial trials of the training session were always Haptic trials. For the subsequent Visual imagery trials, participants were instructed to use the previously acquired haptic information to calibrate the mental visual images of the three stimulus sizes. As such, the Visual imagery task relied exclusively on information acquired through haptic exploration. In Haptic trials, participants were asked to use their thumb and index finger to haptically explore the target ring by performing circular movements along the corresponding groove on the tablet.

A video camera placed in the magnet room recorded participants' hand movements during the experiment for off-line analysis of errors. Errors included incorrect task execution, such as exploring more than one groove within a single trial due to mislocalization of the target groove or unintentionally performing an action during a Visual imagery trial. These trials were excluded from further analysis, resulting in the removal of 3.6% of trials in total from the dataset. To help the experimenter distinguish between the three differently sized rings in the video recordings, the grooves were marked with distinct colours (small groove: black; medium groove: red; large groove: yellow; Fig. 1C).

Each run lasted approximately nine minutes and included five trials for each of the six experimental conditions, for a total of 30 trials per run. The order of the six conditions was pseudorandomized within each run and counterbalanced across all runs so that each trial type was preceded and followed equally often by other trial types across the experiment. Participants completed six functional runs for a total of 180 trials per subject (30 trials per condition). One

participant was excluded from the analyses due to technical issues that prevented complete data acquisition.

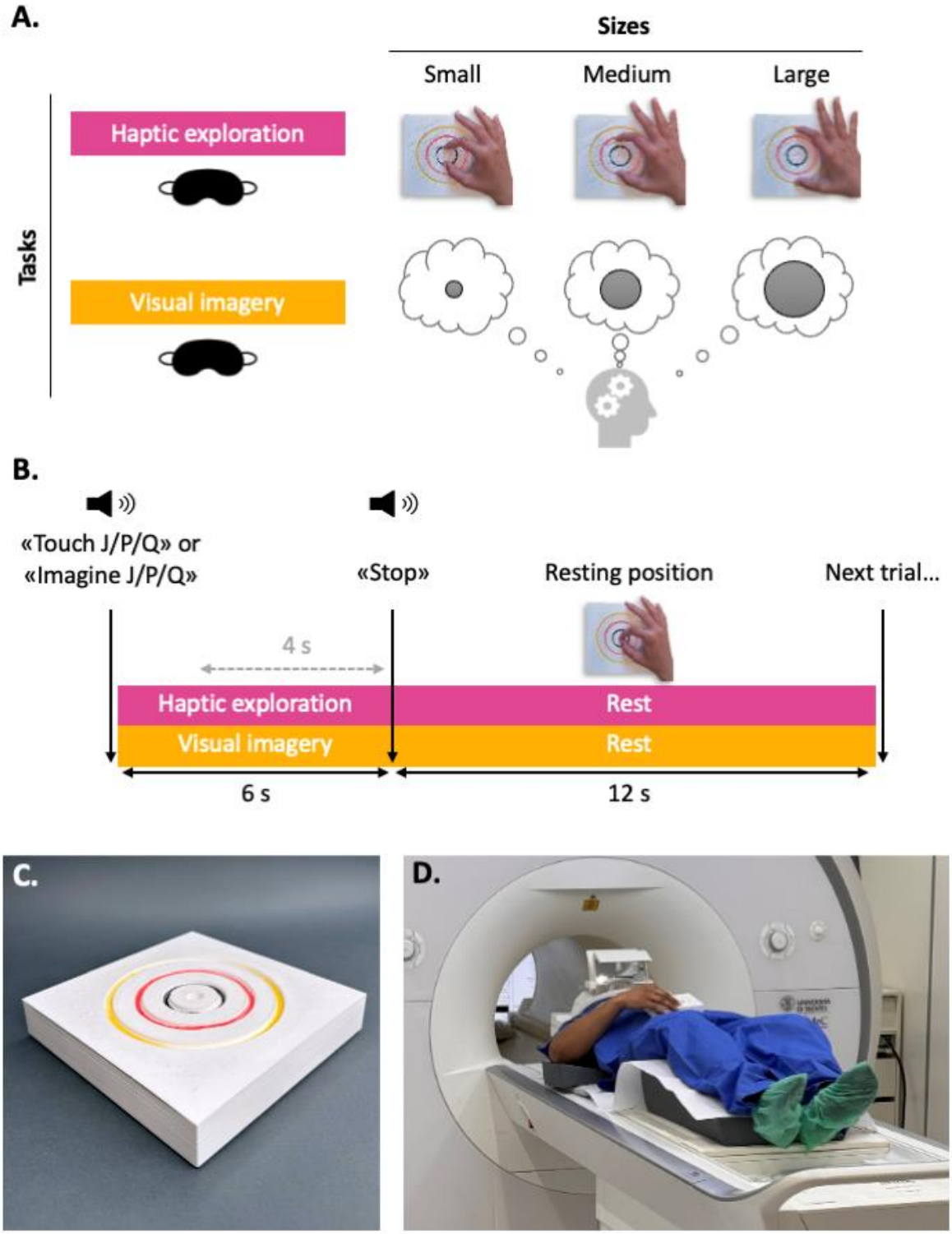

Figure 1. Experimental design, paradigm, stimulus and setup.
A. We employed a 2 x 3 repeated-measures design with three ring sizes (Small, Medium, and Large) and two tasks (Haptic exploration and Visual imagery) as factors. Participants were blindfolded during the training and experimental sessions. **B.** At the beginning of each trial, a recorded voice instructed

participants about the task that they had to perform, which was to either haptically explore or visually imagine one of the three stimulus sizes. Participants performed the task for 6 s; after that, a "stop" cue prompted participants to stop performing the task, and to return the hand to the resting position when performing Haptic exploration trials. We used an inter-trial interval (ITI) of 12 s. We performed the analysis on the last 4 s of the 6 s task phase as indicated by the dashed grey line. **C.** The experimental stimulus consisted of a three-dimensional (3D) plastic tablet with three concentric circular rings of different sizes engraved on its surface. The grooves had diameters of 3 cm, 6.5 cm, and 10 cm, respectively. We marked the grooved with different colors to facilitate the distinction between the three differently sized rings from in the video recordings. **D.** The setup required participants to lay supine with the stimulus placed on their abdomen. The right upper arm was supported with foam, while the left arm rested beside the body.

3.2.3 Stimuli and apparatus

We used a real and tangible three-dimensional (3D) stimulus that consisted of a plastic tablet featuring three concentric circular rings engraved on its surface (Fig. 1C). We selected rings in the form of grooves because they can be reliably explored for size while retaining a consistent shape, texture, and weight across conditions. The grooves had diameters of 3 cm, 6.5 cm, and 10 cm, respectively. The stimulus was designed with Autodesk Fusion 360 and printed on a 3D printer (UltiMaker 2+ Connect). While lying on the magnetic resonance (MR) bed, participants had the tablet placed on their abdomen (Fig. 1D); the tablet was attached with Velcro to a belt worn by the participants during the experiment. The position of the tablet could be adjusted to ensure that each participant could comfortably and naturally explore the stimulus. The right upper arm of the participants was supported with foam, and the left arm rested beside the body. Auditory cues were played through ePrime software, which was triggered by a computer that received a signal from the magnetic resonance imaging (MRI) scanner.

3.2.4 MRI parameters

The study was conducted at the Center for Mind/Brain Sciences (University of Trento, Italy) using a 3-T SIEMENS MAGNETOM Prisma MRI system with a 64-channel head coil. Functional images were acquired with a T2*-weighted segmented gradient echo-planar imaging sequence (Repetition time (TR) 2 s; Echo time (TE) 28 ms; Flip angle (FA) 75 deg; Field of

view (FOV): 200 x 200 mm; in-slice resolution of 2 x 2 mm; slice thickness: 2 mm; multiband slice acceleration: 3). Each volume comprised 69 slices acquired in ascending interleaved order. At the beginning of each experimental session, a T1-weighted anatomical reference volume was acquired using a MPRAGE sequence (TR: 2530 ms; Inversion time (TI): 1100 ms; FA: 7 deg; FOV: 256 mm; 176 slices; 1 mm isotropic voxel resolution).

3.2.5 MRI Data preprocessing

We analysed the imaging data using Brain Voyager QX 2.8.4 (Brain Innovation, Maastricht, The Netherlands). Functional data were superimposed on anatomical brain images, aligned with the anterior commissure–posterior commissure line, and transformed into Talairach space (Talairach & Tournoux, 1988).

Functional data were pre-processed with temporal smoothing to remove frequencies below 2 cycles per run. We applied slice-time correction with a cubic spline interpolation algorithm. Each functional run was motion-corrected using a trilinear/sinc interpolation algorithm, such that each volume was aligned to the volume of the functional scan closest to the anatomical scan. The motion correction parameters of each run were also checked. Functional data from each run were screened to ensure that no obvious motion artifacts (e.g., rims of activation) were present in the activation maps of individual participants. For univariate analysis, we applied spatial smoothing using a Gaussian kernel with an 8-mm full width at half maximum. In contrast, no spatial smoothing was applied for multivariate analysis.

3.2.6 Univariate analysis

We used univariate analysis to localize areas that are well known to be involved in haptic and imagery tasks. To do so, we defined a general linear model (GLM) including seven predictors for each participant. The predictors were: (1) Touch Small, (2) Touch Medium, (3) Touch Large, (4) Imagine Small, (5) Imagine Medium, (6) Imagine Large, (7) Audio instruction.

We also included six motion parameters (3 rotations and 3 translations) and error trials, if present, as predictors of no interest. The estimated beta weight (β) for each condition was converted to percent signal change; therefore, β values were scaled with respect to the mean signal level, and a random-effects (RFX) analysis was performed at the group level. We applied cluster-level correction (Forman et al., 1995) using the Brain Voyager's cluster-level statistical threshold estimator plug-in (Goebel et al., 2006), which implements Monte Carlo simulations (1000 iterations). Only foci that survived cluster threshold correction at an alpha-correction level of 0.01 are shown.

We created the average cortical surface using the anatomical images of 20 participants with cortex segmentation and cortex-based alignment procedures as implemented in Brain Voyager. Statistical activation maps were then projected onto the average surface map.

We performed a univariate conjunction analysis of Haptic exploration and Visual imagery (Haptic exploration AND Visual imagery). The conjunction analysis showed the recruitment of a widespread cluster of regions on both left and right hemispheres, including prefrontal, parietal, superior temporal, and occipital cortices (Fig. 2). We used the activation map of the conjunction analysis to functionally localize areas that showed above baseline activation for Haptic and Visual imagery trials. This allowed us to select areas involved in both tasks while also avoiding biases towards either task. The main focus of the study was to examine whether the activity pattern in the EVC can be used to decode the size of haptically explored stimuli and eventually exclude the potential role of visual imagery. Therefore, the selection criterion used to functionally localize our regions of interest (Haptic exploration AND Visual imagery) was independent from the key comparison explored in further analyses (Small vs. Medium, Medium vs. Large, and Small vs. Large stimulus size), ensuring no bias towards our predictions (Kriegeskorte et al., 2010; Vul & Kanwisher, 2010).

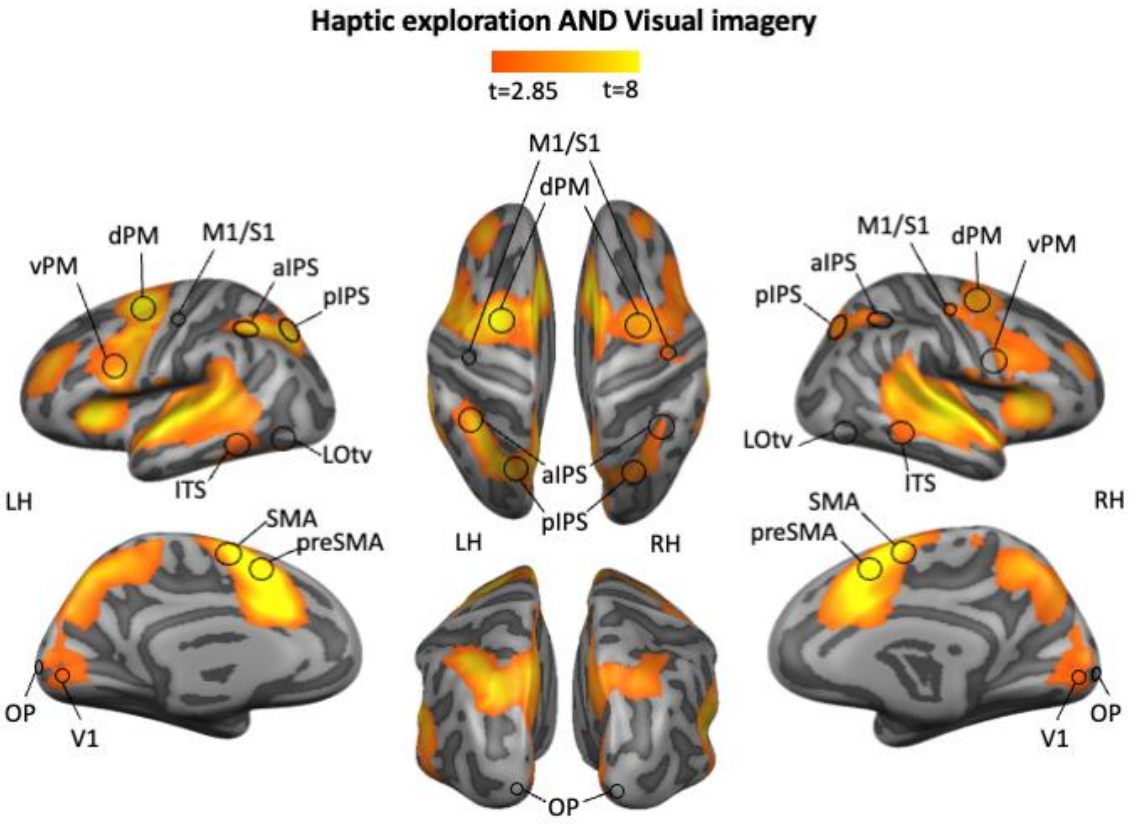

Figure 2. Conjunction analysis of Haptic exploration and Visual imagery, and group ROIs. The figure shows the voxelwise statistical map obtained from the Haptic and Visual imagery univariate conjunction analysis. The group activation map is overlaid on the average cortical surface derived from the cortex-based alignment performed on 20 participants. Overlaid on the statistical map are regions of interest (ROIs) selected bilaterally for multivoxel pattern analysis (MVPA), including the primary motor/somatosensory area (M1/S1), dorsal and ventral premotor areas (dPM and vPM), supplementary and presupplementary motor areas (SMA and preSMA), anterior and posterior intraparietal sulci (aIPS and pIPS), inferior temporal sulcus (ITS), lateral-occipital tactile-visual area (LOtv), primary visual cortex (V1), occipital pole (OP).

3.2.7 Regions of Interest

The main objective of this study was to investigate whether 1) imagined and haptically explored size of unseen stimuli can be decoded from fMRI activity patterns, especially in early visual areas including V1 and the foveal cortex in OP, and whether 2) this representation, if present, is shared across haptic exploration and visual imagery. To this end, we localized areas V1 and OP, as well as specific ROIs in the dorsal and ventral visual streams, known for their involvement in movement execution, visual imagery, and object recognition. In particular, we

explored the role of haptic exploration and visual imagery in 11 cortical regions in the left and right hemisphere, including areas that are known to support specific functions like visual information processing (i.e., V1, OP, inferior temporal cortex), visuo-tactile information processing (i.e., lateral-occipital tactile-visual area; LOtv), action execution and somatosensory processing (i.e., primary motor and somatosensory cortex), action planning, preparation and monitoring (i.e., supplementary and pre-supplementary motor area, dorsal and ventral premotor area) and coding of movement intention along with motor imagery processes (anterior and posterior intraparietal sulcus).

We localized our ROIs based on functional and anatomical methods. For functional localization, we used the group-level conjunction map of the RFX-GLM (Haptic exploration AND Visual imagery, $p < 0.01$) and searched for significant activation that coincided with the expected anatomical location. We used the same threshold for all ROIs. The activation map was corrected for multiple comparisons using the Monte Carlo simulation approach implemented in the BrainVoyager's cluster threshold plug-in (Forman et al., 1995; Goebel et al., 2006). We used an alpha-correction level of 0.01. Only foci that survived cluster threshold correction are shown in Figure 2. When the univariate conjunction analysis did not reveal significant activation around one of our regions of interest (e.g., left M1/S1, bilateral OP and LOtv), we localized the area based on group-level anatomical landmarks and Talairach coordinates reported in previous studies. Talairach (TAL) coordinates of our ROIs are listed in Table 1 and illustrated in Fig. 2.

We defined our ROIs with region-specific radii optimized for anatomical and functional considerations. For early sensory and primary motor regions—specifically V1, OP, and primary motor/somatosensory cortex (M1/S1)—we used a 6-mm radius (925 mm3) for each ROI. We reasoned that, since these areas are known for their high functional specificity and consistent anatomical landmarks, a small ROI would reliably capture the core activity without incorporating adjacent, functionally distinct areas. For regions that show greater spatial

heterogeneity and less sharply defined boundaries (e.g., higher-order visual, multisensory, and association areas), we used a larger, 9-mm radius (3071 mm^3). This radius ensures adequate coverage of the distributed and potentially variable functional representations observed in higher-order regions and across individuals.

We identified seven bilateral ROIs in frontal and parietal lobes known for their role in action planning and execution (Gallivan, McLean, Valyear, et al., 2011), as well as in motor imagery (Hardwick et al., 2018). As shown in Fig. 2, the dorsal premotor cortex (dPM) was located at the intersection of the superior frontal sulcus and the precentral sulcus (Monaco et al., 2014). The primary motor/somatosensory cortex (M1/S1) was defined by selecting voxels in the fundus of the central sulcus and spanning pre- and post-central gyri at the omega-shaped hand knob. The ventral premotor cortex (vPM) was identified by selecting voxels slightly below and behind the junction of the inferior frontal sulcus and precentral sulcus (Gallivan, McLean, Valyear, et al., 2011). The supplementary motor area (SMA) was identified at the junction of the superior frontal gyrus and the cingulate gyrus, while the pre-supplementary motor area (preSMA) was located more anteriorly compared to SMA. The anterior intraparietal sulcus (aIPS) was selected at the intersection of the intraparietal sulcus and the inferior segment of the postcentral sulcus (Culham et al., 2003), while the posterior intraparietal sulcus (pIPS) was located more posteriorly along the intraparietal sulcus compared to the aIPS.

We also identified four bilateral ROIs in occipital and temporal lobes known for their specialization in visual and multisensory processing, as well as object recognition. In particular, V1 was located in the calcarine sulcus, while the OP was localized at the most posterior region of the occipital lobe, corresponding to the caudal end of the calcarine sulcus. The LOtv was mapped to the junction of the ascending limb of the inferior temporal gyrus and the lateral occipital sulcus (Amedi et al., 2001). Finally, the inferior temporal sulcus (ITS) was localized at the inferior aspect of the temporal lobe.

Table 1. ROIs Talairach coordinates.

ROI	Coordinates (Talairach)		
	x	y	z
Left preSMA	-9	9	52
Right preSMA	9	9	52
Left SMA	-9	-9	58
Right SMA	9	-9	58
Left dPM	-27	-6	53
Right dPM	27	-10	55
Left vPM	-54	8	28
Right vPM	54	8	28
Left M1S1*	-39	-20	52
Right M1S1	41	-16	50
Left aIPS	-38	-48	45
Right aIPS	32	-43	40
Left pIPS	-17	-68	43
Right pIPS	22	-64	40
Left OP*	-11	-96	1
Right OP*	12	-96	1
Left V1	-9	-83	0
Right V1	9	-83	1
Left LOtv*	-48	-62	-7
Right LOtv*	48	-60	-6
Left ITS	-55	-44	-7
Right ITS	56	-42	-7

Note: all ROIs have the same number of anatomical voxels (3071 mm3; ROI radius of 9 mm), except for bilateral M1S1, V1, and OP (925 mm3; ROI radius of 6 mm). Asterisks (*) indicate the ROIs localized based on group-level anatomical landmarks and Talairach coordinates reported in previous studies. The remaining ROIs were defined by the intersection of the group-level conjunction map of the RFX-GLM (Haptic exploration AND Visual imagery) and their expected anatomical locations.

3.2.8 Multivoxel Pattern Analysis

To perform MVPA, we employed a Linear Discriminant Analysis (LDA) classifier using the CoSMoMVPA Toolbox (Oosterhof et al., 2016). For each participant and each of the 22

ROIs, β weights were estimated from non-spatially smoothed data using the design matrix specified in the GLM. Activity patterns were decoded from individual runs, and classification accuracy was assessed using a 'leave-one-run-out' cross-validation approach. Since the classifier requires at least two samples per class for the training, and error trials were excluded, we had to discard some functional runs (5 runs across 3 participants) from the MVPA due to an insufficient number of trials for the training phase. Thus, a new GLM was estimated for these participants, excluding the above-mentioned runs to satisfy the requirements of the CoSMoMVPA Toolbox.

MVPA was conducted using both ROI-based and whole-brain searchlight approaches (Kriegeskorte & Bandettini, 2007), performing decoding analysis across all voxels in the brain. The searchlight analysis served to replicate and potentially extend the ROI-based results, though its spatial specificity is inherently limited, as decoding results for each searchlight are assigned to its central voxel (Oosterhof et al., 2011). Each searchlight was defined using the beta values of the selected voxel and its surrounding neighbours within a sphere of three-voxel radius, averaging 123 anatomical voxels per searchlight.

To investigate whether the haptically explored and imagined size of stimuli could be decoded from activity patterns in our ROIs, we trained the classifier to discriminate between two sizes within each of the three stimulus size pairs, separately for Haptic trials (Touch Small vs. Touch Medium, Touch Medium vs. Touch Large, and Touch Small vs. Touch Large) and Visual imagery trials (Imagine Small vs. Imagine Medium, Imagine Medium vs Imagine Large, and Imagine Small vs. Imagine Large). Classification accuracies were then averaged to obtain a mean accuracy for each ROI. To assess whether the representation of stimulus size, if present, is shared across Haptic exploration and Visual imagery, we performed cross-decoding. Specifically, we trained the classifier on the distinction between two sizes within each of the three pairs of sizes in Haptic trials (e.g., Touch Small vs. Touch Medium) and tested its

performance to distinguish between the same size pairs in Visual imagery trials (e.g., Imagined Small vs. Imagined Medium), and vice-versa. Classification accuracies for the cross-decoding of the three comparisons were also averaged.

For ROI-based MVPA, we evaluated the statistical significance of mean classification accuracies using a two-tailed, one-sample t-test against chance-level decoding (50%) for each ROI. To account for multiple comparisons (22 ROIs × 3 comparisons), statistical results were corrected using the False Discovery Rate (FDR) method (Benjamini & Hochberg, 1995). To test for significant differences in the mean decoding accuracies between Haptic exploration, Visual imagery, and Cross-decoding conditions, we also performed a two-tailed, paired sample t-test between each pair of decoding type (e.g., Haptic size decoding vs. Visual imagery size decoding, Haptic size decoding vs. Cross-decoding, Visual imagery size decoding vs. Cross-decoding), for each ROI. Statistical results were corrected for multiple comparisons using the FDR procedure. The rationale for these comparisons is as follows: comparing Haptic vs. Visual imagery size decoding allows us to assess whether size information is more accurately discriminated in one task than the other within a given ROI. Comparisons between Haptic size vs. Cross-decoding, and Visual imagery size vs. Cross-decoding, inform us about whether the abstract representation of size, reflected in the Cross-decoding, differs from either the haptic or imagined representation. For instance, above-chance Cross-decoding but lower accuracy than within-task modality decoding would indicate that an abstract size representation exists, but that one task modality (the one with higher decoding accuracy) provides a more precise representation than the abstract one. Conversely, above-chance Cross-decoding with no difference with Haptic or Visual imagery decoding would suggest that a region contains an abstract representation of size that is independent of the task modality used to acquire it. A third possibility is that Cross-decoding is not significant, indicating that size representations in that region are task-specific. We do not expect Cross-decoding to exceed within-task modality

decoding accuracy because generalizing across two different tasks typically results in a lower signal-to-noise ratio.

For searchlight-based MVPA, we identified brain areas where decoding exceeded chance level (50%) by performing t-tests across individual decoding accuracy maps. Each resulting map corresponds to the average of the individual comparisons (Small vs. Medium, etc. for Haptic, Visual imagery trials, and Cross-decoding). As for the univariate analysis, statistical maps were corrected for multiple comparisons using the Brain Voyager's cluster-level statistical threshold estimator plug-in (Forman et al., 1995, Goebel et al., 2006), which implements Monte Carlo simulations (1000 iterations). Only foci that survived cluster threshold correction at an alpha-correction level of 0.05 for Visually imagined size decoding and Size cross-decoding searchlight statistical maps, and 0.001 for the Haptic size decoding searchlight statistical map are shown. We then projected the average statistical maps originating from the searchlight analysis onto the average surface map.

3.2.9 Psychophysiological interaction (PPI) analysis

We used the PPI method (Friston et al., 1997; McLaren et al., 2012; O'Reilly et al., 2012) to estimate the task-specific changes in functional connectivity between our seed regions (left OP and V1) and the rest of the brain during the Haptic exploration versus Visual imagery task. PPI identifies brain regions in which functional connectivity is modified by the task above and beyond simple interregional correlations ("physiological component") and task-modulated activity ("psychological component"). For each seed region, and for each run of each participant, we created a PPI model that included the following: (1) the physiological component, corresponding to the z-normalized time course extracted from the seed region; (2) the psychological component, corresponding to the task model (boxcar predictors convolved with a standard hemodynamic response function); and (3) the PPI component, corresponding to the z-normalized time course multiplied, volume by volume, with the task model. The boxcar

predictors of the psychological component were set to 1 for the Haptic task, to -1 for the Visual imagery task, and to 0 for baseline. Motion correction parameters from each run of each participant were included as co-variates of no interest. The individual GLM design matrix files were used for a random-effects model analysis (Friston et al., 1999). The functional connectivity map was corrected for multiple comparisons using the Monte Carlo simulation approach implemented in the BrainVoyager's cluster threshold plug-in (Forman et al., 1995; Goebel et al., 2006). The minimum cluster sizes were 178 and 181 functional voxels for maps originated with left hemisphere (LH) OP and V1 as seed regions, respectively (F=2.2; 1424 and 1448 mm3). We used an alpha-correction level of 0.05.

3.2.10 Subjective vividness rating

The ability to generate vivid visual images varies significantly across individuals (Cui et al., 2007). We assessed the vividness of visual imagery in our participants to ensure they possessed a robust ability to form mental images. To do so, at the end of the experimental session, participants completed the Vividness of Visual Imagery Questionnaire (VVIQ), which evaluates the quality of their visual imagery (Marks, 1995). The questionnaire includes 16 items, each requiring participants to rate the vividness of their visual imagery for various scenarios (e.g., a shop, a person, the sky) on a scale from 1 (no image present) to 5 (perfectly clear and vivid image). The total score ranges from 16 to 80, with higher scores indicating higher vividness of visual imagery. We calculated the mean vividness score as an indicator of each participant's visual imagery ability.

To explore potential relationships between imagery vividness and neural activity, we computed Pearson's correlation coefficient (r) to measure the correlation between the vividness scores and classification accuracies in Visual imagery trials, Haptic trials, and in the Cross-decoding condition, separately, for each ROI. Importantly, the analysis of correlation for the Haptic and Cross-decoding conditions allowed us to examine whether individual differences in

imagery vividness might be reflected in different neural mechanisms, and potentially different processing strategies, to represent haptic size and to generalize size information across the two tasks.

3.3 Results

3.3.1 ROI-based Multivoxel pattern analysis

We performed MVPA in each ROI to test whether the size of unseen stimuli can be decoded from brain activity patterns during Haptic exploration, Visual imagery, and across Haptic and Visual imagery tasks. For each ROI, decoding accuracies and significant differences between each pair of decoding accuracies are shown in Figs. 3,4 and statistical values are reported in Tables 2,3. The statistical values of decoding accuracies for each of the three pairs of sizes are reported in Supplementary Table 3.1.

Nearly all ROIs in the occipital and temporal cortices, including the left V1, bilateral OP, LOtv, and ITS showed significant decoding accuracy of stimulus size during Haptic exploration (Fig. 3, magenta dots). In addition, the left LOtv showed above chance size decoding also during Visual imagery (yellow dots). Haptic size decoding was significantly higher than Visual imagery size decoding in all occipital and temporal ROIs, except in the right OP and left V1. These results suggest that Haptic size decoding in visual areas (especially left OP and right V1) is not merely driven by visual imagery processes, as decoding was observed during Haptic exploration but not during Visual imagery alone, which is in contrast to what would be expected if the visual imagery hypothesis were true. In addition, the results suggest that LOtv contains distinct yet overlapping representations of haptically explored and imagined stimulus size. None of these areas showed significant decoding of size information across Haptic and Visual imagery tasks (orange dots), indicating that the representation of stimulus

size does not generalize across tasks in areas specialized in processing low-level visual features of objects (OP, V1) and object recognition (LOtv, ITS). All areas, except the right V1, showed higher accuracy for Haptic size than Cross-decoding.

As expected, the patterns of activity in all frontal and parietal ROIs enabled successful decoding of size during Haptic exploration (Fig. 4). These regions include bilateral preSMA, SMA, vPM, dPM, M1/S1, aIPS, and pIPS. Decoding of stimulus size during Visual imagery trials was significantly accurate in left SMA, bilateral dPM, aIPS, and pIPS. We also found higher decoding accuracy for Haptic than Visual imagery trials in parietal and frontal ROIs. Therefore, although these areas show a predominant role in haptic size processing, they can flexibly represent size information regardless of whether it is based on Haptic exploration or Visual imagery. Interestingly, bilateral dPM, aIPS, and pIPS also showed above-chance cross-decoding accuracy, suggesting that in these areas haptically explored and imagined size is represented using similar neural mechanisms. Moreover, we found higher decoding accuracy for Haptic size than Cross-decoding in frontal and parietal ROIs, and the left aIPS also showed higher decoding accuracy for Visually imaged size than Cross-decoding.

Taken together, these results suggest that both distinct and shared neural mechanisms underlie the representation of stimulus size during Haptic exploration and Visual imagery, with higher-order cortical areas flexibly representing size information across these tasks. In addition, the differential involvement of various brain regions highlights not only the complexity of processing stimulus-related features under different cognitive tasks, but also the role of both early visual and higher-order brain regions in encoding size information.

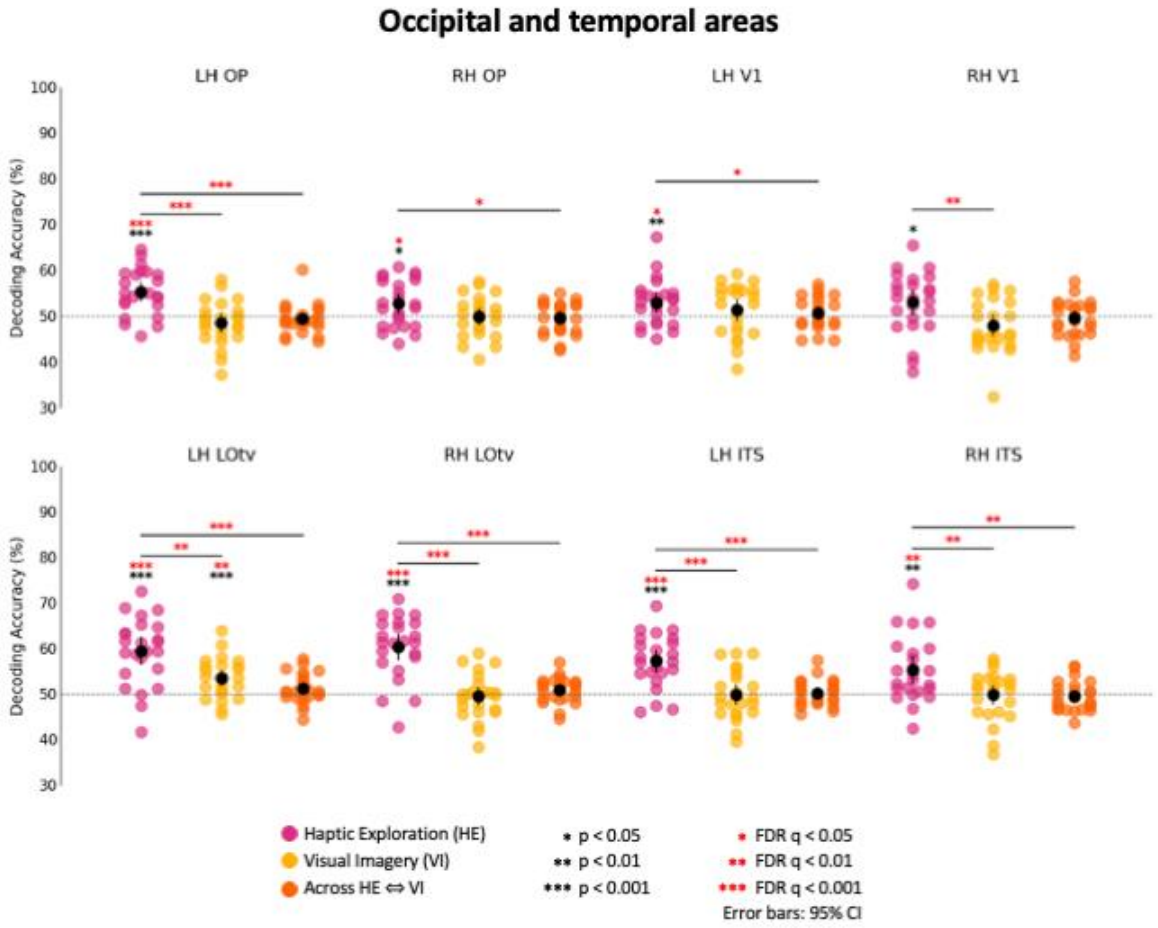

Figure 3. Classifier decoding accuracies in occipital and temporal ROIs.
The scatterplots show decoding accuracies for each participant along with the average (black circles) in occipital and temporal areas in both the left and right hemisphere for size information in Haptic Exploration (HE) trials (magenta circles), Visual Imagery (VI) trials (yellow circles), and across HE and VI (orange circles). Chance level is indicated with a line at 50% of decoding accuracy. Error bars represent 95% confidence intervals (CI). Asterisks (*) indicate statistical significance based on paired-samples, two-tailed t-tests across subjects with respect to 50%, and pairwise comparisons for each pair of decoding type (i.e., HE vs. VI, HE vs. Across HE and VI). Black asterisks denote uncorrected statistical significance, whereas red asterisks indicate statistical significance based on an FDR correction of $q < 0.05$. While all areas show significant above chance decoding accuracy of size information in HE trials, except for the right V1, in VI trials size information can only be decoded from the activity patterns of the left LOtv. In addition, no area shows significant above chance decoding accuracy of size information across HE and VI conditions.

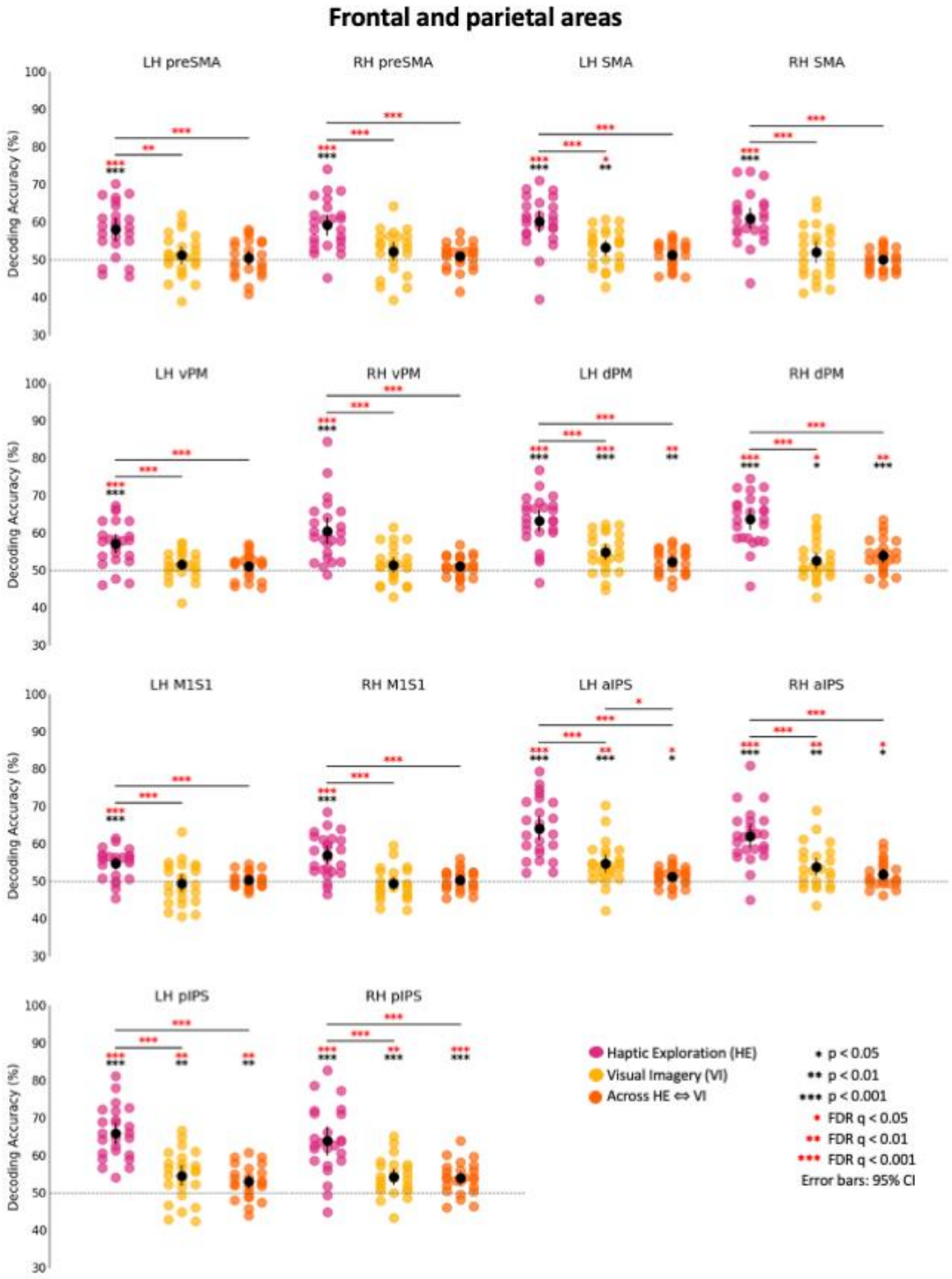

Figure 4. Classifier decoding accuracies in frontal and parietal ROIs.
The scatterplots show decoding accuracies for each participant along with the average (black circles) in frontal and parietal areas in both the left and right hemisphere for size information in Haptic Exploration (HE) trials (magenta circles), Visual Imagery (VI) trials (yellow circles), and across HE and VI (orange circles). Chance level is indicated with a line at 50% of decoding accuracy. Error bars represent 95% confidence intervals (CI). Asterisks (*) denote statistical significance based on paired-samples, two-tailed t-tests across subjects with respect to 50%, and pairwise comparisons for each pair of decoding

type (i.e., HE vs. VI, HE vs. Across HE and VI, VI vs. Across HE and VI). Black asterisks indicate uncorrected statistical significance, whereas red asterisks indicate statistical significance based on an FDR correction of $q < 0.05$. While all areas show significant above chance decoding accuracy of size information in HE trials, in VI trials size information can only be decoded from the activity patterns of the left SMA, bilateral dPM area, bilateral aIPS, and pIPS. As for the decoding of size across HE and VI conditions, significant above chance accuracy is observed in bilateral dPM, aIPS, and pIPS.

Table 2. Statistical values for ROI-based MVPA results.

ROI	Decoding accuracy for size, t(23)		
	Haptic exploration	**Visual imagery**	**Cross-decoding**
Left preSMA	***p*<.001 t=5.60**	*p*=.311 t=1.04	*p*=.617 t=0.51
Right preSMA	***p*<.001 t=6.70**	*p*=.082 t=1.82	*p*=.210 t=1.29
Left SMA	***p*<.001 t=7.33**	***p*=.005 t=3.11**	*p*=.076 t=1.86
Right SMA	***p*<.001 t=7.98**	*p*=.185 t=1.37	*p*=.975 t=0.03
Left dPM	***p*<.001 t=9.52**	***p*<.001 t=4.65**	***p*=.002 t=3.41**
Right dPM	***p*<.001 t=9.95**	***p*=.025 t=2.39**	***p*<.001 t=4.23**
Left vPM	***p*<.001 t=5.84**	*p*=.060 t=1.98	*p*=.109 t=1.67
Right vPM	***p*<.001 t=6.21**	*p*=.164 t=1.44	*p*=.070 t=1.90
Left M1S1	***p*<.001 t=5.76**	*p*=.634 t=-0.48	*p*=.477 t=0.72
Right M1S1	***p*<.001 t=5.94**	*p*=.453 t=-0.76	*p*=.568 t=0.58
Left aIPS	***p*<.001 t=8.84**	***p*=.001 t=4.00**	***p*=.024 t=2.42**
Right aIPS	***p*<.001 t=8.07**	***p*=.004 t=3.21**	***p*=.018 t=2.55**
Left pIPS	***p*<.001 t=11.18**	***p*=.003 t=3.36**	***p*=.003 t=3.30**
Right pIPS	***p*<.001 t=7.49**	***p*<.001 t=4.15**	***p*<.001 t=4.46**
Left OP	***p*<.001 t=5.25**	*p*=.134 t=-1.55	*p*=.328 t=-1.00
Right OP	***p*=.018 t=2.56**	*p*=.853 t=-0.19	*p*=.525 t=-0.65
Left V1	***p*=.010 t=2.81**	*p*=.248 t=1.19	*p*=.432 t=0.80
Right V1	*p*=.043 t=2.14	*p*=.086 t=-1.79	*p*=.543 t=-0.62
Left LOtv	***p*<.001 t=6.29**	***p*=.001 t=3.84**	*p*=.072 t=1.89
Right LOtv	***p*<.001 t=7.42**	*p*=.619 t=-0.50	*p*=.143 t=1.52
Left ITS	***p*<.001 t=6.13**	*p*=.923 t=-0.10	*p*=.729 t=0.35
Right ITS	***p*=.001 t=3.65**	*p*=.841 t=-0.20	*p*=.478 t=-0.72

Note: Statistically significant values after False Discovery Rate (FDR) correction ($q < 0.05$) for multiple comparisons are indicated in boldface.

Table 3. Statistical values for ROI-based MVPA results: pair-wise comparisons.

ROI	Decoding accuracy for size, t(23)		
	Haptic exploration vs. Visual imagery	Haptic exploration vs. Cross-decoding	Visual imagery vs. Cross-decoding
Left preSMA	***p*=.001 t=3.95**	***p*<.001 t=4.76**	*p*=.658 t=0.45
Right preSMA	***p*<.001 t=4.41**	***p*<.001 t=6.11**	*p*=.301 t=1.06
Left SMA	***p*<.001 t=4.86**	***p*<.001 t=5.54**	*p*=.184 t=1.37
Right SMA	***p*<.001 t=5.34**	***p*<.001 t=7.42**	*p*=.205 t=1.30
Left dPM	***p*<.001 t=6.12**	***p*<.001 t=6.80**	*p*=.049 t=2.07
Right dPM	***p*<.001 t=6.88**	***p*<.001 t=6.12**	*p*=.241 t=-1.21
Left vPM	***p*<.001 t=4.10**	***p*<.001 t=4.64**	*p*=.715 t=0.37
Right vPM	***p*<.001 t=4.38**	***p*<.001 t=6.02**	*p*=.787 t=0.27
Left M1S1	***p*<.001 t=4.15**	***p*<.001 t=5.34**	*p*=.479 t=-0.72
Right M1S1	***p*<.001 t=4.49**	***p*<.001 t=4.88**	*p*=.289 t=-1.09
Left aIPS	***p*<.001 t=4.81**	***p*<.001 t=7.79**	***p*=.007 t=2.93**
Right aIPS	***p*<.001 t=4.96**	***p*<.001 t=6.35**	*p*=.043 t=2.14
Left pIPS	***p*<.001 t=6.53**	***p*<.001 t=10.58**	*p*=.343 t=0.97
Right pIPS	***p*<.001 t=5.06**	***p*<.001 t=5.57**	*p*=.814 t=0.24
Left OP	***p*<.001 t=4.94**	***p*<.001 t=4.45**	*p*=.456 t=-0.76
Right OP	*p*=.075 t=1.86	***p*=.014 t=2.65**	*p*=.800 t=0.26
Left V1	*p*=.325 t=1.00	***p*=.031 t=2.30**	*p*=.581 t=0.56
Right V1	***p*=.001 t=3.63**	*p*=.043 t=2.14	*p*=.222 t=-1.26
Left LOtv	***p*=.005 t=3.11**	***p*<.001 t=5.20**	*p*=.039 t=2.19
Right LOtv	***p*<.001 t=6.74**	***p*<.001 t=6.75**	*p*=.164 t=-1.44
Left ITS	***p*<.001 t=4.47**	***p*<.001 t=5.87**	*p*=.826 t=-0.22
Right ITS	***p*=.002 t=3.42**	***p*=.001 t=3.89**	*p*=.844 t=0.20

Note: Statistically significant values after False Discovery Rate (FDR) correction ($q < 0.05$) for multiple comparisons are indicated in boldface.

3.3.2 Searchlight-based MVPA

We complemented the ROI-based analysis with searchlight-based MVPA over the whole brain to identify brain regions where neural activity patterns reflected reliable decoding of the size during Haptic exploration, Visual imagery, and across the two tasks.

Overall, ROI-based and searchlight MVPA results were highly consistent. Specifically, for the Haptic condition, searchlight analysis revealed significant size decoding in widespread

bilateral clusters encompassing frontal (including vPM, dPM, SMA, preSMA, and M1), parietal (including S1, aIPS, and pIPS), temporal (including ITS), and occipital regions (including lateral occipital areas and OP), in both hemispheres (Fig. 5A). Although the calcarine sulcus did not show Haptic size decoding at the chosen threshold in the searchlight map, this information emerged at lower, yet still significant thresholds, consistent with the ROI analysis. Decoding of Visually imaged size was significantly accurate in several clusters located in bilateral parietal cortices (including aIPS and pIPS), the left superior temporal cortex, bilateral lateral occipital cortices, while frontal decoding was markedly left-lateralized (including SMA and dPM) (Fig. 5B). Cross-decoding of size information yielded significant results in a large cluster spanning bilateral parietal cortices (including IPS), as well as additional clusters in bilateral frontal (including dPM areas), prefrontal, temporal, and superior occipital cortices (Fig. 5C).

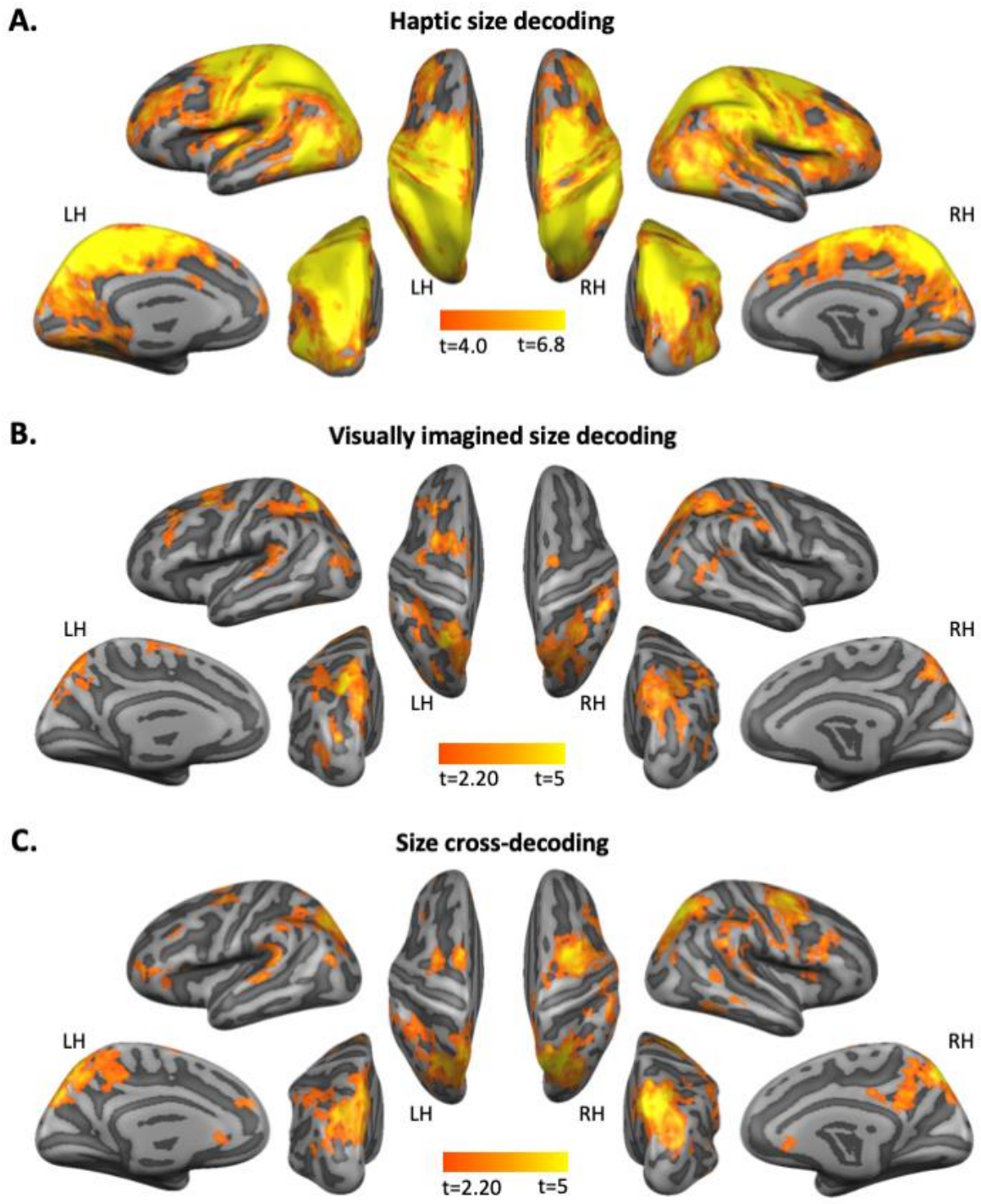

Figure 5. Searchlight results for Haptic size, Visually imagined size, and Cross-decoding of size. **A.** The figure shows the decoding accuracy map for Haptic size which demonstrated a widespread cluster where decoding accuracies for haptically explored size were above chance-level. **B.** The figure shows the decoding accuracy map for Visually imagined size which revealed clusters in bilateral frontal cortices, bilateral parietal cortices, the left superior temporal cortex, and bilateral occipital cortices where decoding accuracies for visually imagined size were above chance-level. **C.** The figure shows the decoding accuracy map for the Cross-decoding of size which revealed clusters in bilateral prefrontal and

frontal cortices, bilateral parietal cortices, the left superior temporal cortex, and bilateral occipital cortices where decoding accuracies for cross-decoding of size information were above chance-level. All maps are overlaid on the average cortical surface

3.3.3 PPI analysis

To summarize, our MVPA results show that the activity pattern from the patch of visual cortex corresponding to foveal vision (OP) and primary visual cortex (V1) can be used to decode stimulus size during Haptic exploration even if participants are blindfolded. These results might be due to feedback from high-level sensory-motor areas in the premotor cortex and intraparietal sulcus. To examine whether functional connectivity between left hemisphere OP and V1 and other regions (e.g., premotor and parietal areas) is modulated by the nature of the task, we used a PPI approach. When comparing Haptic with Visual imagery task, we found that the left OP and V1 (Fig. 6) showed stronger functional connectivity with several areas, including those implicated in sensory-motor control of grasping actions (left aIPS), multimodal recognition of objects (LOtv), somatosensory/motor function (premotor cortex). In particular, left OP (Fig. 6A) showed stronger connections for Haptic than Imagery tasks with left hemisphere cortical regions including aIPS, vPM, ITS, and LOtv. Similarly, left V1 (Fig. 6B) showed enhanced connectivity during Haptic exploration as compared to Visual imagery task with predominantly left-lateralized clusters, which include aIPS, pIPS, vPM, ITS, and LOtv. However, it is important to note that, for both PPI analyses, the results observed in parietal (aIPS, pIPS) and premotor (vPM) regions did not survive cluster-level correction. Together, the PPI results reinforce the suggestion that the OP and V1 play a role in haptic size exploration because of feedback connections from high-level sensory-motor areas.

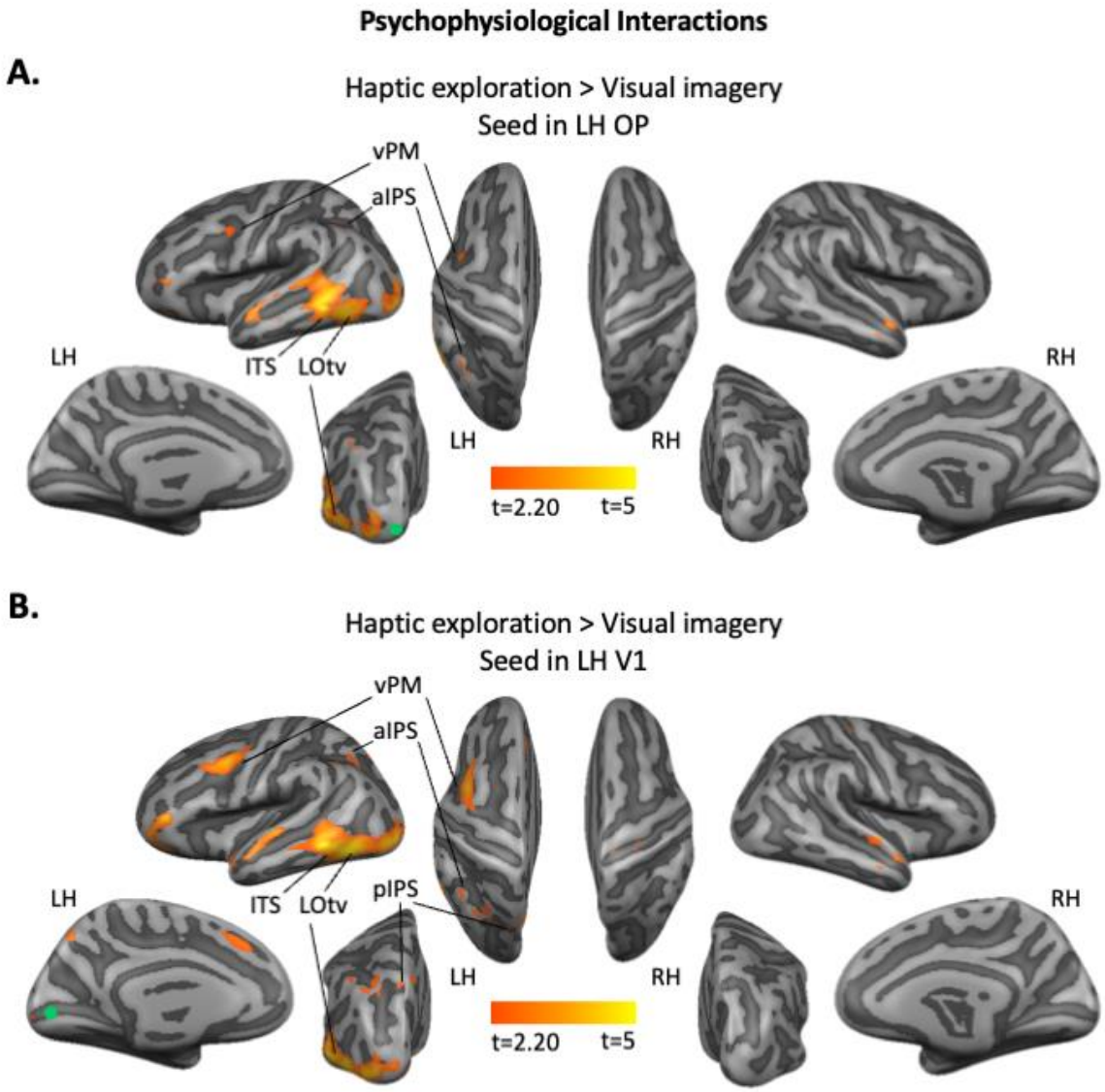

Figure 6. Task-related functional connections between early visual areas and the rest of the brain.
A. The figure shows the psychophysiological interaction results using left OP as seed region (green circle). The map indicates the brain areas that show stronger functional connections with left OP for Haptic exploration as compared to Visual imagery. The map is overlaid on the average cortical surface.
B. The figure shows the psychophysiological interaction results using left V1 as seed region (green circle). The map indicates the brain areas that show stronger functional connections with left V1 for Haptic exploration as compared to Visual imagery. The map is overlaid on the average cortical surface.
Note: Results are shown at $p < 0.05$ uncorrected. Clusters in parietal (pIPS, aIPS) and premotor (vPM) cortices did not survive Cluster-threshold correction.

3.3.4 Vividness of visual imagery

Overall, participants' performance in the VVIQ demonstrated average visual imagery ability (mean VVIQ score: 62.04; SD: 8.5; range: 47-75). Note that higher values indicate greater imagery vividness. We found a significant positive correlation between decoding accuracy in the Visual imagery condition and imagery vividness scores in left preSMA ($r(22) = .43$, $p < 0.05$; Fig. 7A). None of the other ROIs showed a significant correlation. In addition, we found a significant negative correlation between VVIQ scores and decoding accuracy in the Haptic exploration condition in right M1/S1 ($r(22) = -0.47$, $p < 0.05$; Fig. 7B). No significant correlation was found in the other ROIs. None of our ROIs showed a significant correlation between VVIQ scores and Cross-decoding accuracy. All Pearson's correlation coefficients (r) and statistical significance values are reported in Supplementary Table 3.2.

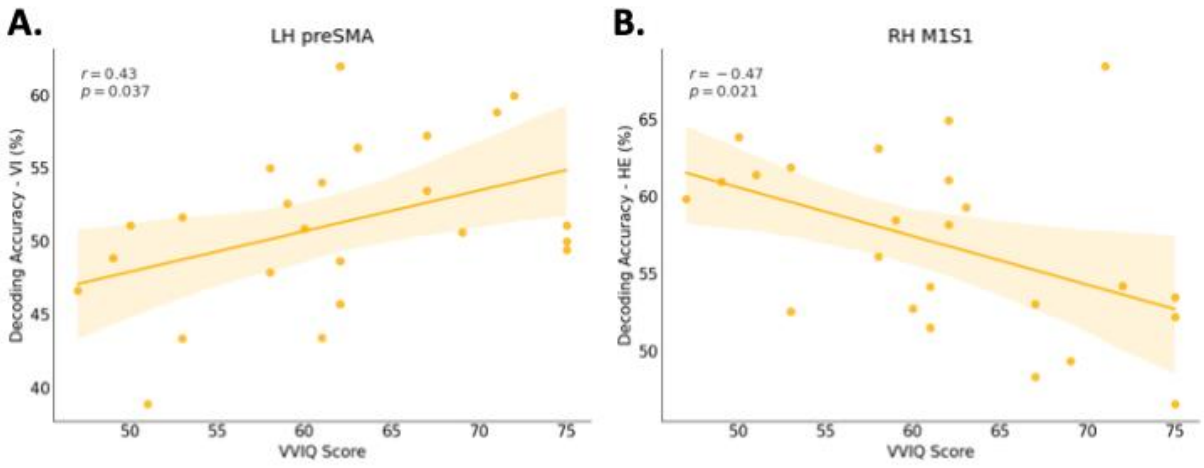

Figure 7. Correlation between VVIQ scores and decoding accuracy (%).
A. The scatterplot shows the correlation between the average decoding accuracy (%) for visually imagined size and the average VVIQ score of each participant, in left preSMA. **B.** The scatterplot shows the correlation between the average decoding accuracy (%) of haptically explored size and the average VVIQ score of each participant, in right M1S1. In both Panels, Pearson's correlation coefficient (r) and statistical significance are also shown on the top left. The translucent band around the regression line represents 95% confidence interval (CI). HE: Haptic Exploration; VI: Visual Imagery.

3.4 Discussion

Previous research has shown that haptic exploration of objects recruits early visual areas, despite the absence of concurrent visual input (Merabet et al., 2007; Monaco et al., 2017; Singhal et al., 2013; Snow et al., 2014). However, the specific aspects of haptic processing that drive this activation in EVC remain unclear. Here, we used MVPA to examine whether the dimension of haptically explored stimuli can be decoded based on the activity patterns in EVC, as well as in the action and perception networks. We also examined whether this effect could be related to visual imagery. Our results revealed that activity patterns in occipito-temporal areas, including early visual areas such as OP and V1, as well as in frontal and parietal areas, allowed discriminating the sizes of haptically explored stimuli. Interestingly, the lack of imagined size decoding in the EVC suggests that the current findings are not driven by visual imagery. In contrast, haptically explored and visually imagined stimulus size could be decoded in LOtv, a multisensory area in the ventral visual stream, along with associative areas in frontal and parietal cortices, such as SMA, dPM, aIPS, and pIPS, suggesting that these regions flexibly represent size information based on task demands. We also performed cross-decoding to identify brain regions that potentially store a representation of size shared across the two tasks. This analysis yielded significant results in dPM, aIPS, and pIPS, indicating the existence of an abstract representation of size. Interestingly, in these areas haptic information still provides a more precise representation than the abstract one.

Taken together, these results not only provide evidence that EVC is recruited during haptic exploration of objects, but also demonstrate that stimulus dimensions can be discriminated based on activity patterns in the visual cortex despite the lack of visual input, and that this information cannot be merely attributed to visual imagery. Our findings also give an overview of the brain networks supporting the representation of stimulus size both within and across Haptic exploration and Visual imagery. Specifically, while haptically explored size can

be decoded in early visual areas, higher-order parietal and premotor regions encode size information across the two tasks. This suggests that these regions may play a pivotal role in abstracting perceptual representations independently of the task modality. In line with this view, IPS has been associated with the processing of object-related features (Konen & Kastner, 2008; Mruczek et al., 2013; for a review, see Erlikhman et al., 2018) and with multisensory processing mechanisms (Huang & Sereno, 2018). Additionally, dPM area has been found to process both intrinsic and extrinsic object properties (e.g., size and location), which are relevant for accurately positioning our digits during grasping actions (Monaco et al., 2015).

3.4.1 Occipital and temporal areas

So far, several neuroimaging studies have investigated the role of visual areas in haptic object exploration without visual input. However, most of these studies have used a univariate approach, which reveals whether an area is engaged during haptic exploration but does not provide information about the content-specific nature of the elicited activity patterns. Moreover, the majority of these previous studies has focused on haptic shape (Monaco et al., 2017; Snow et al., 2014), texture (Eck et al., 2013; Sathian et al., 2011; Stilla & Sathian, 2008), and dot patterns processing (Merabet et al., 2007), leaving the neural mechanisms underlying haptic size processing relatively underexplored. Yet, object size is critical, as it is an inherently relevant object property that guides hand actions.

Evidence from several neuroimaging studies supports the involvement of visual cortical areas in haptic shape processing, including LOC in the ventral visual stream and EVC (Lee Masson et al., 2016; Monaco et al., 2017; Snow et al., 2014). Further, the occipital cortex has a modality-independent representation (i.e., shared across haptic and vision) of basic shape features like curvature and rectilinearity (Tian et al., 2023). Interestingly, haptic exploration of object shape in the dark also activates the foveal representation in the OP (Monaco et al., 2017). This suggests that tactile information about the shape of objects can recruit high-acuity visual

processing areas, even when objects are explored in the absence of visual input. Our results extend these findings by showing that LOtv, V1, and OP are engaged during haptic exploration of stimuli in blindfolded participants, and that haptic size information is represented in these areas. The representation of haptic size in LOtv is in line with the known foveal representation in this region and may reflect cross-talk between the broader lateral occipital complex and the OP. Despite evidence of haptic information content being represented in early and higher-order visual areas, their causal role in haptic perception remains unclear. Causal evidence from a patient with bilateral LOC lesions has challenged the notion that the ventral visual stream plays a critical role in haptic object recognition. Notably, despite the absence of LOC activation, the patient exhibited intact haptic shape recognition and preserved activation in regions of the dorsal visual stream (Snow et al., 2015). This dissociation suggests that, although LOC is fundamental for visual size processing in neurologically intact individuals and is engaged even earlier than the EVC (Zeng et al., 2020), LOtv, a subregion of LOC, is recruited during haptic tasks but may not be essential for haptic recognition. We found haptic size representation also in ITS, a ventral visual stream area involved in object recognition. This result is in agreement with a previous univariate fMRI study (Merabet et al., 2007), which showed that tactile exploration of raised-dot patterns recruited brain regions including V1 and, to a lesser extent, a region in the ventral occipital and inferior temporal cortex (ITC). Overall, these findings support the idea that both early and higher-order visual cortical areas contribute to haptic information processing, regardless of the specific task (i.e., haptic exploration of size, shapes, or dot patterns).

Although a recent study has investigated the brain regions involved in representing haptic size information (Perini et al., 2020), a direct comparison between haptic exploration and visual imagery of differently sized stimuli, especially in early visual areas, has not yet been examined. More specifically, Perini et al. (2020) examined the brain regions involved in haptic

judgements of object size by applying searchlight MVPA to fMRI data. The authors found that areas of the IPS and the lateral prefrontal cortex contain a representation of haptic size that is independent of the hand used (either left or right). However, they did not find such representations in occipital and temporal areas. As the authors pointed out, one possible explanation is that the occipital and temporal lobes were not fully covered during fMRI data acquisition in some participants. As such, the lack of data from these areas makes it difficult to draw conclusions on the role of ventral visual stream areas in encoding haptic size information from their study. Additional methodological differences could also account for the discrepancy in results compared to our study. For example, while Perini et al. (2020) asked participants to perform a haptic size comparison task using either hand with a movement similar to a pincer grasp, in our experiment participants explored three differently sized rings using the thumb and index finger of their dominant right hand. These methodological differences may have contributed to the detection of haptic size information in the occipital and temporal cortices.

One possible explanation for the involvement of visual areas in haptic object perception is that their recruitment is mediated by top-down visual imagery processes and, therefore, may not be essential for haptic processing.

In line with this hypothesis, an fMRI study by Lee Masson et al. (2016) showed that haptic shape representations could be detected in the EVC and the right LOC, but only when participants had prior visual experience with the objects. Based on this evidence, the authors proposed that top-down mechanisms may engage visual imagery to support haptic shape processing. As for the role of EVC in visual imagery and perception, a recent fMRI study using voxel-wise encoding models, revealed that neural representations in early visual areas (like V1) during imagery resemble those activated during actual visual perception, not only for simple, Gabor-like features (i.e., oriented edge-detection features), but also for more complex ones (Huang et al., 2023). This supports the idea that imagery and perception share overlapping

neural substrates in the EVC. However, while this may be true for visual perception, the same might not apply to haptic perception in the EVC. Furthermore, although it may be tempting to attribute the significant Haptic size decoding in early visual areas to visual imagery, our results show that visually imagined size cannot be accurately decoded in either V1 or OP. Besides, we found a significant difference between the accuracy of Haptic and Visual imagery size decoding in left OP and right V1. It is important to note that the absence of Visual imagery size decoding in early visual areas may reflect the fact that participants never had visual experience of the stimulus, neither before nor during the experiment. It might also be argued that the lack of significant visually imagined size discrimination based on activity patterns in these areas is likely due to a lower signal-to-noise ratio in the Visual imagery than Haptic task. Another possible interpretation of the results in the EVC is that the Haptic exploration task does involve visual imagery to some extent, as imagery may be facilitated by the tactile referent making Haptic size decoding more robust and significant. Along the same lines, the lack of tactile input during the pure Visual imagery task might hamper decoding of visually imagined size. However, if this were the case, we would expect Visual imagery size decoding to be similarly unreliable across all ROIs. Instead, we found significant decoding of visually imagined size in ventral and dorsal stream regions such as the left LOtv, SMA, bilateral dPM, and IPS, indicating that the imagery signal was robust enough to yield significant decoding in brain regions that are known to be involved in imagery representations. In addition, if tactile information was sufficient to boost visual imagery during the Haptic task, then significant cross-decoding should occur whenever both Haptic and Visual imagery size decoding are significant as the visual imagery component should be present in both conditions. Yet, the fact that both left SMA and left LOtv showed successful decoding of visually imagined and haptically explored size, but not across tasks makes it unlikely that the tasks share similar representational content represented by visual imagery.

We found no significant correlation between VVIQ and Visual imagery size decoding in the EVC. This result is in line with previous findings showing a lack of correlation, in the EVC, between VVIQ and pure visual imagery decoding of common objects varying in orientation, shape, and colour (e.g., car, lamp, umbrella, etc.), although a significant correlation was found between VVIQ and the decoding across visual imagery and visual perception (Lee et al., 2012). The lack of correlation in EVC supports the idea that activity patterns might not reflect the subjective offline evaluations regarding the vividness and strength of visual imagery. One possible explanation for the lack of correlation is associated with the different nature of the visual imagery content assessed with VVIQ and the one required by our Visual imagery task. While our stimuli might be so basic that participants did not have to summon effortful visual imagery to mentally visualize them, the VVIQ assesses the ability to vividly visually imagine more complex scenes and objects. Therefore, the vividness of one's visual imagery as assessed by the VVIQ might not correlate with the decoding accuracies of imagined size of basic stimuli. However, we found a significant correlation between VVIQ scores and Visual imagery size decoding accuracies in left preSMA which provides evidence against this interpretation. Another possibility is that the lack of correlation might be due to the fact that participants were never allowed to view the stimuli. With no prior visual experience, it may have been difficult for them to generate visual mental images of the rings, even if we instructed them to engage in visual imagery. Nevertheless, the haptic size representation observed in early visual cortical areas in our study cannot be explained entirely by visual imagery.

Interestingly we found that the left LOtv stores a flexible representation of object size that is independent of whether participants were imagining or haptically exploring the stimuli. This finding indicates that the left LOtv encodes size-based spatial information in a format that is not strictly bound to one task modality, but rather, is available as a size-related magnitude representation accessible across tasks. Notably, such size-sensitive regions may share a

common functional architecture with temporal lobe networks that specialize in the processing of allocentric, object-centered spatial information. For example, Schenk (2006) showed that patient D.F., who suffers from bilateral ventral stream lesions, exhibits an allocentric rather than a purely perceptual deficit, implying that object-based spatial metrics (e.g., relative position and size in space) processed in the ventral visual stream are crucial for certain types of visuomotor tasks. Likewise, the frameworks proposed by Goodale and Haffenden (1998) and further elaborated in Milner and Goodale's reviews (2006, 2008) emphasize that distinct neural streams, including those in the temporal lobe, preferentially process spatial metrics that afford object-centered (allocentric) reference frames. Taken as a whole, these findings reinforce the idea that the left LOtv may be part of a broader network of size-sensitive regions that encode spatial information in an object-based (allocentric) manner, that is accessible across both imagery and haptic modalities.

While there is evidence showing that LOtv is a multimodal area processing both visual and tactile information (Lacey et al., 2009), there is no clear evidence for its involvement in imagery processes. Previous work has shown that LOC, which contains LOtv, is involved in imagery of haptically explored shapes (Lee Masson et al., 2016; Zhang et al., 2004). In a recent review, Spagna et al. (2024) have proposed a heterarchical neural architecture at the basis of visual imagery which involves both domain-general and domain-specific neural mechanisms. The authors identified a region in the left mid-fusiform gyrus, along with frontoparietal areas, as core components of the network supporting visual imagery regardless of the semantic domain (e.g., faces, colours, shapes imagery). Moreover, the authors provided evidence that imagery and visual perception recruit similar cortical regions both in the ventral and dorsal visual streams if the content is from a preferred domain (e.g., fusiform face areas for faces and parahippocampal place area for places; O'Craven & Kanwisher, 2000). While Spagna et al. (2024) highlighted the shared engagement of domain-preferring regions during visual

perception and imagery, our findings extend this framework by showing that a shape selective region in the ventral stream, such as LOtv, supports both visual imagery and haptic perception through distinct neural mechanisms.

Why would the EVC and ventral stream areas, known to primarily process visual information, code the size of haptically explored stimuli? It is possible that the visual system predicts and simulates the expected size of a haptically explored object based on prior experience, in order to assess whether the haptic input matches the internal visual prediction and, if not, update the internal model accordingly.

Predicting an object's visual size from haptics is computationally efficient, and since we often use vision to confirm what we touch, the visual system may be deeply embedded in this prediction loop. In our daily life, we often see what we touch, leading to frequent co-activation of visual and somatosensory cortices. As such, it is possible that signals from one sensory modality trigger activation also in other sensory areas. Hence, the recruitment of EVC for non-visual, haptic tasks is likely due to feedback signals coming from sensory-motor brain regions, as indicated by the results of the PPI analysis.

The occipitotemporal cortex contains neural representations of the real-world size of visually presented objects (Coutanche and Koch, 2018), suggesting that semantic information might also play a role. To minimize potential semantic processing related to ring size we used letter-based instructions which were randomly assigned to size conditions across participants. Moreover, semantic information is typically linked to object identity, whereas in our study the stimuli were simple geometric shapes (i.e., rings) with the same identity. If our rings had been associated with real-world objects of corresponding sizes, thereby engaging semantic size processing during both the Haptic exploration and Visual imagery tasks, we would expect significant decoding of size in the Visual imagery condition and possibly also in the Cross-decoding condition, particularly in early visual areas but not in more anterior temporal regions,

in line with the study by Coutanche and Koch (2018). This pattern contrasts with our findings, making a semantic explanation unlikely.

3.4.2 Frontal and parietal areas

Our Haptic exploration task required the active movement of the thumb and index finger to extract size-related features. These movements inherently demand the dynamic coordination of finger aperture and trajectories, which varied slightly across our differently sized stimuli. The acquired sensory inputs are integrated within the haptic system, known to be subserved by a network of frontal and parietal regions (James et al., 2007; Sathian, 2016). Consistent with this notion, we observed successful decoding of stimulus size based on Haptic trials across all frontal and parietal ROIs. Specifically, Haptic size decoding in M1/S1 likely reflects a combination of afferent cutaneous and proprioceptive input, as well as kinematic differences related to the motor execution of exploration strategies for the three different sizes, such as adjustments in grip aperture and spatial scaling of finger movements. Interestingly, right M1/S1 showed a significant negative correlation between vividness imagery scores and Haptic size decoding accuracy. This result suggests that participants with higher vividness of visual imagery, compared to those with low imagery vividness, have a haptic size representation that is likely less dependent on motor and somatosensory information. Instead, participants who score low on VVIQ might rely more on haptic and kinesthetic information to represent size information when haptically exploring it.

Beyond M1/S1, successful decoding of haptic stimulus size was also observed in a distributed frontoparietal network, notably including bilateral dPM and vPM, aIPS and pIPS, SMA, and preSMA. This pattern partially aligns with previous findings showing that these regions, especially aIPS, dPM and SMA, are involved in processing intrinsic object properties, such as size, and integrating them with action-relevant spatial information during grasping (e.g., Monaco et al., 2015), making them key regions for sensorimotor transformations. Specifically,

decoding in aIPS and pIPS is especially informative. Here, we observed successful decoding of size not only in Haptic but also Visual imagery trials, and across the two tasks. The IPS is well-known for its role in sensorimotor integration as well as in visual imagery (Spagna et al., 2021). Interestingly, both regions have also been implicated in supramodal encoding of spatial and metric object features (Reed et al., 2005; Stilla & Sathian, 2008), suggesting a high-level representation of properties such as size that transcends input modality. Furthermore, Harvey et al. (2015) found that the human parietal cortex contains topographic maps for visually processed object size, similar to those for numerosity. These maps overlap, though not completely, suggesting a spatial organization that is shared across different types of quantity information. This further supports the role of the IPS in abstract processing of size information. Therefore, the engagement of the IPS during both haptically explored and visually imagined size conditions, and across conditions, is consistent with its role as a hub where multimodal spatial information converge into a unified representation that is also accessed during visual imagery. The successful decoding of size in the dorsal visual stream aligns well with neuropsychological data from patients with ventral visual stream lesions. In particular, patients with severe visual agnosia resulting from bilateral ventral pathway damage showed spared recognition of graspable objects, but only when their physical size matched the expected real-world size (Holler et al., 2019). Although this study did not investigate haptic perception, their finding is in line with our results showing more widespread size decoding in dorsal than ventral visual stream areas, as the dorsal visual stream links visual and real-world action-related object information.

The dPM also showed robust decoding not only within both Haptic and Visual imagery trials, but also across the two tasks. Although dPM is not consistently engaged during visual imagery across studies (Spagna et al., 2021), it is possible that when participants imagine the size of circles, an interaction between visual and somatosensory representations occurs to create

a spatial or metric map in the brain. This process could involve regions like the IPS and possibly the dPM, depending on the task context. The observed size decoding across Haptic exploration and Visual imagery tasks in dPM aligns with the multimodal functions attributed to the premotor cortex (Hardwick et al., 2018).

The size of a stimulus is indicative of whether and how an object can be grasped and manipulated, and helps predict its weight. This information is essential for planning accurate grasping movements. As such, the abstract representation of size is unsurprising in areas that are well-known to be involved in grasping actions, such as aIPS, pIPS, and dPM (for reviews, see Culham et al., 2006; Gallivan & Culham, 2015). These findings reinforce the idea that the degree of content-similarity (stimulus size) across tasks (Haptic exploration and Visual imagery) is strongly dependent on the degree of specialization of a brain area in processing that particular content for action, such as the aIPS, pIPS, and dPM for grasping movements.

Interestingly, the left SMA showed decoding of haptically explored but also imagined size, although no cross-modal size decoding was found here. This pattern of results was also observed in left LOtv, suggesting that both regions represent size-related magnitude information in a context-dependent way. Our results align with previous research showing that the left SMA is involved in visual imagery (for a meta-analysis, see Spagna et al., 2021). In addition, they also reveal that the higher the Visual imagery size decoding accuracy in the left preSMA, the greater the visual imagery vividness. These findings are consistent with the prominent role of frontoparietal areas in sustaining imagery over time, as this process relies on working memory mechanisms supported by the same frontoparietal, especially prefrontal, networks (Miller et al., 2018). The preSMA is strongly involved in motor imagery (for a meta-analysis, see Hardwick et al., 2018) and the SMA proper exerts a strong inhibitory effect on the forward connection to M1 during motor imagery (Kasess et al., 2008). This mechanism is likely

responsible for preventing the execution of internally simulated actions and might also involve the preSMA along with the SMA proper.

3.4.3 PPIs: functional connectivity during the Haptic task

The representation of size information in the EVC is likely due to the stronger functional connections during the Haptic exploration than Visual imagery task with areas involved in multimodal perception, like the LOtv (Amedi et al., 2001), and haptic shape processing of objects for subsequent actions, like the aIPS (Króliczak et al., 2008; Marangon et al., 2016; Monaco et al., 2017). The functional connection between the EVC and ventral and dorsal stream areas has already been found during haptic shape exploration in the dark (Monaco et al., 2017). Here, we confirm and extend those findings by showing that haptic size processing is also supported by functional connections between the EVC and ventral as well as dorsal visual stream areas, and premotor cortex.

3.4.4 Limitations

One limitation of the current study is related to the possible recruitment of mental motor imagery during our Visual imagery task. Although we specifically asked our participants to visually imagine the size of the stimulus they had previously explored, we cannot completely rule out the possibility that participants, even involuntarily, also visually imagined the exploratory movement associated with a given size. In fact, while they did not have any prior visual experience of the stimulus, they could still rely on previous haptic experience with the same stimulus, which, in turn, could have helped them create a visual mental image of the associated size during the Visual imagery task. Additionally, participants may have engaged in tactile imagery as the major source of information about the stimulus was the haptic system, as discussed in sections 2.2. and 4.1.

3.5 Conclusions

By applying MVPA to fMRI data, we demonstrated for the first time that information about stimulus size can be decoded not only during haptic exploration but also during visual imagery of unseen stimuli. First, we found that early visual areas, including V1 and OP, successfully decoded haptic but not visually imagined size, suggesting that haptic processing in the EVC does not simply reflect visual imagery of the haptically explored stimulus. Instead, higher-order and associative regions, such as LOtv, aIPS, pIPS, dPM, and SMA, showed overlapping but distinct representations of size for both Haptic and Visual imagery tasks. Second, cross-decoding yielded significant results in parietal and premotor areas, including dPM, aIPS, and pIPS, thus suggesting the existence of an abstract representation of size that is independent of the task demands. Overall, these findings advance our understanding of how the brain represents object properties when we haptically explore and visually imagine them. While the EVC represents haptic size information, associative areas show overlapping but distinct representations of haptic and visually imagined size, respectively. Last, but not less important, the premotor and parietal cortices have a shared representation of size.

Chapter 4

Behavioural relevance of foveal cortex processing for haptic size estimation

The content of this chapter is going to be submitted to the Journal of Experimental Psychology: Human Perception and Performance.

Abstract

Recent evidence points to a role of the early visual cortex (EVC), including the primary visual cortex (V1), in haptic processing, even in the absence of visual input. However, it remains unclear whether V1 plays a functionally relevant role at the behavioural level. To this aim, we conducted three behavioural experiments to investigate whether: i) size estimates of haptically explored stimuli are influenced by stimulus location relative to gaze direction and body midline; ii) the EVC is functionally relevant for haptic size processing. To this aim, we asked participants to use their right-dominant hand to haptically explore differently sized cylinders placed behind a monitor, while fixating a cross. Participants were then instructed to manually estimate the size of the explored stimulus. Size estimates and their variability were not modulated by the location of the exploring hand and the stimulus relative to neither gaze direction nor body midline (Experiment 1). When dynamic foveal visual noise was presented in central vision during haptic size exploration to interfere with processing in the foveal cortex, size estimation was larger as compared to the no-noise baseline condition, suggesting a size estimation bias when noise is present (Experiment 2). Further, foveal noise increased variability but not the average of size estimates when we increased task difficulty (Experiment 3). While the results of Experiment 1 show that hand location relative to gaze direction and body midline does not influence haptic size estimation, Experiments 2 and 3 suggest that the foveal cortex supports haptic size estimation although future research is needed to replicate our findings and better understand the underlying neural mechanisms.

keywords: manual size estimation, foveal visual noise, early visual cortex (EVC), functional relevance, reference frames

4.1 Introduction

Although vision is the dominant sense to perceive the world around us, we often rely on haptic perception to generate representations of object properties like shape, size, or texture. Haptic perception involves the integration of both cutaneous and kinesthetic inputs and plays a central role in the human motor control system. In fact, it allows us to process several physical properties of objects that are relevant for planning and executing actions to successfully interact with them. Haptic processing is supported by various brain structures, including the ventral posterior lateral nucleus of the thalamus where sensory signals are then relayed to higher-order cortical regions like the primary somatosensory cortex (SI), secondary somatosensory cortex (SII), insula, and superior parietal lobule (Hsiao & Yau, 2008). Interestingly, also the early visual cortex (EVC), including the primary visual cortex (V1), seems to play a role in haptic object processing (Sathian, 2016). However, it remains unclear whether V1 plays a functionally relevant role at the behavioural level.

The involvement of the EVC in haptic processing has been demonstrated by neuroimaging studies on sighted individuals performing different haptic and motor tasks in the absence of concurrent visual input. For instance, V1 was found to be recruited during tactile processing of raised-dot patterns (Merabet et al., 2007), haptic exploration of object shape (Marangon et al., 2016; Monaco et al., 2017; Snow et al., 2014), and execution of delayed actions in the dark towards stimuli that had been previously seen or touched (Monaco et al., 2017; Singhal et al., 2013). Interestingly, multivoxel pattern analysis (MVPA) further revealed that haptically explored object properties are represented in early visual areas, like haptic shape and size (Lee Masson et al., 2016; Sartin et al., 2026). While these studies indicate the involvement of EVC in haptic tasks, they do not inform us about the possible functional relevance of early visual areas for haptic behaviour. To gain information about the behavioural significance of a brain area, we need to perturb activity within that area to assess whether this

causes a change in behaviour. If so, this would provide evidence for the functional significance of the given brain area for the behaviour under investigation. In this regard, lesion approached (both irreversible and reversible, i.e., single-case studies and non-invasive brain stimulation (NIBS) techniques, respectively) are among the available tools that enable us to investigate the functional relevance of brain areas for given behaviours.

Patient M.C., with extensive bilateral occipitotemporal infarctions, showed preserved haptic shape recognition despite only a small region of tissue in the occipital lobe (representing peripheral vision) being spared from the lesion (Snow et al., 2015). This finding suggests that the lesioned cortical visual areas, including the lateral occipital complex (LOC) which is involved in both visual (Grill-Spector et al., 2001) and haptic (Amedi et al., 2001) shape processing, are not necessary for object recognition through touch. As the authors point out, preserved haptic shape processing might also reflect potential cortical reorganization such that intact cortical areas functionally similar and near to LOC could be recruited to compensate for haptic shape processing (Snow et al., 2015).

In contrast with patient work, previous NIBS studies in neurologically intact, sighted participants showed that transient disruption of the visual cortex interferes with fine tactile discrimination, providing causal evidence that visual cortical areas support the processing of tactile object properties in a functionally relevant manner (e.g., Amemiya et al., 2017; Bola et al., 2019; Merabet et al. 2004, 2008; Siuda-Krzywicka et al., 2016; Zangaladze et al., 1999). This discrepancy might indicate that, while visual cortical areas are not necessary for haptic shape recognition possibly due to long-term neural reorganization after a brain lesion, they may still be recruited and necessary for accurate haptic information processing in people with no neurological deficits. However, it remains unclear whether the EVC is behaviourally relevant for more complex haptic tasks, like haptic estimation of object size.

While many studies have explored how visually guided hand movements rely on coordinates linked to the eyes, head, body, and hand (Batista, 2002), the ways in which these coordinates influence haptically guided responses have been less investigated. Yet, there is evidence that the visual and haptic systems interact during grasping actions towards previously haptically explored objects. For instance, fingers' kinematics of grasping movements towards haptically explored, occluded stimuli have been found to be affected by gaze direction despite the absence of stimulus-related visual input (Pirruccio et al., 2020). Therefore, gaze direction might similarly affect perceptual manual size estimation of haptically explored, unseen cylinders.

As such, we aimed at extending previous findings in three main directions: 1) by examining whether and how gaze direction and hand location might influence participants' size estimates, 2) by investigating the functional relevance of the EVC for manual size estimation of haptically explored objects, and 3) by using a behavioural paradigm that physiologically disrupts processing in the visual cortex, including V1, via a dynamic patch of visual noise presented in fovea, while participants haptically explored the size of the occluded stimuli. If haptic information processing recruits the EVC in a functionally relevant way such as to support size estimation, then the dynamic visual noise should compete with haptic size information processing and consequently interfere with haptic size estimates.

Therefore, in Experiment 1 we explored whether hand location relative to gaze direction and body midline influences haptic size estimation. Is manual size estimate, in absence of visual information, more accurate or precise when the location of the exploring hand is aligned with the gaze or body midline as opposed to when it is not? The purpose of this study was twofold. First, the study aimed at assessing whether haptic size information is influenced by the location of the exploring hand relative to gaze, body midline or both. Indeed, the properties of haptically explored stimuli can be memorized for subsequent object manipulations by storing a mental

representation of the object. This representation engages not only somatosensory areas, but also the early visual cortex (Sartin et al., 2026). Therefore, if the haptic system uses size information stored in retinotopic coordinates in the visual cortex, then the retrieval of such information might depend also on eye position. Similarly, if the haptic system uses size information stored in body-centered coordinates, then the retrieval of this information might depend on body coordinates. While Pirruccio et al. (2020) have shown that systematic finger configuration errors during a grasping task toward previously haptically explored unseen stimuli depend on gaze direction, it remains unclear whether this effect generalizes to perceptual manual estimation and extend to a coordinate system centered on body midline. We hypothesize that these biases might reflect a fundamental property of haptic representations within the egocentric reference frame. Specifically, if haptic size is represented within a coordinate system that is more precisely calibrated at gaze direction or at the body midline and becomes distorted toward the periphery, then a misalignment between the relevant anchor (gaze or body midline, or both) and the exploring hand should result in a systematic scaling or estimation error. In addition, we analyzed the variability of manual size estimates to assess whether misalignment also reduces the precision of the haptic representation. In fact, previous evidence has shown that uncertainty of perceptual estimates is reflected in higher variability (Ernst & Banks, 2002; Niechwiej-Szwedo et al., 2022). Therefore, we hypothesized that the variability of size estimates would be higher when the hand is not aligned with the body midline or gaze direction as opposed to when it is. While an increase in variability would indicate higher sensory noise or uncertainty during coordinate integration, a systematic bias would point toward a distortion in the underlying spatial map. By using a manual size estimation task, we aim to investigate whether coordinate-dependent biases are a general feature of haptic spatial representation rather than a phenomenon limited to object-directed hand movement, and whether the precision of perceptual size estimates might be affected as well. Second, this experiment allowed us to define the

experimental setup and paradigm for the subsequent behavioural studies (Experiments 2 and 3) with an ideal configuration of hand location relative to gaze direction and body midline, in order to control for the effects of additional variables other than foveal noise on haptic size estimation.

The aim of Experiment 2 was to investigate whether foveal noise affects haptic size estimation of previously haptically explored, occluded stimuli, aligned with both body midline and gaze direction. The hypothesis we wanted to test is that, if V1 is functionally relevant for perceptual size estimation of haptically explored objects, then the introduction of noisy visual information in fovea while participants haptically explore the size of the stimulus should interfere with accurate encoding of haptic size information, thus modulating participants' manual size estimates. Specifically, we investigated whether the recruitment of the primary visual cortex (V1) during haptic processing of the size on unseen cylinders is behaviourally relevant. To do so, we asked our participants to haptically explore the size of occluded cylinders of different widths, followed by a manual size estimation task. To test for the behavioural relevance of V1 for haptic size processing, we presented a patch of dynamic visual noise in the fovea while participants haptically explored the occluded cylinders. We then compared the manual size estimation performance in the noise trials with performance in baseline no-noise trials to test whether foveal noise might affect haptic size estimation. Previous studies showed that foveal visual noise impairs peripheral object discrimination by interfering with task-relevant feedback from higher-order visual areas to the foveal cortex in V1 (Fan et al., 2016), thus providing evidence for the role of the foveal cortex in the processing of objects presented in the periphery (for a review, see Stewart et al., 2020). As such, we adapted the visual paradigm used by Fan et al. (2016) to test our hypothesis on the role of V1 in haptic size processing, despite the absence of any stimulus-related visual input. Finally, the aim of Experiment 3 was to examine whether the effect of foveal noise on haptic size processing and manual size estimation would persist under more constrained conditions, including a more difficult task

(i.e., increased number of stimuli with sizes differing to a small extent between each other) and a smaller foveal noise precisely interfering with processing of visual information within the perifoveal region of the visual field. We hypothesized that if V1 contributes to haptic size processing in a functionally relevant manner, then we would expect the visual noise interference effect to persist or even increase under high-demand conditions as finer discrimination and higher precision are needed to distinguish very similar stimuli within a narrow range of sizes. Specifically, since the higher task demands in Experiment 3 require fine haptic discrimination, we expect haptic size processing to rely on the foveal region, whereas high spatial resolution might help refining the spatial details of size representations. By reducing the retinal extent of the visual noise, we tested whether the noise-related interference was: i) specific to the retinotopic location of the stimulus, or ii) related to a broader and more general disruption of early visual cortical processing. In addition, we hypothesized that the increased demand for precision would make haptic size processing even more susceptible to spatially specific disruptions in V1.

4.2 Experiment 1

4.2.1 Participants

A total of 30 healthy volunteers participated in Experiment 1 (18 females; age: M_{age} = 22.80 years, *SD* = 4.12, range 18-38). We excluded the data of one subject from the analyses due to technical problems during the experiment. All subjects were right-handed and had normal or corrected-to-normal vision. All participants provided their written informed consent after the study procedures were explained. The experimental procedures were approved by the Research Ethics Committee of the University of Trento (Ethics protocol n. 2021-040).

4.2.2 Stimuli and apparatus

We used three-dimensional (3D) stimuli which consisted of three plastic cylinders of different widths. Each object had magnetic tape attached to its base such that we could place the stimulus on an inclined metal panel positioned on the top of an adjustable support placed behind the monitor (Fig. 1a). This configuration ensured that participants never saw the stimuli neither before nor during the experimental session. The cylinders had a diameter of 20 mm (small), 40 mm (medium), and 60 mm (large). While the three stimuli were included in the design, the main analyses were restricted to small and large stimuli. The medium sized stimulus was used as a catch stimulus to prevent participants from adopting a binary "small/large" response strategy when exploring and later estimating stimulus sizes. In addition, we included fewer trials for the medium as opposed to the other stimuli to keep the total duration of the experimental session within a feasible range while avoiding participants' fatigue, which could have hampered performance throughout the experimental session. As such, by focusing the analysis on small and large stimuli, which included a balanced number of trials, we ensured stronger statistical power and unbiased results for our statistical comparisons while preventing participants from using a simple binary strategy to perform the task. All stimuli were 3 cm high. We designed the stimuli using Autodesk Fusion 360 (Autodesk, Inc., 2021) and we then printed them using a 3D printer (UltiMaker 2+ Connect).

Throughout the experiment, participants had their chin fixed on a chin rest while sitting in front of an LCD (Liquid Cristal Display) monitor with a frame rate of 59.95 Hz, a resolution of 1,920 × 1,200 pixel, and a size of 52 × 32.4 cm, with a viewing distance of ~28 cm. During the experiment, participants maintained fixation on a cross displayed on the monitor and aligned with their body midline or displaced by ~15° visual angle to the right of the body midline. The stimulus attached on the platform behind the monitor could be aligned with the participant body midline or shifted to the right by~15°. The fixation cross and the stimulus could either be

aligned with each other or misaligned. We ensured the alignment between the fixation point and the stimulus using a laser pointer which defined the point in space where gaze would fall both on the screen and behind it. The experimental paradigm was programmed in MATLAB R2020a, using the Psychophysics Toolbox extensions (i.e., PsychToolbox version 3.0.16; Brainard, 1997; Pelli, 1997). A QWERTY keyboard was connected to the main computer. Two speakers were placed on each side of the monitor to deliver auditory cues throughout the experimental session.

We used a digital calliper to accurately measure participants' manual estimates, which allowed a sensitivity of measurement as small as 0.01 mm (0.0005 inch). In particular, we measured the distance between the tips of the thumb and index finger. Before the onset of the experiment, an experimenter drew two millimetric dots on participants' thumb and index finger, respectively, of their right hand using a pen. These were used as reference points where to position the digital calliper when, at the end of each trial, participants opened their index finger and thumb to give the estimation of the size of the previously explored object. The aim of this procedure was to obtain measures that were consistent across trials for each participant and, therefore, to minimize the risk of adding variability across measures related to inaccurate measuring procedure.

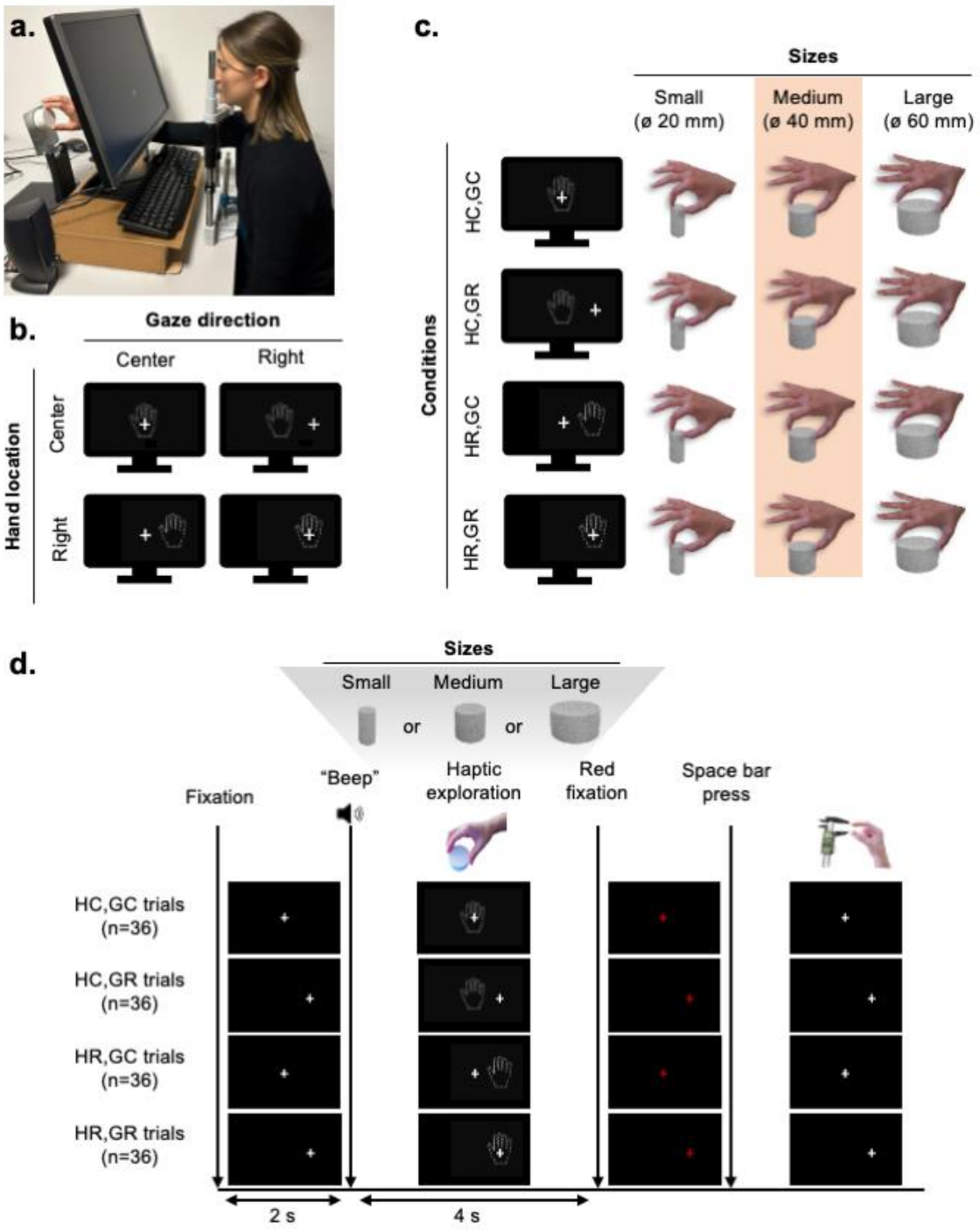

Figure 1. Experiment 1: experimental setup, design, and paradigm.
a. Experimental setup. Participants sat in front a monitor displaying a fixation cross with their chin fixed on a chin rest. The 3D stimuli (i.e., cylinders) were attached to a metal platform located at the top of a reclinable support, which was placed behind the screen. Therefore, participants could never see the stimuli. A keyboard was connected to the main computer and was used to receive participants' input. Auditory cues throughout the experiment were delivered by two speakers placed on the sides of the monitor. **b.** Independent variables of main interest. We manipulated both Hand location relative to Body Midline (aligned at the centre vs. shifted to the right; Hand Centre, HC, and Hand Right, HR) and Gaze direction (at the centre of the screen vs. to the right; Gaze Centre, GC, and Gaze Right, GR, respectively). Therefore, we had 4 experimental conditions: 1) the Hand Centre, Gaze Centre (HC,GC) condition; 2) the Hand Centre, Gaze Right (HC,GR) condition; 3) the Hand Right, Gaze Centre (HR,GC) condition;

4) the Hand Right, Gaze Right (HR,GR) condition. **c.** Schematic representation of the full experimental design. We had a 2×2×3 factorial design with 2 Hand locations (Hand Centre, HC, Hand Right, HR), 2 Gaze directions (Gaze Centre, GC, Gaze Right, GR), and 3 Sizes (Small, Medium, Large; 20, 40, 60 mm in diameter, respectively) resulting in a total of 12 conditions. The medium cylinder was used only in catch trials and therefore not considered for the main analysis. Hence, the final design consisted of a 2 (Hand location) by 2 (Gaze direction) by 2 (Size) factorial design, which yielded 8 conditions in the final analyses. **d.** Schematic representation of the paradigm. The total of 144 trials was divided into 4 experimental blocks of 36 trials each. In two blocks, the hand explored the cylinder which was aligned at the centre with the body midline (HC), while in the remaining 2 blocks the hand reached to and explored the cylinder which was placed to the right of the body midline (HR). Before the onset of each experimental block, participants were told where the target was located. Each trial started with a 2 s-fixation period during which participants were instructed to fixate on a small cross that could appear either at the centre or to the right of the screen. Next, a 'beep' sound signalled the beginning of the exploration phase during which participants were asked to reach and explore haptically with their right hand a cylinder which was placed behind the screen. Participants haptically explored the cylinder for 4 s. The change in colour of the fixation cross from white to red signalled them to release the object and press the space bar on the keyboard. Finally, participants performed the manual size estimation task by opening the thumb and index finger, and their estimates represented by the distance between the fingers were measured by the experimenter by means of a digital calliper.

4.2.3 Experimental design

To test our hypotheses, we asked participants to haptically explore with their right hand the size of unseen cylinders placed behind the monitor while fixating a cross. At the end of each trial, they were asked to provide a manual estimate of the size of the stimulus they had just explored. Therefore, participants' manual size estimates represented our dependent variable.

We manipulated Hand location relative to body midline (aligned with the centre vs. shifted to the right; Hand Centre, HC, and Hand Right, HR; Fig. 1b) and Gaze direction (centre vs. right; Gaze Centre, GC, and Gaze Right, GR; Fig. 1b). As such, we had 4 experimental conditions: 1) the Hand Centre, Gaze Centre (HC,GC) condition; 2) the Hand Centre-Gaze Right (HC,GR) condition; 3) the Hand Right, Gaze Centre (HR,GC) condition; 4) the Hand Right, Gaze Right (HR,GR) condition. Therefore, stimulus Size, Hand location, and Gaze direction were varied over a 3 (Size; Small, Medium, Large) by 2 (Hand location; Centre, Right) by 2 (Gaze direction; Centre, Right) factorial design, resulting in 12 conditions (Fig. 1c). Catch

trials were excluded from further analysis. As such, for the analysis we used a 2 (Size; Small, Large) by 2 (Hand location) by 2 (Gaze direction) factorial design, which yielded 8 conditions.

Each participant performed a total of 144 trials which were split in four blocks of 36 trials each, to allow participants to briefly rest in between separate blocks. In particular, in two blocks the hand was at the centre relative to body midline (HC), while in the remaining two blocks the hand was to the right of the body midline (HR). To deal with blocks' order effects, we identified all the six possible orders of the four blocks and randomly assigned them to our participants, while ensuring that an equal number of participants completed each possible order of conditions' blocks. Each block (either HC or HR) consisted of 8 trials for each of the four Gaze direction x Size combinations (GC,Small; GR,Small; GC,Large; GR,Large), and four trials for each of the two Gaze direction x Size catch conditions (GC,Catch Cylinder; GR,Catch Cylinder). The order of presentation of the six conditions (Gaze direction x Size) was randomized for each experimental block, for each participant.

4.2.4 Experimental paradigm

Before the onset of each experimental block, participants were informed about the location of the platform and the attached stimulus placed behind the monitor (centre or right). At the beginning of each trial, a white fixation cross appeared over a black background either at the centre of the screen (i.e., in HC,GC and HR,GC trials) or to the right (i.e., in HC,GR and HR,GR trials) (Fig. 1d). The cross was displayed for the whole duration of the experiment and participants were instructed to always maintain fixation on it. After 2 *s*, a "beep" sound cued participants to start haptically exploring the size of the stimulus. Specifically, subjects were asked to reach with their right hand the cylinder, which was placed behind the screen in one of the two previously defined locations (i.e., HC, HR). Participants haptically explored the size of the stimulus with the thumb and index fingers until the colour of the fixation cross turned to red after 4 *s*. Therefore, they had to return the hand to the keyboard and press the spacebar, after

which the fixation cross turned to white. This indicated to participants to perform the manual estimation task (Sperandio et al., 2012; Franz, 2003), that is they had to manually report the width of the stimulus they had just haptically explored. Thus, they opened their thumb and index fingers such that the aperture matched the width of the explored stimulus. Their size estimates were measured and recorded by an experimenter using the digital calliper. To start a new trial, participants had to press the spacebar on the keyboard. Subjects ran a short training session of 4 trials for each block type (with HC and HR, respectively) before the experiment to familiarize with the procedures and the task.

4.2.5 Statistical analysis

To have an overview of the size estimates and their variability in each task, we computed a repeated-measures (RM) analysis of variance (ANOVA) on size estimates as well as on the standard deviation of size estimates for each condition and each participant with main factors: 2 Hand locations (Centre, Right) × 2 Gaze directions (Centre, Right) × 2 Sizes (Small, Large). We performed post-hoc pairwise comparisons with Bonferroni corrections to further investigate any significant ANOVA results.

Since previous evidence has shown that uncertainty of perceptual estimates is reflected in higher variability (Ernst & Banks, 2002; Niechwiej-Szwedo et al., 2022), we expected that *SD*s would be higher in those conditions where the hand is not aligned with the body midline or gaze direction (HC,GR; HR,GC; HR,GR) as opposed to when it is (HC,GC). Therefore, we conducted planned paired-samples one-tailed t-tests on *SDs* based on this hypothesis. We used Bonferroni correction for all pairwise comparisons.

Previous work exploring whether gaze direction influences grip aperture during grasping movement towards previously haptically explored objects has shown that fingers configuration errors depend on gaze direction, with systematic higher biases when gaze was not aligned with the grasping hand as compared to when it was (Pirruccio et al., 2020). Based on

these findings, we tested whether gaze and body coordinates have an effect on perceptual size estimation bias. Specifically, we hypothesized a size estimation bias when Hand location and Gaze direction were not aligned with each other (HC,GR; HR,GC), but not when they were aligned (HC,GC; HR,GR), irrespective of Hand and target location relative to Body Midline. We named this Hand-Gaze alignment effect. In addition, we hypothesized a size estimation bias when the Hand location was not aligned with Body Midline (HR,GR; HR,GC), but not when they were aligned with each other (HC,GC; HC,GR), irrespective of Gaze direction. We named this Hand-Body Midline alignment effect. To measure size estimation bias between conditions, we calculated the signed difference in size estimation between misaligned vs. aligned conditions. Positive values would indicate an overestimation of the size of the haptically explored stimuli in the misaligned as compared to the aligned conditions while negative values would indicate an underestimation of the size of the haptically explored stimuli in the misaligned as compared to the aligned conditions. To determine whether the effect of misalignment was robust across the stimulus range, we analyzed size estimation biases for the Small and Large stimuli. This allowed us to assess if the influence of gaze and body coordinates was consistent regardless of the physical size of the haptically explored object. We then performed two-tailed t-tests to evaluate whether size estimation biases for both Small and Large stimuli differed significantly from zero.

Finally, as an indication of whether size estimations accurately scaled with stimulus size, we performed a linear regression analysis relating real and estimated stimulus' sizes in the four experimental conditions (HC,GC; HC,GR; HR,GC; HR,GR). We then compared the 4 slope values resulting from the linear regression using two-way RM ANOVA with Hand location and Gaze direction as main factors. While we focused our main analyses on the Small and Large stimulus sizes to maintain a balanced design, as the Medium stimulus was a catch stimulus and therefore contained fewer trials, in the linear regression analysis we included all three stimulus

sizes (Small, Medium, and Large). This allowed for a more robust evaluation of the linearity of the perceptual size estimates across the full stimulus range.

Data visualization and statistical analyses for all three experiments were conducted in PyCharm (JetBrains, 2023), integrated development environment (IDE) software used for Python programming. Specifically, we used matplotlib 3.5.2 (Hunter, 2007), pandas 1.4.2 (McKinney, 2010), numpy 2.2 (Harris et al., 2020), scipy 1.8.0 (Virtanen et al., 2020), statsmodels 0.14.1 (Seabold & Perktold, 2010), and seaborn 0.11.2 (Waskom, 2021).

4.2.6 Results

The ANOVA on size estimates revealed a significant main effect of Size ($F_{(1,28)}$ = 452.848, $p < .001$, $\eta p^2 = .94$), with higher size estimates for the Large as compared to the Small cylinder. We found no significant main effect neither of Hand location ($F_{(1,28)} = .265$, $p = .610$, $\eta p^2 = .01$) nor of Gaze direction ($F_{(1,28)} = .663$, $p = .423$, $\eta p^2 = .02$). The interaction between Hand location and Gaze direction ($F_{(1,28)} = 3.351$, $p = .078$, $\eta p^2 = .11$), and between Size and Gaze direction ($F_{(1,28)} = 3.551$, $p = .070$, $\eta p^2 = .11$) did not reach statistical significance. Likewise, the Hand location × Size interaction ($F_{(1,28)} = .006$, $p = .938$, $\eta p^2 < .001$) and Hand location × Gaze direction × Size interaction ($F_{(1,28)} = .055$, $p = .816$, $\eta p^2 = .002$) were not statistically significant (Fig. 2a). Since the main effect of Size was significant, we performed post-hoc pairwise comparisons with Bonferroni correction which revealed significant differences between Small and Large sizes within each condition (all $p < .001$ Bonferroni corrected; Supplementary Table 4.1). Since the experiment included a Medium Catch Cylinder which was not included in the primary analysis (see Section 4.2.2), Supplementary Figure 4.1 (Panel a) shows the average size estimates for Small, Medium, and Large stimuli across experimental conditions to provide an overview of participants' manual estimation performance considering all the explored sizes. Full statistical results of the pair-wise comparisons are reported in Supplementary Table 4.6.

To assess the variability of size estimates, we calculated the standard deviation for each condition. A 3-way repeated measures ANOVA with Hand location (Centre, Right), Gaze direction (Centre, Right), and Size (Small, Large) as main factors was performed on standard deviations. We found a significant main effect of Size ($F_{(1,28)}$ = 64.020, p < .001, $\eta p2$ = 0.70), with higher variability for the Large as compared to the Small cylinder, in line with Weber's law. The ANOVA revealed no significant main effect of Hand location ($F_{(1,28)}$ = 0.216, p = .645, $\eta p2$ = 0.01) and Gaze direction ($F_{(1,28)}$ = 1.088, p = .307, ηp^2= 0.04), as well as no interaction between factors (Fig. 2b). Since the main effect of Size was significant, we performed post-hoc pairwise comparisons with Bonferroni correction which revealed significant differences between Small and Large sizes within each condition (all p < .001 Bonferroni corrected; Supplementary Table 4.2). Full statistical results of the ANOVA are reported in Table 1. The planned one-tailed t-tests between conditions where the hand is not aligned with the body midline or gaze direction (HC,GR; HR,GC; HR,GR) as opposed to when it is (HC,GC) did not reach statistical significance (HC,GR > HC,GC: $t_{(28)}$ = -0.421, p_{uncorr} = . 661, p_{corr} = 1.00; HR-GC > HC-GC: $t_{(28)}$ = 0.820, p_{uncorr} = .210, p_{corr} = .629; HR-GR > HC-GC: $t_{(28)}$ = -0.217, p_{uncorr} = .585, p_{corr} = 1.00).

To test the hypothesis that misalignment between the Hand and Gaze direction and/or Body Midline would induce a bias, we analyzed the size estimation bias for Small and Large stimuli. Two-tailed t-tests revealed no significant over or underestimation of stimulus size in the Hand-Gaze misaligned relative to the aligned condition (Small stimulus: $t_{(28)}$ = 1.60, p = .121; Large stimulus: $t_{(28)}$ = 1.149, p = .260; Fig. 2, Panel c). Regarding the Hand-Body Midline alignment effect, we found no bias for the Small or the Large stimulus size in the misaligned relative to the aligned condition (Small stimulus: $t_{(28)}$ = -0.913, p = .369; Large stimulus: $t_{(28)}$ = -0.281, p = .781; Fig. 2, Panel c). Collectively, these results suggest that neither Hand-Gaze nor Hand-Body Midline misalignment induce a size estimation bias.

Finally, we performed a linear regression analysis relating real and estimated stimulus' Sizes in the four experimental conditions (HC,GC; HC,GR; HR,GC; HR,GR) to compute the slope of the regression line. To test for differences between the regression slopes, we conducted a two-way ANOVA which revealed no significant main effect neither of Hand location ($F_{(1,28)}$ = .006, p = .938, $\eta p2$ < .001) nor of Gaze direction ($F_{(1,28)}$ = 3.551, p = .070, $\eta p2$ = .11; Fig. 3). The interaction between Hand location and Gaze direction was not significant ($F_{(1,28)}$ = .055, p = .816, $\eta p2$ = .002). To note, the value of the slope for all four experimental conditions was very close to 1 (HC,GC: M = 0.98, SD = 0.25; HC,GR: M = 0.99, SD = 0.26; HR,GC: M = 0.98, SD = 0.25; HR,GR: M = 0.99, SD = 0.26) indicating that participants were able to discriminate object sizes with high levels of accuracy.

Table 1. Results of the 2 × 2 × 2 ANOVA on the variability (SD) of perceptual size estimates.

	$F_{(1,28)}$	p-value	η_p^2
Hand loc.	.216	.645	.01
Gaze dir.	1.088	.306	.04
Size	64.021	<.001	.70
Hand loc. × Gaze dir.	.210	.650	.01
Hand loc. × Size	.951	.338	.03
Gaze dir. × Size	.419	.523	.01
Hand loc. × Gaze dir. × Size	.080	.780	.003

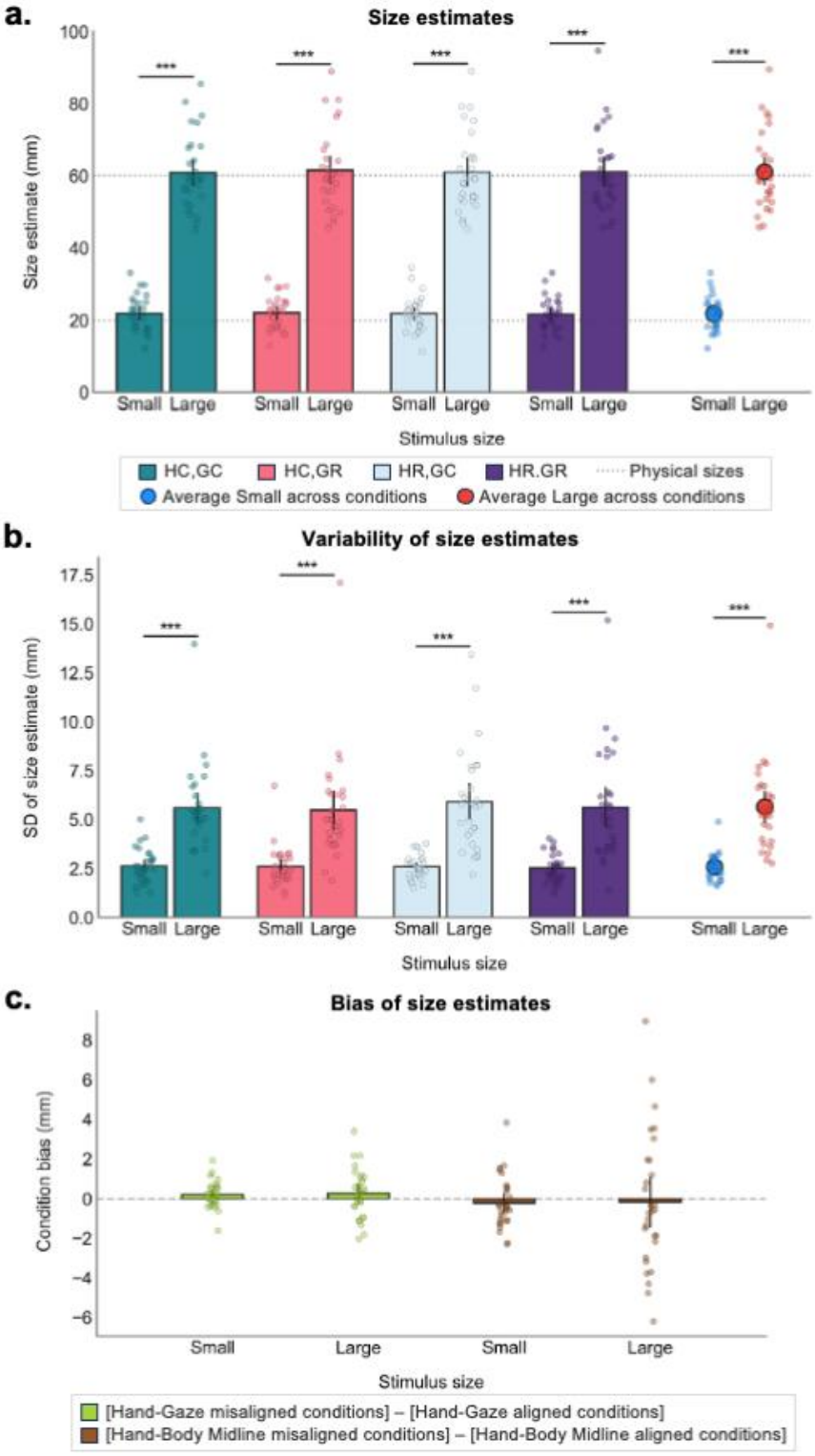

Figure 2. Accuracy, precision, and bias of size estimates in Experiment 1.
a. Size estimates: Average size estimates (mm) for Small and Large stimuli across four hand-gaze configurations: HC,GC (teal); HC,GR (pink); HR,GC (light blue); HR,GR (purple). Horizontal dotted lines represent the physical sizes of the stimuli (20 and 60 mm). The blue and red circles on the right represent the grand average for Small (blue circle) and Large (red circle) stimuli across all conditions, respectively. Significant differences between sizes both within and across conditions are indicated (***).
b. Variability of size estimates: Standard deviation (SD) of size estimates (mm) for Small and Large

stimuli across the four conditions. As indicated by asterisks (***), variability significantly increased for Large stimuli compared to Small ones across all hand-gaze configurations, consistent with Weber's Law. Circles on the right represent the grand average variability for each stimulus size (Small: blue circle; Large: red circle) across all conditions. **c.** Bias of size estimates: The panel shows the Condition Bias (directional under-/over-estimation) in millimeters. The condition bias represents the mean difference in size estimates between misaligned and aligned conditions separately for Small and Large stimuli, for both Hand-Gaze and Hand-Body Midline alignment effects. A positive value indicates that misalignment led to an overestimation of size relative to the aligned condition, while a negative value indicates underestimation. Note: Individual subjects' data points are shown as semi-transparent scatter dots. Error bars represent 95% confidence intervals (CI). Asterisks (***) denote significance at $p < .001$. Post-hoc pairwise comparisons shown in Panels a and b are Bonferroni corrected for multiple comparisons (all $p < .001$). Abbreviations: HC (Hand Centre), HR (Hand Right), GC (Gaze Centre), GR (Gaze Right).

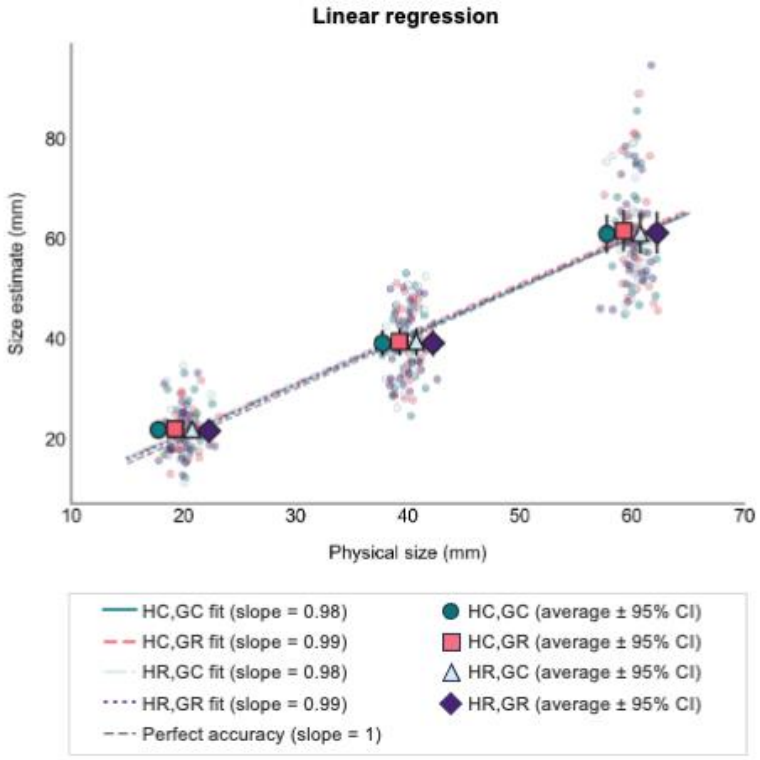

Figure 3. Linear regression between Physical stimulus size and Estimated size (Experiment 1).
The figure shows a linear regression analysis of size estimates (y-axis) plotted against the physical stimulus sizes (x-axis) across the four hand-gaze configurations (HC,GC; HC,GR; HR,GC; HR,GR). Individual subjects' size estimates are shown as semi-transparent scatter points. Data points are scattered around the distinct physical sizes tested (Small: 20 mm; Medium: 40 mm; Large: 60 mm). Mean estimated size for each condition is represented by symbols (circle: HC,GC; square: HC,GR; triangle: HR,GC; rhombus: HR,GR); error bars denote 95% confidence intervals (CI). Regression fits for all conditions (coloured lines; teal: HC,GC; pink: HC,GR; light blue: HR,GC; purple: HR,GR) indicate high veridicality, with slopes ranging from 0.98 to 0.99, closely following the line of perfect accuracy (dashed grey line, slope = 1).

4.2.7 Discussion

The aim of Experiment 1 was to investigate whether Gaze direction (relative to Hand location) and Hand location (relative to Body Midline) influence haptic processing and estimation of the size of occluded targets. As expected, the results showed that size estimation aperture scaled with stimulus size. Indeed, we found a significant effect of Size on the average size estimates suggesting that participants accurately scaled the distance between the thumb and index finger to the physical dimension of the stimuli. In addition, we found a significant effect of Size on the variability of size estimates, with more variable (i.e., less precise) size estimates for the Large compared to the Small stimulus. This result is in line with Weber's law, suggesting that the precision of size estimates decreases as the size of the stimulus increases. Gaze direction and Hand location alone had no significant effect neither on the average nor on the variability of manual size estimates; likewise, the interaction effect between the two factors on the average size estimates, as well as the interaction effect between Size and Gaze direction did not reach the threshold for statistical significance. We did not find significantly higher variability of size estimates when the hand was not aligned with gaze direction or body midline as compared to the aligned condition. In addition, we did not find a significant size estimation bias for the Hand-Gaze and Hand-Body Midline alignment effects.

Overall, these results do not provide evidence that the misalignment between Gaze direction and the exploring Hand, as well as between Hand location and Body Midline, influences haptic size estimation. Based on these results, we could not define an optimal configuration of hand, gaze and stimulus alignment for size estimation to be used in Experiment 2 where we explored whether the EVC plays a role in haptic size estimation of unseen stimuli. Therefore, we decided to keep the stimulus and the exploring hand aligned with both body midline and gaze direction in the following Experiment for simplicity.

4.3 Experiment 2

4.3.1 Participants

A group of 30 healthy individuals took part in Experiment 2 (15 females; age: M_{age} = 22.80, *SD* = 2.14, range 20-28). Data of 4 subjects in Experiment 2 were excluded from the analyses due to technical problems during the experiment. All subjects were right-handed and had normal or corrected-to-normal vision. All participants provided their written informed consent after the study procedures were explained. The experimental procedures were approved by the Research Ethics Committee of the University of Trento.

4.3.2 Stimuli and apparatus

The experimental stimuli were the same as described in Experiment 1 (20, 40, and 60 mm; small, medium, and large). All three cylinders were included in the analyses.

Throughout the experiment, participants had their chin fixed on a chin rest while sitting in front of an LCD (Liquid Cristal Display) monitor. The latter had a frame rate of 120 Hz, a resolution of 1,920 × 1,080 pixel, and a size of 53.3 × 30 cm, with a viewing distance of ~24 cm. As in Experiment 1, the 3D stimuli and the associated support were placed behind the screen, as shown in Fig. 4a. Consequently, participants could never see the stimuli, neither before nor during the experimental session. Here, the metal platform was always aligned with participants' body midline. To ensure that the stimulus on the platform was aligned with the central fixation cross displayed on the screen and, thus also with participants' gaze direction, we used a laser pointer which defined the point in space where gaze would fall both on the screen and behind it, as explained in Section 4.2.2.

A dynamic visual noise (also referred to as flickering patched square or dynamic noise patch; 20 x 20°; Fig. 4a-b), centered at the fixation, was randomly presented in half of trials. It consisted of five distinct high-contrast Mondrian patterns flickering at a rate of 10 Hz (e.g.,

Sperandio et al., 2018). The total presentation time of the dynamic visual noise was 4 s. The experimental paradigm was programmed in E-Prime 2.0 Professional Software (Schneider et al., 2012). As in Experiment 1, A QWERTY keyboard was connected to the main computer and two speakers were placed on the sides of the monitor to deliver auditory cues throughout the experimental session.

To measure participants' manual size estimates we used the same tool and procedure described in Section 4.2.2.

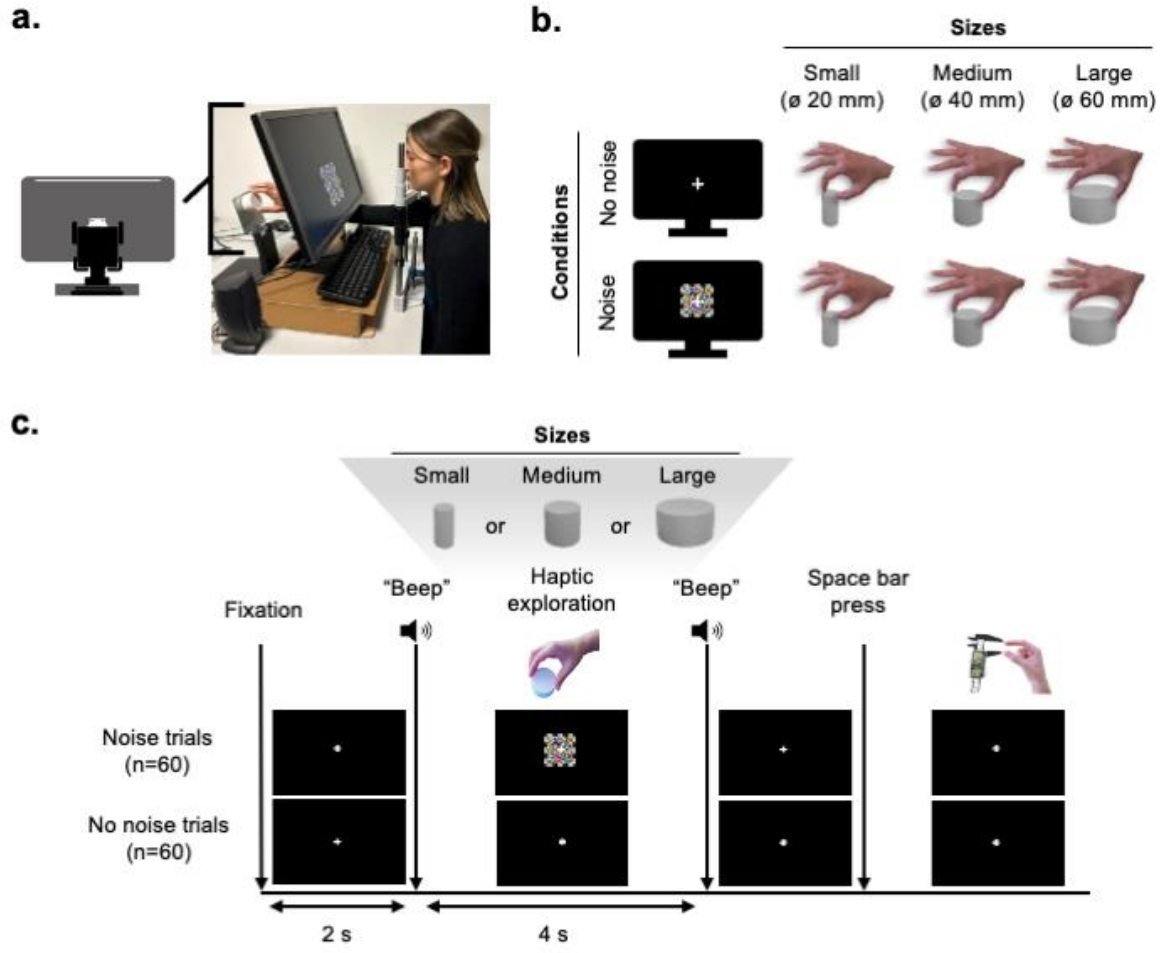

Figure 4. Experiment 2: experimental setup, design, and paradigm.
a. Experimental setup. Participants sat in front a monitor displaying a fixation cross with their chin fixed on a chin rest. The 3D stimuli (i.e., cylinders) were attached to a metal platform located at the top of a reclinable support, which was placed behind the screen. Therefore, participants could never see the stimuli. Unlike Experiment 1, here the stimulus location was aligned with participants' gaze direction and body midline at the center, and it remained fixed throughout the experiment. A keyboard was connected to the main computer and was used to receive participants' input. Auditory cues throughout the experiment were delivered by two speakers placed on the sides of the monitor. **b.** Experimental

design. We had a 2×3 factorial design with two Noise conditions (Noise, No noise), and 3 stimulus sizes (Small, Medium, Large; 20, 40, 60 mm in diameter, respectively) resulting in a total of 6 conditions. **c.** Schematic representation of the paradigm. Each trial started with a 2 s-fixation period during which participants were instructed to fixate on a small cross that appeared at the center of the screen. Next, a 'beep' sound signaled the beginning of the exploration phase during which participants were instructed to reach with their right hand and haptically explore a cylinder placed behind the screen. Participants haptically explored the cylinder for 4 s. Then, a second 'beep' cued them to release the object and position their hand back to the starting position by pressing the space bar. Finally, participants performed the manual estimation task, and their estimates were measured by the experimenter by means of a digital caliper.

4.3.3 Experimental design

As in Experiment 1, participants were asked to haptically explore and manually estimate the size of unseen cylinders of three different sizes. In half of trials, a patch of flickering noise was displayed on the screen while participants haptically explored the stimulus. As such, stimulus size and noise condition were varied over a three (stimulus size; Small, Medium, Large) by two (noise condition; Noise, No noise) factorial design, resulting in a total of six conditions (Fig. 4b). Each participant performed a total of 120 trials (20 trials per condition) which were split in three blocks of 40 trials each, to allow participants to briefly rest in between separate blocks. The order of presentation of the six conditions was randomized for each experimental block, for each participant.

4.3.4 Experimental paradigm

The experimental paradigm was similar to the paradigm used in Experiment 1 (Fig. 4c). At the beginning of each trial, a white fixation cross appeared in the center of the screen, over a black background. The cross was displayed for the whole duration of the experiment and participants were instructed to always maintain fixation on it. After 2 s, a 'beep' sound cued participants to start haptically exploring the size of the stimulus. Specifically, subjects were asked to reach with their right hand the cylinder that was placed behind the screen and aligned with participants' gaze direction and body midline. Participants were required to haptically explore the width of the stimulus with the thumb and index fingers until they heard another

beep signal after 4 s. Subsequently, they had to release the stimulus and press the space bar on the keyboard. Finally, participants manually reported the width of the stimulus they had just haptically explored. Thus, they opened their thumb and index fingers such that the aperture had to match the width of the explored stimulus. Then, an experimenter measured their size estimates using the digital caliper and recorded them. To start a new trial, the experimenter pressed the space bar on the keyboard.

In half of the trials, dynamic visual noise was presented at the center of the screen while participants haptically explored the stimulus (Noise condition). Specifically, the visual noise began at $t = 2\ s$ and ended at $t = 6\ s$. In the remaining half of the trials, only the fixation cross was displayed on the screen during haptic exploration (No noise condition). Subjects ran a short training session before the experiment to familiarize with the procedures and the task.

4.3.5 Statistical analysis

As in Experiment 1, participants' size estimates were calculated by measuring the distance between the dots located on the index finger and thumb, respectively. We computed mean size estimates for each condition and each participant. A 2×2 repeated-measures analysis of variance (ANOVA) with Noise condition (Noise, No noise) and stimulus Size (Small, Medium, Large) as main factors was performed on size estimates. Further, we analyzed standard deviations of size estimates for each condition and each participant to assess the variability of size estimates. A 2×2 repeated-measures ANOVA with Noise condition (Noise, No noise) and stimulus Size (Small, Medium, Large) as main factors was performed on standard deviations of size estimates. We then performed post-hoc pairwise comparisons with Bonferroni correction to further investigate any significant ANOVA results.

Since previous evidence has shown that uncertainty of perceptual estimates is reflected in higher variability (Ernst & Banks, 2002; Niechwiej-Szwedo et al., 2022), we expected that

SDs would be higher in the Noise as compared to No noise conditions. Therefore, we conducted a one-tailed t-test on *SDs* based on this a-priori hypothesis.

Finally, we performed a linear regression analysis relating real and estimated stimulus' sizes in the Noise and No noise conditions to compute the slope of the regression lines. We then compared the 2 slope values using a paired-samples t-test.

4.3.6 Results

The ANOVA on size estimates revealed a significant main effect of Noise ($F_{(1,25)}$ = 4.678, p = .040, ηp^2 = .16; Fig. 5a). Specifically, the average size estimate was higher in the Noise (M = 46.75, SD = 7.59) as compared to No noise condition (M = 46.36, SD = 7.51). As expected, there was also a significant main effect of Size ($F_{(2,50)}$ = 642.083, p < .001, ηp^2 = .96), with higher estimates for the Large than Medium and for the Medium than Small object. Post-hoc pair-wise comparisons with Bonferroni correction revealed significant differences between each pair of sizes within both Noise and No noise conditions (all p < .001 Bonferroni corrected; Supplementary Table 4.3). The Noise × Size interaction was not significant ($F_{(2,50)}$ = 1.315, p = .278, ηp^2 = .05). Supplementary Figure 4.1 (Panel b) shows the average size estimates for Small, Medium, and Large stimuli across experimental conditions to provide an overview of the overall participants' manual size estimation performance for each stimulus size. Full statistical results of the pair-wise comparisons are reported in Supplementary Table 4.6.

To assess the precision of size estimates in the Noise vs No noise conditions, we calculated the standard deviation for each condition. A 2-way repeated measures ANOVA with Noise (Noise, No noise) and Size (Small, Medium, Large) was performed on standard deviations. The results of the ANOVA showed a significant main effect of Size ($F_{(2,50)}$ = 32.370, p < .001, ηp^2 = .56), but not Noise ($F_{(1,25)}$ = .810, p = .377, ηp^2= .03; Fig. 5b). Post-hoc pair-wise comparisons with Bonferroni correction revealed significant differences between each pair of sizes within both Noise and No noise conditions (all p < .05 Bonferroni corrected;

Supplementary Table 4.4). The Noise × Size interaction was not significant ($F_{(2,50)}$ = .860, p = .429, ηp^2 = .03). Based on our a priori directional hypothesis that higher uncertainty of perceptual estimates is reflected in higher variability (Ernst & Banks, 2002; Niechwiej-Szwedo et al., 2022), we conducted a one-tailed paired-samples t-test between average *SD* in Noise vs No noise conditions. However, this comparison did not reach statistical significance ($t_{(25)}$ = -0.900, p = .812).

We then performed a linear regression analysis relating real and estimated stimulus' sizes in Noise and No noise conditions to compute the slope of the regression lines. A paired-samples t-test revealed no significant difference between the mean slopes for the Noise vs No noise condition ($t_{(25)}$ = -0.602, p = .091, Fig. 6). To note, the slope for Noise and No noise conditions approached a value of 1 (Noise: M = 0.90, SD = 0.17; No noise: M = 0.89, SD = 0.17) indicating that participants were able to discriminate the three object sizes with high levels of accuracy.

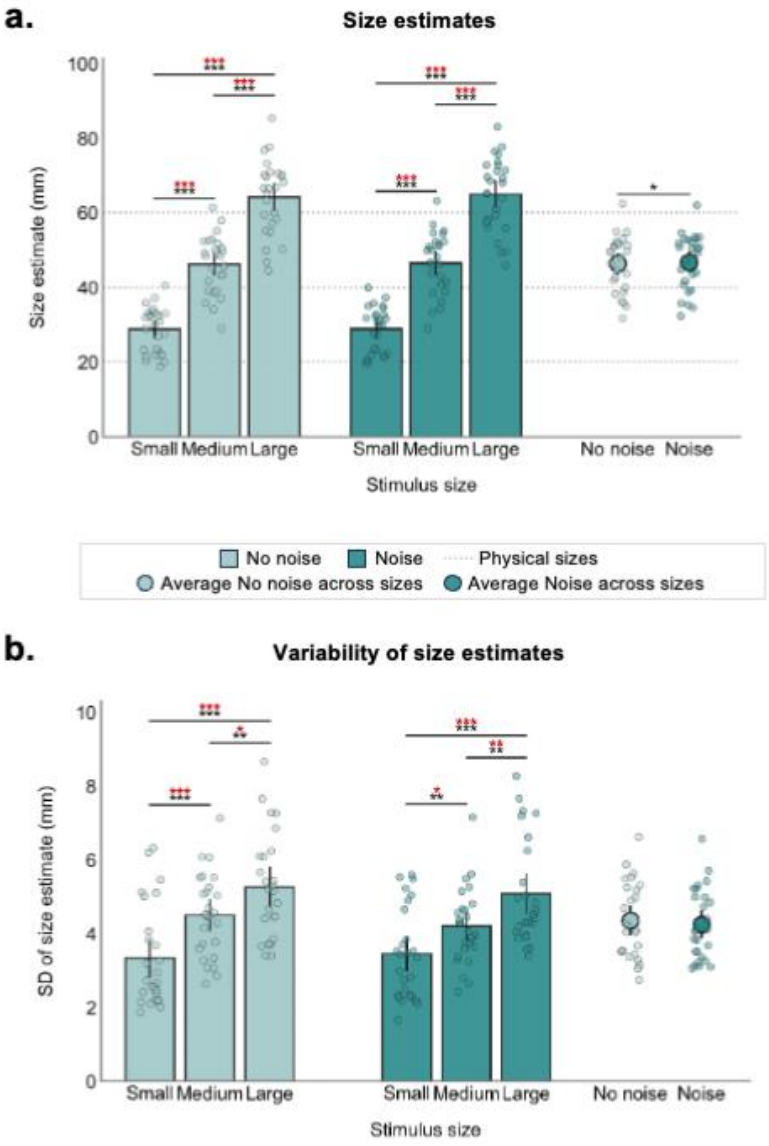

Figure 5. Accuracy and precision of size estimates in Experiment 2.
a. Size estimates: Average size estimates (mm) for Small, Medium, and Large stimuli within No noise (light teal) and Noise (dark teal) conditions. Horizontal dotted lines represent the actual physical sizes of the stimuli (20, 40, and 60 mm). The circles on the right represent the grand average size estimates across all sizes for each condition, indicating a significant increase in perceived size in the Noise condition compared to the No noise condition (*). **b.** Variability of size estimates: Standard deviation (*SD*) of size estimates (mm). Bars indicate variability for each specific stimulus size within No noise and Noise conditions, while circles on the right represent the grand average variability across all sizes. As indicated by asterisks (** and ***), variability increased significantly as a function of stimulus size within both noise conditions, a result consistent with Weber's Law. Note: Individual subjects' data points are shown as semi-transparent scatter dots. Error bars represent 95% confidence intervals (*CI*). Asterisks (*, **, ***) denote significance levels at $p < .05$, $p < .01$, and $p < .001$, respectively. Post-hoc pairwise comparisons are Bonferroni corrected; corrected *p-values* are shown in red, while uncorrected *p-values* are shown in black.

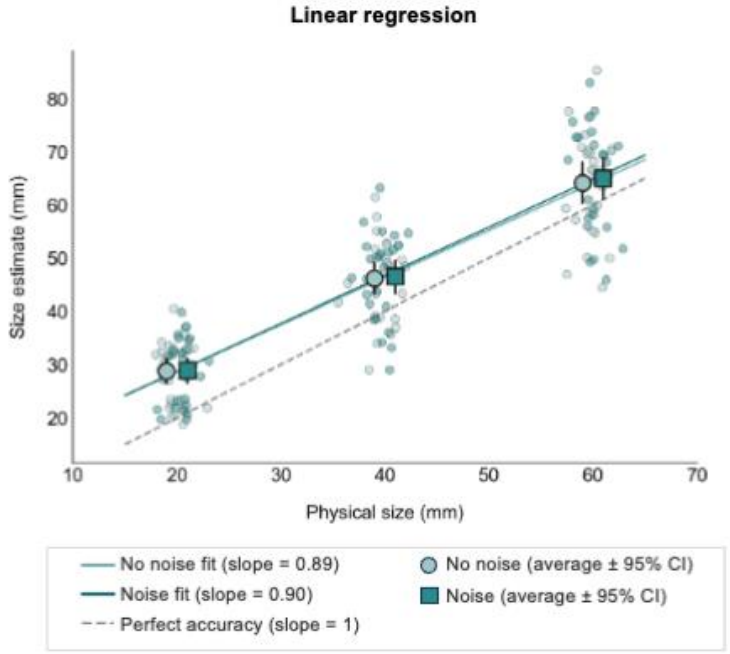

Figure 6. Linear regression between Physical stimulus size and Estimated size (Experiment 2).
The figure shows a linear regression analysis of size estimates (y-axis) plotted against the physical stimulus sizes (x-axis) across No noise and Noise conditions. Individual subjects' size estimates are shown as semi-transparent scatter points. Data points are scattered around the distinct physical sizes tested (Small: 20 mm; Medium: 40 mm; Large: 60 mm). Mean estimated size for each condition is represented by symbols (circle: No noise; square: Noise); error bars denote 95% confidence intervals (CI). Regression fits for the two conditions (colored lines; light teal: No noise; dark teal: Noise) indicate high veridicality, with slopes equal to 0.89 to 0.90 for No noise and Noise conditions, respectively, following the line of perfect accuracy (dashed grey line, slope = 1).

4.3.7 Discussion

In Experiment 2, we aimed at investigating whether the haptic and visual systems interact with each other to process the size of occluded, haptically explored objects. Specifically, we assessed whether V1 is behaviourally and functionally relevant for haptic size processing. To this aim, we asked our participants to haptically explore the width of different sized cylinder which were placed behind a screen and always aligned with the participants' gaze direction and body midline. At the end of each trial, participants were asked to provide a manual estimate of the size of the previously haptically explored stimulus, without the possibility to rely on visual information about the hand. In half of trials, we presented a patch of flickering

visual noise in fovea to interfere with V1 processing while participants haptically explored the size of stimuli. We hypothesized that, if V1 is behaviourally relevant for haptic size processing despite the absence of target-related visual information, then we should see an effect of visual noise oh haptic size estimation performance. While we hypothesized higher variability in the Noise compared to the No noise condition, our results show that Noise had a significant effect on perceptual size estimates but not on their variability. In fact, there were significantly greater estimates when noise was presented during haptic size exploration compared to the No noise condition, indicating a bias in size estimation in the Noise as compared to the No noise condition.

Also, Size had a significant effect on perceptual size estimates, with larger manual estimates as the size of the stimulus increased. This result suggests that perceptual size estimates scale with the physical dimension of stimuli. The analysis of regression slopes further revealed that size estimates accurately scaled with the real stimulus size. To note, accuracy is not affected by Noise. In fact, we found that the difference between the slopes of the two regression lines representing Noise and No noise conditions did not reach statistical significance.

Interestingly, the variability of size estimates was significantly modulated by Size, but not Noise. Specifically, the average standard deviation of size estimates increased as a function of stimulus size, similar to the results observed in Experiment 1. These results suggest that the precision of manual estimates follows Weber's law, therefore the precision of perceptual estimates scales with object size.

In Experiment 3 we explored whether Noise would affect performance even with increased task difficulty.

4.4 Experiment 3

4.4.1 Participants

A third group of 34 people participated in Experiment 3 (18 females; age: M_{age} = 25.32, *SD* = 7.19, range 18-46). All subjects were right-handed and had normal or corrected-to-normal vision. All participants provided their written informed consent after the study procedures were explained. The experimental procedures were approved by the Research Ethics Committee of the University of Trento.

4.4.2 Stimuli and apparatus

For this experiment, we used three plastic cylinders similar to those used in Experiment 1 and 2 but with different sizes. Specifically, we reduced the difference between the stimulus sizes to make them more similar and therefore increasing task difficulty. The stimuli had a diameter of 55 (Small), 60 (Medium), and 65 mm (Large). We also used two additional cylinders with a diameter of 57.5 mm (Catch Cylinder 1) and 62.5 mm (Catch Cylinder 2) in catch trials. All stimuli were 3 cm high. The increased number of stimulus sizes also contributed to increase task difficulty as compared to Experiment 2. Similar to what we did in Experiment 1 and 2, each object was attached to the same metallic support thanks to a layer of magnetic tape attached at the base of the stimulus. The procedures used to design and print the stimuli are the same applied to Experiment 1 and 2.

Throughout the experiment, participants had their chin fixed on a chin rest while sitting in front of an LCD (Liquid Cristal Display) monitor with a frame rate of 59.95 Hz, a resolution of 1,920 × 1,200 pixel, and a size of 52 × 32.4 cm, with a viewing distance of ~28 cm. As in the previous experiments, the 3D stimuli and the associated support were placed behind the screen. Consequently, participants could never see the stimuli, neither before nor during the experimental session. Similar to Experiments 1 and 2, we ensured that the metal platform along

with the attached stimulus was aligned with the central fixation cross displayed on the screen and, thus also with participants' gaze direction, by using a laser pointer which defined the point in space where gaze would fall both on the screen and behind it. Here, the dynamic visual noise (8 x 8 cm; 16.26° x 16.26°), centered at the fixation, was smaller in size as compared to the one used in Experiment 2. It consisted of five distinct high-contrast Mondrian patterns flickering at a rate of 4 Hz. The total presentation time of the dynamic visual noise was 4 s. The viewing distance (i.e., the between the fixation cross on the monitor and the point between the eyes) of ~28 cm ensured that the patch of dynamic visual noise fell within 17° of visual angle, corresponding to central vision (perifovea, Strasburger et al., 2011). A QWERTY keyboard was connected to the main computer. In addition, two speakers were placed on the sides of the monitor to deliver auditory cues throughout the experimental session. The experimental paradigm was programmed in MATLAB R2020a, using the Psychophysics Toolbox extensions (i.e., PsychToolbox version 3.0.16; Brainard, 1997; Pelli, 1997).

To measure participants' manual size estimates we used the same tool and procedure described in Section 4.2.2.

4.4.3 Experimental design

As in Experiment 1 and 2, participants haptically explored and manually estimated the size of unseen cylinders of different sizes. Similar to Experiment 2, in half of trials, a patch of flickering visual noise was presented on the screen during the haptic exploration phase. As such, we had a 2 (noise condition: Noise, No noise) by 5 (stimulus size: Small, Catch 1, Medium, Catch 2, Large) factorial design. Catch trials were excluded from further analysis. As such, the final design consisted of a 2 (noise condition) x 3 (stimulus size) design, with two levels of visual interference (noise and no noise) and 3 object sizes (Small, Medium, and Large), which yielded 6 conditions in the final analyses (Fig. 7a).

Each participant performed a total of 112 trials which were split in 4 blocks of 28 trials each, to allow participants to briefly rest in between separate blocks. In particular, each block consisted of 4 trials for each of the six experimental conditions (Noise-Small, Noise-Medium, Noise-Large, No noise-Small, No noise-Medium, No noise-Large), and 1 trial for each of the four catch conditions (Noise-Catch Cylinder 1, Noise-Catch Cylinder 2, No noise-Catch Cylinder 1, No noise-Catch Cylinder 2). The order of presentation of the 10 conditions was randomized for each experimental block, for each participant.

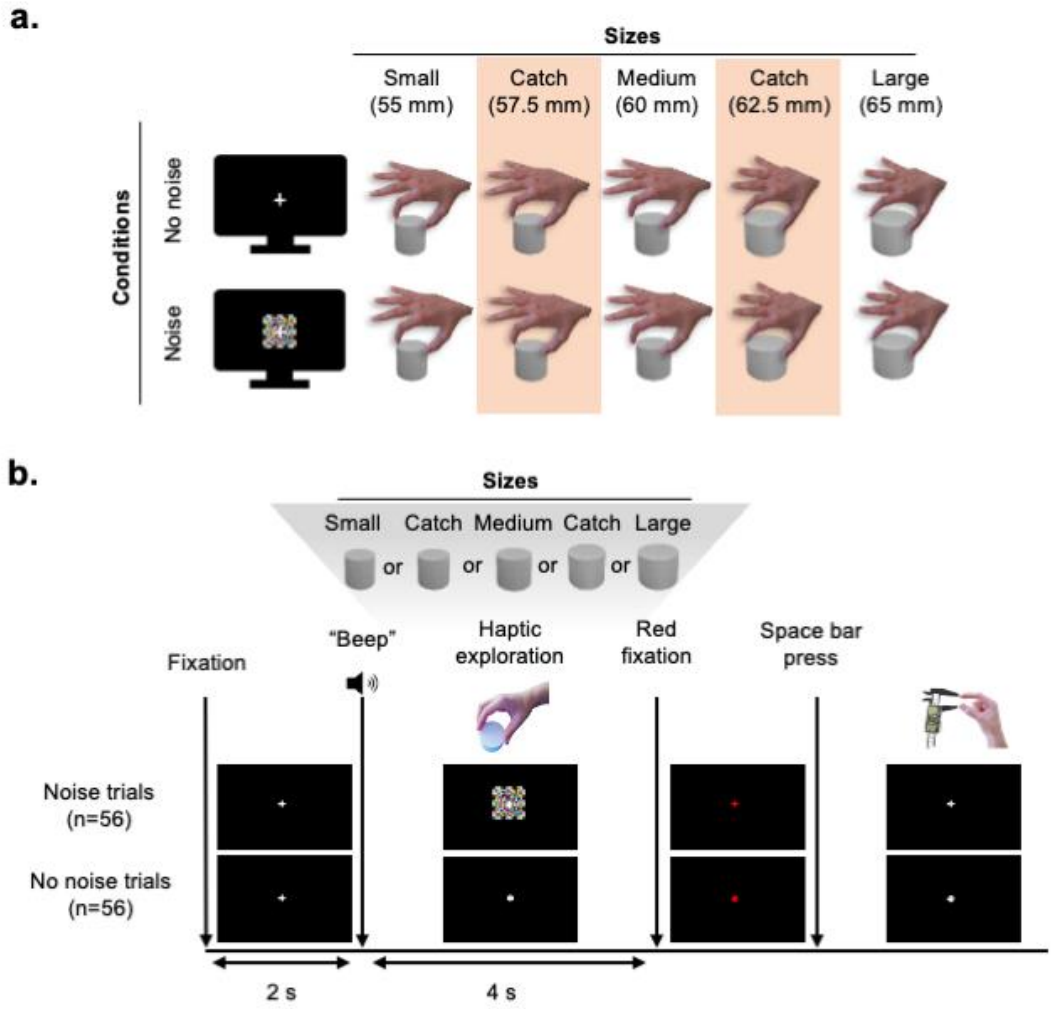

Figure 7. Experiment 3: experimental setup, design, and paradigm.
a. Experimental design. We had a 2×5 factorial design with two Noise conditions (noise, no noise), and 5 stimulus sizes (Small, Catch, Medium, Catch, Large; 55, 57.5, 60, 62.5, 65 mm in diameter, respectively) resulting in a total of 10 conditions. The Catch Cylinders were used in catch trials only to increase task difficulty and therefore were not considered for the analysis. Hence, the final design consisted of a 2 (noise) by 3 (stimulus size) factorial design, which yielded 6 conditions in the final analyses. **b.** Schematic representation of the paradigm. Each trial started with a 2 s-fixation period during

which participants were instructed to fixate a cross that was displayed at the center of the screen. Next, a 'beep' sound signaled the beginning of the exploration phase during which participants were asked to reach with their right hand and haptically explored a cylinder which was placed behind the screen thereby avoiding visual processing of the stimulus and the hand. Participants haptically explored the cylinder for 4 s, after which a color change of the fixation cross (from white to red) prompted them to release the object and press the space bar on the keyboard. After that, participants performed the manual estimation task, and their estimates were measured by the experimenter by means of a digital caliper.

4.4.4 Experimental paradigm

The experimental paradigm was similar to the paradigm used in Experiment 1 (Fig. 7b). At the beginning of each trial, a white fixation cross appeared in the centre of the screen, over a black background. The cross was displayed for the whole duration of the experiment and participants were instructed to always maintain fixation on it. After two seconds, a 'beep' sound cued participants to start haptically exploring the size of the stimulus. Specifically, subjects were asked to reach with their right hand one of the cylinders which was placed behind the screen and in alignment with the fixation point. Participants were required to haptically explore the width of the stimulus with the thumb and index fingers until the colour of the fixation cross became red ($t = 6\ s$). Afterwards, they had to release the stimulus and press the space bar on the keyboard; after pressing the space bar, the colour of the fixation cross returned white. Finally, participants performed the manual estimation task. Then, their size estimates were measured by the experimenter using the digital calliper and eventually recorded.

To start a new trial, participants were instructed to press the space bar on the keyboard. In half of the trials, dynamic visual noise was presented at the centre of the screen while participants haptically explored the stimulus (Noise condition). Specifically, the visual noise began at $t = 2\ s$ and persisted until participants pressed the space bar after finishing stimulus exploration. In the remaining half of the trials, only the fixation cross was displayed on the monitor during haptic exploration (No noise condition). Subjects ran a short training session of 6 trials before the experiment to familiarize with the task.

4.4.5 Statistical analysis

As in Experiments 1 and 2, we computed mean size estimates for each condition and each participant. A 2×3 repeated-measures ANOVA with Noise condition (Noise, No noise) and stimulus Size (Small, Medium, Large) as main factors was performed on size estimates. Further, we analyzed standard deviations (*SDs*) of size estimates for each condition and each participant to assess the variability of size estimates. A 2×3 repeated-measures ANOVA with Noise condition (Noise, No noise) and Size (Small, Medium, Large) as main factors was performed on standard deviations of size estimates. We performed post-hoc pairwise comparisons with Bonferroni correction to further investigate any significant ANOVA results.

Since previous evidence has shown that uncertainty of perceptual estimates is reflected in higher variability (Ernst & Banks, 2002; Niechwiej-Szwedo et al., 2022), we expected that *SDs* would be higher in the Noise as compared to No noise conditions. Therefore, we conducted a one-tailed t-test on *SDs* based on this a-priori hypothesis.

Finally, we performed a linear regression analysis relating real and estimated stimulus' sizes in the Noise and No noise conditions to compute the slope of the regression lines. We then compared the 2 slope values using a paired-samples t-test.

4.4.6 Results

The ANOVA on size estimates revealed no significant main effect of Noise ($F_{(1,33)}$ = .294, p = .592, η_p^2 = .01; Fig. 8a). As expected, there was a significant main effect of Size ($F_{(2,66)}$ = 232.453, p < .001, η_p^2 = .88). Post-hoc pair-wise comparisons with Bonferroni correction revealed significant differences between each pair of sizes within both Noise and No noise conditions (all p < .001; Fig. 8a; Supplementary Table 4.5). The Noise × Size interaction was not significant ($F_{(2,66)}$ = .477, p = .623, η_p^2 = .01). Given that the experiment included two catch stimuli that were not included in the primary analysis (see Section 4.4.2), Supplementary Figure

4.1 (Panel c) shows the average size estimates for Small, Catch 1, Medium, Catch 2, and Large stimuli across experimental conditions to provide an overview of participants' manual size estimation performance considering all the explored sizes. Full statistical results of the pair-wise comparisons are reported in Supplementary Table 4.6.

To assess the precision of size estimates in the Noise vs No noise conditions, we calculated the *SD* for each condition. A 2-way repeated measures ANOVA with Noise (Noise, No noise) and Size (Small, Medium, Large) was performed on *SDs*. The results of the ANOVA showed no significant main effect of Noise ($F_{(1,33)} = 2.922$, $p = .097$, $\eta_p^2 = .08$). Based on our a priori directional hypothesis that higher uncertainty of perceptual estimates is reflected in higher variability (Ernst & Banks, 2002; Niechwiej-Szwedo et al., 2022), we performed a one-tailed paired-samples t-test between the average *SD* in Noise vs No noise conditions. Consistent with our hypothesis, the results of the t-test revealed a significant difference between *SD* in the Noise relative to No noise condition ($t_{(33)} = -1.709$, $p = .048$; Fig. 8b). In addition, there was no significant main effect of Size ($F_{(2,66)} = .255$, $p = .775$, $\eta_p^2 = .008$; Fig. 8b) and no significant interaction between Noise and Size ($F_{(2,50)} = .860$, $p = .429$).

We then performed a linear regression analysis relating real and estimated stimulus' sizes in both Noise and No noise conditions to compute the slope of the regression lines. A paired-samples t-test revealed no significant difference between the mean slopes for the Noise vs No noise condition ($t_{(33)} = -0.822$, $p = .417$, Fig. 9). To note, the slope for both Noise and No noise conditions was close to 1 (Noise: $M = 1.19$, $SD = 0.41$; No noise: $M = 1.23$, $SD = 0.52$) indicating that participants were able to discriminate the three object sizes with high levels of accuracy in both conditions.

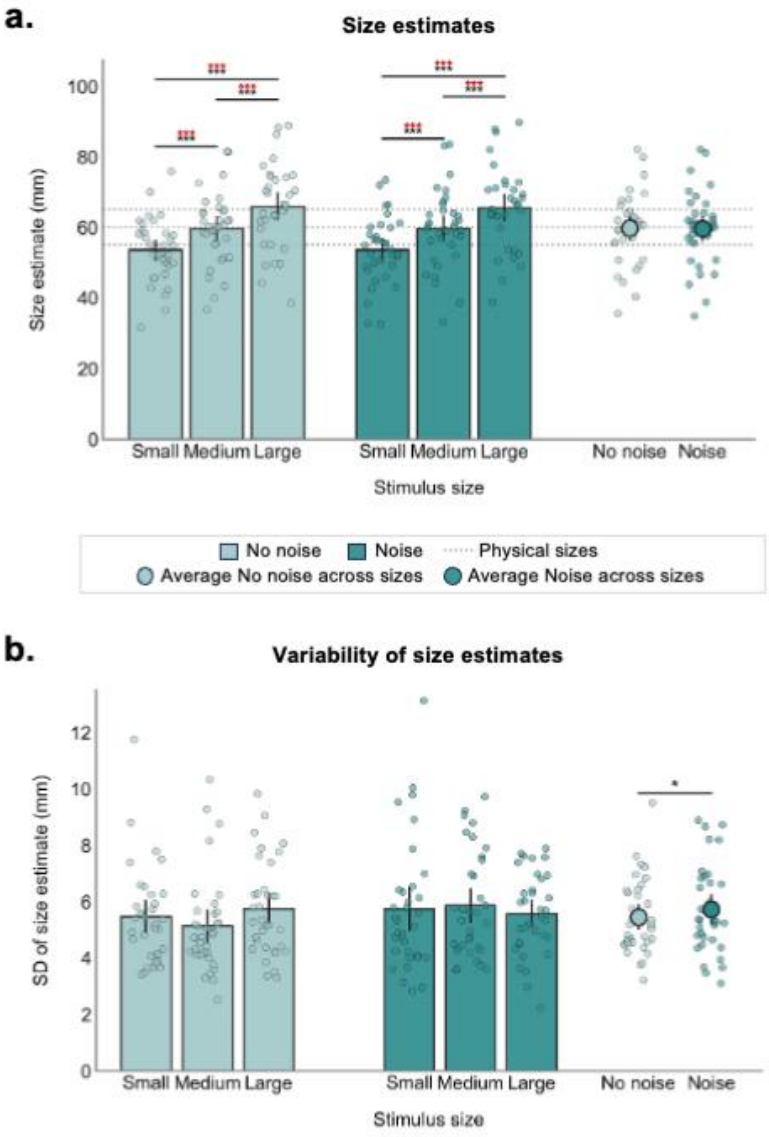

Figure 8. Accuracy and precision of size estimates in Experiment 3.
a. Size estimates: Average size estimates (mm) for Small, Medium, and Large stimuli within No noise (light teal bars) and Noise (dark teal bars) conditions. Horizontal dotted lines represent the actual physical sizes of the stimuli (55, 60, and 65 mm). The circles on the right represent the grand average size estimates across all sizes for No noise (light teal circle) and Noise (dark teal circle) condition. Asterisks (***) indicate statistically significant differences between each pair of stimulus sizes. **b.** Variability of size estimates: Standard deviation (SD) of size estimates (mm) for Small, Medium, and Large stimuli within No noise (light teal) and Noise (dark teal) conditions. Bars indicate variability for specific stimulus sizes within No noise (light teal bars) and Noise (dark teal bars) conditions, while circles on the right represent the grand average variability across all sizes for the No noise (light teal circle) and Noise (dark teal circle) conditions. As indicated by the asterisk (*), average variability was significantly higher in the Noise compared to the No noise condition, indicating a decrease in precision in the Noise condition. Note: Individual subjects' data points are shown as semi-transparent scatter dots. Error bars represent 95% confidence intervals (*CI*). Asterisks (*, ***) denote significance levels at $p < .05$ and $p < .001$, respectively. Post-hoc pairwise comparisons for stimulus size effects on size estimation shown in Panel a are Bonferroni corrected; corrected p-values are shown in red, while uncorrected p-values are shown in black.

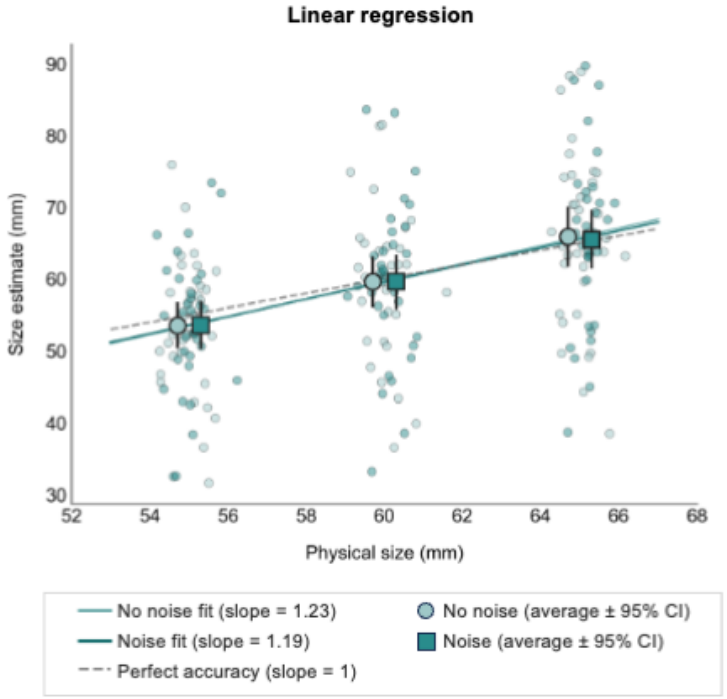

Figure 9. Linear regression between Physical stimulus size and Estimated size (Experiment 3).
The figure shows a linear regression analysis of size estimates (y-axis) plotted against the physical stimulus sizes (x-axis) across No noise and Noise conditions. Individual subjects' size estimates are shown as semi-transparent scatter points. Data points are scattered around the distinct physical sizes tested (Small: 55 mm; Medium: 60 mm; Large: 65 mm). Mean estimated sizes for each condition are represented by symbols (circle: No noise; square: Noise); error bars denote 95% confidence intervals (*CI*). Regression fits for the two conditions (coloured lines; light teal: No noise; dark teal: Noise) indicate high veridicality, with slopes equal to 0.89 to 0.90 for No noise and Noise conditions, respectively, following the line of perfect accuracy (dashed grey line, slope = 1).

4.4.7 Discussion

In the present experiment, we examined whether the effect of noise on manual estimation of the size of previously haptically explored stimuli observed in Experiment 2 would persist under more stringent conditions, that is increased task difficulty. To do so, we increased the number of stimulus sizes from three to five, and we reduced the distance between sizes from 20 mm to 2.5 mm. We also reduced the retinal size of the visual noise to ensure that it precisely fell within the perifoveal region of the visual field. The task was the same as in Experiment 2, that is participants had to haptically explore the size of unseen cylinders while fixating a central

fixation cross on a screen. Subsequently, they were asked to perform a manual size estimation task solely based on the haptic size information previously acquired during the exploration phase. Like in Experiment 2, a patch of dynamic visual noise was presented in half of trials to test whether visual Noise modulates manual size estimates of haptically explored stimuli even in the absence of direct stimulus-related visual input. In the present experiment, we hypothesized that if V1 is behaviourally relevant for haptic size processing under increased task difficulty, the effect of Noise on perceptual size estimation would persist or even increase as finer discrimination is required to perform the task. Unlike Experiment 2 where Noise had an effect on the average perceptual size estimates, the results of Experiment 3 suggest a different nature of noise-related interference under high-demand conditions. Notably, while we could not replicate the effect of Noise on average size estimates, we found a significant effect of Noise on the variability of size estimates, with increased standard deviations during Noise compared to No noise trials as revealed by the planned directional comparison between the two conditions. This suggests that under high-demand conditions, Noise may modulate manual size estimates by reducing participants' size estimation precision, which likely reflects an increase in participants' uncertainty about the size of the haptically explored objects when Noise was present and interfered with V1 processing. In fact, evidence shows that higher variability of perceptual estimates is linked to participants' uncertainty about the target stimulus (Ernst & Banks, 2002). Taken together, the evidence across Experiment 2 and 3 suggests that the role of V1 in haptic size processing may be context dependent. Indeed, while foveal noise interferes with haptic size estimation, the specific nature of this interference (i.e., an overestimation of stimulus size vs. a decrease in precision of size estimation) might depend on the specific task demands and experimental contexts. However, given that the effect of foveal noise on variability as measured by the ANOVA did not reach significance, and that we could not

replicate the interference effect on the average size estimates, these mixed findings should be interpreted with caution.

Similar to what we found in Experiment 2, Size had a significant effect of the average size estimates, with higher estimates for increasingly larger stimulus sizes indicating that perceptual size estimates scale with the real dimension of stimuli even when finer tactile discrimination is required for a more difficult task. The analysis of regression slopes showed that manual size estimates were indeed accurate even with greater task difficulty, as they were very close to the real size of stimuli. Further, this accuracy was not modulated by Noise as indicated by the non-significant difference between Noise and No noise regression slopes.

Interestingly, the variability of size estimates was not modulated by Size, suggesting that when fine tactile discrimination is needed to distinguish stimuli which widths differ to a very small extent between each other (from a minimum of 2.5 to a maximum of 10 mm), Weber's law is disrupted.

4.5 General discussion

We conducted three experiments to investigate the potential influence of specific variables on the manual size estimation of previously haptically explored, occluded cylinders. In Experiment 1, we aimed at determining the best possible configuration of gaze direction and hand/target location for optimal performance. The results of this experiment indicated that participants accurately discriminated the different sizes, and that hand location relative to gaze direction and body midline did not influence perceptual size estimation. As such, we cannot draw conclusions about the use of reference frames centered on either gaze or body midline for haptic size processing, therefore further research is warranted to disentangle the reference frames involved in these processes. Therefore, we designed the subsequent experiments with a

gaze and hand configuration characterized by hand alignment relative to gaze and body midline for simplicity.

In Experiment 2, we assessed whether foveal visual noise modulates the manual estimation of the size of previously haptically explored, occluded stimuli by interfering with EVC activity during the encoding of hypothetical competing haptic size information. The results showed that Noise influenced the average perceptual size estimates, but not their variability as initially hypothesized, resulting in overestimation of stimulus Size, suggesting a functional role of the EVC for haptic size processing. In Experiment 3, however, foveal noise appeared to modulate the precision rather than the accuracy of perceptual size estimates when participants performed a more difficult task. Because of the discrepancy between the effects of Experiment 2 and 3 (i.e., overestimation vs. reduced precision, respectively) and the fact that significance of the noise-related interference effect in Experiment 3 was not confirmed by the ANOVA, we need to interpretate these findings with caution. Given this, we speculate that foveal noise may influence haptic size processing in the EVC through different mechanisms depending on the specific task demands and experimental context. This hypothesis, however, remains speculative and should be tested in future studies.

4.5.1 Influence of gaze direction and hand location on perceptual size estimation

Pirruccio et al. (2020) showed that gaze direction modulates grasping kinematics while participants grasped occluded and previously haptically explored stimuli of different sizes. The authors found wider finger aperture when participants were looking to the right as compared to the left or towards the occluded object, which was always aligned with body midline (Pirruccio et al., 2020). These results suggest that memory of the haptically explored objects might be stored in the EVC in eye-centered retinotopic coordinates. The influence of gaze direction has also been observed on reaching movements toward proprioceptive targets in sighted and late blind individuals (Reuschel et al., 2012). However, the findings of our study on perceptual,

haptically guided size estimation, did not reveal a size estimation bias when gaze direction and hand location were not aligned with each other relative to the aligned condition. In addition, we found no significant main effect of gaze on accuracy and precision of manual size estimates. All in all, these results indicate that while the processing of haptically acquired stimulus information, like size, for action depend on gaze direction, the same might not be true also for perception. Nevertheless, a possible influence of gaze on haptic object discrimination was found by Lawson et al. (2014) who showed that head direction, which likely correlated with gaze direction, had an effect on haptic object recognition with improved performance when the visual and haptic frames of reference were aligned in space.

Overall, while we hypothesized that the hand-gaze and hand-body midline misalignment as compared to the aligned condition would introduce a bias in the manual estimation of the size of haptically explored stimuli, our data did not provide evidence in support of this hypothesis. Likewise, our results did not support the hypothesis that variability of size estimates is higher when the hand is not aligned with the body midline or gaze direction as opposed to when it is, suggesting that misaligned conditions do not induce higher sensory noise or uncertainty as compared to the aligned condition.

Our findings revealed no influence of hand location relative to body midline on haptic size estimation. In fact, the misalignment between hand location and body midline, irrespective of gaze direction, induced no size estimation bias of significant direction in haptic size estimates for either Small and Large stimuli compared to the aligned condition. Similarly, hand location had no significant main effect neither on the average nor on the variability of size estimation aperture. On the contrary, the psychophysical findings of Armstrong and Marks (1999) on haptic perception of linear extent revealed that while the lateral position of a haptic stimulus does not consistently bias the mean magnitude of perceived extent, haptic perception is fundamentally anchored to body-centered movement directions (e.g., radial vs. tangential)

(Armstrong & Marks, 1999). The significant magnitude of condition-related size estimation bias we observed in the Hand-Body Midline misaligned vs aligned conditions might reflect the cost of coordinate transformation associated with shifting the hand-centered reference frame away from the body midline, which seemingly influences haptic size processing more than gaze-centered mapping in purely haptic tasks.

Furthermore, the interaction between gaze direction and hand location did not reach statistical significance. Yet the use of mixed body- and gaze-centered reference frames has been shown for reaching towards proprioceptive-tactile target when an effector movement is introduced before reaching (Mueller & Fiehler, 2016). To note, target locations previously encoded within a gaze-centered reference frame are hypothesized to undergo transformations into head, body, or combined frames of reference prior to the computation of muscular commands, especially when visual feedback is not available during the movement phase (Andersen & Buneo, 2002; Blohm et al., 2009; Flanders et al., 1992; McIntyre et al., 1998; Snyder et al., 1997). Based on this evidence, we might speculate that similar mechanisms occur when planning and executing haptic exploration of stimuli despite of the absence of direct stimulus-related visual information, and that both types of reference frames participate during haptic size processing, probably at different processing stages. However, since we did not find evidence suggesting the use of reference frames centered on either gaze direction or body midline, this remains a speculation that requires further investigation.

4.5.2 Effects of dynamic visual noise on perceptual size estimation

Evidence for the role of V1 in haptic processing comes from studies that showed activation in the EVC while participants haptically explored objects in the absence of visual input (Merabet et al., 2007; Monaco et al., 2017; Sartin et al., 2026; Singhal et al., 2013; Snow et al., 2014). Notably, Bola et al. (2017, 2019) additionally found that the visual cortex in sighted, blindfolded participants trained in tactile Braille reading for eight months is causally

involved in tactile processing required for the discrimination of Braille letters. Interestingly, they also found that the visual cortex supports tactile processing in a hierarchical fashion, with early tactile processing occurring in early visual areas, and more complex tactile processing recruiting higher-order visual areas (Bola et al., 2019). Merabet et al. (2008) also demonstrated that the visual cortex of sighted subjects shows an increase in the blood-oxygen-level-dependent (BOLD) signal after five days of blindfolding (i.e., complete visual deprivation) and concomitant tactile training. Further, they found that transient disruption of the occipital cortex via repetitive TMS (rTMS) on the fifth day impaired the ability to discriminate Braille letters in the blindfold group, but not in the non-blindfolded control subjects (Merabet et al., 2008). As the authors pointed out, these results indicate that intensive tactile training and a period of visual deprivation can induce the recruitment of latent connections and rapid cortical reorganization which result in the functionally relevant recruitment of the visual cortex in tactile tasks. Nevertheless, previous TMS studies demonstrated the functional relevance of the visual cortex for the perception and discrimination of orientation and motion through touch (Amemiya et al., 2017; Zangaladze et al., 1999) without having participants undergo a period of intensive training or visual deprivation. Therefore, our results extend our knowledge on the functional relevance of the visual cortex for haptic perception, by showing that haptic size processing in the occipital cortex, precisely in V1, is behaviourally relevant, and that neural mechanisms like cortical reorganization and unmasking of latent connections are likely not necessary to induce the functional recruitment of the visual cortex for haptic size processing.

To accurately estimate the size of an object explored through touch only, the brain needs to translate proprioceptive and kinematic inputs into a representation of object size that ultimately allows us to provide a perceptual size estimate. We suggest that the visual cortex participates in this process by providing a stable and accurate spatial reference scale where the haptically acquired size-related information are mapped onto. Interestingly, we found that

interfering with V1 activity through the foveal noise differentially affected this process based on experimental context and task demands. In fact, in Experiment 2 we observed a significant difference between the average size estimates in the Noise vs No noise conditions, with greater size estimates (i.e., reduced accuracy) in Noise trials, whereas in Experiment 3 there was a significant difference in the SD of size estimates between Noise and No noise conditions, with greater variability (i.e., lower precision) when Noise was presented. Given the mixed results observed across the two experiments, along with the fact that the influence of noise on the variability of size estimates reached significance in the planned directional comparison but not in the ANOVA, the interpretation of the effects of foveal noise on size estimation require caution. With this in mind, we can only speculate that the apparent discrepancy between the results of Experiment 2 (systematic overestimation) and 3 (increased variability) could be associated with the difference in task demands. When size differences were broad (20 mm steps) like in Experiment 2, the task was easier as it required a coarse discrimination between stimulus sizes. In contrast, when size differences were small (2.5 mm steps) like in Experiment 3, the task was more difficult as finer discrimination was needed to distinguish very similar stimuli within a narrow range of sizes. Hence, it is possible that when task demands are low (larger differences between stimuli), participants primarily need to maintain a consistent internal spatial representation of the size of stimuli. Instead, when task demands are high (smaller differences between stimuli), they need to focus on sensory precision to distinguish between very similar stimuli. As such, when foveal noise interferes with haptic processing in a low-demanding task, it might cause a change in size calibration due to the lack of a stable spatial reference scale, thereby leading to systematic directional bias in size estimation. In the case of a high-demanding task, foveal noise might influence the precision of size estimates, resulting in more variable size estimates with no directional bias. In sum, these results may indicate that V1 is recruited for haptic size processing in a task-dependent manner, by providing a spatial

reference scale for size representation during haptic processing for a coarse size discrimination task and by supporting a finer-grained resolution of size information during haptic processing for a finer discrimination task. However, this remains a speculation that should be tested in future studies in order to unveil the specific mechanisms mediating the effect of foveal noise on size estimation performance.

Alternatively, we might also hypothesize the potential involvement of bimodal neurons. In fact, our manual estimation task requires participants to open the thumb and index fingers such that the gap between fingers matches the size of the explored stimuli. This process likely relies on the dorsal stream, which translates the haptically-acquired perceptual size information into a motor output. The posterior parietal cortex, which is part of the dorsal stream, is therefore an important step for the processing of haptic size-related information (Perini et al., 2020; Sartin et al., 2026). Interestingly, this region contains the so-called bimodal neurons which respond to both visual and somatosensory inputs. Notably, these visuo-tactile neurons have been identified in various cortical and subcortical regions of the macaque brain, including area 7b of the inferior posterior parietal lobe (Hyvärinen, 1981; Hyvärinen & Poranen, 1974), the ventral intraparietal area (VIP) in the fundus of the intraparietal sulcus (Colby et al., 1993, Duhamel et al., 1998), the caudal portion of the premotor cortex (Graziano et al., 1997; Rizzolatti et al., 1981), superior temporal sulcus (Bruce et al., 1981), superior colliculus (Wallace et al., 1996), and putamen (Graziano & Gross, 1993). The multisensory interactions in parietal and frontal regions are especially relevant for the construction of representations of the peripersonal space (i.e., the region of space immediately surrounding the body, where we can manipulate objects), which are in turn crucial for sensory guidance of motor behaviour, including object-oriented hand actions (di Pellegrino & Làdavas, 2015). Since representations of size-related information acquired through haptic exploration alone have been found in intraparietal sulcus (Perini et al., 2020) and premotor areas (Sartin et al., 2026), it may be possible that bimodal neurons in these

regions are recruited to process haptic size information. If this is true, then the involvement of these neurons might also explain the results observed in the present behavioural studies showing the effect of visual noise on haptically guided perceptual size estimation of occluded stimuli. When participants haptically explore the stimuli to acquire information about their size, proprioceptive and tactile inputs might be processed by visuo-tactile neurons to build a representation of the size of the explored stimulus. Since the visual receptive field of bimodal neurons is anchored to the tactile receptive field located on the arm or hand (Graziano et al., 1994), if concomitantly foveal noise is presented in the region of space overlapping with the spatial location of the exploring hand, then the integration of visual noise information with the size-related haptic input might increase the signal-to-noise ratio or degrade the purely haptic information. Nevertheless, while this may be an interesting alternative interpretation of our behavioural findings, it does not necessarily and completely exclude the role of V1 in haptic size processing. In fact, facilitatory cross-modal influences on unisensory processes may occur through feedback connections from multimodal areas to more specialized unimodal areas in order to strengthen and refine the perception of stimuli (Magosso et al., 2010). Complementarily, when the degraded cross-modal information is fed back to the unisensory brain region (i.e., V1), the task-relevant representation of the stimulus might lack the necessary refinement due to the degraded information coming from higher-order visuo-tactile regions. As such, bimodal neurons in frontal and parietal cortices and V1 might simultaneously contribute to haptic size processing through potential feed-forward and feed-back mechanisms. However, as mentioned previously, the specific neural mechanisms at the basis of the visuo-haptic interference observed in our behavioural experiments should be further tested in future studies.

The effect of Noise on size estimation might also by explained by reduced awareness of the tactile input as attention is focused on the foveal visual noise. In this regard, one study has shown that tactile detection sensitivity was reduced in response to an increase in the visual

perceptual load during a concurrent visual task, suggesting that vision and touch share perceptual resources (Murphy & Dalton, 2016). As such, perceptual size estimation would be affected because the shared attentional capacity is engaged by visual information processing leaving no available resources for haptic information. However, while the study by Murphy & Dalton (2016) required participants to perform a visual task which poses a high cognitive load, our participants simply had to ignore (i.e., passively view) the flickering foveal noise thereby inducing a low cognitive load. Therefore, our finding that noise interferes with haptic performance despite the lack of a visual task suggests that the attentional load explanation might be less likely. Yet, our data do not allow us to completely exclude the attentional argument. It might also be possible that both V1 functional recruitment and attentional load mechanisms are at play, but not mutually exclusive. To rule out the hypothesis that attentional load that could be induced by visual noise, future studies could test whether flickering noise in the periphery of the visual field would interfere with haptic estimation performance.

4.5.3 Weber's law in haptic processing

Interestingly, we found a significant effect of Size on standard deviations in Experiments 1 and 2, indicating that haptically guided size estimation adheres to Weber's law. Observed and documented across sensory modalities (Holway & Pratt, 1936), this psychophysical principle posits that discrimination thresholds scale proportionally with the magnitude of the stimulus (Fechner, 1948). In the context of haptic tasks, this implies that larger objects are perceived with less precision than smaller ones. Evidence suggests that this holds true for haptic size estimation but not haptic grasping (Pettypiece et al., 2010), in line with a functional dissociation between the dorsal and ventral streams which differentially process visual information for action and perception, respectively (Goodale & Milner, 1992). However, recent evidence suggests that the dissociation between action and perceptual tasks may be driven by the availability of sensory feedback rather than by distinct visual processing streams, as pantomime

grasps without online visual and final haptic feedback adhered to Weber's law (Deng et al., 2024). Our results align well with these findings confirming that haptically-guided manual size estimation follows Weber's law.

Yet, while the variability of manual estimates in Experiments 1 and 2 scaled linearly with stimulus size consistent with Weber's law, we did not find the same pattern in Experiment 3. This result is likely due to the restricted stimulus size range in Experiment 3 (55-65 mm) compared to the wider stimulus range used in Experiments 1 and 2 (20-60 mm). Specifically, over such a narrow 10 mm-range of sizes used in Experiment 3, the subtle increase in the variability of size estimates predicted by Weber's law was probably overshadowed by other sources of variance, including intrinsic measurement noise and motor variability associated with the moving hand, making the scaling effect too small to be statistically detected.

4.5.4 The potential role of the EVC in haptic processing

Based on the findings of the current study, we tentatively propose that the EVC might play a role in haptic processing of stimulus properties, like size. Notably, early visual areas enable us to process visual information with a high level of detail. As such, other sensory systems might take advantage of these high-resolution processing mechanisms to achieve the same level of accuracy for representations based on non-visual information. For instance, when we need to process the size of haptically explored stimuli, in the absence of visual information, we may need to remap size-related tactile input into a visual frame to complement the haptic size representation with finer-grained size processing that characterizes the early visual areas. This speculative interpretation would rely on known functional connections between the EVC and higher-order visual and multisensory cortical regions that process object shape or size using vision and touch, like the LOtv and aIPS (Amedi et al., 2001; Króliczak et al., 2008; Marangon et al., 2016; Monaco et al., 2017; Perini et al., 2020; Sartin et al., 2026). In this regard, the EVC might receive haptic object information from higher-order cortical regions to help with refining

the spatial details of the size representations given its high spatial resolution. As such, the patch of foveal noise might disrupt this feedback mechanism, thus interfering with the refinement of the haptic size representation which results in a change of perceptual size estimates. In our experiments, the presentation of flickering visual noise while participants haptically explore occluded stimuli would recruit the EVC, thus leaving no available resources in this cortical area for the processing of haptic size information. This would force the haptic system to rely solely on somatosensory processing mechanisms that, in this context, might be less precise than the visual ones, thus leading to a disruption of size estimation processing. However, the high spatial resolution of visual information processing is specific to the foveal visual cortex. Therefore, to specifically test the above-mentioned hypothesis, future studies should examine whether interference with visual processing in the periphery would similarly affect perceptual size estimates.

While our findings suggest that foveal noise can interfere with haptic size processing, the precise mechanisms through which the EVC supports haptic processing under varying task demands remain to be elucidated. We propose a task-dependent hypothesis, speculating that the EVC may differentially support haptic size processing based on task demands (i.e., biasing estimates when size differences are large vs. increasing uncertainty when finer discrimination is required). However, whether these different patterns of noise interference effects reflect distinct neural mechanisms remains an open question. In addition, given that foveal noise differentially influenced accuracy and precision of size estimation across experimental contexts and that the noise interference effect on precision was not consistent across different analyses, the hypothesis about the role of EVC in haptic size processing remains a speculative framework. Future research is needed to determine whether the different patterns of noise interference effects on accuracy and variability of size estimation can be reliably replicated. Likewise, future studies using targeted manipulations of task difficulty are needed to test whether and how the

EVC involvement in haptic processing might differ across experimental contexts of varying difficulty.

4.5.5 Limitations

The present study has some limitations. In Experiment 1, hand location (center vs. right) varied across blocks and participants were informed about the object's spatial location (center vs. right) prior to the onset of each block. This design choice was necessary to allow participants to accurately reach and interact with the object in the absence of online visual information about the moving hand and the target object. However, providing prior spatial information about object location may have facilitated performance, thereby potentially masking possible effects of gaze direction and hand location on size estimation performance. Future studies could randomize object location on a trial-by-trial basis to increase task demands and to induce the need to frequently update spatial and size-related representations, potentially providing a better understanding of the spatial reference frames used for haptic size processing. In addition, regarding Experiment 1, we focused our investigation on specific gaze directions and hand locations (i.e., center vs. right). Future research using a full-factorial design including the left visual field and left side of the body (e.g., gaze left, hand left), along with varying eccentricities, could provide a clearer and more informative picture about the reference frames used for haptic size processing. In relation to Experiments 2 and 3, the additional control of the location of foveal noise in the visual field (i.e., in peripheral locations) could shed light onto the potential role of attentional mechanisms in mediating the observed effects of noise on perceptual size estimation. Finally, as discussed in Section 4.5.4, the discrepancy in the noise effect on haptic size estimation (accuracy in Experiment 2 vs. precision in Experiment 3) suggests that the role of the EVC may depend on task demands and experimental context. Given that the noise effect on variability in Experiment 3 was not consistent across different analyses, our task-dependent hypothesis remains speculative. Therefore, future research is needed to replicate the noise

interference effects on haptic size estimation using targeted manipulations of task difficulty to confirm whether the EVC contributes to haptic size processing through different mechanisms depending on task demands.

4.6 Conclusions

In this study, we investigated whether the location of the occluded target and the exploring hand relative to gaze direction and body midline influence haptic size processing for a perceptual manual estimation task. We showed that the misalignment between hand and gaze, as well as the misalignment between hand and body midline do not appear to influence haptically guided size estimation. As such, although our results seem to not support the use of reference frames centered on gaze direction and body midline for haptic size processing in the absence of stimulus-related visual information, further research is warranted in order to thoroughly investigate the frames of reference involved in haptic processing of the size of unseen stimuli.

To the best of our knowledge, this is the first study examining the functional relevance of V1 for haptic size processing by using a behavioural paradigm that interferes with the visual cortex via a dynamic patch of visual noise presented in fovea, while participants process haptic size information that are relevant for performance in a subsequent manual size estimation task. Our results suggest that foveal visual noise can influence haptic size processing, though the nature of the noise-related interference seems to vary with task demands. Indeed, in Experiment 2 we found that foveal visual noise induced an overestimation of stimulus size, indicating an effect of noise on estimation accuracy. In Experiment 3, under increased task difficulty, the noise interference was reflected in increased variability of size estimation performance, suggesting a reduction in estimation precision. While these findings require a cautious

interpretation, they nevertheless suggest a behavioural relevance of V1 for haptic size processing. In addition, we speculate that V1 might support haptic size processing through different mechanisms depending on task demands and experimental context, with low and high-demanding tasks affecting the accuracy and the variability of size estimation, respectively. Future research is needed to replicate foveal noise interference effects on haptic size estimation and test whether the proposed task-dependent hypothesis can account for the discrepancy of the effects observed in our studies.

Chapter 5

General Discussion and Conclusion

5.1 Thesis summary

Humans are equipped with a powerful biological "tool", namely the hand, which is capable of executing goal-directed actions and haptically exploring objects, allowing us to shape our surroundings and, at the same time, to perceive and understand it. In this thesis, we investigated the neural mechanisms at the basis of grasping, reaching, and haptic exploration, particularly focusing on the role of the ventral visual stream and EVC in these processes when visual input is unavailable. We did so by levering different methodologies (i.e., ALE meta-analysis, fMRI and behavioural experiments) to gain deeper insights into the network of brain areas involved in the execution of skilled hand actions and haptic object exploration, and the behavioural relevance of visual areas in haptically guided estimation of object properties. This is key to understanding whether the frequent co-occurrence of visual and haptic information during everyday life interactions with our environment might induce the development of shared processing mechanisms across primary sensory areas that allow these cortical regions to be recruited even in absence of inputs from the native sensory modality. In addition, this investigation could also shed light on the potential role of early visual areas in generating predictions for actions, especially in the absence of direct visual information.

In Chapter 2, we capitalized on a coordinate-based meta-analysis to systematically aggregate and analyze the existing neuroimaging literature which used univariate analyses to investigate the neural bases of the execution of human hand reaching and grasping actions, with and without online visual input. This allowed us to summarize the brain areas consistently involved in reaching and grasping actions across the literature, but more importantly for the focus of this thesis, we addressed the controversial involvement of ventral visual stream areas in delayed actions without online visual feedback. The results of our meta-analysis confirmed the well-known role of the dorsal stream in the guidance and execution of skilled hand actions, by showing its consistent involvement in both reaching and grasping actions, with slightly

higher involvement in no-visual conditions, likely reflecting the increased effort in maintaining and updating the internal representation of the arm for guiding the action. In contrast, the ventral visual stream was consistently involved in the guidance of reaching and grasping only when visual information about the target and the moving hand was available during action execution, in line with its well-known role in visual processing. In addition, we hypothesized a stronger recruitment of the ventral visual stream for grasping than reaching, as grasping but not reaching require the processing of object properties like size and shape that are crucial for hand pre-shaping and, in turn, for efficient hand-object interactions. However, contrary to our expectations, we found the ventral stream to be similarly recruited across grasping and reaching actions. Overall, these results suggest that parietal and frontal cortices are consistently involved in grasping and reaching regardless of the availability of visual information, while the occipital-temporal cortex is only recruited when hand actions are performed with vision. Yet, while the EVC and ventral stream regions do not show a consistent and significant above baseline activation during action execution, they might still represent action-related information in a more complex pattern of activation distributed across voxels which cannot be detected by classical univariate analysis. In support of this, recent work using MVPA has shown that the EVC and ventral visual stream represent specific action intentions (i.e., reaching vs grasping) (Monaco et al., 2020), regardless of the availability of visual information (Monaco et al., 2019). As such, this growing body of evidence leaves the possibility for the EVC and the ventral stream to play a role in action execution. Therefore, in the following chapter we examined if these brain areas play a role in processing action-relevant information about object properties acquired solely through active touch in absence of visual information, by using multivoxel pattern analysis.

In fact, in Chapter 3 we focused on the perceptual component of hand-object interactions, that is haptic processing of object attributes which occurs while we haptically

explore objects through active touch. We focused on a specific property of objects, namely size, which is crucial for planning efficient hand-object interactions, especially for grasping, and it is also a property that can be easily manipulated and controlled for in the experimental setting. In addition, we investigated whether the potential representation of haptically explored object size could be explained by top-down visual imagery. To achieve our aim, we performed an event-related fMRI experiment during which blindfolded participants haptically explored or visually imagined the size of different rings. We then used MVPA to investigate if EVC and other task-relevant brain regions contain a representation of the haptically explored stimulus size, and whether this effect might be due to visual imagery. The MVPA results in V1 and OP showed accurate decoding of size only during haptic exploration, suggesting that visual imagery cannot explain the activity patterns observed during the haptic task. In addition, we found overlapping but distinct representations of haptically explored and visually imagined size in frontal and parietal regions, along with the multisensory area LOtv, whereas only aIPS, pIPS and dPM also showed successful cross-decoding of size. Interestingly, the PPI analysis indicated that V1 and OP show stronger functional connections with ventral and dorsal visual stream areas during haptic exploration relative to the visual imagery task. In sum, these findings demonstrate that frontal and parietal regions specialized for action, haptic exploration, and visual imagery similarly represent haptic and imagined stimulus size. In contrast, early visual areas represent haptic but not imagined size information, thereby providing evidence against their top-down recruitment by visual imagery processes. Instead, early visual areas might play a role in haptic size processing through connections with higher-order brain regions in ventral and dorsal visual stream regions, including LOtv and aIPS, which are involved in action planning and execution, as well as processing shape-related information acquired through both touch and vision (Amedi et al., 2001; Króliczak et al., 2008; Marangon et al., 2016; Monaco et al., 2017; Perini et al., 2020). While these findings demonstrate that haptic size information is

represented within the EVC, the presence of such representations does not necessarily imply that this brain region is also relevant for haptically-guided behaviour. To investigate the behavioural relevance of haptic processing in EVC, we conducted the third study presented in the following chapter of the thesis.

Specifically, in Chapter 4, we further investigated haptic size processing from a behavioural perspective. We conducted three behavioural experiments each investigating the influence of specific variables on haptic processing of the size of occluded stimuli for a perceptual manual estimation task. In Experiment 1, we investigated the influence of gaze direction and hand location on haptic size processing. The results showed that neither gaze direction nor hand location relative to the stimulus and the exploring hand modulates performance in the manual size estimation task. While we expected performance to worsen when the exploring hand was not aligned with gaze direction and body midline, our results did not reveal any estimation bias or higher perceptual uncertainty in the misaligned compared to the aligned conditions. Overall, these findings do not support the use of reference frames centered on gaze direction and body midline for haptic processing of the size of occluded stimuli. Therefore, further research is needed to better understand the frames of reference used for haptic size processing. In light of these results, for simplicity we defined a configuration of gaze direction and hand location for two subsequent behavioural studies where both were aligned with the stimulus location. In fact, in Experiments 2 and 3 we focused our investigation on the functional relevance of the EVC for haptically-guided perceptual size estimation. To this aim, we adapted a behavioural paradigm generally used in the visual domain (Fan et al., 2016) to the haptic one. Specifically, we physiologically disrupted processing in V1 by presenting a patch of dynamic visual noise while participants haptically explored different sized cylinders for the subsequent manual size estimation. We hypothesized that, if haptic size processing in the EVC is behaviourally relevant, then the presentation of visual noise should compete with

the processing of haptic size information, thereby interfering with and worsening perceptual size estimation. The results of Experiment 2 demonstrated that foveal visual noise indeed disrupts haptic size processing by inducing an overestimation of size relative to the no-noise condition, highlighting V1's role in this process. Further, the results of Experiment 3 revealed that under increased task difficulty, the noise-induced interference manifested as an increase in the variability of size estimation performance, suggesting a reduction in estimation precision. Although these findings need to be interpreted with caution, they altogether suggest a behavioural relevance of V1 for haptic size processing. Based on these findings, we speculated that V1 might support haptic size processing through different mechanisms depending on task demands and experimental context. However, future research is needed to replicate the effects of noise on haptic size estimation and test whether the proposed task-dependent hypothesis can account for the discrepancy of the effects observed in our studies. Overall, the behavioural results appear to align with and extend previous findings on the functional relevance of the visual cortex for tactile orientation and motion discrimination in sighted individuals (Amemiya et al., 2017; Zangaladze et al., 1999), by showing that also haptic size perception might rely on V1.

5.2 General discussion

The contributions presented in this thesis indicate that the EVC might subserve important functions not only for perception while our hands acquire information about object attributes through active tactile exploration, but also for planning and executing actions with our hands towards objects. Based on this evidence, we propose two possible explanations for the functional recruitment of the EVC for haptic size processing and haptically guided action execution. One possibility is that EVC may contain mechanisms for the processing of fine-

grained spatial information that are shared across sensory modalities, especially because sensory inputs frequently co-occur in time and space during everyday life. Another non-mutually exclusive explanation is that EVC may process sensory information that is useful to predict the sensory consequences of upcoming actions.

5.2.1 Shared or distinct neural mechanisms across sensory modalities?

Previous studies showed the existence of multisensory and modality-independent representations of object properties, supported by either distinct or shared neural mechanisms, in higher order visual processing areas (Xu et al., 2023; Van Kemenade et al., 2014). There are now multiple, compelling sources of evidence for the multisensory modulation of V1, where both convergence and integration of multiple sensory inputs occur (for a review, see Murray et al., 2016). The fMRI and behavioural findings presented in this thesis seem to corroborate the cross-modal modulation of the visual cortex even at the earliest stage of the visual cortical hierarchy, by showing haptic size representations in early visual areas that cannot be merely explained by visual imagery, and that V1 might also be functionally relevant for haptic size processing. All in all, this indicates that the visual cortex is traditionally a unimodal area that exhibits cross-modal and multisensory modulation for inputs acquired through non-visual sensory modalities, namely touch. Importantly, this doesn't seem to be an epiphenomenon of visual imagery.

The finding that we can decode the size of unseen, haptically explored stimuli in early visual areas (Sartin et al., 2026) might be linked to the fine spatial resolution that characterizes early visual areas. In fact, receptive fields (RFs) of visual neurons in early visual areas are relatively small, with the smallest ones located in V1, and increasingly larger ones as we go through higher order regions along the visual cortical hierarchy (e.g., V2, V3, V4). In addition, the size of RFs in all these visual areas is relatively small in the foveal representation and it becomes larger and larger as we move away from the fovea toward more eccentric locations in

the periphery of the visual field (Smith et al., 2001; Zeki, 1978). The scaling of RFs' size adheres to a scale-invariant principle: the size of the population receptive field (pRF) is inversely proportional to the spatial frequency preference, while maintaining a constant sampling density (i.e., cycles per RF) throughout the visual hierarchy (Wiecek et al., 2026). The combination of the small size of high-frequency-tuned RFs and the high cortical magnification factor of the foveal representation (i.e., disproportionately larger amount of visual cortex devoted to the processing of central compared to peripheral vision) ensures that V1 and precisely its foveal representation is equipped with high-spatial resolution for precise spatial discrimination (Harvey & Dumoulin, 2011). This makes V1 and especially its foveal representation a good candidate region for the processing of fine-grained sensory information necessary to represent basic geometrical object properties, like size and shape. In line with this, modality-independent representations (i.e., shared across haptic and vision) of basic shape features like curvature and rectilinearity have been found in the occipital cortex (Tian et al., 2023).

However, the evidence for shared domain preferences in the visual cortex, regardless of the sensory modality through which information is acquired, has been and still is a matter of debate. More than two decades ago, Pascual-Leone and Hamilton (2001) advanced the hypothesis of a metamodal organization of the brain, which proposed that sensory cortical areas have intrinsic cognitive (i.e., "metamodal") functions (e.g., detailed spatial discrimination) applicable to inputs from any sensory modality, with experience modifying the sensory input over which they are applied. For instance, the fusiform face area (FFA), a human visual area which plays a key role in visual face perception (for a review, see Kanwisher & Yovel, 2006), is involved in face recognition based on vision in the sighted and based on sound or touch in the blind (Bola et al., 2022; Ratan Murty et al., 2020). Later, in a literature review, Ricciardi and Pietrini (2011) discussed evidence that both congenitally blind and sighted individuals

recruit task-related regions in the visual cortex to process tactile information, in support of the existence of supramodal, abstract representations that are independent of the sensory modality receiving the input, do not require visual experience or visual imagery to form, and can be accessed through bottom-up or top-down mechanisms. A common abstract representation would integrate different types of information from different sensory modalities, thereby promoting a coherent and unified perceptual experience (Ricciardi & Pietrini, 2011). As Kupers & Ptito (2014) argue, the rapid cross-modal responses in visual areas during tactile tasks suggests that the sighted brain possesses connections between occipital and parietal cortices likely conveying non-visual inputs to visual areas. Under normal vision conditions, non-visual inputs can influence processing in the visual cortex (Macaluso et al., 2000) in a functionally relevant way for tactile performance (Zangaladze et al., 1999) without producing tactile sensations (Kupers et al., 2006; Ptito et al., 2008) due to masking by the dominant visual input, while a period of visual deprivation might unmask or strengthen non-visual processing in the occipital cortex (Kupers & Ptito, 2014). Hence, according to this hypothesis, visual areas are not strictly unisensory, but rather multisensory modulated brain regions wherein non-visual inputs are typically masked by competitive visual information. Despite variations in assumptions across the proposed metamodal accounts, they all propose that cortical areas have consistent cognitive and behavioural functions across adults, regardless of early experience or behavioural needs. Yet, it is important to mention that several findings challenge the idea of intrinsic metamodal functions, by showing that visual cortices have seemingly different functional profiles in sighted and blind subjects (for a review, see Saccone et al., 2024). These findings provide evidence in favor of a functional pluripotent view of the brain in early development, which posits that the functional specialization of a brain area depends on an individual developmental experience and behavioural needs, as well as on long-range innate connectivity patterns of that brain region (Saccone et al., 2024). Overall, these frameworks

suggest a cross-modal nature of visual areas. Whether through the unmasking of existing connections, the encoding of abstract representations, or the innate flexibility of the developing brain, the theories discussed above support the premise that early visual areas can process haptic information, not only in the blind but also in the sighted brain.

In this context, we provide evidence for the functional recruitment of the visual cortex of blindfolded sighted individuals in tactile tasks, by demonstrating haptic size representations in V1 and OP that cannot be explained by visual imagery, and that are likely relevant for behaviour as suggested by our behavioural findings, especially when visual information about the stimulus is not directly available. The finding that haptic representation of size information in the EVC is likely due to functional connections with areas involved in visuo-tactile perception of object shape, like the LOtv (Amedi et al., 2001), and haptic object shape processing for subsequent actions, like the aIPS (Króliczak et al., 2008; Marangon et al., 2016; Monaco et al., 2017), is in line with the idea that existing connections between the occipital and higher order brain areas play an important role in mediating the recruitment of the visual cortex for haptic tasks, and that these connections might intensify in the absence of visual information.

While our findings provide evidence in support of the cross-modal modulation of the EVC, they do not inform us about potentially abstract or amodal representations of stimulus size. In fact, amodal representations correspond to symbolic representations of concepts that abstract from the details of a situation, as well as from the characteristics of any particular sensory modality, making the representational content modality-unspecific despite originating from different sensory experiences (Kaup et al., 2024). Our fMRI study included two tasks, namely haptic exploration and visual imagery, as we were focused on investigating whether the size of haptically explored, occluded stimuli is represented in the EVC, and if so, whether this could be explained by top-down visual imagery processes. As such, we did not explore representations of stimulus size in the visual modality. Yet, by directly testing for

representations of visually and haptically explored stimulus size within the same experimental design one could precisely investigate if abstract or amodal representations of size are subtended by a shared, distributed pattern of activity in early visual areas, that enables the representation of the size of stimuli regardless of the characteristics of the sensory modality through which information was initially acquired. The finding of Tian et al. (2023) that basic object features (i.e., curvature and rectilinearity) are represented in the occipital cortex through modality-independent representations, accessible through both vision and haptics, opens the possibility that also size might be similarly represented in EVC irrespective of the sensory input conveying size information.

However, it is also possible that the processing of visual and haptic information is underpinned by different neural mechanisms, especially if we consider the microstructural organization of the visual cortex. In fact, evidence from animal studies shows that non-visual inputs from non-visual regions terminate mainly in layers 1 and 5/6 of the visual cortex, thus avoiding layer 4 (Pennartz et al., 2023), while bottom-up sensory input coming from the retina passes through the lateral geniculate nucleus (LGN) of the thalamus and reaches layer 4 and, to a lesser extent, layer 6 (Felleman & Van Essen, 1991; Roth et al., 2016) of the visual cortex via thalamocortical connections, with information then propagating to layers 2/3 which is reciprocally connected with layer 5 (Douglas & Martin, 2004). As such, while neurons in layer 4 of V1 are driven by bottom-up, thalamocortical visual inputs, neurons in superficial and deep layers of V1 receive non-visual inputs which might help contextualize and update visual representations based on non-visual signals (e.g., Douglas & Martin, 2004). Recent high-resolution fMRI evidence seems to confirm a similar dissociation in human early visual regions (V1-V3), with bottom-up modulations strongest in the middle layer (layer 4) and top-down attentional modulations stronger in superficial than middle and deep layers of the cortex (Lawrence et al., 2019). Therefore, we might speculate that if haptic information is conveyed

to early visual areas through feedback connections from higher order brain regions, as we hypothesize, then these inputs could be processed by different neuronal populations in different layers of the visual cortex, thereby indicating overlapping but distinct neural mechanisms dedicated to the processing of haptic and visual information. However, the nature of cross-sensory representations in early visual areas still need to be thoroughly investigated. As a last note, it might be important to mention that the idea of bottom-up tactile information directly reaching V1 to recruit cross-modal or amodal representations seems very unlikely for the sighted brain given the dominance of visual and tactile input over visual and somatosensory cortices, respectively. On the contrary, a re-routing of tactile information to the occipital cortex through a thalamocortical pathway seems possible in congenitally blind people (Müller et al., 2019) as a consequence of plastic changes following sensory loss.

Interestingly, animal studies also provide evidence for the modulation of V1 activity by non-visual sensory modalities, including somatosensation, as well as by non-sensory factors like body movement (for a review, see Pennartz et al., 2023). For instance, several studies found that somatosensory and proprioceptive stimuli influence V1 activity (Bouvier et al., 2020; Iurilli et al., 2012; Vasconcelos et al., 2011; Vélez-Fort et al., 2018). Therefore, results from animal models and human data seem to converge to some extent, thereby corroborating the idea that early visual cortices are not strictly unisensory, rather they are able to process non-visual inputs, including haptic-related information.

5.2.2 Predictive coding

Despite the inconsistent activation of the ventral stream and EVC during the execution of grasping and reaching actions in the absence of visual information across the neuroimaging literature (Sartin et al., 2023), some pieces of evidence still point to a role of early visual areas, precisely V1, in high-level cognitive and motor-related functions, including planning and executing goal-directed actions. Indeed, activity patterns in V1 before the onset of the

movement can predict the upcoming actions towards visible targets (Gallivan et al., 2019; Gutteling et al., 2015, Monaco et al., 2020). In addition, the execution of actions in the dark, directed towards stimuli previously explored through vision or haptics, activates the EVC (Monaco et al., 2017; Singhal et al., 2013; Styrkowiec et al., 2019). Importantly, visual cortical activation during action execution is not entirely explained by motor imagery since real actions elicit higher activation than imagined actions in EVC likely due to the fact that real actions, unlike imagined ones, involve proprioceptive feedback and efference copy, potentially leading to higher EVC activation during execution compared to motor imagery (Monaco et al., 2017). Likewise, Monaco et al. (2020) found that the activation level in the EVC during motor imagery was around baseline; still, they could decode action content during motor imagery as well as during action planning but not across tasks, thus further supporting the role of the EVC in action-related processes.

What specific purpose might the EVC serve when we plan and execute skilled hand actions? A possible explanation is related to the involvement of predictive coding mechanisms in the visual system. In the context of visual perception, there is evidence for top-down modulations of early visual processing in both animals and humans which have been discussed within the framework of predictive coding (Rauss et al., 2011). According to the predictive coding theory, the brain not only processes incoming sensory input but also generates internal models of the external world based on context and prior experience to generate predictions about the upcoming sensory information. As soon as we receive sensory signals, these are then compared with the prediction based on the internal model, and in case of a mismatch (i.e., prediction error) the internal model is updated based on the new sensory experience. In this regard, the ability of the EVC to predict the visual appearance of objects is supported by evidence showing that the visual cortex generates sensory stimulus templates based on prior expectations, even in the absence of sensory input, potentially facilitating efficient processing

of expected sensory information (Kok et al., 2014, 2017). These predictive representations likely also play a role in the completion of partially visible scenes (Smith & Muckli, 2010; Morgan et al., 2019) and are dynamically updated to account for changes in the environment (Aldegheri et al., 2026). In light of these findings, it is plausible that the EVC uses similar predictive processes to anticipate changes in the environment and the sensory consequences of self-generated actions which are inherently dynamic. Such a mechanism may be facilitated by possible cross-modal feedback signals from somatomotor regions, which have been shown to maintain intrinsic visual representations of the hand even at rest (El Rassi et al., 2024), potentially providing the EVC with additional hand-related information crucial for the prediction of the sensory consequences of an impending movement. In the context of predictive coding for motor control, dominant theories propose that the brain predicts the sensory consequences of upcoming movements using an internal forward model along with an efference copy (i.e., a copy of the motor command) (McNamee & Wolpert, 2019; Shadmehr & Krakauer, 2008; Wolpert & Flanagan, 2001). This prediction allows for motor error correction and enhances the estimation of the body's state by combining predicted and actual sensory input (Scott, 2004; Shadmehr & Krakauer, 2008). According to these dominant theories, the attenuation of sensory reafference (i.e., self-generated sensory input) is necessary to prioritize the perception of externally generated stimuli over expected self-generated stimuli (McNamee & Wolpert, 2019). The finding that action intentions and movement plans can be decoded in V1 prior to movement (Gallivan et al., 2019; Gutteling et al., 2015, Monaco et al., 2020), suggests predictive coding mechanisms in early visual areas. In addition, the fact that V1, which stores haptic representations of object properties like size (Sartin et al., 2026), is involved in action execution and haptic object exploration despite the absence of visual information (e.g. Monaco et al., 2017), further suggests that V1 might help predict the somatosensory consequences of the upcoming reaching and grasping movement toward an occluded target. Since the system

uses internal models of object properties, like size (e.g., Flanagan et al., 2008), to predict the sensory consequences of actions and adjust movements accordingly, it seems plausible that haptic size information in V1 might be used to make sensory predictions based on efference copy and internal models, even when visual information is not available, thus participating in motor control. Other theories have been proposed to describe predictive coding for motor control (e.g., the active inference model by Friston et al., 2011), yet a detailed description of predictive coding theories goes beyond the purpose of this thesis.

Overall, we propose that the results of this thesis could be ultimately explained within the predictive coding framework. Specifically, the visual system likely processes action-related and non-visual perceptual information, even in the absence of visual input, by integrating top-down signals to make predictions that are useful for appropriate hand-object interactions. In fact, sensory, cognitive, and motor domains are strongly interdependent in everyday life interactions with the environment, influencing each other at the neural level. Our experience of stimuli in the external world comprises a myriad of sensory signals coming from multiple senses, that need to be processed and integrated at the neural level. As such, visual, tactile, and motor-related information, among other types of sensory information, are often processed simultaneously, in space and time. Consequently, visual, somatosensory, and motor cortices are often recruited at the same time to make sense of the outside world by integrating multiple sensory signals, and to produce an appropriate motor output through which we can change the state of the world. Therefore, the interdependence between sensory and motor systems is likely crucial for building predictions and generating appropriate outcomes. This makes it possible for the visual system to be strongly involved in predictive mechanisms necessary to generate appropriate movements but also to process sensory information acquired through senses other than vision, like touch, through top-down recruitment likely involving sensory-motor brain regions.

Finally, it is interesting to mention the review by Pennartz et al. (2023) who discuss evidence of multisensory properties of V1 of the rodent brain in light of predictive coding mechanisms. Notably, the authors argue that the fact that non-visual signals terminate in superficial and deep layers of V1, while visual inputs mainly target layer 4 of V1 aligns well with predictive processing, whereby sensory input enters via layer 4, prediction errors are computed in layers 2/3 due to motor feedback and non-visual sensory signals, and predictive representations are coded in layer 5/6 consistent with local and long-range output projections to other brain areas and perceptual outcome feedback to LGN (Pennartz et al., 2023). While we cannot use this evidence to draw conclusions on predictive coding in the human, it still provides compelling evidence for action-related properties of early visual areas that might be shared across different species.

5.3 Methodological considerations and limitations

The first contribution of this thesis, presented in Chapter 2, allowed us to clarify the consistency across neuroimaging studies on the neural bases of goal-directed hand actions with and without online visual information as investigated with univariate analysis. We demonstrated the involvement of the frontal and parietal areas in reaching and grasping, while also exploring the potential role of the temporal-occipital cortex, especially when online visual input is unavailable during action execution. However, as discussed in Section 2.4.3, limitations of the work include the type of univariate contrasts used in primary studies categorized as Grasp with Vision. In fact, half of these experiments used contrasts involving visual processing of the reaching limb and grasping hand only, thereby excluding visual processing of the object. This may have hindered the possibility to find consistent activation in brain areas associated with visual processing during action execution, consequently influencing the results of our analysis

contrasting actions performed with vision, with actions performed without vision. As such, the results of our meta-analysis highly depend on the type of contrasts used by the included neuroimaging studies. In addition, an increasing number of neuroimaging studies proved MVPA to be crucial for the investigation of action-related representations in early visual areas (Gallivan et al., 2013, 2019; Gallivan, McLean, Valyear, et al., 2011; Gutteling et al., 2015; Monaco et al., 2019, 2020; Velji-Ibrahim et al., 2022). However, these MVPA studies could not be included in our coordinate-based meta-analysis as MVPA and univariate analysis produce different types of data (i.e., percentage of classification accuracy and activation level, respectively) that cannot be collapsed with each another. Further, the number of studies using MVPA is not yet large enough to neither motivate nor permit a meta-analysis of MVPA data on this topic. Therefore, we need to keep in mind these limitations when interpreting the results of our meta-analysis. Notably, we cannot completely rule out the potential role of EVC in action-related processes especially if we consider the evidence beyond the one included in our study.

In the fMRI study described in Chapter 3, we focused on the role of the EVC in haptic processing of stimulus size. Nevertheless, it would be worth investigating if stimulus size could be similarly decoded also in the visual modality. In this regard, we could directly test for the presence of shared processing mechanisms accessible from different sensory modalities, namely vision and touch, which might be subtended by similar or distinct neural mechanisms. This would further clarify the nature of size representations in the visual cortex, which could be either bimodal/multimodal (i.e., distinct activity patterns underly visual and haptic size representations) or amodal (i.e., vision and touch share the same activity patterns to represent the geometrical size of stimuli, regardless of the sensory input conveying information about the object attribute). In addition, we also tested whether haptic size decoding in early visual areas could be due to visual imagery. We found no successful decoding of visually imagined size in early visual areas, providing evidence in support of the hypothesis that visual imagery cannot

completely explain the haptic processing observed in these areas (for a detailed discussion, see Section 3.4.1). However, as mentioned in Section 3.4.4, since participants could solely rely on previous haptic experience with the stimuli (i.e., they never viewed the stimuli, neither before nor during the experiment), they might have used this haptic information to create a visual mental image of the stimulus size during the visual imagery task. Therefore, they might have engaged also motor or tactile imagery to some extent, even though we explicitly asked to just visually imagine the size of stimuli. Yet, the finding that we can decode size in the visual imagery tasks in frontal and parietal regions known for their role in visual imagery somehow supports the visual nature of the imagery task. In addition, it also makes it unlikely for the visual imagery task to not be able to sufficiently activate brain regions, especially early visual areas, due to lower signal-to-noise ratio (SNR) compared to the haptic exploration task. Instead, our finding is line with the inconsistent recruitment of early visual areas in visual imagery tasks (Spagna et al., 2021). In this regard, an important methodological consideration, as shown by Arbuckle et al. (2019), is that multivariate discriminability measures can scale with overall BOLD signal amplitude and SNR, even though the underlying representational geometry remains stable. In our study, across most ROIs, Haptic exploration elicited overall stronger activation amplitude (i.e., higher β-weight values) compared to Visual imagery (Supplementary Figure 3.1 and 3.2). Therefore, it is possible that the non-significant or significantly lower decoding accuracy for visually imagined compared to haptically explored size, especially in early visual areas, is attributable to the lower SNR observed in univariate fMRI results in Visual imagery vs. Haptic trials. Yet the relationship between decoding accuracy and signal amplitude in the Visual imagery condition was not consistent across all ROIs. In particular, in left LOtv activation amplitude in the Visual imagery condition was at baseline while decoding accuracy was significantly above chance level. In other ROIs, specifically bilateral preSMA, right SMA, bilateral vPM, right M1S1, bilateral ITS, we observed the opposite pattern of results:

significantly above baseline activation levels for the Visual imagery condition, while decoding accuracies were at chance level. Therefore, not all brain areas showed a clear modulation of decoding accuracies by SNR and signal amplitude. Overall, while we cannot draw conclusions about the exact nature of the relationship between univariate signal amplitude and decoding accuracy observed in this study, it is still important to consider the possible influence of SNR on decoding accuracies observed especially in early visual areas.

Haptic-related recruitment of and representations in early visual areas are unlikely to be due to imagery-related inputs form higher-order brain regions. Indeed, if haptic activity in early visual areas were primarily driven by involuntary visual imagery processes, then we would expect voluntary visual imagery to elicit at least comparable activation levels and decoding accuracies within a given ROI. On the contrary, our findings revealed successful decoding and significantly above baseline activation levels in early visual areas during Haptic exploration but not Visual imagery. Altogether, our results indicate that higher-order areas like LOtv, aIPS, pIPS, and frontal areas, showed successful size decoding and significant above-baseline activation levels in Haptic and Visual imagery conditions, thereby confirming that our Visual imagery task successfully engaged brain areas typically known to be involved in imagery processes (for a meta-analysis, see Spagna et al., 2021).

The successful cross-decoding of stimulus size in frontal and parietal areas might have been influenced by the experimental context. In fact, we used an event-related design in which the two task modalities were interleaved within runs. In addition, during the training session haptic trials were necessarily presented prior to imagery trials to provide participants with the size information that they later needed in imagery trials. As such, it is possible that imagery results were influenced by the recently acquired haptic information. Therefore, participants might have implicitly relied on short-term haptic memory of the stimulus size during visual imagery trials. Based on this consideration, the observed cross-modal decoding in frontal and

parietal areas might reflect shared tactile and haptic memory-based processes rather than purely abstract size representations that are independent of task modality. Future studies could test whether the effects observed in our event-related fMRI study would persist under conditions of minimal sensory influence during visual imagery, for instance by separating haptic and imagery tasks across experimental sessions or days. Lastly, while our experimental paradigm allowed us to precisely target stimulus size by rigorously controlling for other stimulus properties, it did not enable testing for ecologically valid haptic behaviour. In fact, everyday-life haptic interactions with objects in natural environments typically involve the use of multiple digits at once, often exploring 3D object volume, weight, and material compliance, all of which can provide cues about size. By constraining haptic behaviour to a circular exploration along engraved rings using only the thumb and index finger, we prioritized the isolation of stimulus size and the kinematic variables associated with the exploratory movement over environmental complexity and validity. While this provided the necessary control for our investigation, it may limit the generalizability of our findings to more naturalistic object manipulation. Future research should extend our findings by including naturalistic haptic object exploration to determine whether and how the complex combination of different material properties and motor strategies influence haptic size processing and the underlying neural mechanisms.

Beyond the adoption of widely used fMRI and meta-analytical techniques, I also employed a novel approach to specifically investigate the behavioural relevance of the visual cortex in haptic processing. Notably, the contribution presented in Chapter 4 represents the first attempt to assess this in sighted subjects by using a behavioural paradigm which includes the presentation of foveal visual noise used by Fan et al. (2016) and studies the potential effects of hypothetical interactions between the visual and haptic systems. On the one hand, this contribution tests the effectiveness of this promising paradigm for studying the role of the visual cortex in haptic processing of objects attributes. On the other hand, the novelty of this approach

necessarily requires further testing and replication studies in order to confirm our results, as well as the use of complementary methodologies to gain a deeper understanding of the neural mechanisms behind the observed effects on haptic behaviour. In fact, while the discrepancies in the noise-related effects on size estimation across experimental contexts (i.e., overestimation in Experiment 2 vs. lower precision in Experiment 3 under higher task demands) could be explained by a task-dependent hypothesis, these apparently mixed effects of noise on performance should be replicated in future studies and the speculative hypothesis should be tested with targeted experiments. In addition, the recruitment of V1 might not be the only possible mechanism mediating the interaction between visual and haptic systems as we already discussed in Section 4.5.2 and Section 4.5.5. As such, additional hypotheses should be tested, including the potential role of bimodal neurons, to explain the functional relevance of V1 for haptic processing especially in the sighted population. Likewise, whether the observed effects might be due to attentional load mechanisms and noise-induced distraction, rather than functional recruitment of V1, should be further investigated in future studies. In this regard, NIBS approaches could confirm the causal involvement of the EVC in haptic processing, while techniques like magnetoencephalography (MEG), and electroencephalography (EEG) would shed light on the temporal dynamics of EVC recruitment during haptic exploration thanks to their higher spatial resolution as compared to fMRI. As for the investigation of reference frames centered on gaze direction and body midline potentially involved in haptic exploration of occluded targets, our experimental design only included central and right fields of view, as well as central and right target locations to which the right hand was directed for haptic exploration. While the observed results suggest that neither reference frame is used during haptic object exploration in the absence of visual input, a complete factorial design including both hands and all parts of the space compared to body midline (i.e., left, center, right gaze direction and target location) could provide a more comprehensive understanding of the reference frames used for

haptic size exploration. Further, prior spatial information about object location in Experiment 1 may have facilitated performance in the manual size estimation task, potentially masking any possible effects of gaze direction and hand location on size estimation. Therefore, future studies should randomize object location within blocks and across trials to increase task demands and to possibly provide a better understanding of the spatial reference frames involved in haptic size processing.

5.4 Conclusion

To conclude, this thesis addressed three main questions: i) Are dorsal stream, and especially early visual and ventral visual stream areas differentially recruited during the execution of hand reaching and grasping when online visual input is available compared to when it is not? ii) Do early visual areas represent haptic object attributes, like size, in such a way that visual imagery cannot explain? iii) Pending a positive answer to the previous question, is the recruitments of early visual areas functionally relevant for haptic size processing? To address these three crucial questions, we leveraged three distinct methodological approaches, namely a coordinate-based meta-analysis of neuroimaging studies, an event-related fMRI study, and a behavioural investigation, respectively. Altogether, our contributions revealed that: i) dorsal stream areas are consistently recruited across the neuroimaging literature during the execution of skilled hand actions regardless of the availability of online visual input, while ventral visual stream and early visual areas show consistent activation only when vision is available; ii) early visual areas of blindfolded participants have a representation of the size of stimuli explored through active touch alone, even though participants never saw the stimuli, and this finding is not just an epiphenomenon of visual imagery; iii) the recruitment of EVC, including V1, during haptic exploration might be behaviourally relevant for haptic size

processing, since the physiological disruption of V1 via the presentation of foveal visual noise during haptic size processing appears to modulate performance in a subsequent manual size estimation task.

Overall, this work advances our understanding of the neural bases of the execution of skilled hand actions and haptic processing of object features, with a specific focus on the debated role of early visual areas in such processes. Investigating the neural underpinnings of action execution and haptic perception is fundamental to understanding how humans sense the world and execute appropriate actions to interact with objects and tools, even when they cannot rely on visual information. In addition, with the increasing use of touch-based smart devices and virtual reality (VR) settings including haptic feedback, there is a growing need for more comprehensive studies on haptic perception. A deeper understanding of how the brain handles touch could have valuable implications for the implementation of haptic robotic systems, prosthetic limbs, and haptic sensations in VR environments. In addition, it could also pave the way to the study of how haptic information about object properties is then used to guide our actions towards real world objects in our daily life which we do effortlessly despite the complex neural machinery supporting these processes. This is particularly relevant for deafferented patients who lost proprioceptive and tactile inputs from afferent nerves of a particular part of the body while motor nerves remain intact. As such, these patients lack the haptic feedback necessary for motor control, and become unable to move until they re-learn to do so using continuous visual feedback of their moving effector. Investigating the brain areas underlying haptic processing offers potential cortical targets for rehabilitative strategies, which could leverage cross-modal plasticity, Sensory Substitution Devices (SSD), and Brain-Computer Interfaces (BCI) to improve the fine control of hand-object interactions. Likewise, investigating the neural basis of action execution and predictive coding mechanisms can inform the development of high-fidelity BCIs. Such systems could enable paralyzed patients to restore

movement by decoding action intentions and simulating the sensory consequences of actions, thereby closing the sensorimotor loop.

Supplementary Materials

Chapter 2: Annexes

Annex A. PRISMA Flow diagram for studies on reaching and grasping (adapted from Ranzini et al., 2022).

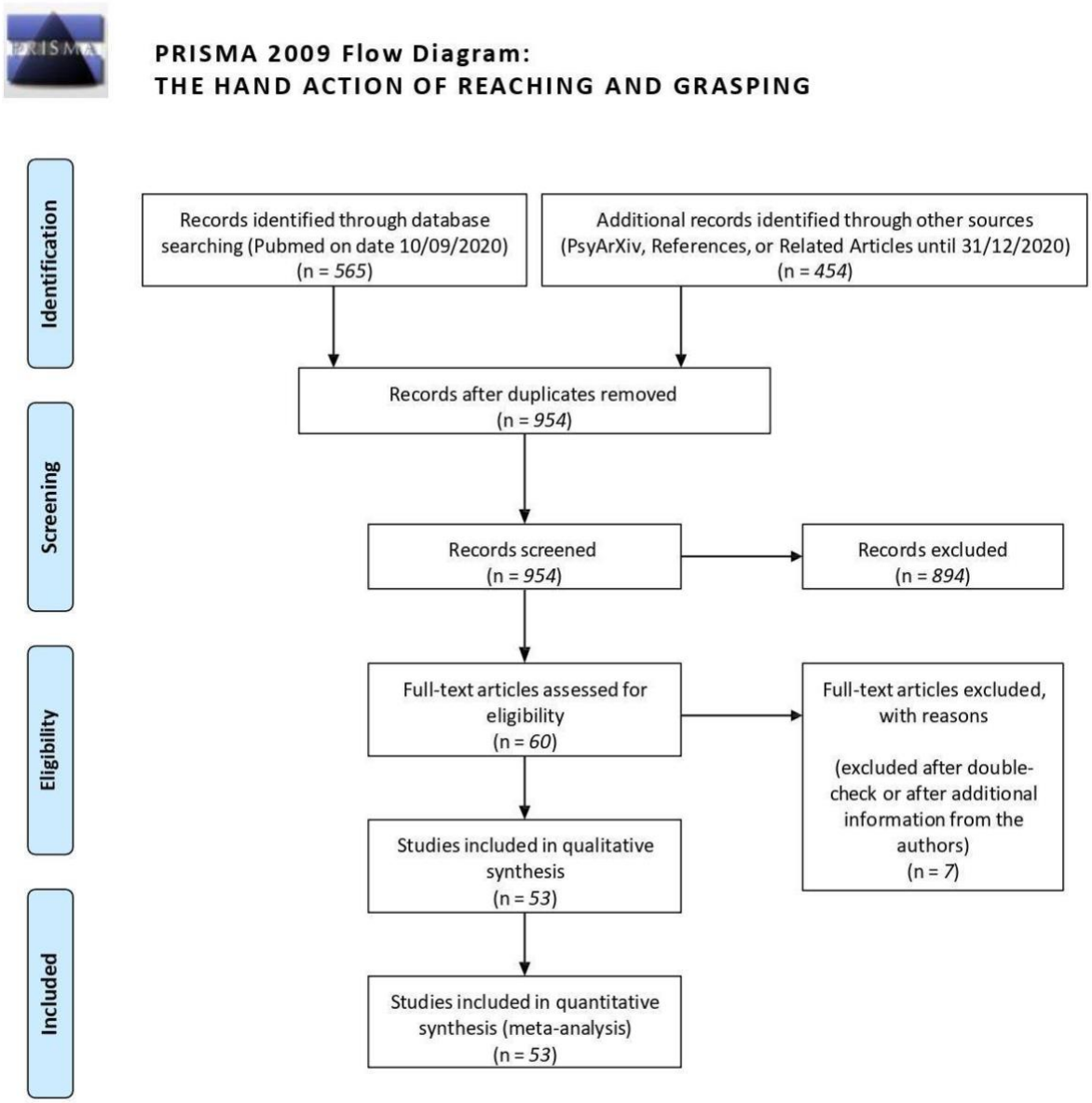

Annex B. Table of the list of included studies and additional details about participants, the task employed, contrast used, category, and number of activation foci (adapted from Ranzini et al., 2022).

Study N°	Study (First author, publication year)	N, Sex, Handedness	Age	Technique	Contrast	Category	Details	N Foci
1	Styrkowiec, 2019	21, 11 F, all RH	23	fMRI	grasp tool > control object	Grasp No vision	Execution w/o vision; real object tools and non-tools	19
2	Chen, 2018	12, 8 F, all RH	33	fMRI	Response: different cue > same cue	Reach No vision	Reach-to-touch-with index finger	9
3	Gorbet, 2018	20, 20 F, all RH	25	fMRI	Reach > dot fixation	Reach Vision	Visuo-motor combination	15
4	Gertz, 2015	19, 11 F, all RH	25	fMRI	Reach-Pro > Reach underspecified	Reach No vision	Pro and Anti reach task in specified (with earlier instruction) or underspecified (with later instruction) condition	7
5	Renzi, 2013	9, 5 F, all RH	24	fMRI	Far > Near in visual feedback	Grasp No vison	Near or far whole or precision grasp with or without visual	4

							feedback	
6	Rossit, 2013	10, 7 F, all RH	27	fMRI	Grasp in Lower > Upper visual field in absence of vision	Grasp No vison	Grasp or look 3D objects central objects with focus on the lower vs. upper visual field	3
7	Bernier, 2012	18, 7 F, all RH	26	fMRI	Uncued > Cued (right hand)	Reach No vision	Short cued or uncued reach with either left or right hand to left or right targets	9
8	Glover, 2012	21, all RH		fMRI	Immediate execution > Observation	Grasp Vision	Four conditions: Observation, Imagination (planning), Immediate execution (Control), Planning + Control	11
9	Fabbri, 2012	13, 8 F, all RH	27	fMRI	changed > adapted test trials	Reach No vision	Adaptation reach direction or	18

							amplitude	
10	Gallivan, 2011	13, 7 F, all RH	28	fMRI	Reach & Grasp > Look (right handers)	Grasp No vision	Reach, Grasp or Look within near or far space in right or left handers	1
11	Fiehler, 2011	21, 15 F, all RH	24	fMRI	Immediate grasp > baseline	Grasp Vision	Reach grasp without visual feedback, immediately or after a delay	7
12	Fabbri, 2010	Exp 1: 14, 6 F, 13 RH	28	fMRI	changed in direction or type of motor act > adapted test trials	Reach No vision	Press or whole grasp (both with reach varying in direction)	8
13	Himmelbach, 2009	16, 8 F, all RH	32	fMRI	Immediate reach > delayed reach	Reach Vision	Reach with left or right hand (healthy control participants)	11
14	Verhagen, 2008	19, 0 F, all RH	22	fMRI	Grasp in binocular & monocular vision > rest	Grasp Vision	Monocular or binocular visually guided precision grip	10

15	Begliomini, 2007	16, all RH	25	fMRI	Precision grip > power grasp	Grasp Vision	Reach to grasp small or large objects with precision or power grip	1
16	Valyear, 2019	17, 0 F, all RH	45	fMRI	Grasp > Touch	Grasp Vision	Brain activity of the healthy control group	2
17	Filimon, 2007	14, all RH	34	fMRI	Reach Execution > Object Viewing	Reach No vision	Reach execution, reach observation, reach imagination	35
18	Milner, 2007	17		fMRI	Complex > Simple grasp	Grasp No vision	Squeezing a soft ball (simple) or balancing a weighted flexible ruler (complex), or rest (precision grip only)	2
19	Begliomini, 2007	12, 8 F, all RH	25	fMRI	Precision grip > Whole hand grasp	Grasp Vision	Precision grip or whole hand grasp	1
20	Ehrsson, 2007	6, 0 F	26	fMRI	Loading > Rest	Grasp No vision	Precision grip during increasing (loading) or decreasing	3

							(unloading) in weight	
21	Prado, 2005	12, 8 F, all RH	23	fMRI	Reach w/o saccade > No reach	Reach No vision	Reaching with saccade, reaching w/o saccade (VT/NSe), reaching with invisible object	13
22	Frey, 2005	14, 5 F, all RH	24	fMRI	Grasp > Point	Grasp Vision	Exp.2: Precision grasp	2
23	Kuhtz-Buschbeck, 2001	8, 0 F, all RH	29	fMRI	Gentle > Firm grasp	Grasp No vision	Precision grip with gentle, normal or firm grip force	4
24	Cavina-Pratesi, 2018	11, 4 F, all RH	31	fMRI	all Reach / Point > Passive viewing	Reach No vision	Reach, point, precision or coarse grip with two or more digits	11
25	Monaco, 2015	11, 5 F, all RH	32	fMRI	Adaptation to both size and location	Grasp Vision	Grasp specific adaptation to object size and location	5
26	Monaco, 2014	13, 8 F, all RH	31	fMRI	Adaptation to Grasp > Adaptation to View	Grasp Vision	Grasp specific adaptation to grasp type or object size	3

27	Monaco, 2011	11, 3 F, all RH	33	fMRI	Adaptation in Grasp > Adaptation in Reach	Grasp Vision	Adaptation to object orientation during grasp, reach or look	5
28	Cavina-Pratesi, 2010b	Exp.1: 10, all RH	29	fMRI	Grasp > Touch (Exp.1)	Grasp Vision	Grasp, touch and look to near or far objects	11
29	Cappadocia, 2017	12, 9 F, all RH	28	fMRI	Pro & Anti Reach > Color detection (execution phase)	Reach No vision	Pro and anti reach task	17
30	Pellijeff, 2006	13, 8 F, 12 RH	25	fMRI	First reach > Later Reaches	Reach No vision	Chin pointing with the index finger (reach, exp.1)	6
31	Króliczak, 2007	10, 5 F, all RH	27	fMRI	Grasp > Reach	Grasp No vision	precision grasp, reach, pantomime grasp, pantomime reach	12
32	Inoue, 1998	9, all RH	23	PET	Reach without feedback > Hold (control task)	Reach No vision	Reach without feedback	30
33	Desmurget, 2001	7, 1 F, all RH	25	PET	Reach > Look (stationary condition)	Reach No vision	Reach or look to stationary or jumping targets	15

34	Kertzman, 1997	6, 3 F, all RH	33	PET	Reach with right hand > Look	Reach Vision	Reach with index finger; right or left hand on right or left visual field	14
35	Keisker, 2009	14, 7 F, all RH	27	fMRI	Grasp > Rest	Grasp Vision	Power grip with three forces	15
36	Keisker, 2010	14, 7 F, all RH	27	fMRI	Grasp static & dynamic > No force	Grasp Vision	Power grip in static or dynamic conditio n	12
37	Ward, 2003	26, 9 F, all RH	47	fMRI	Effect of grip force	Grasp No vision	Power grip with left or right hand	6
38	Hilty, 2010	15, 0 F, all RH	25	fMRI	Succeede d grasp > baseline	Grasp Vision	Power grip with different forces and during interfere nce	5
39	Kurniawa n, 2010	17, all RH	27	fMRI	Grip low effort > grip high effort	Grasp No vision	Power grip or hold with high or low effort, and with or without reward	10
40	Talelli, 2008	27, all RH	42	fMRI	Effect of grip force	Grasp No vision	Dynami c power hand grips with the dominan t right hand	4

41	Vaillancourt, 2003	10, 7 F, all RH	27	fMRI	Grip with visual feedback > rest, no visual feedback or visual stimulus	Grasp No vision	Precision grip with visual feedback, without visual feedback, visual stimulus only or rest	26
42	Spraker, 2009	12, 7 F, all RH	27	fMRI	Grip > relaxation	Grasp No vision	Precision grip or relaxation phase	1
43	Neely, 2013	17, 8 F, 16 RH	27	fMRI	Dynamic grip > static grip	Grasp No vision	Static or dynamic precision grip	13
44	Holmström, 2011	16, 0 F, all RH	32	fMRI	High grip force > low grip force	Grasp Vision	Precision grip with high or low force, and high or low instability	12
45	Saiote, 2016	31, 15 F, all RH	32	fMRI	Action execution > imagination	Grasp No vision	Squeezing a ball or imagine doing it	15
46	Turella, 2009	16, all RH	28	fMRI	Hand action > Look	Grasp Vision	Reach and grasp with precision grip a small ball, or fix the ball	4

47	Gatti, 2017	24, all RH	23	fMRI	Grasp > Simple movement	Grasp No vision	Simple (palm movement), Complex (finger movement), Finalistic (Grasp) hand actions	6
48	Bernier, 2017	15, all RH	23	fMRI	Reach > Finger movement	Reach No vision	Reach a target with the index finger or finger movement in response to target position (no point)	17
49	Begliomini, 2015	16, all RH	25	fMRI	Effect of Grasp	Grasp Vision	Precision grasp with right or left hand	22
50	Fabbri, 2014	15	37	fMRI	Execution > baseline	Grasp No vision	Precision or power grasp, or touch	10
51	Ehrsson, 2003	6, all RH	27	fMRI	Grip & lift > lift only	Grasp No vision	Grip and try to lift, grip, or try to lift w/o grip	7
52	Marangon, 2016	10, 4 F, all RH	28	fMRI	Grasp > Reach	Grasp No vision	Reach or reach and grasp unfamiliar simple or complex objects after exploration	4

53	Monaco, 2017	18, 7 F, all RH	29	fMRI	Delayed Grasping > Delayed Reaching (execution phase)	Grasp No vision	Haptic or visual grasp and/or reach task	16

Supplementary Table 3.1. Statistical values for ROI-based MVPA results for each size pair during Haptic exploration (HE), Visual imagery (VI), and Across HE and VI (Across HE ⇔ VI).

ROI	Task	Decoding accuracy for size, t(23)		
		Small vs. Medium	Medium vs. Large	Small vs. Large
Left preSMA	HE	***p*=.002 t=3.60**	*p*=.122 t=1.61	***p*<.001 t=5.56**
	VI	*p*=.807 t=0.25	*p*=.649 t=-0.46	*p*=.076 t=1.86
	Across HE ⇔ VI	*p*=.155 t=1.47	***p*=.009 t=-2.85**	*p*=.059 t=1.98
Right preSMA	HE	*p*=.025 t=2.40	***p*<.001 t=4.14**	***p*<.001 t=6.93**
	VI	*p*=.048 t=2.09	*p*=.965 t=-0.04	*p*=.110 t=1.66
	Across HE ⇔ VI	*p*=.180 t=1.38	*p*=.962 t=0.05	*p*=.276 t=1.11
Left SMA	HE	***p*<.001 t=5.43**	***p*=.006 t=3.05**	***p*<.001 t=6.04**
	VI	***p*<.001 t=3.80**	*p*=.408 t=-0.84	*p*=.040 t=2.18
	Across HE ⇔ VI	*p*=.235 t=1.22	*p*=.139 t=1.53	*p*=.212 t=1.28
Right SMA	HE	***p*<.001 t=4.07**	***p*=.002 t=3.41**	***p*<.001 t=10.96**
	VI	*p*=.485 t=0.71	*p*=.198 t=1.33	*p*=.252 t=1.17
	Across HE ⇔ VI	*p*=.725 t=-0.36	*p*=.936 t=0.08	*p*=.756 t=0.31
Left dPM	HE	***p*<.001 t=6.54**	***p*<.001 t=4.02**	***p*<.001 t=9.95**
	VI	***p*<.001 t=3.97**	*p*=.084 t=1.80	***p*=.002 t=3.59**
	Across HE ⇔ VI	***p*=.015 t=2.64**	*p*=.262 t=1.15	*p*=.035 t=2.24
Right dPM	HE	***p*<.001 t=7.05**	*p*=.019 t=2.52	***p*<.001 t=11.47**
	VI	*p*=.210 t=1.29	*p*=.841 t=0.20	***p*=.002 t=3.56**
	Across HE ⇔ VI	***p*=.001 t=3.67**	*p*=.024 t=2.42	***p*<.001 t=3.98**
Left vPM	HE	***p*<.001 t=4.59**	*p*=.836 t=0.21	***p*<.001 t=7.51**
	VI	*p*=.194 t=1.34	*p*=.271 t=1.13	*p*=.704 t=0.39
	Across HE ⇔ VI	*p*=.810 t=0.24	*p*=.103 t=1.70	*p*=.102 t=1.70
Right vPM	HE	***p*<.001 t=4.11**	***p*=.010 t=2.82**	***p*<.001 t=8.92**
	VI	*p*=.297 t=1.07	*p*=.627 t=0.49	*p*=.294 t=1.07

	Across HE ⇔ VI	*p*=.748 t=0.32	*p*=.046 t=2.11	*p*=.430 t=0.80
Left M1S1	HE	*p*=.277 t=1.11	***p*=.002 t=3.52**	***p*<.001 t=4.53**
	VI	*p*=.570 t=-0.58	*p*=.726 t=-0.35	*p*=.902 t=0.12
	Across HE ⇔ VI	*p*=.028 t=2.34	*p*=.437 t=-0.79	*p*=.725 t=-0.36
Right M1S1	HE	***p*<.001 t=4.58**	*p*=.136 t=1.55	***p*<.001 t=5.09**
	VI	*p*=.518 t=0.66	*p*=.156 t=-1.47	*p*=.645 t=-0.47
	Across HE ⇔ VI	*p*=.745 t=-0.33	*p*=.081 t=1.82	*p*=.695 t=-0.40
Left aIPS	HE	***p*<.001 t=4.50**	***p*=.001 t=3.62**	***p*<.001 t=14.59**
	VI	***p*=.005 t=3.14**	*p*=.061 t=1.97	***p*=.001 t=3.65**
	Across HE ⇔ VI	*p*=.052 t=2.05	*p*=.130 t=1.57	*p*=.533 t=0.63
Right aIPS	HE	***p*<.001 t=4.94**	***p*<.001 t=4.28**	***p*<.001 t=9.62**
	VI	*p*=.066 t=1.93	*p*=.423 t=0.82	***p*=.002 t=3.51**
	Across HE ⇔ VI	*p*=.369 t=0.92	*p*=.071 t=1.90	*p*=.038 t=2.20
Left pIPS	HE	***p*<.001 t=8.00**	***p*=.006 t=3.03**	***p*<.001 t=16.07**
	VI	*p*=.038 t=2.20	*p*=.136 t=1.55	***p*=.002 t=3.50**
	Across HE ⇔ VI	*p*=.070 t=1.90	*p*=.082 t=1.82	***p*<.001 t=4.05**
Right pIPS	HE	***p*<.001 t=5.07**	***p*=.003 t=3.28**	***p*<.001 t=8.23**
	VI	*p*=.326 t=1.00	***p*=.005 t=3.08**	***p*=.001 t=3.73**
	Across HE ⇔ VI	***p*=.002 t=3.55**	*p*=.861 t=0.18	***p*<.001 t=5.62**
Left OP	HE	***p*=.007 t=2.96**	*p*=.179 t=1.39	***p*<.001 t=4.88**
	VI	*p*=.346 t=-0.96	*p*=.305 t=-1.05	*p*=.448 t=-0.77
	Across HE ⇔ VI	*p*=.681 t=0.42	*p*=.192 t=-1.34	*p*=.323 t=-1.01
Right OP	HE	*p*=.148 t=1.50	*p*=.243 t=1.20	***p*=.007 t=2.97**
	VI	*p*=.920 t=0.10	*p*=.943 t=-0.07	*p*=.729 t=-0.35
	Across HE ⇔ VI	*p*=.753 t=-0.32	*p*=.670 t=-0.43	*p*=.556 t=-0.60
Left V1	HE	*p*=.030 t=2.32	*p*=.064 t=1.94	*p*=.101 t=1.71
	VI	*p*=.692 t=-0.40	*p*=.373 t=0.91	*p*=.051 t=2.05
	Across HE ⇔ VI	*p*=.963 t=0.05	*p*=.819 t=-0.23	*p*=.049 t=2.08
Right V1	HE	*p*=.175 t=1.40	*p*=.258 t=1.16	***p*=.014 t=2.66**

	VI	*p*=.151 t=-1.48	*p*=.107 t=-1.68	*p*=.655 t=-0.45
	Across HE ⇔ VI	*p*=.824 t=0.23	*p*=.055 t=-2.02	*p*=.871 t=0.16
Left LOtv	HE	***p*<.001 t=4.09**	***p*=.002 t=3.49**	***p*<.001 t=5.45**
	VI	*p*=.321 t=1.01	***p*=.013 t=2.71**	***p*=.014 t=2.67**
	Across HE ⇔ VI	*p*=.023 t=2.44	*p*=.392 t=0.87	*p*=.483 t=0.71
Right LOtv	HE	***p*<.001 t=6.27**	***p*=.008 t=2.90**	***p*<.001 t=7.52**
	VI	*p*=.264 t=-1.15	*p*=.825 t=0.22	*p*=.855 t=0.18
	Across HE ⇔ VI	*p*=.733 t=-0.35	*p*=.077 t=1.85	*p*=.262 t=1.15
Left ITS	HE	***p*=.014 t=2.65**	***p*=.003 t=3.39**	***p*<.001 t=6.26**
	VI	*p*=.130 t=-1.57	*p*=.746 t=-0.33	*p*=.093 t=1.75
	Across HE ⇔ VI	*p*=.659 t=0.45	*p*=.849 t=-0.19	*p*=.803 t=0.25
Right ITS	HE	***p*=.009 t=2.85**	*p*=.285 t=1.09	***p*<.001 t=3.86**
	VI	*p*=.612 t=-0.51	*p*=.656 t=-0.45	*p*=.458 t=0.75
	Across HE ⇔ VI	*p*=.840 t=-0.20	*p*=.080 t=-1.83	*p*=.423 t=0.82

Note: Statistically significant values after False Discovery Rate (FDR) correction ($q < 0.05$) for multiple comparisons are indicated in boldface.

Supplementary Table 3.2. Statistical values for the correlation between imagery vividness (VVIQ) scores and decoding accuracy in the Haptic exploration, Visual imagery, and Cross-decoding conditions, separately, in each ROI.

ROI	Pearson's r correlation coefficient, r(22)		
	Haptic exploration	**Visual imagery**	**Cross-decoding**
Left preSMA	r=-0.30 *p*=.158	**r=0.43 *p*=.037**	r=-0.10 *p*=.627
Right preSMA	r=0.08 *p*=.718	r=0.12 *p*=.570	r=0.03 *p*=.895
Left SMA	r=0.02 *p*=.937	r=0.05 *p*=.826	r=-0.32 *p*=.134
Right SMA	r=0.02 *p*=.918	r=-0.17 *p*=.426	r=0.05 *p*=.832
Left dPM	r=0.23 *p*=.277	r=0.08 *p*=.712	r=0.08 *p*=.722
Right dPM	r=0.08 *p*=.704	r=0.12 *p*=.592	r=0.01 *p*=.965
Left vPM	r=-0.31 *p*=.135	r=0.23 *p*=.288	r=-0.16 *p*=.458
Right vPM	r=0.16 *p*=.460	r=0.17 *p*=.437	r=0.05 *p*=.820
Left M1S1	r=-0.04 *p*=.841	r=-0.04 *p*=.839	r=-0.07 *p*=.735
Right M1S1	**r=-0.47 *p*=.021**	r=-0.003 *p*=.989	r=0.18 *p*=.406
Left aIPS	r=-0.02 *p*=.940	r=-0.12 *p*=.569	r=-0.17 *p*=.438
Right aIPS	r=-0.005 *p*=.982	r=0.05 *p*=.817	r=-0.02 *p*=.911
Left pIPS	r=0.07 *p*=.754	r=0.05 *p*=.819	r=0.03 *p*=.903
Right pIPS	r=-0.34 *p*=.108	r=0.11 *p*=.625	r=0.37 *p*=.078
Left OP	r=-0.18 *p*=.395	r=0.02 *p*=.938	r=0.19 *p*=.375
Right OP	r=-0.10 *p*=.637	r=-0.34 *p*=.107	r=0.29 *p*=.162
Left V1	r=0.17 *p*=.427	r=-0.11 *p*=.611	r=0.03 *p*=.900
Right V1	r=-0.13 *p*=.530	r=0.05 *p*=.812	r=0.39 *p*=.062
Left LOtv	r=-0.09 *p*=.690	r=-0.36 *p*=.082	r=0.06 *p*=.798
Right LOtv	r=-0.03 *p*=.892	r=-0.12 *p*=.575	r=-0.34 *p*=.103
Left ITS	r=-0.16 *p*=.445	r=-0.11 *p*=.596	r=0.23 *p*=.269
Right ITS	r=0.18 *p*=.392	r=0.04 *p*=.862	r=0.09 *p*=.688

Note: Statistically significant values are indicated in boldface.

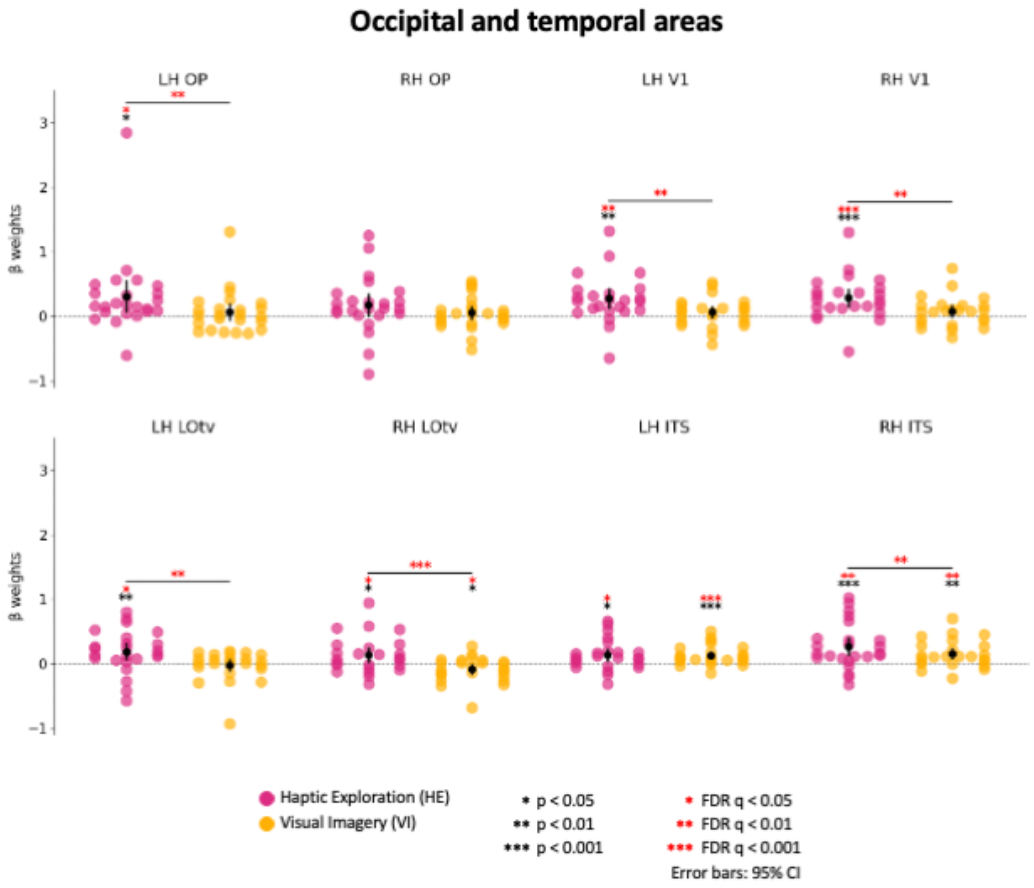

Supplementary Figure 3.1. Univariate β weights in occipital and temporal ROIs.

The scatterplots show univariate β weights for each participant along with the average across participants (black circles) in occipital and temporal areas in both the left and right hemisphere during Haptic Exploration (HE) trials (magenta circles), and Visual Imagery (VI) trials (yellow circles). Error bars represent 95% confidence intervals (CI). Asterisks (*) indicate statistical significance with one-samples, two-tailed t-tests across subjects with respect to baseline (β weight = 0), and significance with paired-samples, two-tailed t-test for comparison between VI and HE. Black asterisks indicate uncorrected statistical significance, while red asterisks indicate statistical significance based on FDR correction.

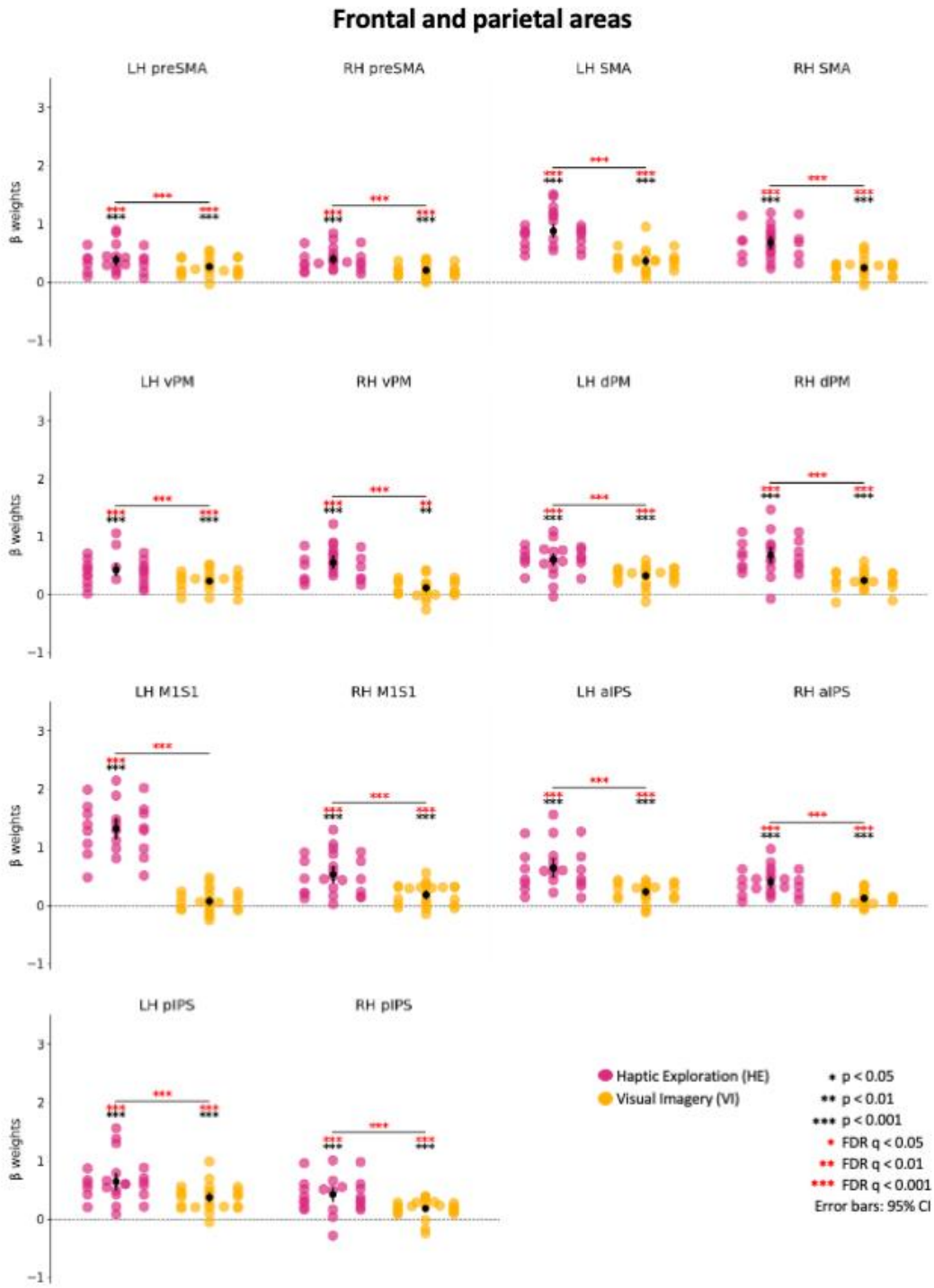

Supplementary Figure 3.2. Univariate β weights in frontal and parietal ROIs.
The scatterplots show univariate β weights for each participant along with the average across participants (black circles) in frontal and parietal areas in both the left and right hemisphere during Haptic Exploration (HE) trials (magenta circles), and Visual Imagery (VI) trials (yellow circles). Error bars represent 95% confidence intervals (CI). Asterisks (*) indicate statistical significance with one-samples, two-tailed t-tests across subjects with respect to baseline (β weight = 0), and significance with paired-samples, two-tailed t-test for comparison between VI and HE. Black asterisks indicate uncorrected statistical significance, while red asterisks indicate statistical significance based on FDR correction.

Supplementary Table 4.1. Results of post-hoc pairwise comparisons between perceptual size estimates for Small and Large sizes within each condition (HC,GC; HC,GR; HR,GC; HR,GR), with Bonferroni correction: Experiment 1.

	$t_{(28)}$	p-value	p-value adjusted
HC,GC			
Small vs. Large	-21.47	<.001	<.001
HC,GR			
Small vs. Large	-20.87	<.001	<.001
HR,GC			
Small vs. Large	-21.18	<.001	<.001
HR,GR			
Small vs. Large	-20.31	<.001	<.001

Note: HC (Hand Center), HR (Hand Right), GC (Gaze Center), GR (Gaze Right).

Supplementary Table 4.2. Results of post-hoc pairwise comparisons between standard deviation (SD) of perceptual size estimates for Small and Large sizes within each condition (HC,GC; HC,GR; HR,GC; HR,GR), with Bonferroni correction: Experiment 1.

	$t_{(28)}$	p-value	p-value adjusted
HC,GC			
Small vs. Large	-8.13	<.001	<.001
HC,GR			
Small vs. Large	-6.83	<.001	<.001
HR,GC			
Small vs. Large	-7.36	<.001	<.001
HR,GR			
Small vs. Large	-6.04	<.001	<.001

Note: HC (Hand Center), HR (Hand Right), GC (Gaze Center), GR (Gaze Right).

Supplementary Table 4.3. Results of post-hoc pairwise comparisons between perceptual size estimates for each pair of Stimulus sizes (Small, Medium, Large) within each Noise condition, with Bonferroni correction: Experiment 2.

	$t_{(25)}$	p-value	p-value adjusted
No noise			
Small vs. Medium	-20.45	<.001	<.001
Small vs. Large	-25.86	<.001	<.001
Medium vs. Large	-23.08	<.001	<.001
Noise			
Small vs. Medium	-22.33	<.001	<.001
Small vs. Large	-26.90	<.001	<.001
Medium vs. Large	-22.03	<.001	<.001

Supplementary Table 4.4. Results of post-hoc pairwise comparisons between SD of size estimates for each pair of Stimulus sizes (Small, Medium, Large) within each Noise condition, with Bonferroni correction: Experiment 2.

	$t_{(25)}$	p-value	p-value adjusted
No noise			
Small vs. Medium	-4.88	<.001	<.001
Small vs. Large	-5.70	<.001	<.001
Medium vs. Large	-2.94	=.007	=.04
Noise			
Small vs. Medium	-3.33	=.003	=.02
Small vs. Large	-5.13	<.001	<.001
Medium vs. Large	-3.63	=.001	=.01

Supplementary Table 4.5. Results of post-hoc pairwise comparisons between perceptual size estimates for each pair of Stimulus sizes (Small, Medium, Large) within each Noise condition, with Bonferroni correction: Experiment 3.

	$t_{(33)}$	p-value	p-value adjusted
No noise			
Small vs. Medium	-13.54	<.001	<.001
Small vs. Large	-13.95	<.001	<.001
Medium vs. Large	-10.38	<.001	<.001
Noise			
Small vs. Medium	-15.27	<.001	<.001
Small vs. Large	-16.76	<.001	<.001
Medium vs. Large	-12.70	<.001	<.001

Average size estimates for all stimuli used in each Behavioural Experiment

To provide an overview of participants' manual estimation performance, for each experiment we calculated the average size estimates for all the sizes used, including catch cylinders which were not considered in the main analyses. For each experiment, we performed paired-samples two-tailed t-tests between each pair of sizes and used Bonferroni correction for multiple comparisons.

As for Experiment 1 (3 sizes: Small, Medium Catch, Large), post-hoc pair-wise comparisons revealed significant differences between each pair of sizes across conditions (all $p < .001$ Bonferroni corrected; Supplementary Fig. 4.1, Panel a). As for Experiment 2 (3 sizes: Small, Medium, Large), post-hoc pair-wise comparisons revealed significant differences between each pair of sizes across conditions (all $p < .001$ Bonferroni corrected; Supplementary Fig. 4.1, Panel b). As for Experiment 3 (5 sizes: Small, Catch, Medium, Catch, Large), post-hoc pair-wise comparisons revealed significant differences between each pair of sizes across conditions (all $p < .001$ Bonferroni corrected; Supplementary Fig. 4.1, Panel c). Full statistical results of the pair-wise comparisons for each Experiment are reported in Supplementary Table 4.6.

Supplementary Table 4.6. Results of pairwise comparisons between perceptual size estimates for each pair of Stimulus sizes across experimental conditions, with Bonferroni correction.

	t statistic	p-value	p-value adjusted
Experiment 1			
Small vs. Medium	$t_{(28)} = -26.02$	<.001	<.001
Small vs. Large	$t_{(28)} = -21.28$	<.001	<.001
Medium vs. Large	$t_{(28)} = -16.48$	<.001	<.001
Experiment 2			
Small vs. Medium	$t_{(25)} = -22.13$	<.001	<.001
Small vs. Large	$t_{(25)} = -26.73$	<.001	<.001
Medium vs. Large	$t_{(25)} = -24.15$	<.001	<.001
Experiment 3			
Small vs. Catch 1	$t_{(33)} = -7.01$	<.001	<.001
Small vs. Medium	$t_{(33)} = 16.27$	<.001	<.001
Small vs. Catch 2	$t_{(33)} = -14.23$	<.001	<.001
Small vs. Large	$t_{(33)} = -15.94$	<.001	<.001
Medium vs. Catch 1	$t_{(33)} = -6.62$	<.001	<.001
Medium vs. Catch 2	$t_{(33)} = -5.61$	<.001	<.001
Medium vs. Large	$t_{(33)} = -12.63$	<.001	<.001
Large vs. Catch 1	$t_{(33)} = -12.32$	<.001	<.001
Large vs. Catch 2	$t_{(33)} = -10.43$	<.001	<.001
Catch 1 vs. Catch 2	$t_{(33)} = -8.67$	<.001	<.001

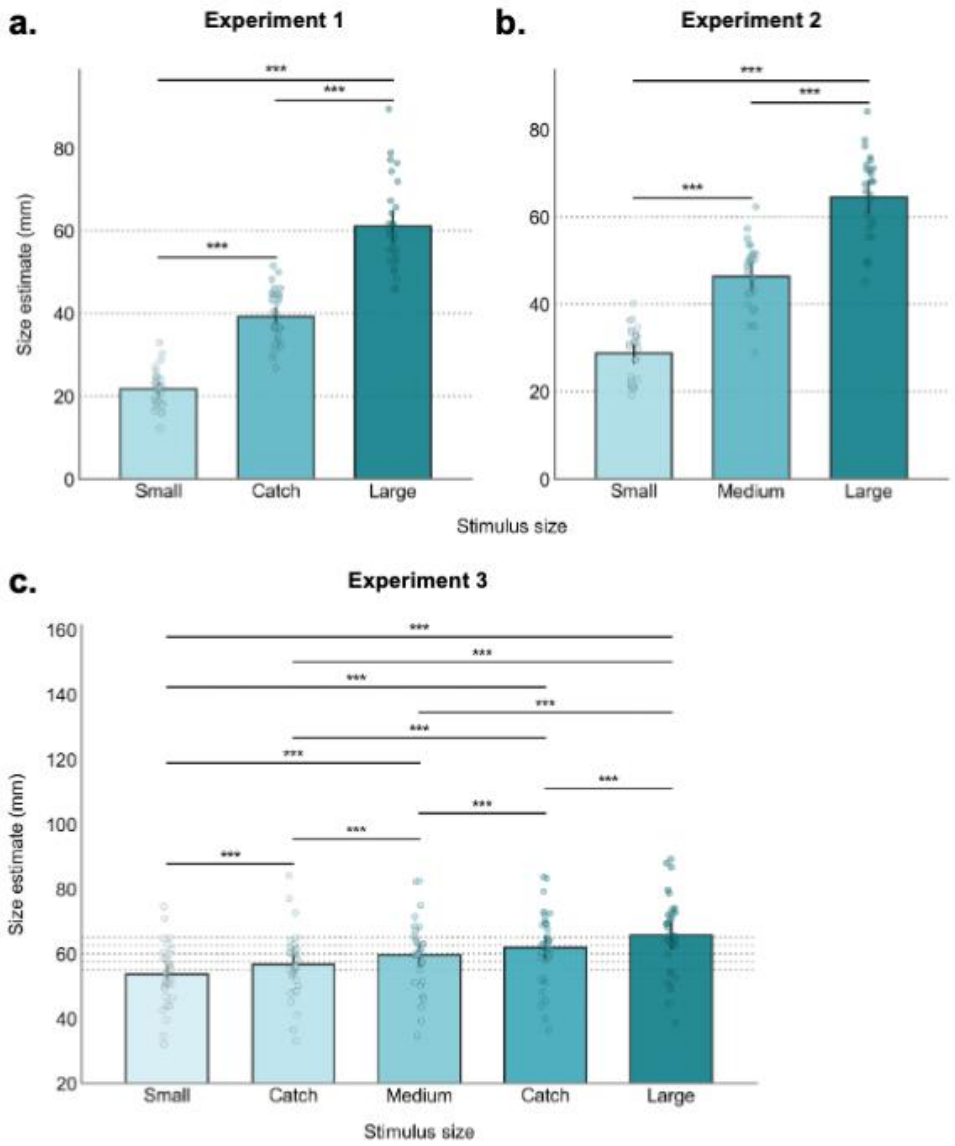

Supplementary Figure 4.1. Accuracy of size estimates for all stimuli used in Experiments 1, 2 and 3. **a.** Experiment 1: Average size estimates (mm) for Small, Medium Catch, and Large stimuli across the four hand-gaze configurations (i.e., HC,GC; HC,GR; HR,GC; HR,GR). Horizontal dotted lines represent the actual physical sizes of the stimuli (20, 40, and 60 mm). **b.** Experiment 2: Average size estimates (mm) for Small, Medium, and Large stimuli across No noise and Noise conditions. Horizontal dotted lines represent the actual physical sizes of the stimuli (20, 40, and 60 mm). **c.** Experiment 3: Average size estimates (mm) for Small, Catch, Medium, Catch, and Large stimuli across No noise and Noise conditions. Horizontal dotted lines represent the actual physical sizes of the stimuli (55, 57.5, 60, 62.5, and 65 mm). Note: Individual subjects' data points are shown as semi-transparent scatter dots. Error bars represent 95% confidence intervals (CI). Asterisks (***) denote significance levels at $p < .001$ Bonferroni corrected for multiple comparisons.

References

Aldegheri, G., Gayet, S., & Peelen, M. V. (2026). Dynamic context–based updating of object representations in the visual cortex. *Science Advances, 12*(4), eadw6726. https://doi.org/10.1126/sciadv.adw6726

Amedi, A., Jacobson, G., Hendler, T., Malach, R., & Zohary, E. (2002). Convergence of visual and tactile shape processing in the human lateral occipital complex. *Cerebral Cortex, 12(*11), 1202–1212. https://doi.org/10.1093/CERCOR/12.11.1202

Amedi, A., Malach, R., Hendler, T., Peled, S., & Zohary, E. (2001). Visuo-haptic object-related activation in the ventral visual pathway. *Nature Neuroscience, 4*(3), 324–330. https://doi.org/10.1038/85201

Amedi, A., Raz, N., Azulay, H., Malach, R., & Zohary, E. (2010). Cortical activity during tactile exploration of objects in blind and sighted humans. *Restorative Neurology and Neuroscience, 28*(2), 143–156. https://doi.org/10.3233/RNN-2010-0503

Amemiya, T., Beck, B., Walsh, V., Gomi, H., & Haggard, P. (2017). Visual area V5/hMT+ contributes to perception of tactile motion direction: a TMS study. *Scientific Reports, 7*(1), 40937. https://doi.org/10.1038/srep40937

Andersen, R. A., & Buneo, C. A. (2002). Intentional maps in posterior parietal cortex. *Annual Review of Neuroscience*, 25, 189–220. https://doi.org/10.1146/annurev.neuro.25.112701.142922

Andersen, R. A., Andersen, K. N., Hwang, E. J., & Hauschild, M. (2014). Optic ataxia: from Balint's syndrome to the parietal reach region. *Neuron, 81*(5), 967-983. https://doi.org/10.1016/j.neuron.2014.02.025

Arbuckle, S. A., Yokoi, A., Pruszynski, J. A., & Diedrichsen, J. (2019). Stability of representational geometry across a wide range of fMRI activity levels. *NeuroImage, 186*, 155–163. https://doi.org/10.1016/j.neuroimage.2018.11.002

Armstrong, L., & Marks, L. E. (1999). Haptic perception of linear extent. *Perception & Psychophysics, 61*(6), 1211-1226. https://doi.org/10.3758/BF03207624

Autodesk. (2021). *Fusion 360* (March 2021 product update) [Computer software]. https://www.autodesk.com/products/fusion-360/overview

Batista, A. (2002). Inner space: Reference frames. *Current Biology, 12*(11), R380-R383. https://doi.org/10.1016/S0960-9822(02)00878-3

Begliomini, C., Caria, A., Grodd, W., & Castiello, U. (2007). Comparing natural and constrained movements: new insights into the visuomotor control of grasping. *PLoS ONE, 2*(10), e1108. https://doi.org/10.1371/journal.pone.0001108

Begliomini, C., Sartori, L., Miotto, D., Stramare, R., Motta, R., & Castiello, U. (2015). Exploring manual asymmetries during grasping: a dynamic causal modeling approach. *Frontiers in Psychology, 6*, 167. https://doi.org/10.3389/fpsyg.2015.00167

Begliomini, C., Wall, M. B., Smith, A. T., & Castiello, U. (2007). Differential cortical activity for precision and whole-hand visually guided grasping in humans. *European Journal of Neuroscience, 25*(4), 1245–1252. https://doi.org/10.1111/j.1460-9568.2007.05365.x

Benjamini, Y., & Hochberg, Y. (1995). Controlling the False Discovery Rate: A Practical and Powerful Approach to Multiple Testing. *Journal of the Royal Statistical Society Series B: Statistical Methodology*, *57*(1), 289–300. https://doi.org/10.1111/j.2517-6161.1995.tb02031.x

Bernier, P. M., Cieslak, M., & Grafton, S. T. (2012). Effector selection precedes reach planning in the dorsal parietofrontal cortex. *Journal of Neurophysiology, 108*(1), 57–68. https://doi.org/10.1152/jn.00011.2012

Bernier, P. M., Whittingstall, K., & Grafton, S. T. (2017). Differential Recruitment of Parietal Cortex during Spatial and Non-spatial Reach Planning. *Frontiers in Human Neuroscience, 11*, 249. https://doi.org/10.3389/fnhum.2017.00249

Bettencourt, K. C., & Xu, Y. (2013). The role of transverse occipital sulcus in scene perception and its relationship to object individuation in inferior intraparietal sulcus. *Journal of Cognitive Neuroscience, 25*(10), 1711–1722. https://doi.org/10.1162/jocn_a_00422

Bettencourt, K. C., & Xu, Y. (2016). Decoding the content of visual short-term memory under distraction in occipital and parietal areas. *Nature Neuroscience, 19*(1), 150–157. https://doi.org/10.1038/nn.4174

Beurze, S. M., De Lange, F. P., Toni, I., & Medendorp, W. P. (2007). Integration of target and effector information in the human brain during reach planning. *Journal of Neurophysiology*, 97(1), 188–199. https://doi.org/10.1152/jn.00456.2006

Beurze, S. M., De Lange, F. P., Toni, I., & Medendorp, W. P. (2009). Spatial and Effector Processing in the Human Parietofrontal Network for Reaches and Saccades. *Journal of Neurophysiology, 101*(6), 3053–3062. https://doi.org/10.1152/jn.91194.2008

Bhandari, A., Gagne, C., & Badre, D. (2018). Just above Chance: Is It Harder to Decode Information from Prefrontal Cortex Hemodynamic Activity Patterns? *Journal of Cognitive Neuroscience, 30*(10), 1473–1498. https://doi.org/10.1162/jocn_a_01291

Binkofski, F., & Buxbaum, L. J. (2013). Two action systems in the human brain. *Brain and Language, 127*(2), 222–229. https://doi.org/10.1016/j.bandl.2012.07.007

Blake, R., Sobel, K. V., & James, T. W. (2004). Neural synergy between kinetic vision and touch. *Psychological Science, 15*(6), 397–402. https://doi.org/10.1111/j.0956-7976.2004.00691.x

Blangero, A., Menz, M. M., McNamara, A., & Binkofski, F. (2009). Parietal modules for reaching. *Neuropsychologia, 47*(6), 1500–1507. https://doi.org/10.1016/J.NEUROPSYCHOLOGIA.2008.11.030

Blohm, G., Keith, G. P., & Crawford, J. D. (2009). Decoding the cortical transformations for visually guided reaching in 3D space. *Cerebral Cortex*, *19*(6), 1372–1393. https://doi.org/10.1093/cercor/bhn177

Bola, Ł., Matuszewski, J., Szczepanik, M., Droździel, D., Sliwinska, M. W., Paplińska, M., Jednoróg, K., Szwed, M., & Marchewka, A. (2019). Functional hierarchy for tactile processing in the visual cortex of sighted adults. *NeuroImage, 202*, 116084. https://doi.org/10.1016/j.neuroimage.2019.116084

Bola, Ł., Siuda-Krzywicka, K., Paplińska, M., Sumera, E., Zimmermann, M., Jednoróg, K., Marchewka, A., & Szwed, M. (2017). Structural reorganization of the early visual cortex following Braille training in sighted adults. *Scientific Reports, 7*(1), 17448. https://doi.org/10.1038/s41598-017-17738-8

Bola, Ł., Yang, H., Caramazza, A., & Bi, Y. (2022). Preference for animate domain sounds in the fusiform gyrus of blind individuals is modulated by shape-action mapping. *Cerebral Cortex, 32*(21), 4913–4933. https://doi.org/10.1093/cercor/bhab524

Borchers, S., Müller, L., Synofzik, M., & Himmelbach, M. (2013). Guidelines and quality measures for the diagnosis of optic ataxia. *Frontiers in Human Neuroscience, 7*, 324. https://doi.org/10.3389/fnhum.2013.00324

Bouvier, G., Senzai, Y., & Scanziani, M. (2020). Head Movements Control the Activity of Primary Visual Cortex in a Luminance-Dependent Manner. *Neuron, 108*(3), 500–511.e5. https://doi.org/10.1016/j.neuron.2020.07.004

Bracci, S., & Op de Beeck, H. P. (2023). Understanding Human Object Vision: A Picture Is Worth a Thousand Representations. *Annual Review of Psychology*, *74*, 113–135. https://doi.org/10.1146/annurev-psych-032720-041031

Bracci, S., Ietswaart, M., Peelen, M. V., & Cavina-Pratesi, C. (2010). Dissociable neural responses to hands and non-hand body parts in human left extrastriate visual cortex.

Journal of Neurophysiology, 103(6), 3389–3397. https://doi.org/10.1152/jn.00215.2010

Brainard, D. H. (1997). The Psychophysics Toolbox. *Spatial vision, 10*(4), 433–436. https://doi.org/10.1163/156856897X00357

Bruce, C., Desimone, R., & Gross, C. G. (1981). Visual properties of neurons in a polysensory area in superior temporal sulcus of the macaque. *Journal of Neurophysiology, 46*(2), 369–384. https://doi.org/10.1152/jn.1981.46.2.369

Cant, J. S., Arnott, S. R., & Goodale, M. A. (2009). fMR-adaptation reveals separate processing regions for the perception of form and texture in the human ventral stream. *Experimental Brain Research, 192*(3), 391–405. https://doi.org/10.1007/s00221-008-1573-8

Cappadocia, D. C., Monaco, S., Chen, Y., Blohm, G., & Crawford, J. D. (2017). Temporal Evolution of Target Representation, Movement Direction Planning, and Reach Execution in Occipital-Parietal-Frontal Cortex: An fMRI Study. *Cerebral Cortex, 27*(11), 5242–5260. https://doi.org/10.1093/cercor/bhw304

Cattaneo, Z., Vecchi, T., Cornoldi, C., Mammarella, I., Bonino, D., Ricciardi, E., & Pietrini, P. (2008). Imagery and spatial processes in blindness and visual impairment. *Neuroscience & Biobehavioral Reviews, 32*(8), 1346–1360. https://doi.org/10.1016/j.neubiorev.2008.05.002

Cavina-Pratesi, C., Connolly, J. D., Monaco, S., Figley, T. D., Milner, A. D., Schenk, T., & Culham, J. C. (2018). Human neuroimaging reveals the subcomponents of grasping, reaching and pointing actions. *Cortex, 98*, 128–148. https://doi.org/10.1016/J.CORTEX.2017.05.018

Cavina-Pratesi, C., Goodale, M. A., & Culham, J. C. (2007). FMRI Reveals a Dissociation between Grasping and Perceiving the Size of Real 3D Objects. *PLoS ONE, 2*(5), e424. https://doi.org/10.1371/JOURNAL.PONE.0000424

Cavina-Pratesi, C., Kentridge, R. W., Heywood, C. A., & Milner, A. D. (2010a). Separate Processing of Texture and Form in the Ventral Stream: Evidence from fMRI and Visual Agnosia. *Cerebral Cortex, 20*(2), 433–446. https://doi.org/10.1093/CERCOR/BHP111

Cavina-Pratesi, C., Monaco, S., Fattori, P., Galletti, C., McAdam, T. D., Quinlan, D. J., Goodale, M. A., & Culham, J. C. (2010b). Functional magnetic resonance imaging reveals the neural substrates of arm transport and grip formation in reach-to-grasp actions in humans. *The Journal of Neuroscience, 30*(31), 10306–10323. https://doi.org/10.1523/JNEUROSCI.2023-10.2010

Chao, L. L., Haxby, J. V., & Martin, A. (1999). Attribute-based neural substrates in temporal cortex for perceiving and knowing about objects. *Nature Neuroscience, 2*(10), 913–919. https://doi.org/10.1038/13217

Chapman, H., Pierno, A. C., Cunnington, R., Gavrilescu, M., Egan, G., & Castiello, U. (2007). The neural basis of selection-for-action. *Neuroscience Letters, 417*(2), 171–175. https://doi.org/10.1016/j.neulet.2007.02.033

Chen, Y., Monaco, S., & Crawford, J. D. (2018). Neural substrates for allocentric-to-egocentric conversion of remembered reach targets in humans. *European Journal of Neuroscience, 47*(8), 901–917. https://doi.org/10.1111/ejn.13885

Chen, Y., Monaco, S., Byrne, P., Yan, X., Henriques, D. Y. P., & Crawford, J. D. (2014). Allocentric versus egocentric representation of remembered reach targets in human cortex. *The Journal of Neuroscience, 34*(37), 12515–12526. https://doi.org/10.1523/JNEUROSCI.1445-14.2014

Chouinard, P. A., Large, M. E., Chang, E. C., & Goodale, M. A. (2009). Dissociable neural mechanisms for determining the perceived heaviness of objects and the predicted weight of objects during lifting: An fMRI investigation of the size–weight illusion. *NeuroImage, 44*(1), 200–212. https://doi.org/10.1016/J.NEUROIMAGE.2008.08.023

Cohen, L. G., Celnik, P., Pascual-Leone, A., Corwell, B., Faiz, L., Dambrosia, J., Honda, M., Sadato, N., Gerloff, C., Catalá, M. D., & Hallett, M. (1997). Functional relevance of cross-modal plasticity in blind humans. *Nature, 389*(6647), 180–183. https://doi.org/10.1038/38278

Cohen, L. G., Weeks, R. A., Sadato, N., Celnik, P., Ishii, K., & Hallett, M. (1999). Period of susceptibility for cross-modal plasticity in the blind. *Annals of Neurology, 45*(4), 451-460. https://doi.org/10.1002/1531-8249(199904)45:4<451::aid-ana6>3.0.co;2-b

Cohen, L., Dehaene, S., Naccache, L., Lehéricy, S., Dehaene-Lambertz, G., Hénaff, M. A., & Michel, F. (2000). The visual word form area: spatial and temporal characterization of an initial stage of reading in normal subjects and posterior split-brain patients. *Brain, 123*(2), 291–307. https://doi.org/10.1093/brain/123.2.291

Cohen, N. R., Cross, E. S., Tunik, E., Grafton, S. T., & Culham, J. C. (2009). Ventral and dorsal stream contributions to the online control of immediate and delayed grasping: a TMS approach. *Neuropsychologia, 47*(6), 1553–1562. https://doi.org/10.1016/j.neuropsychologia.2008.12.034

Colby, C. L., Duhamel, J. R., & Goldberg, M. E. (1993). Ventral intraparietal area of the macaque: anatomic location and visual response properties. *Journal of Neurophysiology, 69*(3), 902–914. https://doi.org/10.1152/jn.1993.69.3.902

Cona, G., Wiener, M., & Scarpazza, C. (2021). From ATOM to GradiATOM: Cortical gradients support time and space processing as revealed by a meta-analysis of

neuroimaging studies. *NeuroImage, 224*, 117407. https://doi.org/10.1016/J.NEUROIMAGE.2020.117407

Coutanche, M. N. (2013). Distinguishing multi-voxel patterns and mean activation: Why, how, and what does it tell us? *Cognitive, Affective and Behavioral Neuroscience, 13*(3), 667–673. https://doi.org/10.3758/s13415-013-0186-2

Coutanche, M. N., & Koch, G. E. (2018). Creatures great and small: Real-world size of animals predicts visual cortex representations beyond taxonomic category. *NeuroImage, 183*, 627-634. https://doi.org/10.1016/j.neuroimage.2018.08.066

Cui, X., Jeter, C. B., Yang, D., Montague, P. R., & Eagleman, D. M. (2007). Vividness of mental imagery: Individual variability can be measured objectively. *Vision Research*, *47*(4), 474–478. https://doi.org/10.1016/j.visres.2006.11.013

Culham, J. C., Cavina-Pratesi, C., & Singhal, A. (2006). The role of parietal cortex in visuomotor control: what have we learned from neuroimaging? *Neuropsychologia, 44*(13), 2668–2684. https://doi.org/10.1016/j.neuropsychologia.2005.11.003

Culham, J. C., Danckert, S. L., De Souza, J. F. X., Gati, J. S., Menon, R. S., & Goodale, M. A. (2003). Visually guided grasping produces fMRI activation in dorsal but not ventral stream brain areas. *Experimental Brain Research, 153*(2), 180–189. https://doi.org/10.1007/S00221-003-1591-5

Davis, T., LaRocque, K. F., Mumford, J. A., Norman, K. A., Wagner, A. D., & Poldrack, R. A. (2014). What do differences between multi-voxel and univariate analysis mean? How subject-, voxel-, and trial-level variance impact fMRI analysis. *NeuroImage, 97*, 271–283. https://doi.org/10.1016/J.NEUROIMAGE.2014.04.037

de Haan, E. H. F., & Cowey, A. (2011). On the usefulness of 'what' and 'where' pathways in vision. *Trends in Cognitive Sciences, 15*(10), 460–466. https://doi.org/10.1016/j.tics.2011.08.005

de Haan, E. H. F., & Dijkerman, H. C. (2020). Somatosensation in the brain: a theoretical re-evaluation and a new model. *Trends in Cognitive Sciences, 24*(7), 529–541. https://doi.org/10.1016/J.TICS.2020.04.003

Delhaye, B. P., Long, K. H., & Bensmaia, S. J. (2018). Neural basis of touch and proprioception in primate cortex. *Comprehensive Physiology, 8*(4), 1575–1602. https://doi.org/10.1002/CPHY.C170033

Deng, A., Cesanek, E., & Domini, F. (2024). Sensory feedback modulates Weber's law of both perception and action. *Journal of Vision, 24*(13), 10. https://doi.org/10.1167/jov.24.13.10

Deshpande, G., Hu, X., Lacey, S., Stilla, R., & Sathian, K. (2010). Object familiarity modulates effective connectivity during haptic shape perception. *NeuroImage, 49*(3), 1991–2000. https://doi.org/10.1016/j.neuroimage.2009.08.052

Deshpande, G., Hu, X., Stilla, R., & Sathian, K. (2008). Effective connectivity during haptic perception: a study using Granger causality analysis of functional magnetic resonance imaging data. *NeuroImage, 40*(4), 1807–1814. https://doi.org/10.1016/j.neuroimage.2008.01.044

Desmurget, M., Gréa, H., Grethe, J. S., Prablanc, C., Alexander, G. E., & Grafton, S. T. (2001). Functional anatomy of nonvisual feedback loops during reaching: a positron emission tomography study. *The Journal of Neuroscience, 21*(8), 2919–2928. https://doi.org/10.1523/JNEUROSCI.21-08-02919.2001

Di Bono, M. G., Begliomini, C., Castiello, U., & Zorzi, M. (2015). Probing the reaching–grasping network in humans through multivoxel pattern decoding. *Brain and Behavior, 5*(11), e00412. https://doi.org/10.1002/brb3.412

di Pellegrino, G., & Làdavas, E. (2015). Peripersonal space in the brain. *Neuropsychologia, 66*, 126–133. https://doi.org/10.1016/j.neuropsychologia.2014.11.011

Dijkerman, H. C., & de Haan, E. H. F. (2007). Somatosensory processes subserving perception and action. *Behavioral and Brain Sciences, 30*(2), 189–201. https://doi.org/10.1017/S0140525X07001392

Dijkstra, N., Bosch, S. E., & van Gerven, M. A. J. (2017). Vividness of visual imagery depends on the neural overlap with perception in visual areas. *The Journal of Neuroscience, 37*(5), 1367–1373. https://doi.org/10.1523/JNEUROSCI.3022-16.2016

Douglas, R. J., & Martin, K. A. (2004). Neuronal circuits of the neocortex. *Annual Review of Neuroscience, 27*, 419–451. https://doi.org/10.1146/annurev.neuro.27.070203.144152

Drucker, D. M., & Aguirre, G. K. (2009). Different spatial scales of shape similarity representation in lateral and ventral LOC. *Cerebral Cortex, 19*(10), 2269–2280. https://doi.org/10.1093/CERCOR/BHN244

Duhamel, J. R., Colby, C. L., & Goldberg, M. E. (1998). Ventral intraparietal area of the macaque: congruent visual and somatic response properties. *Journal of Neurophysiology, 79*(1), 126–136. https://doi.org/10.1152/jn.1998.79.1.126

Eck, J., Kaas, A. L., & Goebel, R. (2013). Crossmodal interactions of haptic and visual texture information in early sensory cortex. *NeuroImage, 75*, 123–135. https://doi.org/10.1016/J.NEUROIMAGE.2013.02.075

Edelman, S., Grill-Spector, K., Kushnir, T., & Malach, R. (1998). Toward direct visualization of the internal shape representation space by fMRI. *Psychobiology, 26*(4), 309-321. https://doi.org/10.3758/BF03330618

Ehrsson, H. H., Fagergren, A., Ehrsson, G. O., & Forssberg, H. (2007). Holding an object: neural activity associated with fingertip force adjustments to external perturbations. *Journal of Neurophysiology, 97*(2), 1342–1352. https://doi.org/10.1152/jn.01253.2005

Ehrsson, H. H., Fagergren, A., Johansson, R. S., & Forssberg, H. (2003). Evidence for the involvement of the posterior parietal cortex in coordination of fingertip forces for

grasp stability in manipulation. *Journal of Neurophysiology, 90*(5), 2978–2986. https://doi.org/10.1152/jn.00958.2002

Eickhoff, S. B., Grefkes, C., Zilles, K., & Fink, G. R. (2007). The somatotopic organization of cytoarchitectonic areas on the human parietal operculum. *Cerebral Cortex, 17*(8), 1800–1811. https://doi.org/10.1093/CERCOR/BHL090

Eickhoff, S. B., Laird, A. R., Fox, P. M., Lancaster, J. L., & Fox, P. T. (2017). Implementation errors in the GingerALE Software: Description and recommendations. *Human Brain Mapping, 38*(1), 7–11. https://doi.org/10.1002/hbm.23342

Eickhoff, S. B., Laird, A. R., Grefkes, C., Wang, L. E., Zilles, K., & Fox, P. T. (2009). Coordinate-based activation likelihood estimation meta-analysis of neuroimaging data: A random-effects approach based on empirical estimates of spatial uncertainty. *Human Brain Mapping, 30*(9), 2907–2926. https://doi.org/10.1002/hbm.20718

Eickhoff, S. B., Nichols, T. E., Laird, A. R., Hoffstaedter, F., Amunts, K., Fox, P. T., Bzdok, D., & Eickhoff, C. R. (2016). Behavior, sensitivity, and power of activation likelihood estimation characterized by massive empirical simulation. *NeuroImage, 137*, 70–85. https://doi.org/10.1016/J.NEUROIMAGE.2016.04.072

El Rassi, Y., Handjaras, G., Perciballi, C., Leo, A., Papale, P., Corbetta, M., Ricciardi, E., & Betti, V. (2024). A visual representation of the hand in the resting somatomotor regions of the human brain. *Scientific Reports, 14*(1), 18298. https://doi.org/10.1038/s41598-024-69248-z

Epstein, R., & Kanwisher, N. (1998). A cortical representation of the local visual environment. *Nature, 392*(6676), 598–601. https://doi.org/10.1038/33402

Erlikhman, G., Caplovitz, G. P., Gurariy, G., Medina, J., & Snow, J. C. (2018). Towards a unified perspective of object shape and motion processing in human dorsal cortex.

Consciousness and Cognition, 64, 106–120. https://doi.org/10.1016/j.concog.2018.04.016

Ernst, M. O., & Banks, M. S. (2002). Humans integrate visual and haptic information in a statistically optimal fashion. *Nature, 415*(6870), 429-433. https://doi.org/10.1038/415429a

Fabbri, S., Caramazza, A., & Lingnau, A. (2010). Tuning curves for movement direction in the human visuomotor system. *The Journal of Neuroscience, 30*(40), 13488-13498. https://doi.org/10.1523/JNEUROSCI.2571-10.2010

Fabbri, S., Caramazza, A., & Lingnau, A. (2012). Distributed sensitivity for movement amplitude in directionally tuned neuronal populations. *Journal of Neurophysiology, 107*(7), 1845–1856. https://doi.org/10.1152/jn.00435.2011

Fabbri, S., Strnad, L., Caramazza, A., & Lingnau, A. (2014). Overlapping representations for grip type and reach direction. *NeuroImage, 94*, 138–146. https://doi.org/10.1016/j.neuroimage.2014.03.017

Fan, X., Wang, L., Shao, H., Kersten, D., & He, S. (2016). Temporally flexible feedback signal to foveal cortex for peripheral object recognition. *Proceedings of the National Academy of Sciences, 113*(41), 11627-11632. https://doi.org/10.1073/pnas.1606137113

Fechner, G. T. (1948). Elements of psychophysics, 1860. In W. Dennis (Ed.), *Readings in the history of psychology* (pp. 206–213). Appleton-Century-Crofts. https://doi.org/10.1037/11304-026

Felleman, D. J., & Van Essen, D. C. (1991). Distributed hierarchical processing in the primate cerebral cortex. *Cerebral Cortex, 1*(1), 1-47. https://doi.org/10.1093/cercor/1.1.1-a

Fiehler, K., Bannert, M. M., Bischoff, M., Blecker, C., Stark, R., Vaitl, D., Franz, V. H., & Rösler, F. (2011). Working memory maintenance of grasp-target information in the

human posterior parietal cortex. *NeuroImage, 54*(3), 2401–2411. https://doi.org/10.1016/j.neuroimage.2010.09.080

Filimon, F. (2010). Human Cortical Control of Hand Movements: Parietofrontal Networks for Reaching, Grasping, and Pointing. *The Neuroscientist*, *16*(4), 388–407. https://doi.org/10.1177/1073858410375468

Filimon, F., Nelson, J. D., Hagler, D. J., & Sereno, M. I. (2007). Human cortical representations for reaching: mirror neurons for execution, observation, and imagery. *NeuroImage, 37*(4), 1315–1328. https://doi.org/10.1016/j.neuroimage.2007.06.008

Flanagan, J. R., Bittner, J. P., & Johansson, R. S. (2008). Experience can change distinct size-weight priors engaged in lifting objects and judging their weights. *Current Biology, 18*(22), 1742-1747. https://doi.org/10.1016/j.cub.2008.09.042

Flanders, M., Tillery, S. I. H., & Soechting, J. F. (1992). Early stages in a sensorimotor transformation. *Behavioral and Brain Sciences, 15*(2), 309-320. https://doi.org/10.1017/S0140525X00068813

Forman, S. D., Cohen, J. D., Fitzgerald, M., Eddy, W. F., Mintun, M. A., & Noll, D. C. (1995). Improved assessment of significant activation in Functional Magnetic Resonance Imaging (fMRI): Use of a cluster-size threshold. *Magnetic Resonance in Medicine*, *33*(5), 636–647. https://doi.org/10.1002/mrm.1910330508

Franz, V. H. (2003). Manual size estimation: a neuropsychological measure of perception? *Experimental Brain Research, 151*(4), 471-477. https://doi.org/10.1007/s00221-003-1477-6

Freud, E., Behrmann, M., & Snow, J. C. (2020). What Does Dorsal Cortex Contribute to Perception? *Open Mind, 4*, 40–56. https://doi.org/10.1162/opmi_a_00033

Freud, E., Ganel, T., Shelef, I., Hammer, M. D., Avidan, G., & Behrmann, M. (2017). Three-Dimensional Representations of Objects in Dorsal Cortex are Dissociable from Those

in Ventral Cortex. *Cerebral Cortex, 27*(1), 422–434. https://doi.org/10.1093/cercor/bhv229

Freud, E., Plaut, D. C., & Behrmann, M. (2016). 'What' is happening in the dorsal visual pathway. *Trends in Cognitive Sciences, 20*(10), 773–784. https://doi.org/10.1016/J.TICS.2016.08.003

Freud, E., Rosenthal, G., Ganel, T., & Avidan, G. (2015). Sensitivity to object impossibility in the human visual cortex: evidence from functional connectivity. *Journal of Cognitive Neuroscience, 27*(5), 1029–1043. https://doi.org/10.1162/jocn_a_00753

Frey, S. H., Vinton, D., Norlund, R., & Grafton, S. T. (2005). Cortical topography of human anterior intraparietal cortex active during visually guided grasping. Brain research. *Cognitive Brain Research, 23*(2-3), 397–405. https://doi.org/10.1016/j.cogbrainres.2004.11.010

Friston, K. J., Buechel, C., Fink, G. R., Morris, J., Rolls, E., & Dolan, R. J. (1997). Psychophysiological and modulatory interactions in neuroimaging. *NeuroImage, 6*(3), 218-229. https://doi.org/10.1006/nimg.1997.0291

Friston, K. J., Holmes, A. P., Price, C. J., Büchel, C., & Worsley, K. J. (1999). Multisubject fMRI studies and conjunction analyses. *NeuroImage, 10*(4), 385-396. https://doi.org/10.1006/nimg.1999.0484

Friston, K., Mattout, J., & Kilner, J. (2011). Action understanding and active inference. *Biological Cybernetics, 104*(1-2), 137–160. https://doi.org/10.1007/s00422-011-0424-z

Gallese, V., Murata, A., Kaseda, M., Niki, N., & Sakata, H. (1994). Deficit of hand preshaping after muscimol injection in monkey parietal cortex. *Neuroreport, 5*(12), 1525–1529. https://doi.org/10.1097/00001756-199407000-00029

Gallivan, J. P., & Culham, J. C. (2015). Neural coding within human brain areas involved in actions. *Current Opinion in Neurobiology, 33*, 141–149. https://doi.org/10.1016/j.conb.2015.03.012

Gallivan, J. P., Chapman, C. S., Gale, D. J., Flanagan, J. R., & Culham, J. C. (2019). Selective modulation of early visual cortical activity by movement intention. *Cerebral Cortex, 29*(11), 4662-4678. https://doi.org/10.1093/cercor/bhy345

Gallivan, J. P., Chapman, C. S., McLean, D. A., Flanagan, J. R., & Culham, J. C. (2013). Activity patterns in the category-selective occipitotemporal cortex predict upcoming motor actions. *European Journal of Neuroscience, 38*(3), 2408–2424. https://doi.org/10.1111/EJN.12215

Gallivan, J. P., McLean, A., & Culham, J. C. (2011). Neuroimaging reveals enhanced activation in a reach-selective brain area for objects located within participants' typical hand workspaces. *Neuropsychologia, 49*(13), 3710–3721. https://doi.org/10.1016/j.neuropsychologia.2011.09.027

Gallivan, J. P., McLean, D. A., Valyear, K. F., Pettypiece, C. E., & Culham, J. C. (2011). Decoding action intentions from preparatory brain activity in human parieto-frontal networks. *The Journal of Neuroscience*, *31*(26), 9599–9610. https://doi.org/10.1523/JNEUROSCI.0080-11.2011

Gatti, R., Rocca, M. A., Fumagalli, S., Cattrysse, E., Kerckhofs, E., Falini, A., & Filippi, M. (2017). The effect of action observation/execution on mirror neuron system recruitment: an fMRI study in healthy individuals. *Brain Imaging and Behavior, 11*(2), 565–576. https://doi.org/10.1007/s11682-016-9536-3

Gertz, H., & Fiehler, K. (2015). Human posterior parietal cortex encodes the movement goal in a pro-/anti-reach task. *Journal of Neurophysiology, 114*(1), 170–183. https://doi.org/10.1152/jn.01039.2014

Glover, S., Wall, M. B., & Smith, A. T. (2012). Distinct cortical networks support the planning and online control of reaching-to-grasp in humans. *European Journal of Neuroscience, 35*(6), 909–915. https://doi.org/10.1111/j.1460-9568.2012.08018.x

Goebel, R., Esposito, F., & Formisano, E. (2006). Analysis of Functional Image Analysis Contest (FIAC) data with BrainVoyager QX: From single-subject to cortically aligned group General Linear Model analysis and self-organizing group Independent Component Analysis. *Human Brain Mapping*, *27*(5), 392–401. https://doi.org/10.1002/hbm.20249

Goodale, M. A., & Haffenden, A. (1998). Frames of reference for perception and action in the human visual system. *Neuroscience & Biobehavioral Reviews, 22*(2), 161–172. https://doi.org/10.1016/s0149-7634(97)00007-9

Goodale, M. A., & Milner, A. D. (1992). Separate visual pathways for perception and action. *Trends in Neurosciences, 15*(1), 20-25. https://doi.org/10.1016/0166-2236(92)90344-8

Goodale, M. A., Jakobson, L. S., & Keillor, J. M. (1994). Differences in the visual control of pantomimed and natural grasping movements. *Neuropsychologia, 32*(10), 1159–1178. https://doi.org/10.1016/0028-3932(94)90100-7

Goodale, M. A., Milner, A. D., Jakobson, L. S., & Carey, D. P. (1991). A neurological dissociation between perceiving objects and grasping them. *Nature, 349*(6305), 154–156. https://doi.org/10.1038/349154a0

Gorbet, D. J., & Sergio, L. E. (2018). Move faster, think later: Women who play action video games have quicker visually-guided responses with later onset visuomotor-related brain activity. *PLoS ONE, 13*(1), e0189110. https://doi.org/10.1371/journal.pone.0189110

Graziano, M. S. A., & Gross, C. G. (1993). A bimodal map of space: somatosensory receptive fields in the macaque putamen with corresponding visual receptive fields. *Experimental Brain Research, 97*(1), 96–109. https://doi.org/10.1007/BF00228820

Graziano, M. S. A., Hu, X. T., & Gross, C. G. (1997). Visuospatial properties of ventral premotor cortex. *Journal of Neurophysiology, 77*(5), 2268–2292. https://doi.org/10.1152/jn.1997.77.5.2268

Graziano, M. S. A., Yap, G. S., & Gross, C. G. (1994). Coding of visual space by premotor neurons. *Science, 266*(5187), 1054–1057. https://doi.org/10.1126/science.7973661

Grill-Spector, K. (2003). The neural basis of object perception. *Current Opinion in Neurobiology, 13*(2), 159–166. https://doi.org/10.1016/s0959-4388(03)00040-0

Grill-Spector, K., & Weiner, K. S. (2014). The functional architecture of the ventral temporal cortex and its role in categorization. *Nature Reviews Neuroscience, 15*(8), 536–548. https://doi.org/10.1038/nrn3747

Grill-Spector, K., Kourtzi, Z., & Kanwisher, N. (2001). The lateral occipital complex and its role in object recognition. *Vision Research, 41*(10-11), 1409–1422. https://doi.org/10.1016/s0042-6989(01)00073-6

Grill-Spector, K., Kushnir, T., Hendler, T., & Malach, R. (2000). The dynamics of object-selective activation correlate with recognition performance in humans. *Nature Neuroscience, 3*(8), 837–843. https://doi.org/10.1038/77754

Gutteling, T. P., Petridou, N., Dumoulin, S. O., Harvey, B. M., Aarnoutse, E. J., Kenemans, J. L., & Neggers, S. F. W. (2015). Action preparation shapes processing in early visual cortex. *The Journal of Neuroscience, 35*(16), 6472–6480. https://doi.org/10.1523/JNEUROSCI.1358-14.2015

Hagen, M. C., Franzén, O., McGlone, F., Essick, G., Dancer, C., & Pardo, J. V. (2002). Tactile motion activates the human middle temporal/V5 (MT/V5) complex. *European Journal of Neuroscience, 16*(5), 957–964. https://doi.org/10.1046/J.1460-9568.2002.02139.X

Hamilton, R., Keenan, J. P., Catala, M., & Pascual-Leone, A. (2000). Alexia for Braille following bilateral occipital stroke in an early blind woman. *Neuroreport, 11*(2), 237-240. https://doi.org/10.1097/00001756-200002070-00003

Hardwick, R. M., Caspers, S., Eickhoff, S. B., & Swinnen, S. P. (2018). Neural correlates of action: Comparing meta-analyses of imagery, observation, and execution. *Neuroscience & Biobehavioral Reviews*, *94*, 31–44. https://doi.org/10.1016/J.NEUBIOREV.2018.08.003

Harris, C. R., Millman, K. J., van der Walt, S. J., Gommers, R., Virtanen, P., Cournapeau, D., Wieser, E., Taylor, J., Berg, S., Smith, N. J., Kern, R., Picus, M., Hoyer, S., van Kerkwijk, M. H., Brett, M., Haldane, A., Del Río, J. F., Wiebe, M., Peterson, P., … Oliphant, T. E. (2020). Array programming with NumPy. *Nature, 585*(7825), 357–362. https://doi.org/10.1038/s41586-020-2649-2

Harvey, B. M., & Dumoulin, S. O. (2011). The relationship between cortical magnification factor and population receptive field size in human visual cortex: constancies in cortical architecture. *The Journal of Neuroscience, 31*(38), 13604–13612. https://doi.org/10.1523/JNEUROSCI.2572-11.2011

Harvey, B. M., Fracasso, A., Petridou, N., & Dumoulin, S. O. (2015). Topographic representations of object size and relationships with numerosity reveal generalized quantity processing in human parietal cortex. *Proceedings of the National Academy of Sciences*, *112*(44), 13525–13530. https://doi.org/10.1073/PNAS.1515414112

Haxby, J. V., Gobbini, M. I., Furey, M. L., Ishai, A., Schouten, J. L., & Pietrini, P. (2001). Distributed and overlapping representations of faces and objects in ventral temporal cortex. *Science, 293*(5539), 2425–2430. https://doi.org/10.1126/science.1063736

Herath, P., Kinomura, S., & Roland, P. E. (2001). Visual recognition: Evidence for two distinctive mechanisms from a PET study. *Human Brain Mapping, 12*(2), 110–119. https://doi.org/10.1002/1097-0193(200102)12:2<110::aid-hbm1008>3.0.co;2-0

Hilty, L., Jäncke, L., Luechinger, R., Boutellier, U., & Lutz, K. (2010). Limitation of physical performance in a muscle fatiguing handgrip exercise is mediated by thalamo-insular activity. *Human Brain Mapping, 32*(12), 2151–2160. https://doi.org/10.1002/hbm.21177

Himmelbach, M., Nau, M., Zündorf, I., Erb, M., Perenin, M.-T., & Karnath, H.-O. (2009). Brain activation during immediate and delayed reaching in optic ataxia. *Neuropsychologia, 47*(6), 1508–1517. https://doi.org/10.1016/j.neuropsychologia.2009.01.033

Holler, D. E., Behrmann, M., & Snow, J. C. (2019). Real-world size coding of solid objects, but not 2-D or 3-D images, in visual agnosia patients with bilateral ventral lesions. *Cortex, 119*, 555-568. https://doi.org/10.1016/j.cortex.2019.02.030

Holmström, L., de Manzano, O., Vollmer, B., Forsman, L., Valero-Cuevas, F. J., Ullén, F., & Forssberg, H. (2011). Dissociation of brain areas associated with force production and stabilization during manipulation of unstable objects. *Experimental Brain Research, 215*(3-4), 359–367. https://doi.org/10.1007/s00221-011-2903-9

Holway, A. H., & Pratt, C. C. (1936). The Weber ratio for intensive discrimination. *Psychological Review, 43*(4), 322–340. https://doi.org/10.1037/h0059748

Hsiao, S., & Yau, J. (2008). Neural basis of haptic perception. In M. Grunwald (Ed.), *Human haptic perception: Basics and applications* (pp. 103–112). Birkhäuser Basel. https://doi.org/10.1007/978-3-7643-7612-3_8

Huang, R. S., & Sereno, M. I. (2018). Multisensory and sensorimotor maps. In Giuseppe Vallar & H. Branch Coslett (Eds.), *Handbook of Clinical Neurology* (Vol. 151, pp. 141–161). Elsevier. https://doi.org/10.1016/B978-0-444-63622-5.00007-3

Huang, Y., Pollick, F., Liu, M., & Zhang, D. (2023). Gabor and Non-Gabor Neural Representations Are Shared between Visual Perception and Mental Imagery. *Journal of Cognitive Neuroscience*, *35*(6), 1045–1060. https://doi.org/10.1162/JOCN_A_01992

Hunter, J. D. (2007). Matplotlib: A 2D graphics environment. *Computing in Science & Engineering, 9*(3), 90–95. https://doi.org/10.1109/MCSE.2007.55

Hyvärinen J. (1981). Regional distribution of functions in parietal association area 7 of the monkey. *Brain Research, 206*(2), 287–303. https://doi.org/10.1016/0006-8993(81)90533-3

Hyvärinen, J., & Poranen, A. (1974). Function of the parietal associative area 7 as revealed from cellular discharges in alert monkeys. *Brain, 97*(4), 673–692. https://doi.org/10.1093/brain/97.1.673

Inoue, K., Kawashima, R., Satoh, K., Kinomura, S., Goto, R., Koyama, M., Sugiura, M., Ito, M., & Fukuda, H. (1998). PET study of pointing with visual feedback of moving hands. *Journal of Neurophysiology, 79*(1), 117–125. https://doi.org/10.1152/jn.1998.79.1.117

Ishai, A., Ungerleider, L. G., Martin, A., Schouten, J. L., & Haxby, J. V. (1999). Distributed representation of objects in the human ventral visual pathway. *Proceedings of the*

National Academy of Sciences, 96(16), 9379–9384. https://doi.org/10.1073/pnas.96.16.9379

Iurilli, G., Ghezzi, D., Olcese, U., Lassi, G., Nazzaro, C., Tonini, R., Tucci, V., Benfenati, F., & Medini, P. (2012). Sound-driven synaptic inhibition in primary visual cortex. *Neuron, 73*(4), 814–828. https://doi.org/10.1016/j.neuron.2011.12.026

James, T. W., Culham, J., Humphrey, G. K., Milner, A. D., & Goodale, M. A. (2003). Ventral occipital lesions impair object recognition but not object-directed grasping: an fMRI study. *Brain, 126*(11), 2463–2475. https://doi.org/10.1093/brain/awg248

James, T. W., Kim, S., & Fisher, J. S. (2007). The neural basis of haptic object processing. *Canadian Journal of Experimental Psychology, 61*(3), 219–229. https://doi.org/10.1037/cjep2007023

Jeannerod, M. (1986). Mechanisms of visuomotor coordination: a study in normal and brain-damaged subjects. *Neuropsychologia, 24*(1), 41-78. https://doi.org/10.1016/0028-3932(86)90042-4

Jeannerod, M., Arbib, M. A., Rizzolatti, G., & Sakata, H. (1995). Grasping objects: the cortical mechanisms of visuomotor transformation. *Trends in Neurosciences, 18*(7), 314–320. https://doi.org/10.1016/0166-2236(95)93921-J

Jeannerod, M., Decety, J., & Michel, F. (1994). Impairment of grasping movements following a bilateral posterior parietal lesion. *Neuropsychologia, 32*(4), 369-380. https://doi.org/10.1016/0028-3932(94)90084-1

Jeong, S. K., & Xu, Y. (2016). Behaviorally Relevant Abstract Object Identity Representation in the Human Parietal Cortex. *The Journal of Neuroscience, 36*(5), 1607–1619. https://doi.org/10.1523/JNEUROSCI.1016-15.2016

JetBrains (2023). PyCharm 2023.3.4 (Community Edition), JetBrains. Available from https://www.jetbrains.com/pycharm/

Jiang, F., Beauchamp, M. S., & Fine, I. (2015). Re-examining overlap between tactile and visual motion responses within hMT + and STS. *NeuroImage, 119*, 187–196. https://doi.org/10.1016/j.neuroimage.2015.06.056

Jimura, K., & Poldrack, R. A. (2012). Analyses of regional-average activation and multivoxel pattern information tell complementary stories. *Neuropsychologia, 50*(4), 544–552. https://doi.org/10.1016/J.NEUROPSYCHOLOGIA.2011.11.007

Kaas, J. H., Nelson, R. J., Sur, M., Lin, C. S., & Merzenich, M. M. (1979). Multiple representations of the body within the primary somatosensory cortex of primates. *Science, 204*(4392), 521–523. https://doi.org/10.1126/SCIENCE.107591

Kanwisher, N. (2010). Functional specificity in the human brain: a window into the functional architecture of the mind. *Proceedings of the National Academy of Sciences, 107*(25), 11163–11170. https://doi.org/10.1073/PNAS.1005062107

Kanwisher, N., & Yovel, G. (2006). The fusiform face area: a cortical region specialized for the perception of faces. *Philosophical transactions of the Royal Society B: Biological sciences, 361*(1476), 2109–2128. https://doi.org/10.1098/rstb.2006.1934

Kanwisher, N., McDermott, J., & Chun, M. M. (1997). The fusiform face area: a module in human extrastriate cortex specialized for face perception. *The Journal of Neuroscience, 17*(11), 4302–4311. https://doi.org/10.1523/JNEUROSCI.17-11-04302.1997

Kappers, A. M. L., & Bergmann Tiest, W. M. (2013). Haptic perception. *Wiley Interdisciplinary Reviews: Cognitive Science, 4*(4), 357–374. https://doi.org/10.1002/WCS.1238

Karnath, H.-O., Rüter, J., Mandler, A., & Himmelbach, M. (2009). The anatomy of object recognition —Visual form agnosia caused by medial occipitotemporal stroke. *The*

Journal of Neuroscience, 29(18), 5854–5862. https://doi.org/10.1523/JNEUROSCI.5192-08.2009

Kasess, C. H., Windischberger, C., Cunnington, R., Lanzenberger, R., Pezawas, L., & Moser, E. (2008). The suppressive influence of SMA on M1 in motor imagery revealed by fMRI and dynamic causal modeling. *NeuroImage*, *40*(2), 828–837. https://doi.org/10.1016/J.NEUROIMAGE.2007.11.040

Kaup, B., Ulrich, R., Bausenhart, K. M., Bryce, D., Butz, M. V., Dignath, D., Dudschig, C., Franz, V. H., Friedrich, C., Gawrilow, C., Heller, J., Huff, M., Hütter, M., Janczyk, M., Leuthold, H., Mallot, H., Nürk, H. C., Ramscar, M., Said, N., Svaldi, J., … Wong, H. Y. (2024). Modal and amodal cognition: an overarching principle in various domains of psychology. *Psychological Research, 88*(2), 307–337. https://doi.org/10.1007/s00426-023-01878-w

Keisker, B., Hepp-Reymond, M.-C., Blickenstorfer, A., & Kollias, S. S. (2010). Differential representation of dynamic and static power grip force in the sensorimotor network. *European Journal of Neuroscience, 31*(8), 1483–1491. https://doi.org/10.1111/j.1460-9568.2010.07172.x

Keisker, B., Hepp-Reymond, M.-C., Blickenstorfer, A., Meyer, M., & Kollias, S. S. (2009). Differential force scaling of fine-graded power grip force in the sensorimotor network. *Human Brain Mapping, 30*(8), 2453–2465. https://doi.org/10.1002/hbm.20676

Kertzman, C., Schwarz, U., Zeffiro, T. A., & Hallett, M. (1997). The role of posterior parietal cortex in visually guided reaching movements in humans. *Experimental Brain Research, 114*(1), 170–183. https://doi.org/10.1007/pl00005617

Kim, J.-H., & Kim, S.-P. (2023). Neuroimaging of tactile information processing. *Investigative Magnetic Resonance Imaging, 27*(1), 1–9. https://doi.org/10.13104/IMRI.2022.1010

Kitada, R., Kochiyama, T., Hashimoto, T., Naito, E., & Matsumura, M. (2003). Moving tactile stimuli of fingers are integrated in the intraparietal and inferior parietal cortices. *NeuroReport, 14*(5), 719–724. https://doi.org/10.1097/00001756-200304150-00012

Kok, P., Failing, M. F., & de Lange, F. P. (2014). Prior expectations evoke stimulus templates in the primary visual cortex. *Journal of Cognitive Neuroscience, 26*(7), 1546–1554. https://doi.org/10.1162/jocn_a_00562

Kok, P., Mostert, P., & de Lange, F. P. (2017). Prior expectations induce prestimulus sensory templates. *Proceedings of the National Academy of Sciences, 114*(39), 10473–10478. https://doi.org/10.1073/pnas.1705652114

Konen, C. S., & Kastner, S. (2008). Two hierarchically organized neural systems for object information in human visual cortex. *Nature Neuroscience, 11*(2), 224–231. https://doi.org/10.1038/nn2036

Konen, C. S., Behrmann, M., Nishimura, M., & Kastner, S. (2011). The functional neuroanatomy of object agnosia: a case study. *Neuron, 71*(1), 49–60. https://doi.org/10.1016/j.neuron.2011.05.030

Kourtzi, Z., & Kanwisher, N. (2001). Representation of perceived object shape by the human lateral occipital complex. *Science, 293*(5534), 1506–1509. https://doi.org/10.1126/science.1061133

Kravitz, D. J., Saleem, K. S., Baker, C. I., & Mishkin, M. (2011). A new neural framework for visuospatial processing. *Nature Reviews Neuroscience, 12*(4), 217–230. https://doi.org/10.1038/nrn3008

Kriegeskorte, N., & Bandettini, P. (2007). Combining the tools: Activation- and information-based fMRI analysis. *NeuroImage*, *38*(4), 666–668. https://doi.org/10.1016/j.neuroimage.2007.06.030

Kriegeskorte, N., Lindquist, M. A., Nichols, T. E., Poldrack, R. A., & Vul, E. (2010). Everything you never wanted to know about circular analysis, but were afraid to ask. *Journal of Cerebral Blood Flow & Metabolism*, *30*, 1551–1557. https://doi.org/10.1038/jcbfm.2010.86

Kriegeskorte, N., Mur, M., Ruff, D. A., Kiani, R., Bodurka, J., Esteky, H., Tanaka, K., & Bandettini, P. A. (2008). Matching categorical object representations in inferior temporal cortex of man and monkey. *Neuron, 60*(6), 1126–1141. https://doi.org/10.1016/j.neuron.2008.10.043

Króliczak, G., Cavina-Pratesi, C., Goodman, D. A., & Culham, J. C. (2007). What Does the Brain Do When You Fake It? An fMRI Study of Pantomimed and Real Grasping. *Journal of Neurophysiology, 97*(3), 2410–2422. https://doi.org/10.1152/jn.00778.2006

Króliczak, G., McAdam, T. D., Quinlan, D. J., & Culham, J. C. (2008). The human dorsal stream adapts to real actions and 3D shape processing: a functional magnetic resonance imaging study. *Journal of Neurophysiology, 100*(5), 2627-2639. https://doi.org/10.1152/jn.01376.2007

Kuhtz-Buschbeck, J. P., Ehrsson, H. H., & Forssberg, H. (2001). Human brain activity in the control of fine static precision grip forces: An fMRI study. *European Journal of Neuroscience, 14*(2), 382–390. https://doi.org/10.1046/j.0953-816X.2001.01639.x

Kupers, R., & Ptito, M. (2014). Compensatory plasticity and cross-modal reorganization following early visual deprivation. *Neuroscience & Biobehavioral Reviews, 41*, 36-52. https://doi.org/10.1016/j.neubiorev.2013.08.001

Kupers, R., Fumal, A., de Noordhout, A. M., Gjedde, A., Schoenen, J., & Ptito, M. (2006). Transcranial magnetic stimulation of the visual cortex induces somatotopically organized qualia in blind subjects. *Proceedings of the National Academy of Sciences, 103*(35), 13256–13260. https://doi.org/10.1073/pnas.0602925103

Kupers, R., Pappens, M., de Noordhout, A. M., Schoenen, J., Ptito, M., & Fumal, A. (2007). rTMS of the occipital cortex abolishes Braille reading and repetition priming in blind subjects. *Neurology, 68*(9), 691-693. https://doi.org/10.1212/01.wnl.0000255958.60530.11

Kurniawan, I. T., Seymour, B., Talmi, D., Yoshida, W., Chater, N., & Dolan, R. J. (2010). Choosing to make an effort: the role of striatum in signaling physical effort of a chosen action. *Journal of Neurophysiology, 104*(1), 313–321. https://doi.org/10.1152/jn.00027.2010

Lacey, S., & Sathian, K. (2014). Visuo-haptic multisensory object recognition, categorization, and representation. *Frontiers in Psychology*, *5*, 730. https://doi.org/10.3389/FPSYG.2014.00730

Lacey, S., Flueckiger, P., Stilla, R., Lava, M., & Sathian, K. (2010). Object familiarity modulates the relationship between visual object imagery and haptic shape perception. *NeuroImage, 49*(3), 1977–1990. https://doi.org/10.1016/j.neuroimage.2009.10.081

Lacey, S., Stilla, R., Sreenivasan, K., Deshpande, G., & Sathian, K. (2014). Spatial imagery in haptic shape perception. *Neuropsychologia, 60*, 144–158. https://doi.org/10.1016/j.neuropsychologia.2014.05.008

Lacey, S., Tal, N., Amedi, A., & Sathian, K. (2009). A putative model of multisensory object representation. *Brain Topography, 21*(3-4), 269–274. https://doi.org/10.1007/S10548-009-0087-4

Laird, A. R., Fox, P. M., Price, C. J., Glahn, D. C., Uecker, A. M., Lancaster, J. L., Turkeltaub, P. E., Kochunov, P., & Fox, P. T. (2005). ALE meta-analysis: Controlling the false discovery rate and performing statistical contrasts. *Human Brain Mapping, 25*(1), 155–164. https://doi.org/10.1002/HBM.20136

Lawrence, S. J., Norris, D. G., & de Lange, F. P. (2019). Dissociable laminar profiles of concurrent bottom-up and top-down modulation in the human visual cortex. *eLife, 8*, e44422. https://doi.org/10.7554/eLife.44422

Lawson, R., Boylan, A., & Edwards, L. (2014). Where you look can influence haptic object recognition. *Attention, Perception, & Psychophysics, 76*(2), 559-574. https://doi.org/10.3758/s13414-013-0579-x

Lederman, S. J., & Klatzky, R. L. (1987). Hand movements: A window into haptic object recognition. *Cognitive Psychology, 19*(3), 342–368. https://doi.org/10.1016/0010-0285(87)90008-9

Lederman, S. J., & Klatzky, R. L. (1993). Extracting object properties through haptic exploration. *Acta Psychologica, 84*(1), 29–40. https://doi.org/10.1016/0001-6918(93)90070-8

Lederman, S. J., & Klatzky, R. L. (2009). Haptic perception: A tutorial. *Attention, Perception, & Psychophysics, 71*(7), 1439–1459. https://doi.org/10.3758/APP.71.7.1439

Lee Masson, H., Bulthé, J., Op de Beeck, H. P., & Wallraven, C. (2016). Visual and haptic shape processing in the human brain: unisensory processing, multisensory convergence, and top-down influences. *Cerebral Cortex, 26*(8), 3402-3412. https://doi.org/10.1093/cercor/bhv170

Lee, S.-H., Kravitz, D. J., & Baker, C. I. (2012). Disentangling visual imagery and perception of real-world objects. *NeuroImage*, *59*(4), 4064–4073. https://doi.org/10.1016/J.NEUROIMAGE.2011.10.055

Macaluso, E., & Maravita, A. (2010). The representation of space near the body through touch and vision. *Neuropsychologia, 48*(3), 782-795. https://doi.org/10.1016/j.neuropsychologia.2009.10.010

Macaluso, E., Frith, C. D., & Driver, J. (2000). Modulation of human visual cortex by crossmodal spatial attention. *Science, 289*(5482), 1206–1208. https://doi.org/10.1126/science.289.5482.1206

Magosso, E., Zavaglia, M., Serino, A., di Pellegrino, G., & Ursino, M. (2010). Visuotactile representation of peripersonal space: a neural network study. *Neural Computation, 22*(1), 190-243. https://doi.org/10.1162/neco.2009.01-08-694

Majdandzić, J., Grol, M. J., van Schie, H. T., Verhagen, L., Toni, I., & Bekkering, H. (2007). The role of immediate and final goals in action planning: An fMRI study. *NeuroImage, 37*(2), 589–598. https://doi.org/10.1016/j.neuroimage.2007.04.071

Malach, R., Reppas, J. B., Benson, R. R., Kwong, K. K., Jiang, H., Kennedy, W. A., Ledden, P. J., Brady, T. J., Rosen, B. R., & Tootell, R. B. (1995). Object-related activity revealed by functional magnetic resonance imaging in human occipital cortex. *Proceedings of the National Academy of Sciences, 92*(18), 8135–8139. https://doi.org/10.1073/PNAS.92.18.8135

Marangon, M., Kubiak, A., & Króliczak, G. (2016). Haptically guided grasping. fMRI shows right-hemisphere parietal stimulus encoding, and bilateral dorso-ventral parietal gradients of object- and action-related processing during grasp execution. *Frontiers in Human Neuroscience, 9*, 691. https://doi.org/10.3389/fnhum.2015.00691

Margalit, E., Jamison, K. W., Weiner, K. S., Vizioli, L., Zhang, R.-Y., Kay, K. N., & Grill-Spector, K. (2020). Ultra-high-resolution fMRI of human ventral temporal cortex reveals differential representation of categories and domains. *The Journal of Neuroscience, 40*(15), 3008–3024. https://doi.org/10.1523/JNEUROSCI.2106-19.2020

Marks, D. F. (1995). New directions for mental imagery research. *Journal of Mental Imagery*, *19*(3–4), 153–167.

Martinaud, O. (2017). Visual agnosia and focal brain injury. *Revue Neurologique, 173*(7-8), 451–460. https://doi.org/10.1016/j.neurol.2017.07.009

Mašić, V., Šečić, A., Bobić, T. T., & Femec, L. (2020). Neuroplasticity and Braille reading. *Acta Clinica Croatica, 59*(1), 147-153. https://doi.org/10.20471/acc.2020.59.01.18

Matteau, I., Kupers, R., Ricciardi, E., Pietrini, P., & Ptito, M. (2010). Beyond visual, aural and haptic movement perception: hMT+ is activated by electrotactile motion stimulation of the tongue in sighted and in congenitally blind individuals. *Brain Research Bulletin, 82*(5-6), 264–270. https://doi.org/10.1016/j.brainresbull.2010.05.001

McIntyre, J., Stratta, F., & Lacquaniti, F. (1998). Short-term memory for reaching to visual targets: psychophysical evidence for body-centered reference frames. *The Journal of Neuroscience, 18*(20), 8423-8435. https://doi.org/10.1523/JNEUROSCI.18-20-08423.1998

McKinney, W. (2010). Data structures for statistical computing in Python. In S. van der Walt & J. Millman (Eds.), *Proceedings of the 9th Python in Science Conference* (pp. 56–61). https://doi.org/10.25080/Majora-92bf1922-00a

McLaren, D. G., Ries, M. L., Xu, G., & Johnson, S. C. (2012). A generalized form of context-dependent psychophysiological interactions (gPPI): a comparison to standard approaches. *NeuroImage, 61*(4), 1277-1286. https://doi.org/10.1016/j.neuroimage.2012.03.068

McNamee, D., & Wolpert, D. M. (2019). Internal Models in Biological Control. *Annual Review of Control, Robotics, and Autonomous Systems, 2*, 339–364. https://doi.org/10.1146/annurev-control-060117-105206

Merabet, L. B., & Pascual-Leone, A. (2010). Neural reorganization following sensory loss: the opportunity of change. *Nature Reviews Neuroscience, 11*(1), 44-52. https://doi.org/10.1038/nrn2758

Merabet, L. B., Hamilton, R., Schlaug, G., Swisher, J. D., Kiriakopoulos, E. T., Pitskel, N. B., Kauffman, T., & Pascual-Leone, A. (2008). Rapid and reversible recruitment of early visual cortex for touch. *PLoS ONE, 3*(8), e3046. https://doi.org/10.1371/journal.pone.0003046

Merabet, L. B., Swisher, J. D., McMains, S. A., Halko, M. A., Amedi, A., Pascual-Leone, A., & Somers, D. C. (2007). Combined activation and deactivation of visual cortex during tactile sensory processing. *Journal of Neurophysiology, 97*(2), 1633-1641. https://doi.org/10.1152/jn.00806.2006

Merabet, L., Thut, G., Murray, B., Andrews, J., Hsiao, S., & Pascual-Leone, A. (2004). Feeling by sight or seeing by touch?.*Neuron, 42*(1), 173-179. https://doi.org/10.1016/S0896-6273(04)00147-3

Miller, E. K., Lundqvist, M., & Bastos, A. M. (2018). Working Memory 2.0. *Neuron*, *100*(2), 463–475. https://doi.org/10.1016/J.NEURON.2018.09.023

Milner, A. D. (2017). How do the two visual streams interact with each other? *Experimental Brain Research, 235*(5), 1297-1308. https://doi.org/10.1007/s00221-017-4917-4

Milner, A. D., & Goodale, M. A. (2006). *The visual brain in action* (2nd ed.). Oxford: Oxford University Press. https://doi.org/10.1093/acprof:oso/9780198524724.001.0001

Milner, A. D., & Goodale, M. A. (2008). Two visual systems re-viewed. *Neuropsychologia*, *46*(3), 774–785. https://doi.org/10.1016/J.NEUROPSYCHOLOGIA.2007.10.005

Milner, A. D., Dijkerman, H. C., Pisella, L., McIntosh, R. D., Tilikete, C., Vighetto, A., & Rossetti, Y. (2001). Grasping the past: delay can improve visuomotor performance. *Current Biology, 11*(23), 1896–1901. https://doi.org/10.1016/s0960-9822(01)00591-7

Milner, A. D., Paulignan, Y., Dijkerman, H. C., Michel, F., & Jeannerod, M. (1999). A paradoxical improvement of misreaching in optic ataxia: new evidence for two separate neural systems for visual localization. *Proceedings of the Royal Society of*

London. Series B: Biological Sciences, 266(1434), 2225–2229. https://doi.org/10.1098/rspb.1999.0912

Milner, A. D., Perrett, D. I., Johnston, R. S., Benson, P. J., Jordan, T. R., Heeley, D. W., Bettucci, D., Mortara, F., Mutani, R., Terazzi, E., & Davidson, D. L. W. (1991). Perception and action in 'visual form agnosia'. *Brain, 114*(1), 405–428. https://doi.org/10.1093/brain/114.1.405

Milner, T. E., Franklin, D. W., Imamizu, H., & Kawato, M. (2007). Central control of grasp: manipulation of objects with complex and simple dynamics. *NeuroImage, 36*(2), 388–395. https://doi.org/10.1016/j.neuroimage.2007.01.057

Moher, D., Liberati, A., Tetzlaff, J., Altman, D. G., & The PRISMA Group. (2009). Preferred reporting items for systematic reviews and meta-analyses: The PRISMA statement. *PLoS Medicine, 6*(7), e1000097. https://doi.org/10.1371/journal.pmed.1000097

Monaco, S., Cavina-Pratesi, C., Sedda, A., Fattori, P., Galletti, C., & Culham, J. C. (2011). Functional magnetic resonance adaptation reveals the involvement of the dorsomedial stream in hand orientation for grasping. *Journal of Neurophysiology, 106*(5), 2248–2263. https://doi.org/10.1152/jn.01069.2010

Monaco, S., Chen, Y., Medendorp, W. P., Crawford, J. D., Fiehler, K., & Henriques, D. Y. P. (2014). Functional magnetic resonance imaging adaptation reveals the cortical networks for processing grasp-relevant object properties. *Cerebral Cortex, 24*(6), 1540–1554. https://doi.org/10.1093/cercor/bht006

Monaco, S., Gallivan, J. P., Figley, T. D., Singhal, A., & Culham, J. C. (2017). Recruitment of foveal retinotopic cortex during haptic exploration of shapes and actions in the dark. *The Journal of Neuroscience, 37*(48), 11572–11591. https://doi.org/10.1523/JNEUROSCI.2428-16.2017

Monaco, S., Malfatti, G., Culham, J. C., Cattaneo, L., & Turella, L. (2020). Decoding motor imagery and action planning in the early visual cortex: Overlapping but distinct neural mechanisms. *NeuroImage, 218*, 116981. https://doi.org/10.1016/j.neuroimage.2020.116981

Monaco, S., Malfatti, G., Zendron, A., Pellencin, E., & Turella, L. (2019). Predictive coding of action intentions in dorsal and ventral visual stream is based on visual anticipations, memory-based information and motor preparation. *Brain Structure and Function, 224*(9), 3291–3308. https://doi.org/10.1007/S00429-019-01970-1

Monaco, S., Sedda, A., Cavina-Pratesi, C., & Culham, J. C. (2015). Neural correlates of object size and object location during grasping actions. *European Journal of Neuroscience*, *41*(4), 454–465. https://doi.org/10.1111/EJN.12786

Moretto, G., & di Pellegrino, G. (2008). Grasping numbers. *Experimental Brain Research*, *188*, 505–515. https://doi.org/10.1007/s00221-008-1386-9

Morgan, A. T., Petro, L. S., & Muckli, L. (2019). Scene Representations Conveyed by Cortical Feedback to Early Visual Cortex Can Be Described by Line Drawings. *The Journal of Neuroscience, 39*(47), 9410–9423. https://doi.org/10.1523/JNEUROSCI.0852-19.2019

Moutoussis, K., & Zeki, S. (2002). The relationship between cortical activation and perception investigated with invisible stimuli. *Proceedings of the National Academy of Sciences, 99*(14), 9527–9532. https://doi.org/10.1073/pnas.142305699

Mruczek, R. E. B., von Loga, I. S., & Kastner, S. (2013). The representation of tool and non-tool object information in the human intraparietal sulcus. *Journal of Neurophysiology*, *109*(12), 2883-2896. https://doi.org/10.1152/JN.00658.2012

Mueller, S., & Fiehler, K. (2016). Mixed body- and gaze-centered coding of proprioceptive reach targets after effector movement. *Neuropsychologia, 87*, 63-73. https://doi.org/10.1016/j.neuropsychologia.2016.04.033

Müller, F., Niso, G., Samiee, S., Ptito, M., Baillet, S., & Kupers, R. (2019). A thalamocortical pathway for fast rerouting of tactile information to occipital cortex in congenital blindness. *Nature Communications, 10*(1), 5154. https://doi.org/10.1038/s41467-019-13173-7

Müller, V. I., Cieslik, E. C., Laird, A. R., Fox, P. T., Radua, J., Mataix-Cols, D., Tench, C. R., Yarkoni, T., Nichols, T. E., Turkeltaub, P. E., Wager, T. D., & Eickhoff, S. B. (2018). Ten simple rules for neuroimaging meta-analysis. *Neuroscience & Biobehavioral Reviews, 84*, 151–161. https://doi.org/10.1016/j.neubiorev.2017.11.012

Murata, A., Gallese, V., Kaseda, M., & Sakata, H. (1996). Parietal neurons related to memory-guided hand manipulation. *Journal of Neurophysiology, 75*(5), 2180–2186. https://doi.org/10.1152/jn.1996.75.5.2180

Murata, A., Gallese, V., Luppino, G., Kaseda, M., & Sakata, H. (2000). Selectivity for the shape, size, and orientation of objects for grasping in neurons of monkey parietal area AIP. *Journal of Neurophysiology, 83*(5), 2580–2601. https://doi.org/10.1152/jn.2000.83.5.2580

Murphy, S., & Dalton, P. (2016). Out of touch? Visual load induces inattentional numbness. *Journal of experimental psychology: Human Perception and Performance, 42*(6), 761–765. https://doi.org/10.1037/xhp0000218

Murray, M. M., Thelen, A., Thut, G., Romei, V., Martuzzi, R., & Matusz, P. J. (2016). The multisensory function of the human primary visual cortex. *Neuropsychologia, 83*, 161–169. https://doi.org/10.1016/j.neuropsychologia.2015.08.011

Nakashita, S., Saito, D. N., Kochiyama, T., Honda, M., Tanabe, H. C., & Sadato, N. (2008). Tactile-visual integration in the posterior parietal cortex: A functional magnetic resonance imaging study. *Brain Research Bulletin, 75*(5), 513–525. https://doi.org/10.1016/j.brainresbull.2007.09.004

Neely, K. A., Coombes, S. A., Planetta, P. J., & Vaillancourt, D. E. (2013). Segregated and overlapping neural circuits exist for the production of static and dynamic precision grip force. *Human Brain Mapping, 34*(3), 698–712. https://doi.org/10.1002/hbm.21467

Niechwiej-Szwedo, E., Cao, M., & Barnett-Cowan, M. (2022). Binocular viewing facilitates size constancy for grasping and manual estimation. *Vision, 6*(2), 23. https://doi.org/10.3390/vision6020023

O'Craven, K. M., & Kanwisher, N. (2000). Mental Imagery of Faces and Places Activates Corresponding Stimulus-Specific Brain Regions. *Journal of Cognitive Neuroscience*, *12*(6), 1013–1023. https://doi.org/10.1162/08989290051137549

O'Reilly, J. X., Woolrich, M. W., Behrens, T. E. J., Smith, S. M., & Johansen-Berg, H. (2012). Tools of the trade: psychophysiological interactions and functional connectivity. *Social Cognitive and Affective Neuroscience, 7*(5), 604-609. https://doi.org/10.1093/scan/nss055

Ogawa, S., Tank, D. W., Menon, R., Ellermann, J. M., Kim, S. G., Merkle, H., & Ugurbil, K. (1992). Intrinsic signal changes accompanying sensory stimulation: Functional brain mapping with magnetic resonance imaging. *Proceedings of the National Academy of Sciences*, *89*(13), 5951–5955. https://doi.org/10.1073/pnas.89.13.5951

Oosterhof, N. N., Connolly, A. C., & Haxby, J. V. (2016). CoSMoMVPA: multi-modal multivariate pattern analysis of neuroimaging data in Matlab/GNU Octave. *Frontiers in Neuroinformatics*, *10*, 27. https://doi.org/10.3389/fninf.2016.00027

Oosterhof, N. N., Wiestler, T., Downing, P. E., & Diedrichsen, J. (2011). A comparison of volume-based and surface-based multi-voxel pattern analysis. *NeuroImage*, *56*(2), 593–600. https://doi.org/10.1016/j.neuroimage.2010.04.270

Op de Beeck, H. P., Torfs, K., & Wagemans, J. (2008). Perceived shape similarity among unfamiliar objects and the organization of the human object vision pathway. *The Journal of Neuroscience, 28*(40), 10111–10123. https://doi.org/10.1523/JNEUROSCI.2511-08.2008

Page, M. J., McKenzie, J. E., Bossuyt, P. M., Boutron, I., Hoffmann, T. C., Mulrow, C. D., Shamseer, L., Tetzlaff, J. M., Akl, E. A., Brennan, S. E., Chou, R., Glanville, J., Grimshaw, J. M., Hróbjartsson, A., Lalu, M. M., Li, T., Loder, E. W., Mayo-Wilson, E., Mcdonald, S., … Moher, D. (2021). The PRISMA 2020 statement: an updated guideline for reporting systematic reviews. *International Journal of Surgery, 88*, 105906. https://doi.org/10.1136/bmj.n71

Pascual-Leone, A., & Hamilton, R. (2001). Chapter 27 The metamodal organization of the brain. *Progress in Brain Research, 134*, 427–445. https://doi.org/10.1016/s0079-6123(01)34028-1

Pearson, J. (2019). The human imagination: the cognitive neuroscience of visual mental imagery. *Nature Reviews Neuroscience, 20*(10), 624–634. https://doi.org/10.1038/s41583-019-0202-9

Peelen, M. V., & Downing, P. E. (2005). Selectivity for the human body in the fusiform gyrus. *Journal of Neurophysiology, 93*(1), 603–608. https://doi.org/10.1152/jn.00513.2004

Pelli, D. G. (1997). The VideoToolbox software for visual psychophysics: Transforming numbers into movies. *Spatial Vision, 10*(4), 437–442. https://doi.org/10.1163/156856897X00366

Pellijeff, A., Bonilha, L., Morgan, P. S., McKenzie, K., & Jackson, S. R. (2006). Parietal updating of limb posture: an event-related fMRI study. *Neuropsychologia, 44*(13), 2685–2690. https://doi.org/10.1016/j.neuropsychologia.2006.01.009

Penfield, W., & Boldrey, E. (1937). Somatic motor and sensory representation in the cerebral cortex of man as studied by electrical stimulation. *Brain, 60*(4), 389–443. https://doi.org/10.1093/brain/60.4.389

Pennartz, C. M. A., Oude Lohuis, M. N., & Olcese, U. (2023). How 'visual'is the visual cortex? The interactions between the visual cortex and other sensory, motivational and motor systems as enabling factors for visual perception. *Philosophical Transactions of the Royal Society B: Biological Sciences*, 378(1886). https://doi.org/10.1098/rstb.2022.0336

Perenin, M. T., & Vighetto, A. (1988). Optic ataxia: A specific disruption in visuomotor mechanisms: Different aspects of the deficit in reaching for objects. *Brain, 111*(3), 643-674. https://doi.org/10.1093/brain/111.3.643

Perini, F., Powell, T., Watt, S. J., & Downing, P. E. (2020). Neural representations of haptic object size in the human brain revealed by multivoxel fMRI patterns. *Journal of Neurophysiology, 124*(1), 218–231. https://doi.org/10.1152/JN.00160.2020

Pettypiece, C. E., Goodale, M. A., & Culham, J. C. (2010). Integration of haptic and visual size cues in perception and action revealed through cross-modal conflict. *Experimental Brain Research, 201*(4), 863-873. https://doi.org/10.1007/s00221-009-2101-1

Pirruccio, M., Monaco, S., Della Libera, C., & Cattaneo, L. (2020). Gaze direction influences grasping actions towards unseen, haptically explored, objects. *Scientific Reports, 10*(1), 15774. https://doi.org/10.1038/s41598-020-72554-x

Pisella, L., Binkofski, F., Lasek, K., Toni, I., & Rossetti, Y. (2006). No double-dissociation between optic ataxia and visual agnosia: multiple sub-streams for multiple visuo-manual integrations. *Neuropsychologia, 44*(13), 2734–2748. https://doi.org/10.1016/j.neuropsychologia.2006.03.027

Pisella, L., Sergio, L., Blangero, A., Torchin, H., Vighetto, A., & Rossetti, Y. (2009). Optic ataxia and the function of the dorsal stream: contributions to perception and action. *Neuropsychologia, 47*(14), 3033-3044. https://doi.org/10.1016/j.neuropsychologia.2009.06.020

Planetta, P. J., & Servos, P. (2012). The postcentral gyrus shows sustained fMRI activation during the tactile motion aftereffect. *Experimental Brain Research, 216*(4), 535–544. https://doi.org/10.1007/s00221-011-2957-8

Podrebarac, S. K., Goodale, M. A., & Snow, J. C. (2014). Are visual texture-selective areas recruited during haptic texture discrimination? *NeuroImage, 94*, 129–137. https://doi.org/10.1016/J.NEUROIMAGE.2014.03.013

Prado, J., Clavagnier, S., Otzenberger, H., Scheiber, C., Kennedy, H., & Perenin, M. T. (2005). Two cortical systems for reaching in central and peripheral vision. *Neuron, 48*(5), 849–858. https://doi.org/10.1016/j.neuron.2005.10.010

Ptito, M., Fumal, A., De Noordhout, A. M., Schoenen, J., Gjedde, A., & Kupers, R. (2008). TMS of the occipital cortex induces tactile sensations in the fingers of blind Braille readers. *Experimental Brain Research, 184*(2), 193-200. https://doi.org/10.1007/s00221-007-1091-0

Ranzini, M., Scarpazza, C., Radua, J., Cutini, S., Semenza, C., & Zorzi, M. (2022). A common neural substrate for number comparison, hand reaching and grasping: A SDM-PSI meta-analysis of neuroimaging studies. *Cortex, 148*, 31–67. https://doi.org/10.1016/J.CORTEX.2021.12.007

Ratan Murty, N. A., Teng, S., Beeler, D., Mynick, A., Oliva, A., & Kanwisher, N. (2020). Visual experience is not necessary for the development of face-selectivity in the lateral fusiform gyrus. *Proceedings of the National Academy of Sciences, 117*(37), 23011–23020. https://doi.org/10.1073/pnas.2004607117

Rauss, K., Schwartz, S., & Pourtois, G. (2011). Top-down effects on early visual processing in humans: a predictive coding framework. *Neuroscience & Biobehavioral Reviews, 35*(5), 1237–1253. https://doi.org/10.1016/j.neubiorev.2010.12.011

Reed, C. L., Klatzky, R. L., & Halgren, E. (2005). What vs. where in touch: an fMRI study. *NeuroImage, 25*(3), 718–726. https://doi.org/10.1016/j.neuroimage.2004.11.044

Renzi, C., Ricciardi, E., Bonino, D., Handjaras, G., Vecchi, T., & Pietrini, P. (2013). The effects of visual control and distance in modulating peripersonal spatial representation. *PLoS ONE, 8*(3), e59460. https://doi.org/10.1371/journal.pone.0059460

Reuschel, J., Rösler, F., Henriques, D. Y. P., & Fiehler, K. (2012). Spatial updating depends on gaze direction even after loss of vision. *The Journal of Neuroscience, 32*(7), 2422-2429. https://doi.org/10.1523/JNEUROSCI.2714-11.2012

Ricciardi, E., & Pietrini, P. (2011). New light from the dark: what blindness can teach us about brain function. *Current Opinion in Neurology, 24*(4), 357-363. https://doi.org/10.1097/WCO.0b013e328348bdbf

Ricciardi, E., Bonino, D., Pellegrini, S., & Pietrini, P. (2014). Mind the blind brain to understand the sighted one! Is there a supramodal cortical functional architecture? *Neuroscience & Biobehavioral Reviews, 41*, 64–77. https://doi.org/10.1016/j.neubiorev.2013.10.006

Ricciardi, E., Vanello, N., Sani, L., Gentili, C., Scilingo, E. P., Landini, L., Guazzelli, M., Bicchi, A., Haxby, J. V., & Pietrini, P. (2007). The effect of visual experience on the development of functional architecture in hMT+. *Cerebral Cortex, 17*(12), 2933–2939. https://doi.org/10.1093/CERCOR/BHM018

Riddoch, M. J., & Humphreys, G. W. (1987). A case of integrative visual agnosia. *Brain, 110*(6), 1431–1462. https://doi.org/10.1093/BRAIN/110.6.1431

Rizzolatti, G., & Matelli, M. (2003). Two different streams form the dorsal visual system: anatomy and functions. *Experimental Brain Research, 153*(2), 146–157. https://doi.org/10.1007/s00221-003-1588-0

Rizzolatti, G., Scandolara, C., Matelli, M., & Gentilucci, M. (1981). Afferent properties of periarcuate neurons in macaque monkeys. II. Visual responses. *Behavioural Brain Research, 2*(2), 147–163. https://doi.org/10.1016/0166-4328(81)90053-x

Roland, P. E., O'Sullivan, B., & Kawashima, R. (1998). Shape and roughness activate different somatosensory areas in the human brain. *Proceedings of the National Academy of Sciences, 95*(6), 3295–3300. https://doi.org/10.1073/pnas.95.6.3295

Rolls, E. T., Deco, G., Huang, C.-C., & Feng, J. (2023). The human posterior parietal cortex: effective connectome, and its relation to function. *Cerebral Cortex, 33*(6), 3142–3170. https://doi.org/10.1093/CERCOR/BHAC266

Rossit, S., McAdam, T., McLean, D. A., Goodale, M. A., & Culham, J. C. (2013). fMRI reveals a lower visual field preference for hand actions in human superior parieto-occipital cortex (SPOC) and precuneus. *Cortex, 49*(9), 2525–2541. https://doi.org/10.1016/j.cortex.2012.12.014

Roth, M. M., Dahmen, J. C., Muir, D. R., Imhof, F., Martini, F. J., & Hofer, S. B. (2016). Thalamic nuclei convey diverse contextual information to layer 1 of visual cortex. *Nature Neuroscience, 19*(2), 299-307. https://doi.org/10.1038/nn.4197

Saccone, E. J., Tian, M., & Bedny, M. (2024). Developing cortex is functionally pluripotent: evidence from blindness. *Developmental Cognitive Neuroscience, 66*, 101360. https://doi.org/10.1016/j.dcn.2024.101360

Sadato, N., Pascual-Leone, A., Grafman, J., Deiber, M. P., Ibañez, V., & Hallett, M. (1998). Neural networks for Braille reading by the blind. *Brain, 121*(7), 1213–1229. https://doi.org/10.1093/BRAIN/121.7.1213

Saiote, C., Tacchino, A., Brichetto, G., Roccatagliata, L., Bommarito, G., Cordano, C., Battaglia, M., Mancardi, G. L., & Inglese, M. (2016). Resting-state functional connectivity and motor imagery brain activation. *Human Brain Mapping, 37*(11), 3847–3857. https://doi.org/10.1002/hbm.23280

Sakata, H., & Taira, M. (1994). Parietal control of hand action. *Current Opinion in Neurobiology, 4*(6), 847–856. https://doi.org/10.1016/0959-4388(94)90133-3

Sakata, H., Taira, M., Kusunoki, M., Murata, A., & Tanaka, Y. (1997). The TINS Lecture. The parietal association cortex in depth perception and visual control of hand action. *Trends in Neurosciences, 20*(8), 350–357. https://doi.org/10.1016/s0166-2236(97)01067-9

Sakata, H., Taira, M., Murata, A., & Mine, S. (1995). Neural mechanisms of visual guidance of hand action in the parietal cortex of the monkey. *Cerebral Cortex, 5*(5), 429–438. https://doi.org/10.1093/cercor/5.5.429

Sakreida, K., Effnert, I., Thill, S., Menz, M. M., Jirak, D., Eickhoff, C. R., Ziemke, T., Eickhoff, S. B., Borghi, A. M., & Binkofski, F. (2016). Affordance processing in segregated parieto-frontal dorsal stream sub-pathways. *Neuroscience & Biobehavioral Reviews, 69*, 89–112. https://doi.org/10.1016/J.NEUBIOREV.2016.07.032

Sartin, S., Danaj, F., Del Giudice, F., Chen, J., Schwarzkopf, D. S., Sperandio, I., & Monaco, S. (2026). Decoding haptic and imagined stimulus size in the human cortex. *NeuroImage*, 121774. https://doi.org/10.1016/j.neuroimage.2026.121774

Sartin, S., Ranzini, M., Scarpazza, C., & Monaco, S. (2023). Cortical areas involved in grasping and reaching actions with and without visual information: An ALE meta-analysis of neuroimaging studies. *Current Research in Neurobiology, 4*, 100070. https://doi.org/10.1016/j.crneur.2022.100070

Sathian, K. (2016). Analysis of haptic information in the cerebral cortex. *Journal of Neurophysiology, 116*(4), 1795–1806. https://doi.org/10.1152/jn.00546.2015

Sathian, K., & Lacey, S. (2022). Cross-modal interactions of the tactile system. *Current Directions in Psychological Science, 31*(5), 411–418. https://doi.org/10.1177/09637214221101877

Sathian, K., Lacey, S., Stilla, R., Gibson, G. O., Deshpande, G., Hu, X., LaConte, S., & Glielmi, C. (2011). Dual pathways for haptic and visual perception of spatial and texture information. *NeuroImage, 57*(2), 462–475. https://doi.org/10.1016/J.NEUROIMAGE.2011.05.001

Schenk, T. (2006). An allocentric rather than perceptual deficit in patient D.F. *Nature Neuroscience*, *9*(11), 1369–1370. https://doi.org/10.1038/nn1784

Schenk, T., & McIntosh, R. D. (2010). Do we have independent visual streams for perception and action? *Cognitive Neuroscience, 1*(1), 52-62. https://doi.org/10.1080/17588920903388950

Schiltz, C., Sorger, B., Caldara, R., Ahmed, F., Mayer, E., Goebel, R., & Rossion, B. (2006). Impaired face discrimination in acquired prosopagnosia is associated with abnormal response to individual faces in the right middle fusiform gyrus. *Cerebral Cortex, 16*(4), 574–586. https://doi.org/10.1093/cercor/bhj005

Schneider, W., Eschman, A., & Zuccolotto, A. (2012). *E-Prime 2.0* [Computer software]. Psychology Software Tools.

Scott, S. H. (2004). Optimal feedback control and the neural basis of volitional motor control. *Nature Reviews Neuroscience, 5*(7), 532–545. https://doi.org/10.1038/nrn1427

Seabold, S., & Perktold, J. (2010). Statsmodels: Econometric and statistical modeling with Python. In *Proceedings of the 9th Python in Science Conference* (pp. 92–96). https://doi.org/10.25080/Majora-92bf1922-011

Shadmehr, R., & Krakauer, J. W. (2008). A computational neuroanatomy for motor control. *Experimental Brain Research, 185*(3), 359–381. https://doi.org/10.1007/s00221-008-1280-5

Silva, P. R., Farias, T., Cascio, F., Dos Santos, L., Peixoto, V., Crespo, E., Ayres, C., Ayres, M., Marinho, V., Bastos, V. H., Ribeiro, P., Velasques, B., Orsini, M., Fiorelli, R., de Freitas, M. R. G., & Teixeira, S. (2018). Neuroplasticity in visual impairments. *Neurology International, 10*(4), 7326. https://doi.org/10.4081/ni.2018.7326

Sim, E.-J., Helbig, H. B., Graf, M., & Kiefer, M. (2015). When Action Observation Facilitates Visual Perception: Activation in Visuo-Motor Areas Contributes to Object Recognition. *Cerebral Cortex, 25*(9), 2907–2918. https://doi.org/10.1093/cercor/bhu087

Singhal, A., Monaco, S., Kaufman, L. D., & Culham, J. C. (2013). Human fMRI reveals that delayed action re-recruits visual perception. *PLoS ONE, 8*(9), e73629. https://doi.org/10.1371/journal.pone.0073629

Siuda-Krzywicka, K., Bola, Ł., Paplińska, M., Sumera, E., Jednoróg, K., Marchewka, A., Śliwińska, M. W., Amedi, A., & Szwed, M. (2016). Massive cortical reorganization in sighted Braille readers. *eLife, 5*, e10762. https://doi.org/10.7554/eLife.10762

Smith, A. T., Singh, K. D., Williams, A. L., & Greenlee, M. W. (2001). Estimating receptive field size from fMRI data in human striate and extrastriate visual cortex. *Cerebral Cortex, 11*(12), 1182–1190. https://doi.org/10.1093/cercor/11.12.1182

Smith, F. W., & Muckli, L. (2010). Nonstimulated early visual areas carry information about surrounding context. *Proceedings of the National Academy of Sciences, 107*(46), 20099–20103. https://doi.org/10.1073/pnas.1000233107

Smyrnis, N., Theleritis, C., Evdokimidis, I., Müri, R. M., & Karandreas, N. (2003). Single-pulse transcranial magnetic stimulation of parietal and prefrontal areas in a memory

delay arm pointing task. *Journal of Neurophysiology, 89*(6), 3344–3350. https://doi.org/10.1152/jn.00810.2002

Snow, J. C., Goodale, M. A., & Culham, J. C. (2015). Preserved haptic shape processing after bilateral LOC lesions. *The Journal of Neuroscience, 35*(40), 13745–13760. https://doi.org/10.1523/JNEUROSCI.0859-14.2015

Snow, J. C., Strother, L., & Humphreys, G. W. (2014). Haptic shape processing in visual cortex. *Journal of Cognitive Neuroscience, 26*(5), 1154–1167. https://doi.org/10.1162/JOCN_A_00548

Snyder, L. H., Batista, A. P., & Andersen, R. A. (1997). Coding of intention in the posterior parietal cortex. *Nature, 386*(6621), 167–170. https://doi.org/10.1038/386167a0

Spagna, A., Hajhajate, D., Liu, J., & Bartolomeo, P. (2021). Visual mental imagery engages the left fusiform gyrus, but not the early visual cortex: A meta-analysis of neuroimaging evidence. *Neuroscience & Biobehavioral Reviews, 122*, 201–217. https://doi.org/10.1016/j.neubiorev.2020.12.029

Spagna, A., Heidenry, Z., Miselevich, M., Lambert, C., Eisenstadt, B. E., Tremblay, L., Liu, Z., Liu, J., & Bartolomeo, P. (2024). Visual mental imagery: Evidence for a heterarchical neural architecture. *Physics of Life Reviews, 48*, 113–131. https://doi.org/10.1016/J.PLREV.2023.12.012

Spence, C., Pavani, F., & Driver, J. (2000). Crossmodal links between vision and touch in covert endogenous spatial attention. *Journal of Experimental Psychology: Human Perception and Performance, 26*(4), 1298–1319. https://doi.org/10.1037/0096-1523.26.4.1298

Sperandio, I., Bond, N., & Binda, P. (2018). Pupil size as a gateway into conscious interpretation of brightness. *Frontiers in Neurology, 9*, 1070. https://doi.org/10.3389/fneur.2018.01070

Sperandio, I., Lak, A., & Goodale, M. A. (2012). Afterimage size is modulated by size-contrast illusions. *Journal of Vision, 12*(2), 18. https://doi.org/10.1167/12.2.18

Spraker, M. B., Corcos, D. M., & Vaillancourt, D. E. (2009). Cortical and subcortical mechanisms for precisely controlled force generation and force relaxation. *Cerebral Cortex, 19*(11), 2640–2650. https://doi.org/10.1093/cercor/bhp015

Stewart, E. E. M., Valsecchi, M., & Schütz, A. C. (2020). A review of interactions between peripheral and foveal vision. *Journal of Vision, 20*(12), 2. https://doi.org/10.1167/jov.20.12.2

Stilla, R., & Sathian, K. (2008). Selective visuo-haptic processing of shape and texture. *Human Brain Mapping*, *29*(10), 1123–1138. https://doi.org/10.1002/HBM.20456

Strasburger, H., Rentschler, I., & Jüttner, M. (2011). Peripheral vision and pattern recognition: a review. *Journal of Vision, 11*(5), 13. https://doi.org/10.1167/11.5.13

Styrkowiec, P. P., Nowik, A. M., & Króliczak, G. (2019). The neural underpinnings of haptically guided functional grasping of tools: An fMRI study. *NeuroImage, 194*, 149–162. https://doi.org/10.1016/j.neuroimage.2019.03.043

Summers, I. R., Francis, S. T., Bowtell, R. W., McGlone, F. P., & Clemence, M. (2009). A functional-magnetic-resonance-imaging investigation of cortical activation from moving vibrotactile stimuli on the fingertip. *The Journal of the Acoustical Society of America, 125*(2), 1033–1039. https://doi.org/10.1121/1.3056399

Taira, M., Mine, S., Georgopoulos, A. P., Murata, A., & Sakata, H. (1990). Parietal cortex neurons of the monkey related to the visual guidance of hand movement. *Experimental Brain Research, 83*(1), 29–36. https://doi.org/10.1007/BF00232190

Talairach, J., & Tournoux, P. (1988). *Co-planar stereotaxic atlas of the human brain: 3-dimensional proportional system: An approach to cerebral imaging*. Thieme.

Talelli, P., Ewas, A., Waddingham, W., Rothwell, J. C., & Ward, N. S. (2008). Neural correlates of age-related changes in cortical neurophysiology. *NeuroImage, 40*(4), 1772–1781. https://doi.org/10.1016/j.neuroimage.2008.01.039

The MathWorks Inc. (2020). MATLAB version: 9.8.0 (R2020a), Natick, Massachusetts: The MathWorks Inc. Available from https://www.mathworks.com

Tian, S., Chen, Y., Fu, Z., Wang, X., & Bi, Y. (2023). Simple shape feature computation across modalities: convergence and divergence between the ventral and dorsal visual streams. *Cerebral Cortex, 33*(15), 9280–9290. https://doi.org/10.1093/CERCOR/BHAD200

Tolkien, J. R. R. (1954). *The Fellowship of the Ring*. George Allen & Unwin.

Tsay, A. J., Giummarra, M. J., Allen, T. J., & Proske, U. (2016). The sensory origins of human position sense. *The Journal of Physiology, 594*(4), 1037–1049. https://doi.org/10.1113/JP271498

Turella, L., Erb, M., Grodd, W., & Castiello, U. (2009). Visual features of an observed agent do not modulate human brain activity during action observation. *NeuroImage, 46*(3), 844–853. https://doi.org/10.1016/j.neuroimage.2009.03.002

Turkeltaub, P. E., Eden, G. F., Jones, K. M., & Zeffiro, T. A. (2002). Meta-analysis of the functional neuroanatomy of single-word reading: Method and validation. *NeuroImage, 16*(3), 765–780. https://doi.org/10.1006/nimg.2002.1131

Uhl, F., Kretschmer, T., Lindinger, G., Goldenberg, G., Lang, W., Oder, W., & Deecke, L. (1994). Tactile mental imagery in sighted persons and in patients suffering from peripheral blindness early in life. *Electroencephalography and Clinical Neurophysiology, 91*(4), 249–255. https://doi.org/10.1016/0013-4694(94)90188-0

Ungerleider, L. G., & Mishkin, M. (1982). *Two cortical visual systems*. In D. J. Ingle, M. A. Goodale, & R. J. Mansfield (Eds.), Analysis of visual behavior. Cambridge, M.A.: MIT Press.

Vaillancourt, D. E., Thulborn, K. R., & Corcos, D. M. (2003). Neural basis for the processes that underlie visually guided and internally guided force control in humans. *Journal of Neurophysiology, 90*(5), 3330–3340. https://doi.org/10.1152/jn.00394.2003

Valyear, K. F., Mattos, D., Philip, B. A., Kaufman, C., & Frey, S. H. (2019). Grasping with a new hand: Improved performance and normalized grasp-selective brain responses despite persistent functional changes in primary motor cortex and low-level sensory and motor impairments. *NeuroImage, 190*, 275–288. https://doi.org/10.1016/j.neuroimage.2017.09.052

Van De Winckel, A., Sunaert, S., Wenderoth, N., Peeters, R., Van Hecke, P., Feys, H., Horemans, E., Marchal, G., Swinnen, S. P., Perfetti, C., & De Weerdt, W. (2005). Passive somatosensory discrimination tasks in healthy volunteers: Differential networks involved in familiar versus unfamiliar shape and length discrimination. *NeuroImage, 26*(2), 441–453. https://doi.org/10.1016/J.NEUROIMAGE.2005.01.058

Van Dromme, I. C., Premereur, E., Verhoef, B.-E., Vanduffel, W., & Janssen, P. (2016). Posterior parietal cortex drives inferotemporal activations during three-dimensional object vision. *PLoS Biology, 14*(4), e1002445. https://doi.org/10.1371/journal.pbio.1002445

Van Kemenade, B. M., Seymour, K., Wacker, E., Spitzer, B., Blankenburg, F., & Sterzer, P. (2014). Tactile and visual motion direction processing in hMT+/V5. *NeuroImage, 84*, 420–427. https://doi.org/10.1016/j.neuroimage.2013.09.004

Vasconcelos, N., Pantoja, J., Belchior, H., Caixeta, F. V., Faber, J., Freire, M. A. M., Cota, V. R., Anibal de Macedo, E., Laplagne, D. A., Gomes, H. M., & Ribeiro, S. (2011). Cross-modal responses in the primary visual cortex encode complex objects and correlate with tactile discrimination. *Proceedings of the National Academy of Sciences, 108*(37), 15408–15413. https://doi.org/10.1073/pnas.1102780108

Vélez-Fort, M., Bracey, E. F., Keshavarzi, S., Rousseau, C. V., Cossell, L., Lenzi, S. C., Strom, M., & Margrie, T. W. (2018). A circuit for integration of head- and visual-motion signals in layer 6 of mouse primary visual cortex. *Neuron, 98*(1), 179–191.e6. https://doi.org/10.1016/j.neuron.2018.02.023

Velji-Ibrahim, J., Crawford, J. D., Cattaneo, L., & Monaco, S. (2022). Action planning modulates the representation of object features in human fronto-parietal and occipital cortex. *European Journal of Neuroscience, 56*(6), 4803–4818. https://doi.org/10.1111/EJN.15776

Verhagen, L., Dijkerman, H. C., Grol, M. J., & Toni, I. (2008). Perceptuo-motor interactions during prehension movements. *The Journal of Neuroscience, 28*(18), 4726–4735. https://doi.org/10.1523/JNEUROSCI.0057-08.2008

Virtanen, P., Gommers, R., Oliphant, T. E., Haberland, M., Reddy, T., Cournapeau, D., Burovski, E., Peterson, P., Weckesser, W., Bright, J., van der Walt, S. J., Brett, M., Wilson, J., Millman, K. J., Mayorov, N., Nelson, A. R. J., Jones, E., Kern, R., Larson, E., … Vázquez-Baeza, Y. (2020). SciPy 1.0: fundamental algorithms for scientific computing in Python. *Nature Methods, 17*(3), 261–272. https://doi.org/10.1038/s41592-019-0686-2

Vul, E., & Kanwisher, N. (2010). Begging the question: The non-independence error in fMRI data analysis. In S. J. Hanson & M. Bunzl (Eds.), *Foundational Issues in Human Brain Mapping* (pp. 71–91). The MIT Press. https://doi.org/10.7551/mitpress/9780262014021.003.0007

Wacker, E., Spitzer, B., Lützkendorf, R., Bernarding, J., & Blankenburg, F. (2011). Tactile motion and pattern processing assessed with high-field fMRI. *PLoS ONE, 6*(9), e24860. https://doi.org/10.1371/JOURNAL.PONE.0024860

Wager, T. D., Lindquist, M. A., Nichols, T. E., Kober, H., & Van Snellenberg, J. X. (2009). Evaluating the consistency and specificity of neuroimaging data using meta-analysis. *NeuroImage, 45*(1), S210–S221. https://doi.org/10.1016/J.NEUROIMAGE.2008.10.061

Wallace, M. T., Wilkinson, L. K., & Stein, B. E. (1996). Representation and integration of multiple sensory inputs in primate superior colliculus. *Journal of Neurophysiology, 76*(2), 1246–1266. https://doi.org/10.1152/jn.1996.76.2.1246

Ward, N. S., & Frackowiak, R. S. J. (2003). Age-related changes in the neural correlates of motor performance. *Brain, 126*(4), 873–888. https://doi.org/10.1093/brain/awg071

Waskom, M. L. (2021). seaborn: statistical data visualization. *Journal of Open Source Software, 6*(60), 3021, https://doi.org/10.21105/joss.03021

Whitwell, R. L., Milner, A. D., Goodale, M. A., Whishaw, I. Q., & Karl, J. M. (2014). The two visual systems hypothesis: new challenges and insights from visual form agnosic patient DF. *Frontiers in Neurology, 5*. https://doi.org/10.3389/fneur.2014.00255

Wiecek, E., Ramirez, L. D., Klimova, M., & Ling, S. (2026). Spatial frequency tuning follows scale invariance in human visual cortex. *The Journal of Neuroscience, 46*(4), e1490252025. https://doi.org/10.1523/JNEUROSCI.1490-25.2025

Wolpert, D. M., & Flanagan, J. R. (2001). Motor prediction. *Current Biology, 11*(18), R729-R732. https://doi.org/10.1016/s0960-9822(01)00432-8

Xu, Y. (2009). Distinctive neural mechanisms supporting visual object individuation and identification. *Journal of Cognitive Neuroscience, 21*(3), 511–518. https://doi.org/10.1162/jocn.2008.21024

Xu, Y., Vignali, L., Sigismondi, F., Crepaldi, D., Bottini, R., & Collignon, O. (2023). Similar object shape representation encoded in the inferolateral occipitotemporal cortex of

sighted and early blind people. *PLOS Biology, 21*(7), e3001930. https://doi.org/10.1371/JOURNAL.PBIO.3001930

Yau, J. M., Kim, S. S., Thakur, P. H., & Bensmaia, S. J. (2016). Feeling form: The neural basis of haptic shape perception. *Journal of Neurophysiology, 115*(2), 631–642. https://doi.org/10.1152/jn.00598.2015

Zachariou, V., Nikas, C. V., Safiullah, Z. N., Behrmann, M., Klatzky, R., & Ungerleider, L. G. (2015). Common dorsal stream substrates for the mapping of surface texture to object parts and visual spatial processing. *Journal of Cognitive Neuroscience, 27*(12), 2442-2461. https://doi.org/10.1162/jocn_a_00871

Zangaladze, A., Epstein, C. M., Grafton, S. T., & Sathian, K. (1999). Involvement of visual cortex in tactile discrimination of orientation. *Nature, 401*(6753), 587-590. https://doi.org/10.1038/44139

Zeki, S. M. (1978). Uniformity and diversity of structure and function in rhesus monkey prestriate visual cortex. *The Journal of Physiology, 277*(1), 273–290. https://doi.org/10.1113/jphysiol.1978.sp012272

Zeng, H., Fink, G. R., & Weidner, R. (2020). Visual Size Processing in Early Visual Cortex Follows Lateral Occipital Cortex Involvement. *The Journal of Neuroscience*, *40*(22), 4410–4417. https://doi.org/10.1523/JNEUROSCI.2437-19.2020

Zhang, M., Weisser, V. D., Stilla, R., Prather, S. C., & Sathian, K. (2004). Multisensory cortical processing of object shape and its relation to mental imagery. *Cognitive, Affective and Behavioral Neuroscience*, *4*(2), 251–259. https://doi.org/10.3758/CABN.4.2.251